Analysis of electrolyte solvation within the primitive equation of state framework

Juan Sebastián Roa Pinto

Sorbonne Université

Faculté des Sciences et Ingénierie
ED 388 : Ecole doctorale de Chimie Physique
et de Chimie Analytique de Paris Centre

Modèle thermodynamique prédictif pour les systèmes complexes électrolytiques.

par
Juan Sebastian Roa Pinto

Thèse de doctorat
Discipline : Génie des Procédés
Dirigé par Jean-Charles DE HEMPTINNE

Présentée et soutenue publiquement le 22 Septembre 2022
Devant un jury composé de :

KONTOGEORGIS Georgios	Prof.	DTU Danemark	Rapporteur
PARICAUD Patrice	Prof.	ENSTA Paris	Rapporteur
GALINDO Amparo	Prof.	Imperial College London	Examinatrice
SIMONIN Jean-Pierre	Dir.	Recherche. Lab. Phenix	Examinateur (président du jury)
DE HEMPTINNE Jean-Charles	Prof.	IFP School	Directeur de thèse
FERRANDO Nicolas	Dr.	IFP Energies Nouvelles	Promoteur de thèse

Dedicado a mis padres, familia y amigos.

Dedicated to my parents, family and friends.

Dédié à mes parents, ma famille et mes amis.

Acknowledgements

This thesis is written for the requirement for the PhD degree in process engineering at Sorbonne University, Paris, France. The research work was done at the Department of Thermodynamics and Molecular Modeling at IFP Energies Nouvelles (IFPEN) in collaboration with Imperial College of London and JIP EleTher from October 2019 to September 2022. I would like to thank Thierry Becue and Pascal Mougin for providing an opportunity at IFPEN for carrying out this research work.

I would like to convey my deepest and sincere gratitude to Jean-Charles de-Hemptinne as the main supervisor and Nicolas Ferrando as co-supervisor of this thesis at IFPEN. They have been an excellent guide for the research journey which involved numerous scientific discussions while realizing the goals of this thesis. I would also like to extend this gratitude to Amparo Galindo, for her excellent guidance during this thesis which involved several discussions deep down into electrolyte thermodynamics. To all the members of the EleTher project for their continuous and productive collaboration in various discussions that have made this thesis very important for the industry. I extend my expression of sincere gratitude to the jury of this thesis for their time and effort in examining this thesis.

I would like to extend my heartiest thanks to my colleagues and friends Angie, Aurelie, Benoit, Carlos, Catherine, Elena, Fernanda, Isabelle, Jonathan, Jose, Karen, Martha, Natalia, Philip, Robert, Saheb, Theo, Tri Dat, Veronique. Finally, I must express my deepest gratitude to my family, especially my parents, grandparents and my brother for their support and encouragement throughout these years. This achievement would not have been possible without them. Thank you all for your encouragement!

Abstract

Electrolytic solutions are involved in many classical and emerging industries such as underground storage, biorefining, pharmaceutical, wastewater treatment, etc. To correctly design units, an accurate thermodynamic model is required to describe phase equilibrium and thermophysical properties of such solutions. Many authors have proposed electrolyte extensions of SAFT-type equations of state, with some success. Yet, the approach often consists in adding an additional Debye-Hückel-type contribution and then fit parameters on a selection of experimental data. Consequently, the extrapolations of these models to high concentrations, high temperatures or mixed solvents are questionable. The thesis work aims at elaborating a SAFT-type model that not only 'fits the data' but for which the physical consistency of parameters is analysed, to make the model more reliable for extrapolations.

In a first step of this work, a large and comprehensive database has been built and analysed, including mean ionic activity coefficients (MIAC), osmotic coefficients, apparent molar volumes, and enthalpies of solution, for aqueous solutions concerning 20 monovalent salts. An analysis of the behaviour of the MIAC with respect to temperature, concentration and the diameter of each ion shows that the solvation behaviour follows the law of matching water affinities. Regarding the behaviour of the salts with respect to temperature, a trend is also identified. Such trends will be used to evaluate the capability of the proposed models to correctly reproduce these specific behaviours.

The modelling approach is carried out with the PPC-SAFT equation of state. An extensive literature review shown that the physical part of the model does not have a major impact on calculations for electrolytic systems, and that either the primitive MSA model or the Debye Hückel model can be used to model long-range cation-anion interactions. The main differentiator between the models used to study electrolyte systems is the way in which short-range interactions between ion-solvent (solvation) and between ion-ion (non-coulombic) are taken into account. Two theories are studied in this work to model such interactions: dispersion and association.

This work shown that equivalent results can be obtained for NaCl aqueous solutions with both theories. Furthermore, various formulations of the dielectric constant are also investigated: the most accurate results are found when the salt concentration is not explicitly considered. For each approach, the most sensitive parameters are identified, which makes it possible to reduce the number of adjustable parameters without significantly affecting the overall quality of the model. Nevertheless, none of the models can describe accurately and with physically meaningful parameters the correct low-temperature trend of the mean ionic activity coefficient observed experimentally, and the behaviour at very high salinity.

To address this issue, two modifications to the association theory are proposed. First, a distinction is made between ion-solvent association sites (several sites per ion) and cation-anion association sites (a single site per ion). Secondly, the calculation of the cation-anion association constant is modified by including the Bjerrum theory in the Wertheim association model. It is found that these modifications make the model more accurate, more specifically at very high salinity (up to 20 molal for LiBr aqueous solution). The effect of the number of associative sites per ion is also studied, finding that they significantly affect the quality of the model. Three lithium salts have been studied separately with this model, and deviations less than 5% for both MIAC and osmotic coefficient are obtained. On the whole concentration range. Further work would consist in optimizing model parameters on many salts simultaneously, in order to increase its predictivity.

Résumé

Les solutions électrolytiques sont présentes dans un grand nombre d'industries classiques et émergentes telles que le stockage souterrain, le bioraffinage, la pharmacie, le traitement des eaux usées, etc. Afin de concevoir correctement les unités opérationnelles, un modèle thermodynamique précis est requis pour décrire les équilibres de phase et les propriétés thermophysiques de ce type de solutions. De nombreux auteurs ont proposé des extensions électrolytiques à des équations d'état de type SAFT, avec un certain succès. Pourtant, l'approche consiste très souvent à ajouter une contribution supplémentaire de type Debye-Hückel puis à ajuster les paramètres sur à une sélection de données expérimentales. En conséquence, les extrapolations de ces modèles à des concentrations élevées, des températures élevées ou des solvants mixtes sont discutables. Ce travail de thèse vise à élaborer un modèle de type SAFT qui non seulement reproduit les données, mais pour lequel la cohérence physique des paramètres est analysée, afin de rendre le modèle plus fiable pour les extrapolations.

Dans une première étape de ce travail, une vaste base de données a été constituée et analysée, regroupant les coefficients d'activité ionique moyen (MIAC), les coefficients osmotiques, les volumes molaires apparents et les enthalpies de solution, pour des solutions aqueuses contenant 20 sels monovalents. L'analyse du comportement des MIAC en fonction de la température, de la concentration et du diamètre de chaque ion montre que le comportement de solvatation suit la loi dite de « matching water affinity ». En ce qui concerne le comportement des sels par rapport à la température, une tendance est également identifiée. Ces tendances seront utilisées pour évaluer la capacité des modèles proposés à les reproduire correctement.

L'approche de modélisation est réalisée avec l'équation d'état PPC-SAFT. Une revue de la littérature a montré que la partie physique du modèle n'a pas d'impact majeur sur les calculs des systèmes électrolytiques, et que le modèle MSA primitif ou le modèle de Debye-Hückel peuvent être utilisés pour modéliser les interactions cation-anion à longue portée. Le principal facteur de différenciation entre les modèles utilisés pour étudier les systèmes électrolytiques est la manière dont les interactions courte-portée ion-solvant (solvatation) et ion-ion (non-coulombiennes) sont prises en compte. Deux théories sont étudiées dans ce travail pour modéliser ces interactions : la dispersion et l'association.

Ce travail a montré que des résultats équivalents peuvent être obtenus avec les deux théories pour les solutions aqueuses de NaCl. De plus, plusieurs formulations de la constante diélectrique sont également étudiées. Les résultats les plus précis sont obtenus lorsque la concentration en sel n'est pas explicitement considérée. Pour chaque approche, les paramètres les plus sensibles sont identifiés, ce qui permet de réduire le nombre de paramètres ajustables sans affecter de manière significative la qualité globale du modèle. Cependant, aucun des modèles proposés ne peut décrire avec précision et avec des paramètres physiquement corrects la tendance à basse température du coefficient d'activité ionique moyen observé expérimentalement, ainsi que le comportement à très forte salinité.

Pour résoudre ce problème, deux modifications à la théorie d'association ont été proposées. Premièrement, une distinction a été faite entre les sites d'association ion-solvant (plusieurs sites disponibles sur l'ion) et cation-anion (un unique site disponible sur l'ion). Deuxièmement, le calcul de la constante d'association cation-anion a été modifié en incluant la théorie de Bjerrum dans le modèle d'association de Wertheim. Ces modifications permettent au modèle d'être plus précis, en particulier à très forte salinité (jusqu'à 20 molal pour LiBr). L'effet du nombre de sites d'association des ions a également été étudié, ceux-ci impactant nettement la qualité du modèle. En étudiant séparément plusieurs sels de lithium (LiCl, LiI, LiBr), des écarts de moins de 5% pour le MIAC et le coefficient osmotique sont obtenus par le modèle, sur toute la gamme de concentration en sel. Une perspective à ce travail consistera à optimiser les paramètres de ce modèle sur plusieurs sels simultanément, pour gagner en prédictivité.

Table of contents

List of figures

List of tables

Chapter 1 Electrolytic systems and their challenges

1.1 Introduction

The world population experiences a substantial growth over the last century. This growing population causes an increase in consumption, and therefore an increase in the production demand of different industries. These increases in both production and population, accompanied by a lack of environmental consciousness, have caused, among other things, an increase in the earth's temperature. At present, efforts are being made to mitigate the impact of humans on the environment and that is why terms such as climate change, greenhouse gases, green energy and energy transition are becoming more and more important. These terms refer to the need to change the way we generate energy, to meet the needs of a growing world population. In 2015, 196 countries signed the Paris agreement [1] whose objective is to limit global warming below 2°C, preferably 1.5°C, compared to pre-industrial levels. To achieve this long-term temperature goal, countries aim to reach greenhouse gas emissions neutrality, as soon as possible to achieve a climate-neutral planet by mid-century (2050).

The goal of improving the quality of life and the environment generates the need to develop advanced engineering materials, environmentally friendly chemicals and improve process efficiency. The chemical industry uses different unit operations to transform raw materials into products. In general, a chemical process is mainly composed of 2 steps: chemical reactions and purification (separation) of the products. In each of these steps, the compounds will behave according to their chemical potential, which is a thermodynamic property. Thermodynamic is one of the most important tools in chemical industry. It is used to design and operate equipments (mainly separation and purification equipments). The purification of a mixture is generally performed using unit operations such as distillation, extraction and filtration. For example, distillation consists in separating the chemical components of a mixture by taking advantage of the differences between the volatilities of each component, while extraction is carried out using the difference in the affinity of each compound with a third chemical compound, the solvent (solubility).

The design of the separation units requires an accurate thermodynamic model which can be correlative or predictive. Correlative models have to be calibrated with experimental data,

which can be a disadvantage, since there are still many systems for which experimental data are scarce. Predictive models can overcome this problem as they do not depend completely on existing experimental data, but there are consequently less accurate. Two main theories exit, the first one describes deviations from an ideal mixture using activity coefficient models. They suit well for liquid state, but their predictive capability is limited. The second one describes deviations from an ideal gas using equations of state. Some of these equations have a high predictive capability because they are constructed on the foundation of statistical thermodynamics. The choice of a thermodynamic model depends largely on the composition of the solution and the process conditions.

The thermodynamic of systems with strong and weak electrolytes has gained great importance in recent years in the chemical industry. However, the capabilities of thermodynamic models are far from being fully optimized, due to the complexity of molecular interactions in this type of solutions [2]. The long- and short-range interactions that take place in electrolyte systems, make difficult to perform accurate calculations of phase equilibria and solubilities, among others. Consequently, thermodynamic models based on electrolyte systems require continuous developments and research.

This chapter defines the main needs and applications of electrolytic systems. It also describes the main objectives of the present work and the methodology that will be used.

1.2 Scope of the work

This thesis is part of the IFPEN scientific project 1 "Characterizing materials and fluids for energy at different scales", and more precisely in the challenge 1.2 "Physico-chemical description of fluids". One of the stakes of this challenge is to perfect and develop new methodological and computational tools (equation of state in particular) to predict the thermodynamic and physico-chemical properties of complex fluids. Objective 3 of this challenge clearly identifies electrolytic systems as an area of research since significant progress is to be made in this field.

The interest in the study of electrolytic systems has become a topical subject not only for IFPEN but worldwide. An article [3] compiling the main requirements at industrial level, points out that electrolytic systems are one of the most important topics, being one of the most

mentioned among the companies consulted. Some of the statements from the participating companies are:

"Electrolytes are more prominent in processes, possibly due to the expansion of bioprocessing. The electrolyte models are more complex than the non-electrolyte ones, and much more difficult to use for practicing chemical engineers. One perceives a lack of standardization when it comes to using these models. There is a need for a critical review/comparison/evaluation on these models, similar to what has been done for non-electrolytic models, nonelectrolytic predictive models, etc."

"There is a lack of data to fit the parameters of the e-NRTL model, which is used systematically for electrolyte systems at our company. For our systems, measurements are difficult due to radioactivity and/or toxicity of some compounds.".

In addition to showing concern about the lack of standardization and lack of experimental data, many companies also expressed concern that most existing models are not predictive outside of the experimental range [3]. This creates a need for truly predictive models for electrolytic systems, in which the number of adjustable parameters and data regressions are limited. These models should also work at high concentrations, including speciation behaviour. Kontogeorgis et al. [3] also state that the parameterization of electrolyte models is widely debated, and it is noted that "procedures should also include instructions to include uncertainty in the most effective way".

Although new industries related to the energy transition such as biofuels, batteries and CO_2 capture are increasing the attention on the study of electrolytes, these systems are nothing new as they have already been investigated in other contexts. Figure 1 shows some of the applications industries where electrolyte thermodynamics is needed.

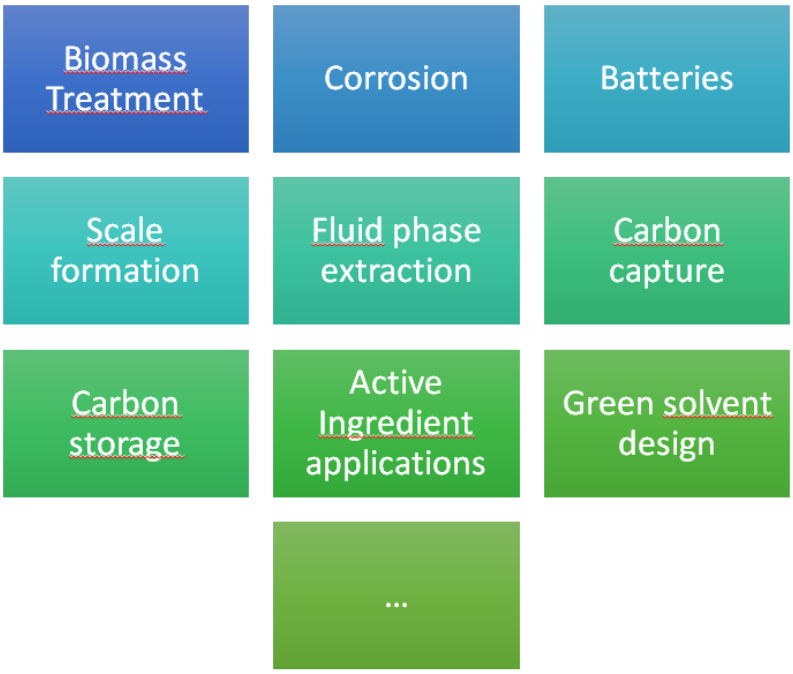

Figure 1 : Some of the applications of electrolyte thermodynamics [4].

IFPEN has created a Joint Industrial Project (JIP) called EleTher (Electrolyte thermodynamics) [5], that was joint by a number of companies with international prestige like Bayer, BP, Orano, BASF, Nouryon, NESTE and Solvay. The objective of this project was to mark a route and to advance on the investigation of the thermodynamics of electrolytic systems. The present work is associated with the EleTher project.

Figure 2 : Industrial community composing the JIP of EleTher.

Industrial applications require good description of several properties of mixtures that contain electrolytes. Electrolytic systems pose two specific problems: the inclusion of long-distance interactions and the reactivity of species. The existing industrial models are not good

at extrapolating the few existing data and the JIP aims at creating an industrial community for electrolyte systems with following goals:

- Communicate regarding the challenges.
- Elaborate a methodology to analyses the data in view of identifying trends that can be used to extrapolate.
- Propose parameterization strategies of industrial models for mixed solvents including acids, alcohols, and aprotic solvents.
- Propose a best practice workflow to model electrolyte systems.

This thesis work focuses on the analysis of the data, the comparison of thermodynamic models, the parameterization of models, as well as the modification and extension of a model for the calculation of thermodynamic properties at very high salt concentration.

1.3 Electrolytes in the industry

As mentioned above, electrolytic solutions are present in many classical and emerging industries. Electrolytes are charged species, meaning that thermodynamic models must contain a description of the long-range electrostatic interactions, as well as short range interactions between the solvent molecules, the ions and the solvent and in some cases between the ions. In addition, many of the compounds considered may chemically react, thus creating additional species that were not initially present in the mixture.

A correct understanding of the speciation is especially important if, for example, the effect of pH on the properties must be understood. Depending on the system, on the pressure and the temperature range, different types of phase equilibria can occur, which obviously affect the properties of interest (a vapour, one or several liquid phases, one or several solid phases). Below we will briefly present how an accurate understanding of the behaviour of electrolyte solutions is required in some industries.

1.3.1 Corrosion

It is common for oil and gas companies to transport crude oil over long distances using pipelines, which saves on transportation and operating costs. Even oil extracted offshore is transported to onshore facilities to be refined. Corrosive components such as CO_2 and H_2S are usually found in these types of fluids without pretreatment, which can significantly affect the steel by corrosion. From an environmental point of view the problem of corrosion in oil transportation creates a serious problem as it can lead to oil leakage which can cause irreversible

environmental damage to the surrounding ecosystem. In addition to this it can also generate large economic losses. Once the oil has been refined, corrosion problems persist. Although petroleum distillates and refinery product streams are generally non-corrosive, the presence of water and salts, even as low as 15 ppm (chlorides, sulfates, nitrates), can cause significant levels of corrosion in refinery process equipment. [6, 7].

One solution is to use corrosion resistant steel, but this increases the cost of pipeline installation. Eliminating corrosion is almost impossible, however, the rate at which steel corrodes can be controlled. For this it is necessary to study this phenomenon taking into account temperature, water content, pH and flow rate. It is also necessary to know the condition in which the iron carbonate formed Fe_2CO_3 will precipitate, since it acts as a protective layer on the surface of the steel. The presence of dissolved salts in the well fluid can further complicate the phenomenon and affect the corrosion rate. Therefore, thermodynamic models capable of calculating thermodynamic properties including reactions and solid phase and the presence of ions are needed.

1.3.2 Hydrate formation

Hydrate formation is another problem that affects the transport of hydrocarbons. Hydrates are formed when natural gas is trapped by water molecules forming in a hydrogen bond structure. This type of structure can block the flow of hydrocarbons (see Figure 3), thus stopping the operation until the obstruction is removed. Hydrate formation can be controlled using chemical, hydraulic, mechanical, or thermal methods. Chemical methods make use of thermodynamic inhibitors, either to change the equilibrium temperature of hydrate formation or to use them as kinetic/dispersant inhibitors. Some of the best known inhibitors are methanol, glycols or electrolyte solutions [8]. The presence of salts reduces the solubility of hydrocarbons in water (salting out effect) [9]. In addition, salts contribute to the breakdown of gas hydrates in pipelines, as the ions interact with water molecules, which is effective in preventing blockage of gas pipelines [4].

Figure 3 Corrosion and gas hydrates problem associated in oil and gas industry [10].

1.3.3 Underground storage in salt caverns

Underground storage in salt caverns is a mature technique for natural gas storage, which ensures flexibility on the gas network and supplies security during the winter season. But for storing new promising green energy vectors such as hydrogen or pressurized air, it remains a challenge. These caverns behave as pressure vessels and may deliver high flow rates on demand. They are used in an increasingly intensive modes, with shorter cycles. Salt caverns present several advantages for massive storage of gases as a pure product [11], notably the very low permeability of salt layers and the flexibility allowed by these structures, compatible with the variable production and usages associated with hydrogen.

In this context, it becomes very important to predict moisture content at the wellhead and in the cavern, in order to design the surface units and optimize exploitation. In the case of gas storage in salt caverns, depending on the usages planned after production, a high purity might be required, which imposes the use of dehydration units at surface. On the other hand, evaluation of gas loss by dissolution may be interesting for operators when considering mechanical integrity tests (cavern in that case is partially filled) or during de-brining phases.

At the end of the creation of the saline cavity (by leaching, see Figure 4), a saturated salt solution remains at the bottom. The presence of this saturated brine and the gas must be taken into account when making thermodynamic calculations. These factors increase the complexity in the calculation of phase equilibria within the salt cavity. It is thus of primary importance for operators to dispose of a thermodynamic model able to accurately predict the vapour-liquid equilibrium (VLE) at wellhead and inside the cavern to correctly dimension surface facilities during the phase of preliminary design, and to determine the storage performance and improve its exploitation during operations [12].

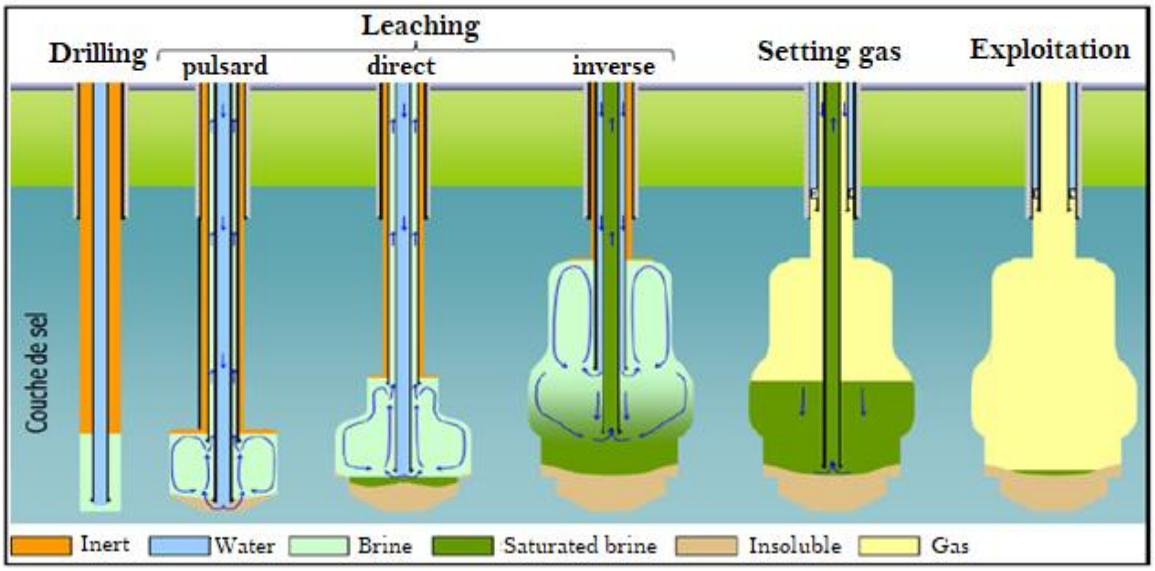

Figure 4 : Steps for the creation of a saline cavity by leaching [13].

1.3.4 Biorefining industry

The objective of this industry is to extract valuable material, such as alcohols, from biomass. One of the main problems in this industry is the extraction of valuable biomass (see figure 5). Numerous methods such as steam stripping, vacuum distillation, solvent extraction, reactive extraction, ion exchange resins, activated carbon or molecular sieve adsorption and zeolite membranes have been used as separation methods for this type of system [10, 14, 15].

The use of ionic liquids and Deep Eutectic Solvents (DES) (also called green solvents), represents an attractive solution due to their excellent dissolving capability for biomass processing, in addition to their low toxicity and cost as well as good biodegradability [16]. The presence of electrolytes causes a significant change in the liquid-liquid equilibrium (LLE), making the modeling of these complex systems particularly difficult. Ions affect the hydrogen bonding structure and other intermolecular forces; therefore, the mutual solubility is affected by their presence (water rich phase and organics rich phase). This is why it is important to have a thermodynamic model capable of making accurate representations of these types of systems. It should include the representation of the mutual solubilities of oxygenated compounds and water in organic and aqueous solvents including salts.

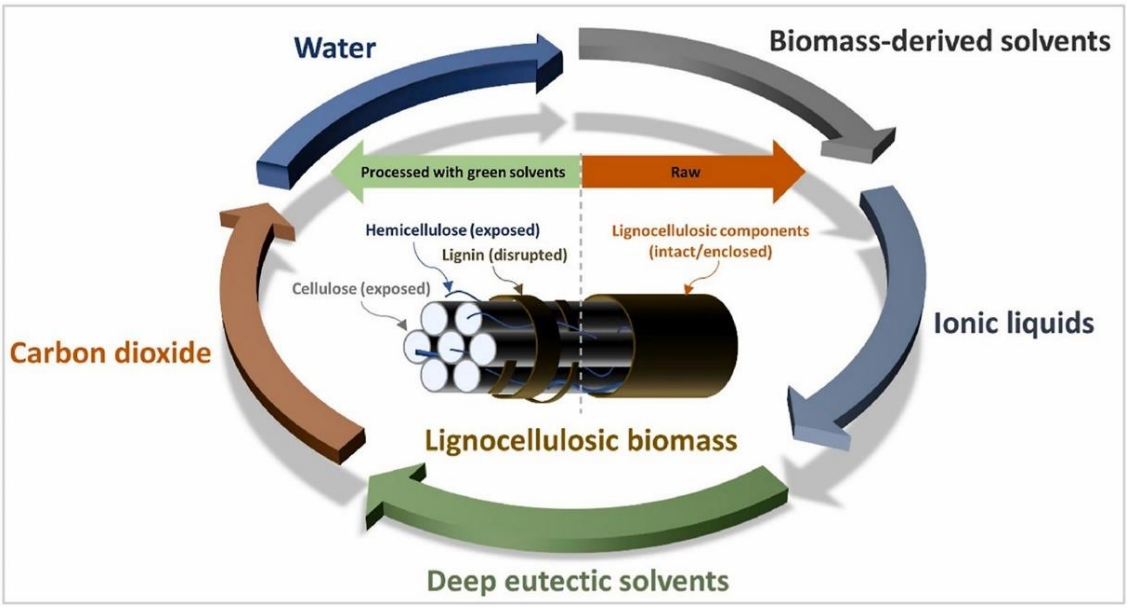

Figure 5 : Use of green solvents in biomass extraction [16].

1.3.5 Batteries

As can be seen in Figure 6, the main elements that form a lithium battery are a cathode, an anode, an electrolyte, and a separator. During the charge process, lithium ions move from the cathode to the anode. The movement is promoted by the electric field via the Li^+-conductive electrolyte. Electrons are simultaneously donated by the cathode host, in order to maintain electric neutrality, and flow to the anode via an external electrically conductive circuit.

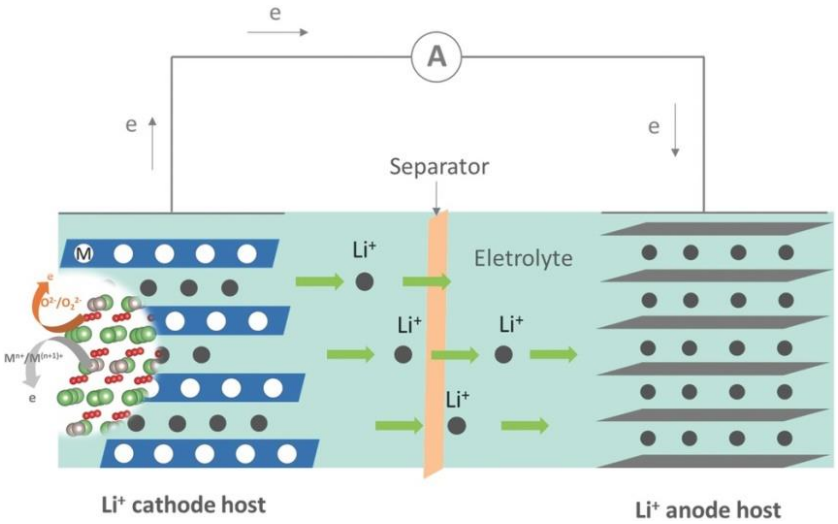

Figure 6 : Mechanism of lithium-ion batteries [17].

Lithium is the lightest of all metals and it can provide the conductivity. When lithium is used as anode in contact with ionic lithium salt electrolytes, it can provide a wider

electropositive potential window. These batteries can contain a very high energy density. In fact, these batteries are being manufactured presently on a large scale and used as rechargeable power packs in a wide variety of applications [17]. This type of device is characterized by the presence of multiple phases. Therefore, understanding and optimizing the management of multiple phases is one of the key factors for the development of electrochemical energy technology. For this, of course, models capable of predicting the different phase equilibria in the presence of ions are necessary [18].

1.3.6 Pharmaceutical industry and life science

Electrolyte systems also play an important role in the pharmaceutical industry. One example of the application of electrolytes can be found in drug delivery and solubility. The skin is the largest organ in the human body and it is considered as an extremely important organ for all the functions of our body. The organ is composed by a tissue organized into different layers: the dermis, epidermis and the hypodermis.

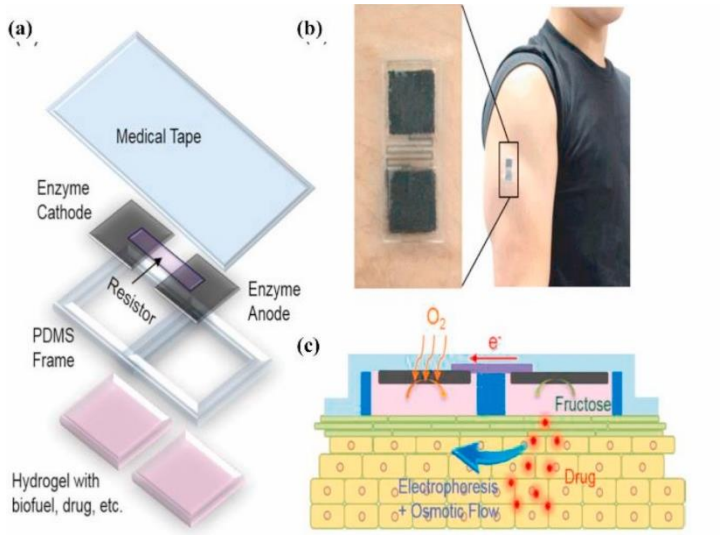

Figure 7 : Disposable organic anodal iontophoresis patch. a). Schematic representation of the transdermal iontophoresis patch that is a built-in enzymatic biofuel cell containing the drug to be delivered. b) Image of the patch placed on a human arm. c) Schematic representation of the iontophoretic drug delivery mechanism [20].

The pharmaceutical industry looks for new techniques to heal the wound of skin injuries and burns. Some engineering techniques facilitate the transport of drugs in the different layers of the skin. For example, polymer electrolytes are polymers capable of conducting ionic drugs (see Figure 7). In addition, these polymers are highly biocompatible and are suitable for reducing rejection. They are as a consequence potential candidates to host the drugs for the delivery on the affected area [19, 20]. Therefore, this industry requires thermodynamic models

capable of predicting the solubility of pharmaceuticals in solutions with the presence of salts (solid-liquid equilibrium SLE). The solubility of pharmaceuticals in water and organic solvents also plays a key role in the discovery and formulation of new drugs in pharmaceutical processes involving several steps, such as design, synthesis, extraction, purification, formulation, absorption and distribution in body fluids [21].

1.3.7 Metal recovery and hydrometallurgy.

The separation of metallic ions by solvent extraction is a well-established and well known hydrometallurgical technology [22, 23]. This technique aims to separate and extract metals either from natural sources or from residues (metal recovery). Solvent extraction of metals, which usually operates as an equilibrium process, is based on thermodynamic principles. However, the thermodynamics of such systems is far from being simple because calculations of liquid-liquid equilibria (LLE) of complex mixtures must be made; indeed, a typical system of practical interest in hydrometallurgy consists of water and an organic solvent, several organic solutes, and several salts.

To design or optimize such processes, the thermodynamic model must accurately describe the LLE behavior of a system with two-solvents plus one electrolyte (two-phase system with three components). Cosolvents or solution modifiers are added to control the density, viscosity, interfacial tension and to improve the solubility of the extractant [22]. Moreover, the chemistry of these solutions introduces several additional complications. Liddell [22] reports that the effects of chemical speciation have not been taken into account in most of the thermodynamic models investigated in his study. He also stressed the importance of including these effects since several of the models obtained poor results when they were evaluated in complex systems or in systems with possible ion pair formation.

1.3.8 Wastewater treatment

Environmental applications include wastewater treatment. In some processes, such as petroleum, leather, or food-processing, recovered industrial wastewater contains high salts concentration and needs an important treatment before its release in the environment. The aim of the treatment is to reduce its content on dissolved hydrocarbons and salts [24]. High concentration of salt in the water has a negative impact in the aquatic life, water quality and agriculture. Various techniques are currently used for salts removal. Some examples of these

processes are reverse osmosis, ion exchange, electrodialysis or biological treatments [25]. All these techniques require a good understanding of the thermodynamics of the aqueous phase.

1.4 Objectives and methodology

This thesis work focuses on the modeling of systems containing electrolytes. By the past, many authors have proposed electrolyte extensions of equation of state, including SAFT-type equations, with some success. Yet, very often, the approach consists in adding an additional Debye-Hückel-type contribution and then to fit parameters to some data. Consequently, it is found very difficult to use the models for extrapolations to high concentrations, high temperatures or mixed solvents.

This work aims to propose deep analysis of the differences and similarities between various modelling approaches, so as to identify the best way to reconcile the theoretical foundation of the model and the expected experimental behaviour, up to saturation concentrations and high temperatures of aqueous solutions of alkali halides. To reach this goal, the following methodology is adopted:

- To create a comprehensive database containing different properties such as mean activity coefficient (MIAC), osmotic coefficient, enthalpies of solution and apparent molar volume (AMV), including the maximum temperatures and concentrations of aqueous electrolyte solutions with alkali halides.

- To analyse the data collected and the existing theories, in order to identify trends and key points in the study of electrolytic systems.

- To propose different variants of SAFT equation of state (EoS), by using different approaches to model ion-solvent and ion-ion short range interactions, and to benchmark them on the same database, in order to identify the best model to reproduce in an accurate and coherent way the electrolytic systems.

- To calibrate the best model so as to make it as predictive as possible, focusing on high salt concentrations.

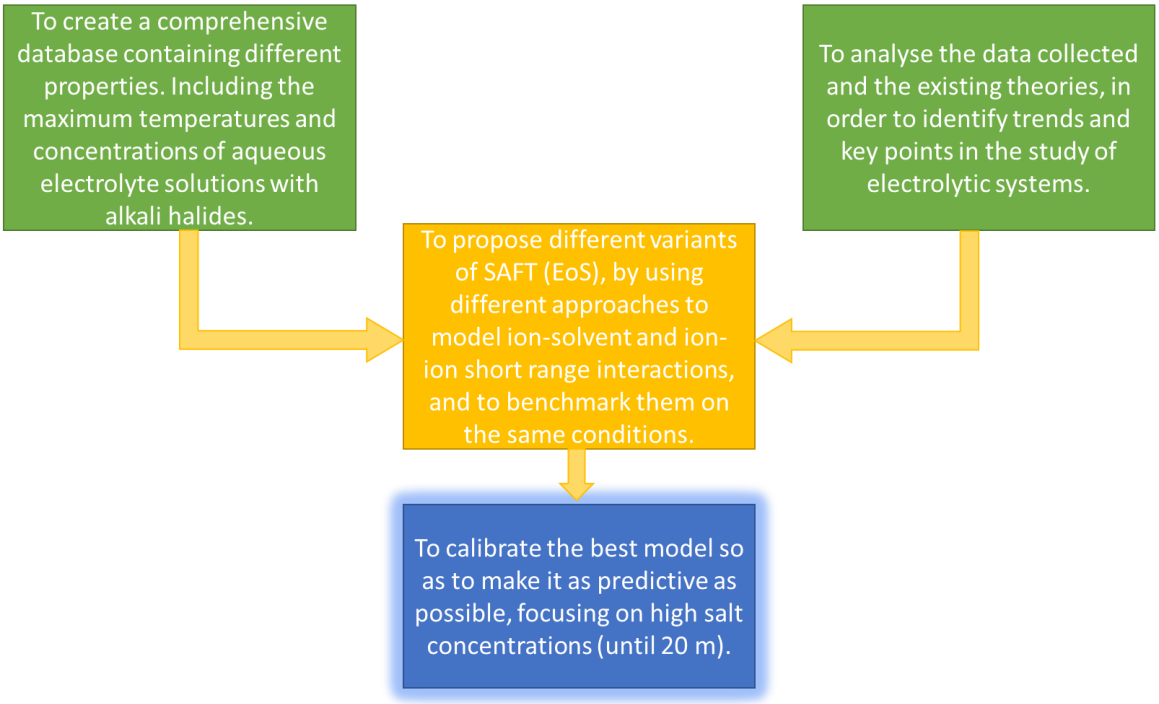

Figure 8: Methodology for thesis project.

This methodology is described in this thesis work in 4 main chapters.

The first chapter deals with the basic concepts and usual properties used in the thermodynamics of electrolytes. This chapter first introduces fundamental concepts in the study of electrolytic systems such as mole fraction, molality, chemical potential and activity coefficients. The thermodynamic properties that will be used throughout the work are presented: mean ionic activity coefficient (MIAC), osmotic coefficient, apparent molar volume and enthalpy of solution. Then, the database creation procedure will be explained and a summary showing the maximum temperature and solubility for each property will be presented. Finally, an analysis of the main trends found as a function of salt concentration, temperature and the difference between the diameters of the ions will be made. The relationship between the variation of MIAC with respect to temperature and the variation of the enthalpy of solution is also presented.

The second chapter is devoted to the presentation of the theoretical framework of the SAFT equation of state, and the physical modeling background of typical electrolytic interactions. For this purpose, the main intermolecular interactions are introduced. Then, the construction of an equation of state based on the principles of perturbation theory is presented. The main theories used to describe each of the interactions present in an electrolytic system are also summarized. Models to describe the interactions between molecules are divided into

several groups. The first group concerns the physical or short-range interactions, involving the hard sphere (repulsion interactions), dispersion (Van der Walls interactions), association (hydrogen bond interactions) and polar (interactions between polar molecules) models. The second group is the coulombic interactions, where the Debye-Hückel (DH) and Mean Spherical Approximation (MSA) theories are presented. The third group presents the SR2 and Born models that are used to consider the ion-solvent interactions. This chapter also presents three models for calculating the dielectric constant, two depending explicitly on the salt concentration and one depending implicitly. Finally, the state of the art of the equations of state for electrolytic systems is presented. In this discussion the main differences and similarities between the SAFT equations of state for modeling electrolytes are highlighted. The main difference is in the way the dispersion and association models are used to model ion-solvent short-range interactions. For ion-ion interactions it is evident that there is "agreement" in the modeling of coulombic interactions, and that most papers do not take into account the formation of ion pairs.

The third chapter focuses on a comparison of various modeling approaches on the example of the NaCl aqueous solutions. Based on the observations of the literature review, two types of models will be compared. The first one called dispersive model considers the short-range ion-solvent and ion-ion interactions with the dispersion model. The second, called associative model takes into account the short-range ion-solvent and cation-anion interactions through the association model. Three different dielectric constants are used for both the dispersive and associative models. All models will be compared using the same conditions (database, objective function, properties, etc). For both types of models, the most sensitive parameters are identified, and an optimization strategy is established to obtain physically consistent parameters. The main challenge in this chapter is to find a model able to correctly describe the MIAC, the osmotic coefficient, the enthalpy of solution and the apparent molar volumes for NaCl aqueous solution, between 0 and 6 molal in a temperature range between 273.15 and 473.15 K. The best models will be also extended to describe 4 salts using ion-specific parameters.

The fourth chapter focuses on the modeling of the very high concentration aqueous solutions, with the example of lithium-based electrolyte aqueous solutions. To this end, this section first introduces Bjerrum's theory. Then, two modifications made to the association model will be discussed. These modifications aim to improve the way ion-solvent and cation-anion interactions are modeled. In the first modification, two types of associative sites are introduced for each ion. The first type of site (ion-solvent) allows multiple interactions between

the ions and the solvent. The second type (cation-anion), allows only one bond between the cation and the anion. In the second modification, the Wertheim cation-anion association constant is replaced by the Bjerrum association constant. In this chapter the impact of the associative sites on the model will be also analyzed. An extension of the model is also made for 3 salts (LiCl, LiBr and LiI). Following the postulate that the smaller the ion size the higher the solvation, the impact of the number of anion-solvent associative sites for Cl, Br and I will be evaluated.

Chapter 2 Thermodynamic properties for electrolytic systems

2.1 Introduction

As discussed in the previous chapter, the phase equilibrium calculations are an essential and recurrent element in the simulation of chemical processes. Algorithms for phase equilibrium calculations are therefore required to be robust as well as efficient. Important applications requiring such calculations comprise single-stage processes, i.e. flash and saturation point calculations, as well as multistage processes such as distillation, adsorption and extraction [26]. This type of calculation is based on an algorithm that minimizes the Gibbs energy of the system for a fixed pressure and temperature. This energy is calculated from the chemical potentials [27]. In addition, the chemical potential is also related to the fugacity and the activity coefficient, two very important concepts in thermodynamics. All these concepts are related, and it is important to know them before starting the study of electrolytic systems. That is why we will begin this chapter by defining these basic concepts (section 2.2).

In this work, different types of properties are considered to investigate electrolyte thermodynamic models: the mean ionic activity coefficients, the osmotic coefficients, the apparent molar volumes, vapor-liquid equilibria, and enthalpies of solution. The two first ones are rightly considered as essential in the study of electrolyte systems by all authors. The apparent molar volume is less often considered. The enthalpy of solution is rarely considered but helps at improving the temperature dependence of other properties. Finally, the VLE is very common datatype (more specifically vapor pressure depression or boiling temperature rise), but the sensitivity of this property to the salt-related parameters of the model is quite small. All these properties will be presented in the section 2.3, and in section 2.4 the way in which the data was collected to create the database used in this study.

An analysis of the data and the different kinds of behaviour found for the 20 alkali-halide salts will also be presented. This study has been published in collaboration with the EleTher Joint Industrial Project [28], and the sections 2.4 and 2.5 present the main results.

2.2 Basic concepts

2.2.1 Concentration units

At a specified temperature and total volume, we consider fluid mixtures consisting of water (the solvent (A)) and a salt (the solute) which is fully dissociated into its constituent ions following an equilibrium reaction. For a salt $X_{\nu_+}Y_{\nu_-}$, the equilibrium can be described as:

$$X_{\nu_+}Y_{\nu_-} \rightleftarrows \nu_+ \cdot X^{Z_+} + \nu_- \cdot Y^{Z_-} \qquad (2.1)$$

where ν_+ and ν_- are the stoichiometric coefficients of the cation (X) with valency Z_+ and the anion (Y) with valency Z_-, respectively. In our case we consider only monovalent salts $\nu_+ = \nu_- = 1$, and the salt is further written as XY.

For modern simulation programs and thermodynamic models, the composition is described in mole fractions. In the field of electrolyte thermodynamics, a concentration unit different from the mole fraction is often used, such as the molality. Consequently, it is essential to define the relation between the molality of the salts in the solvent and the mole fraction.

The mole fractions are defined as the number of moles of a component in a system divided by the total number of moles. Molar fractions are described by x in the liquid phase and are defined as:

$$x_i = \frac{n_i}{n_t} \qquad (2.2)$$

Where x_i is the mole fraction of the ion i, n_i is the number of moles of the ion i and n_t is the total number of moles. The mole fraction differs whether the salt is considered as a single species (apparent mole fractions) or whether the true (ionic) species are considered. In this work we shall always consider full dissociation (true species).

The molality is the most common concentration unit used in the study of electrolyte solutions. The molality (m) of a salt or any solute, is the number of moles of solute (n_{XY}) per kilograms of solvent (A). Molality is a popular unit for salt solutions due to the fact that the concentrations in molality units give practical numbers (often between 0 and 20 for most salts), while the concentrations in mole fraction units are very small (10^{-3}, 10^{-2}) [29]. The molality (m) is defined as:

$$m = \frac{n_B}{mass_A} \qquad (2.3)$$

Where, $mass_A$ is the mass of the solvent. The molality only dependent on the amount of the relevant solute and the amount of solvent.

The relationship between molality and molar fraction can be found by stating:

$$m_i = \frac{n_i}{n_A \cdot M_A} \tag{2.4}$$

Where n_A is the mole number of the solvent and M_A is the molar mass of the solvent. The number of moles can be divided by the total number of moles, in the denominator and the numerator. As the system is defined with salt and solvent, the molar fraction of solvent can be expressed as one minus the molar fraction of the salt. The relation can then be written depending in the molar fraction of salt or ion as:

$$m_i = \frac{x_i}{(1 - \nu x_i) \cdot M_A} \tag{2.5}$$

Where m_i is the molality of the ion i, ν stands for the sum of species valencies in the salt (one if considering apparent species or two for 1:1 salts).

2.2.2 The chemical potential and the activity coefficient

The chemical potential is defined as the Gibbs energy changes (absorbed or released) caused by the change of the particle number of moles of a given component [27]:

$$\mu_i = \left[\frac{\partial G}{\partial n_i}\right]_{P,T,n_j} \tag{2.6}$$

Where μ_i is the chemical potential of the ion i, G is the Gibbs energy, and P,T , n_j are the pressure, temperature, and number of moles of the component j respectively. The chemical potential is used to determine the thermodynamic equilibrium of a system. When equilibrium is reached, the chemical potential of each substance in one phase will be equal to the chemical potential of the substance in the other phases of the system. The chemical potential may also be expressed in terms of fugacity (f). The relation between the chemical potential and the fugacity is defined as:

$$\mu_i = \mu_i^{ref}(T_o, P_o, x_o) + RTln\left(\frac{f_i(P, T, x_i)}{f_i^{ref}(T_o, P_o, x_o)}\right) \tag{2.7}$$

Where the superscript ref refers to reference state, T_0, P_0 and x_o stand for reference temperature, pressure and composition respectively, R is the ideal gas constant, T the temperature, f the fugacity and x_i is the mole fraction of the component i. The fugacity

represents the tendency of the component i to escape from a phase. The fugacity can be calculated as:

$$f_i(P) = c_i f_i^*(P)\gamma_i \qquad (2.8)$$

Where, f_i stands for the fugacity of the component i, f_i^* is the fugacity in the reference state at P of the component i and γ_i is the activity coefficient of the component i. The concentration c_i may be expressed in mole fraction or in molality. Note that the activity coefficient depends on the concentration unit. The activity coefficient describes the deviation of the fugacity with respect to an ideal behaviour.

Four pieces of information define a reference state: temperature, pressure, composition, and physical state. In all the reference states, the temperature is equal to that of the studied fluid. The remaining three pieces of information must be defined. Typically, several choices can be made: ideal gas, pure liquid, infinite dilution or one molal. Table 1 summarizes different references states that can be used.

Table 1 : Reference states for fugacities calculations. P^{σ} is the saturation pressure.

Reference state	Symbol	Definition	Pressure	Physical state	Reference Composition
Ideal gas	#	Ideal Gas	0.1 MPa	Ideal gas $f_i^{ideal} = y_i P$	System composition
Pure liquid	*	Pure liquid	P_i^{σ}	Liquid	Pure $x_i = 1$
Infinite dilution	∞	Infinite dilution	$P^{\sigma}_{solvent}$	Ideal liquid*	Extrapolated to $x_i = 1$
Molality base	m	Molality	$P^{\sigma}_{solvent}$	Ideal liquid**	Unit molality in solvent $m_i^0 = 1 / \text{mol} \cdot \text{kg}^{-1}$

[a] For all reference state the temperature is always the temperature of the system ($\boldsymbol{T}$).

* Defined from the fugacity relationship $f_i^{ideal} = x_i H_i$ where $H_i = \lim_{x_i \to 0} \frac{f_i}{x_i}$.

** Defined from the fugacity relationship $f_i^{ideal} = m_i H_i^m$ where $H_i^m = \lim_{m_i \to 0} \frac{f_i}{m_i}$

The liquid state reference state is used for calculations made with activity coefficient models and can be used only for liquid solvents. The infinite dilution reference state is used for solutes (neutral gases or very dilute compounds), generally in combination with solvents where the pure component reference state is used. The last case (molality base) is most often used for electrolyte systems.

For an activity coefficient model based on mole fractions, equation (2.8) is used with $c_i = x_i$. The fugacity is expressed as:

$$f_i(P) = x_i f_i^*(P_i^\sigma)\gamma_i \qquad (2.9)$$

Where γ_i is the mole fraction-based activity coefficient, which needs to be calculated with the use of a suitable model. The most known being e-NRTL [30, 31], e-UNIQUAC [32, 33], Pitzer [34–36], as well as MSE [37, 38]. f_i^* is the fugacity of the component taken in the reference conditions as shown in the Table 1.

The advantage of using activity coefficient models is that they are simple and easily deployed in process simulators, which makes these models the most widely used in the industry. The main disadvantage of these models is that they are independent of pressure. This means that they are not suitable for use in high-pressure calculations. In some cases, the Poynting correction can be included, which allows working at high pressures, thus correcting the properties of the reference state (f_i^*), but not those of the mixture (γ_i). In addition, the predictive ability of these models is very weak since they are based on the adjustment of many interaction parameters. The success of the adjustment of these parameters depends strongly on the availability of experimental data.

Equations of state (EoS), are used to calculate the fugacities as a function of temperature, pressure and composition using the ideal gas as a reference state. They are appropriate for both liquid and vapour phases. For equations of state, the fugacity is expressed in terms of fugacity coefficient:

$$f_i = x_i \varphi_i P \qquad (2.10)$$

Where, φ_i is the fugacity coefficient of the ion i and P is the pressure. EoS consider all types of interactions and the effect of density on these interactions. Their application range therefore covers all fluid phase conditions. EoS are relationships between pressure, temperature, volume, and composition. A distinction is made between pressure explicit EoS and volume explicit EoS. Volume explicit equations of state are unable to describe multiple phases at a fixed pressure, in contrast to pressure explicit equations of state which could give roots for various molar volumes. These equations can be considered as originating from an expression of Helmholtz energy as a function of temperature, phase volume and phase composition [27]. The fugacity coefficient is obtained from the derivative of the residual Helmholtz energy (A^{res}) with respect to the number of moles, as shown below [39]:

$$ln(\varphi_i) = \frac{1}{RT}\frac{\partial A^{res}(T,V)}{\partial n_i} - ln(Z) \qquad (2.11)$$

Where A^{res} is the residual Helmholtz energy, n_i is the number of moles of the ion i and Z is the compressibility factor, defined as:

$$Z = \frac{Pv}{RT} \qquad (2.12)$$

Where v is the molar volume, R is the ideal gas constant and T is the temperature. The equations of state can be classified into three groups: Virial EoS, Cubic EoS and perturbation theory EoS. Virial EoS are strongly empirical, therefore they will not be discussed here. Cubic EoS and perturbation theory EoS are pressure explicit. Perturbation theory EoS are increasingly used to describe complex systems. This type of equations will be discussed in further details in section 3.

The mole fraction-based activity coefficient can be expressed from the fugacity coefficient as follows:

$$\gamma_i = \frac{\varphi_i}{\varphi_i^*} \qquad (2.13)$$

Where γ_i is the mole fraction-based activity coefficient, φ_i is the fugacity coefficient and φ_i^* is the fugacity coefficient in the reference state. Thanks to equations (2.11) and (2.13), it is possible to write the activity coefficient as:

$$RT\ ln(\gamma_i) = \left(\frac{\partial\left(A^{res}(T,V)\right)}{\partial n_i} - \frac{\partial\left(A^{res,*}(T,V)\right)}{\partial n_i}\right) - RTln\left(\frac{Z}{Z^*}\right) \qquad (2.14)$$

Where the asterisk points to the reference state conditions. For the solvents, pure liquids, but for solutes or electrolytes, infinite dilution is used.

2.3 Properties of electrolyte systems

2.3.1 Mean ionic activity coefficients

As mentioned above, the activity coefficient represents the deviation from an ideal behavior. For electrolyte systems this property is often determined by carrying out electromotive force (EMF) measurements, on cells in which the concentration of the ion of interest is known [40]. In addition, despite some attempts to do so [41, 42], it is in reality very difficult to distinguish between cation and anion activity coefficient, because both are simultaneously present in the solution. Therefore, the mean ionic activity coefficient is then

defined. Considering the general salt $X_{\nu_+}Y_{\nu_-}$ that dissociates into $\nu_+ \cdot X^{z+}$cations and $\nu_- \cdot Y^{z-}$anions (see equation (2.1)). The mean ionic activity coefficient which is defined on a molality basis (indicated by a superscript m) is defined as:

$$\gamma_{\pm}^{m} = \left(\gamma_X^{\nu_+,m} \cdot \gamma_Y^{\nu_-,m}\right)^{\frac{1}{\nu_+ + \nu_-}} \tag{2.15}$$

Where $\gamma_{\pm}^{m}$ is the mean ionic activity coefficient and $\gamma_X^{\nu_+,m}, \gamma_Y^{\nu_-,m}$ are the activity coefficient of the cation and anion respectively. When molality is used as concentration unit, the molality-based activity coefficient is thus defined. Yet, the equation of state framework is based on mole fractions, and the mole fraction-based activity coefficient (γ_i) is obtained from the fugacity coefficients as shown in the equation (2.13). The mole fraction-based activity coefficient is converted into molality-based activity coefficient (γ_i^m) using [40]:

$$\gamma_i^m = \gamma_i \cdot x_A \tag{2.16}$$

Where x_A is the mole fraction of the solvent.

2.3.2 Osmotic coefficient

The osmotic coefficient (ϕ) is a measure of the deviation of the solvent from the ideal behaviour. The usual definition of the osmotic coefficient is [43]:

$$\phi = \frac{-\ln a_A}{M_A \cdot (\nu_+ + \nu_-) \cdot m_{XY}} = -\ln\left(x_A \ \gamma_A\right)\frac{x_A}{1 - x_A} \tag{2.17}$$

where a_A is the activity of the solvent (A), M_A is the molecular weight of the solvent, m_{XY} is the molality of the salt (XY) and γ_A is the mole fraction based activity coefficient of the solvent assuming full dissociation.

Osmotic coefficient can be measured using various methods such as freezing point depression, boiling point elevation and the isopiestic method [40]. It can be calculated from either the difference between the measured freezing point and that expected for an ideal solution, or from differences in boiling temperatures [40]. In the isopiestic method [44] the solvent activity of a sample is determined by placing the sample in equilibrium with a reference solution of known solvent activity. After several days or weeks (when equilibrium is reached between the two samples), the masses of the samples are measured to determine the amount of water in each (salt doesn't evaporate). The solvent activity of the reference salt solution is a known function of the salt concentration. At equilibrium, the water activities in both samples will be equal, therefore, the water activity of the salt solution under study will be known.

As mentioned above, it is important to note also that the osmotic coefficient is directly related to the molality-based activity coefficient through the Gibbs−Duhem relation [45]; i.e.:

$$\phi = 1 + \frac{1}{m_{XY}} \int_0^{m_{XY}} m \frac{\partial ln\left(\gamma_{\pm}^{m}\right)}{\partial m_{XY}} dm_{XY} \qquad (2.18)$$

2.3.3 Vapour-liquid equilibrium (saturation pressure)

A very common datatype is the measurement of the bubble point of salt-containing solutions. Both bubble pressures as bubble temperatures can be measured. In the range of temperature of interest only the solvents are considered to evaporate, and the salts remain in the liquid phase. The saturation pressure is calculated with a flash algorithm, using the following Rachford-Rice equation to be solved:

$$\sum K_i x_i = 1 \text{ with } K_i(P) = \frac{y_i}{x_i} = \frac{{\varphi_i}^L(P)}{{\varphi_i}^V(P)} \qquad (2.19)$$

Where K_i is the partition coefficient, ${\varphi_i}^L$ and ${\varphi_i}^V$ are the liquid and vapor fugacity coefficients respectively, x_i and y_i are the molar fraction in the liquid and vapor phase respectively. In the case of an equation of state calculation, ions are considered absent from de vapor phase ($\varphi_{ions}^{V} = 0$), then $K_i = 0$. The sensitivity of this property to the salt-related parameters of the model is quite small, compared with the mean ionic activity coefficient and the osmotic coefficient [28].

2.3.4 The enthalpy of solution [28]

The molar enthalpy of solution refers to the change of enthalpy when a certain quantity of solute (XY) is mixed with the solvent (A). Experimentally it is obtained by slowly adding a salt to the solution (that is initially pure), and measuring the heat required to maintain a constant temperature with a calorimeter. The molar enthalpy of solution (h^{sol}) may be expressed as:

$$h^{sol} = \frac{H - \left(n_A h_A^* + n_{XY} h_{XY}^{*,S}\right)}{n_{XY}} \qquad (2.20)$$

where the total enthalpy of the solution, H, is written as the sum of number of moles times the partial molar enthalpies ($\bar{h}_i$) of the compounds [28]:

$$H = n_A \bar{h}_A + n_{XY} \bar{h}_{XY} = n_A\left(h_A^* + \bar{h}_A^E\right) + n_{XY}\left(h_{XY}^{\infty} + \bar{h}_{XY}^{E'}\right) \qquad (2.21)$$

Here, h_A^* is the molar enthalpy of pure solvent *A* (which is the reference state enthalpy of the solvent), $\bar{h}_A^E$ is the excess partial molar enthalpy of the solvent *A*, h_{XY}^{∞} is the molar enthalpy of solute (salt XY) at infinite dilution (which is the reference state enthalpy of the solute), $\bar{h}_{XY}^{E\prime}$ is the excess partial molar enthalpy of solute in the asymmetric convention. In equation (2.20), the enthalpy difference is divided by the amount (number of moles) of salt added. Hence:

$$h^{sol} = \frac{n_A\bar{h}_A^E + n_{XY}\left(h_{XY}^{\infty} - h_{XY}^{*,S} + \bar{h}_{XY}^{E\prime}\right)}{n_{XY}} = \frac{n_A\bar{h}_A^E + n_{XY}\bar{h}_{XY}^{E\prime}}{n_{XY}} + \left(h_{XY}^{\infty} - h_{XY}^{*,S}\right)$$
$$= \frac{(n_A + n_{XY}) * h^{M\prime}}{n_{XY}} + \left(h_{XY}^{\infty} - h_{XY}^{*,S}\right) = \frac{h^{M\prime}}{x_{XY}} + \left(h_{XY}^{\infty} - h_{XY}^{*,S}\right) \qquad (2.22)$$

Where the prime (') refers to the asymmetric convention. The asymmetric mixing enthalpy is written as:

$$h^{M\prime} = x_A\bar{h}_A^E + x_{XY}\bar{h}_{XY}^{E\prime} \qquad (2.23)$$

The partial molar excess enthalpy can be obtained from the activity coefficient using Gibbs-Helmholtz as:

$$\bar{h}_A^E = \bar{h}_A - h_A^* = -RT^2\left.\frac{\partial ln\,\gamma_A}{\partial T}\right|_N \qquad (2.24)$$

In the case that an asymmetric activity coefficient is used (electrolyte systems), the excess partial molar enthalpy ($\bar{h}_{XY}^{E\prime}$) can be calculated as:

$$\bar{h}_{XY}^{E\prime} = \bar{h}_{XY} - h_{XY}^{\infty} = -RT^2\left.\frac{\partial ln\,\gamma_{XY}{}'}{\partial T}\right|_N \qquad (2.25)$$

and hence

$$\frac{h^{M\prime}}{RT^2} = -\left(x_A\left.\frac{\partial ln\,\gamma_A}{\partial T}\right|_N + x_{XY}\left.\frac{\partial ln\,\gamma_{XY}{}'}{\partial T}\right|_N\right) \qquad (2.26)$$

Furthermore, most of the data available correspond to highly dilute solutions ($x_A \approx 1$ and therefore $\gamma_A \approx 1$). Therefore, combining equations (2.22) and (2.26), one finds:

$$h^{sol} \approx -x_{XY}RT^2\left.\frac{\partial ln\,\gamma_{XY}{}'}{\partial T}\right|_N + \left(h_{XY}^{\infty} - h_{XY}^{*,S}\right) \qquad (2.27)$$

Section 2.5.4 will show how to convert equation 2.27 in terms of molar based activity coefficient.

2.3.5 Apparent molar volume

Equations of state are based on molar volume. Many authors have developed their equation without considering this property, because it is of less importance for process applications, but it decreases the theoretical foundation of their model (and therefore its predictive capacity). In this work, a special attention is paid to this property. While the density of a salt solution increases with salinity, which means that its specific volume decreases, the molar volume in reality goes up (Figure 9). This is because the apparent molar volume ($v_{\pm}$) of the salt is larger than that of water. This property is defined as:

$$v_{\pm} = \frac{(v - x_A v_A)}{(x_+ + x_-)} \qquad (2.28)$$

where v and v_A are the molar volumes of the solution and of the solvent respectively, and x_+ and x_- are the mole fractions of the cation and the anion. In practice, it is impossible to differentiate the contribution of separate ions, and hence the subscript ± is used to denote the overall apparent molar volume of the salt. The apparent molar volume (AMV) expresses the change in the volume of the solution when a salt is added. Figure 9 shows that this property changes fast with mole fraction, pointing to the fact that it is much more sensitive than the molar volume.

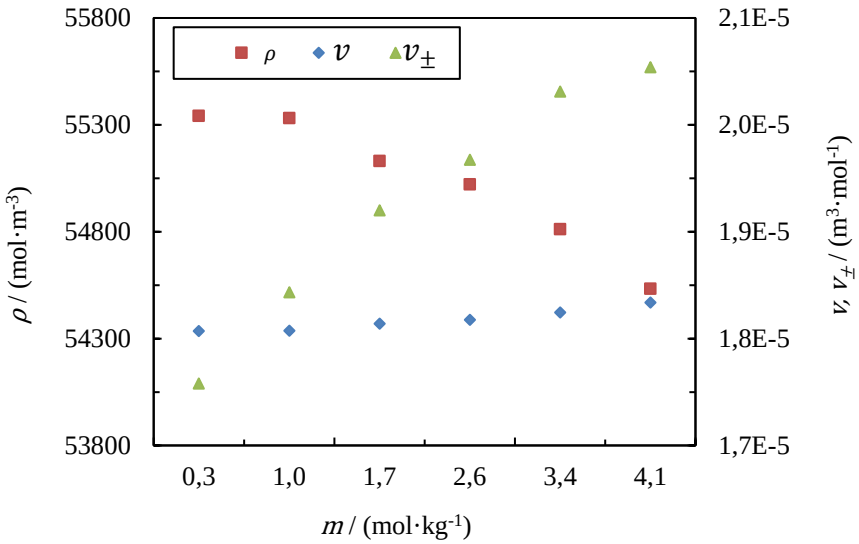

Figure 9 : Molar density ρ, molar volume v and apparent molar volume $\mathbf{v}_{\pm}$ as a function of NaCl concentration at 298 K [46, 47].

2.4 Data collection

Using the Detherm database (2018 release), a database with more than 5800 data points was created, including: mean ionic activity coefficient (MIAC), osmotic coefficient, vapor-liquid equilibrium (VLE), enthalpy of solution and apparent molar volume (AMV). In order to choose the raw data to be considered in the database, all available series for each property were plotted directly in Detherm as a function of concentration, as shown in Figure 10. The series showing a consistency between different authors were chosen. For example, in Figure 10 data with empty symbols were rejected, because they showed different behaviour than the rest of the experimental data.

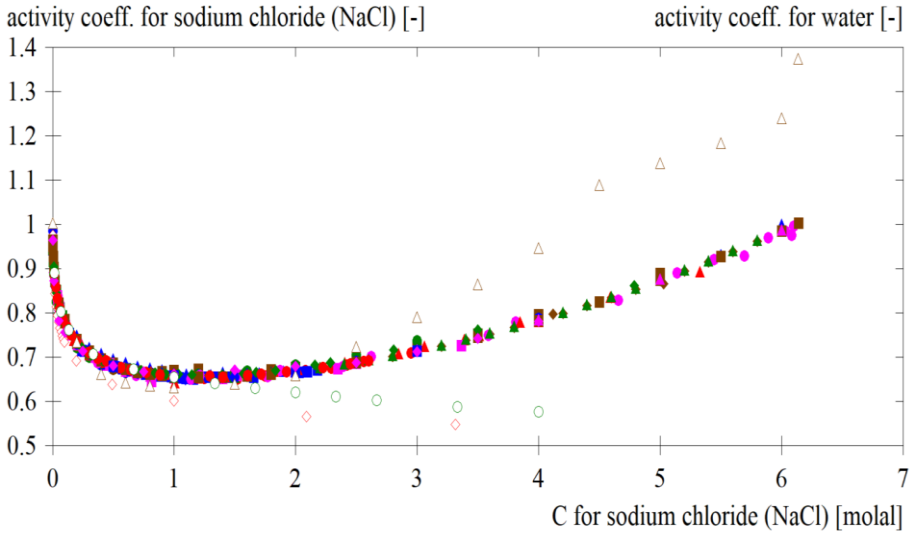

Figure 10: A screenshot of the comparison of experimental mean ionic activity coefficient data ($\gamma_{\pm}^{m}$) in function of the salt concentration (m) for aqueous NaCl at 298.15 K using Detherm database (2018 issue).

The same procedure was used to select data for 20 alkali-halides salts. All data used in the present study are for aqueous solutions, and not mixed solvents. Note that for the same temperature there are several data series (different colors in Figure 10). To choose which data series to use, the concentrations were compared, and the series with the highest concentration data was chosen. This procedure was repeated for all temperatures.

The solubility limit of NaCl as a function of temperature is shown in Figure 11. In this graph, the maximum molality found in experimental data analyses for activity coefficients, osmotic coefficients, VLE (saturation pressure), apparent molar volume and enthalpy of solution is also represented. Figure 11 shows that for NaCl, osmotic coefficient data can be found essentially up to the solubility limit in the full range of temperatures. For the activity

coefficients ($\gamma_{\pm}^{m}$), data are available up to 473 K, while for the osmotic coefficients (ϕ), the highest reported temperature is 573 K. Saturation pressure (P^{σ}) data are available over the entire temperature and concentration range. Apparent molar volume ($v_{\pm}$) and enthalpy of solution (h^{sol}) are found at low temperatures. For the enthalpy of solution data were found up to 6 molal, but only at low temperature.

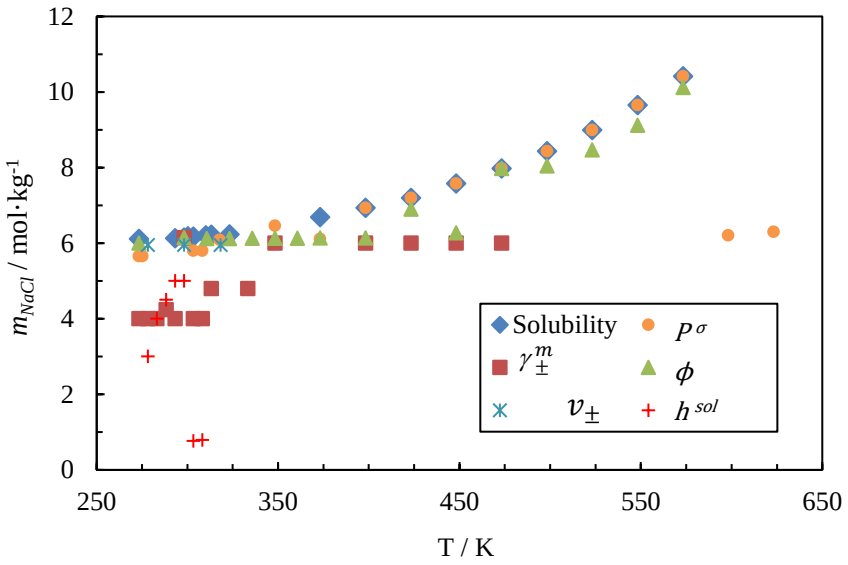

Figure 11 : Maximum molality of available data compared to the solubility limit of NaCl [28]. $\gamma_{\pm}^{m}$ is the activity coefficient, ϕ is the osmotic coefficient, P^{σ} is the saturation pressure, $v_{\pm}$ is the Apparent molar volume and h^{sol} is the enthalpy of solution.

In order to provide a complete picture of the database, Figure 12 present a summary of the database created for all the monovalent salts, showing the same type of graph presented for NaCl (Figure 11).

NaCl is the salt for which the most data is available in the literature. However, no data for all properties were found until saturation for elevated temperatures. The solubility behaviour of salts varies greatly from one salt to another. These changes may be related to a change in the crystalline structure of the salts [28]. Figure 12 shows that the solubility of salts in water increases with temperature except for LiF and NaF. Lithium fluoride (LiF) is the only salt without any data related to activity coefficients: this salt is very insoluble in water. The maximum molality of LiF in water is 0.05 M.

The mean ionic activity coefficient data (activity data for salts) are less abundant than the osmotic coefficient data (activity data for the solvent). Although there is a lot of osmotic coefficient data, it is not found until saturation concentrations at high temperatures. In general, mean ionic activity coefficient data is found for a temperature of 298.15 K. In many cases the

data for the osmotic coefficient are found at higher temperatures and concentrations than for the MIAC. The mean ionic activity coefficient and osmotic coefficient data really refer to the same reality: they can be transformed into one another using Gibbs−Duhem relation (equation (2.18)) . Saturation pressure data (VLE data) is the most abundant, especially at high temperatures. Finally, for enthalpy of solution and apparent molar volume (AMV), data are scarce and only found at low temperatures and low salt concentrations, except in some cases such as NaCl, KBr and KF.

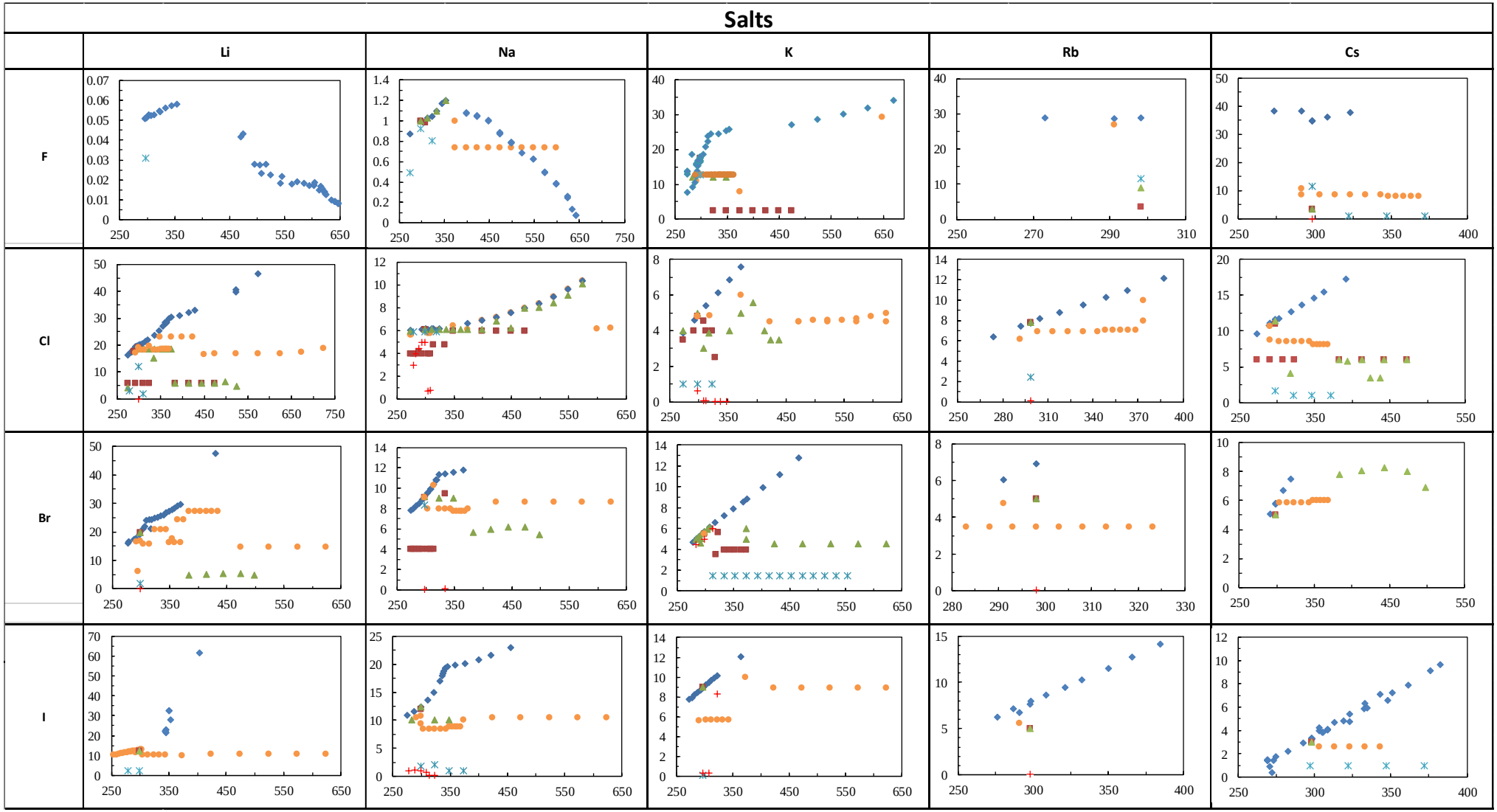

Figure 12: Variation of the solubility with temperature for different salts. On these graphs, the X-axis represent temperature (in K), and the Y-axis represent the maximum molality found for each property studied. The blue diamonds are maximum solubility of the salts in water, the red squares represents the maximum molality found in experimental data of mean ionic activity coefficient ($\gamma_{\pm}^{m}$); the orange circles represents the maximum molality found in experimental data of vapour pressure (P^{σ}); the green triangles are the maximum molality found in experimental data of osmotic coefficient (ϕ); the light blue asterisks represent the maximum molality found in experimental data of the apparent molar volume ($v_{\pm}$) and the red crosses represents the maximum molality found in experimental data of the enthalpies of solution (h^{sol}).

2.5 On the different behaviour of salts

2.5.1 Influence of the salt concentration

Considering the importance of the mean ionic activity coefficient in the study of electrolyte systems, it is important to investigate and understand their behaviour according to the nature of the salts. Figure 13 shows the mean ionic activity coefficient curves for aqueous NaCl at different temperatures. At fixed temperature, it shows first a decrease, attributed to the electrostatic forces (ion-ion interactions), then an increase, related to the increase of the ion-solvent interactions (what is called 'solvation') [28]. This increase may be more or less pronounced depending on temperature and salt considered. It is worth noting that the experimental data presented in Figure 13 were obtained through analytical expression derived from experimental data between 298.15 and 373.15 K, for more details see Gibbard et al. [48].

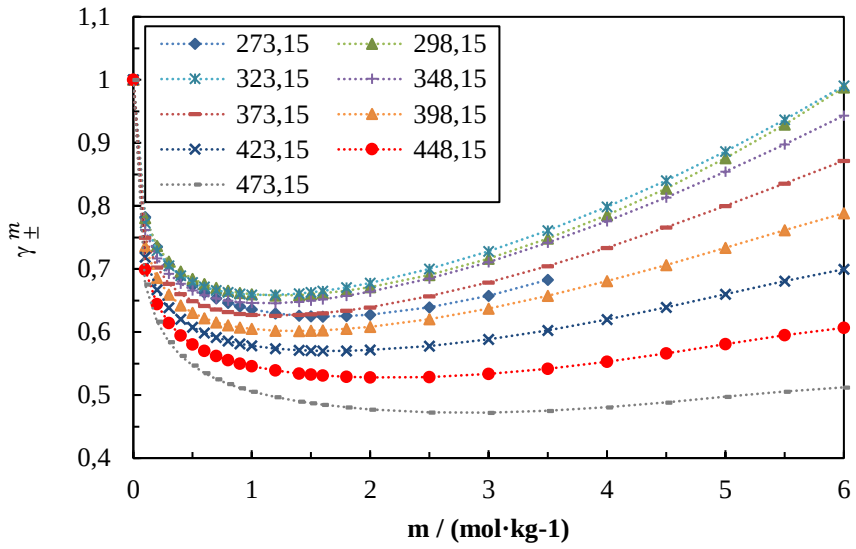

Figure 13 : Experimental mean ionic activity coefficient data for NaCl at different temperatures [48]. The experimental data were obtained through analytical expression and are presented with dotted lines in order to have a better view and interpretation of the variation (mainly at low temperatures).

In some cases, the mean ionic activity coefficient increases strongly, whereas, with other salts, the increase is not notorious. The experimental mean ionic activity coefficient representation of all the monovalent salts in pure water at 298.15 K is shown in Figure 14. The activity coefficient of some salts like a LiI, NaCl, KF, NaI increases at high concentration of salt, which indicates that the ions making up these salts are highly solvated with water. On the other hand, the activity coefficient of some salts like a CsCl or RbBr remains almost constant

after 1 molal. These salts have weak solvation interactions with water, which may lead to more ion pairs as indicated by some authors [49, 50].

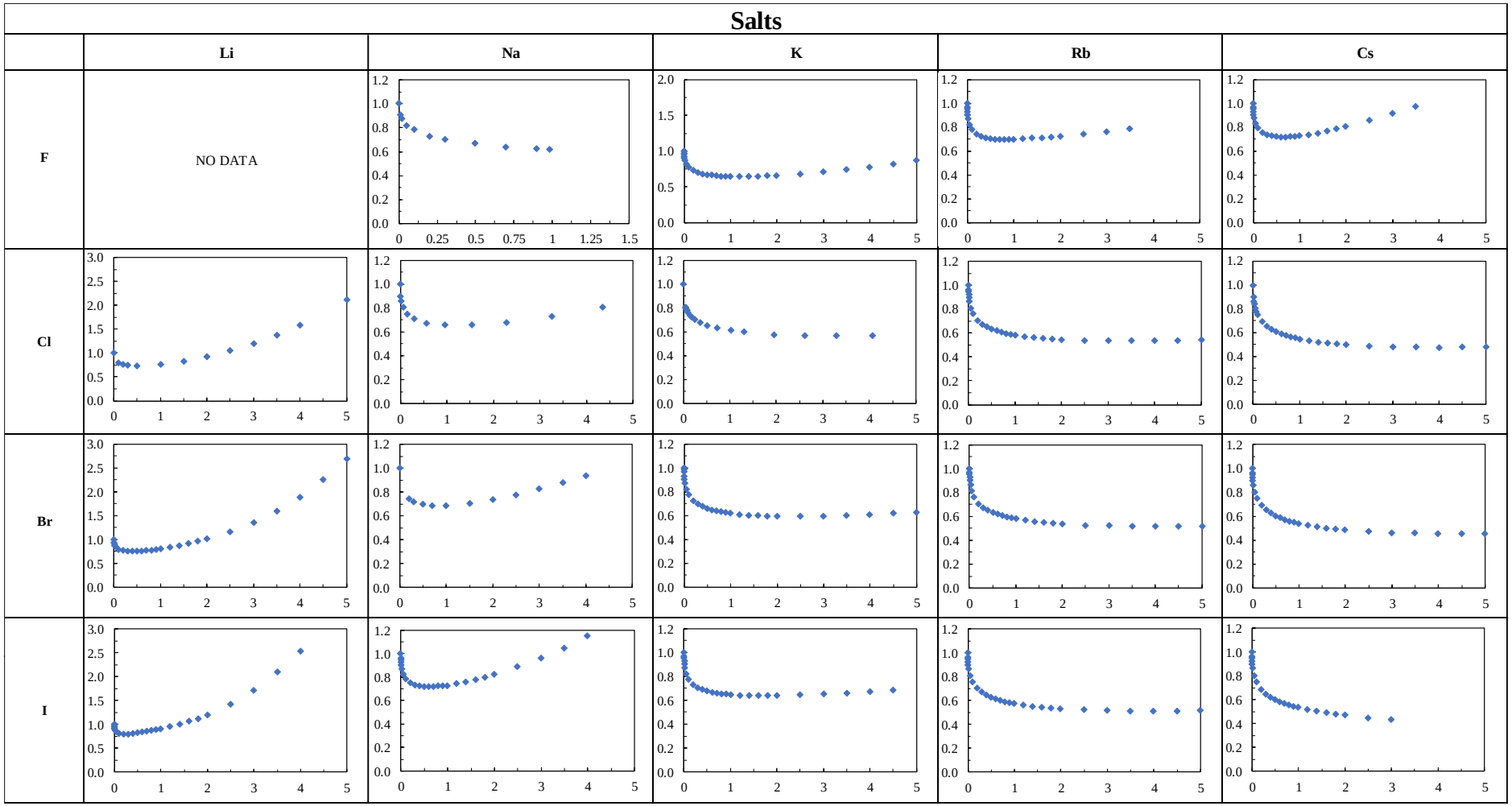

Figure 14: Variation of the experimental mean ionic activity coefficient ($\gamma_{\pm}^{\boldsymbol{m}}$) with molality for different salts. The x axis refers to the molality and the y axis to the mean ionic activity coefficient.

2.5.2 Influence of the ion diameter

In the study realized by Vaque Aura [28], it was shown that the increase in MIAC can be associated with the solvation forces of the ions (ion-water interactions). Figure 15 exhibits the relationship that exists between the parametron B of the Bromley model (correlating the increase in MIAC for each salt [28]) and the difference in the diameter of the ions that form each salt.

The salts that show a large value of activity coefficient at high salinity (Figure 14) have a high B (Figure 15). In contrast, the salts that are close to zero ($B = 0$ kg/mol), are those whose mean ionic activity coefficient remain small in Figure 14.

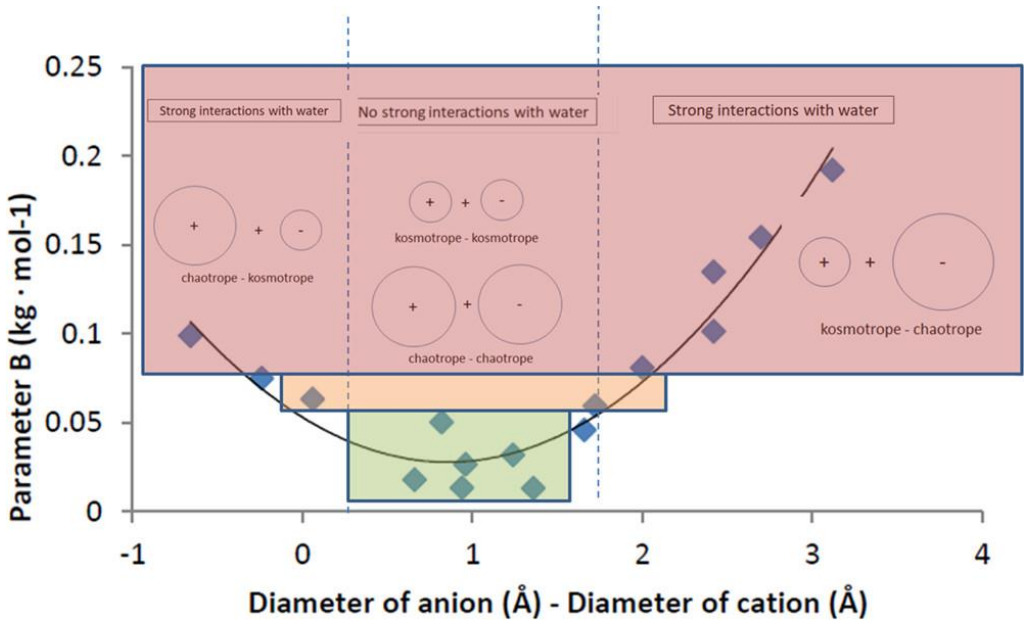

Figure 15: Variation of the parameter B (Bromley model) with the difference of anion and cation diameters. Color code: red, strongly hydrating salts; green, salts with little hydration; and orange, intermediate.

In Figure 15 a clear trend is observed: the smaller the difference between the diameters of the ions, the smaller the value of the parameter B. A study by Collins et all. [52], suggests that ions of the same size tend to stay together, while ions with different sizes prefer to be farther apart. Therefore, the solvation forces for this last type of salts are higher. This phenomenon is explained by Collins [52] using the Law of Matching Water Affinities (LMWA). That law states that there is a different effect on the solvation of ions depending on their charge and their size. According to Collins, small ions (with high charge density) are considered kosmotropes (strongly hydrated ions). In contrast, the big monovalent ions (low charge density) are weakly

hydrated ions and called chaotropes. The combination of two small or two large ions results in an increased trend of ion pairing.

2.5.3 Variation of the mean ionic activity coefficient with the temperature

The trend of the mean ionic activity coefficient with composition and temperature has recently been discussed by some authors [28, 53]. They observed that the temperature behaviour of the activity coefficient is not monotonous. Figure 16 shows on the example of NaCl that the mean ionic activity coefficient curves, increase with increasing temperature up to 323.15. Then as the temperature continues to increase these curves decrease.

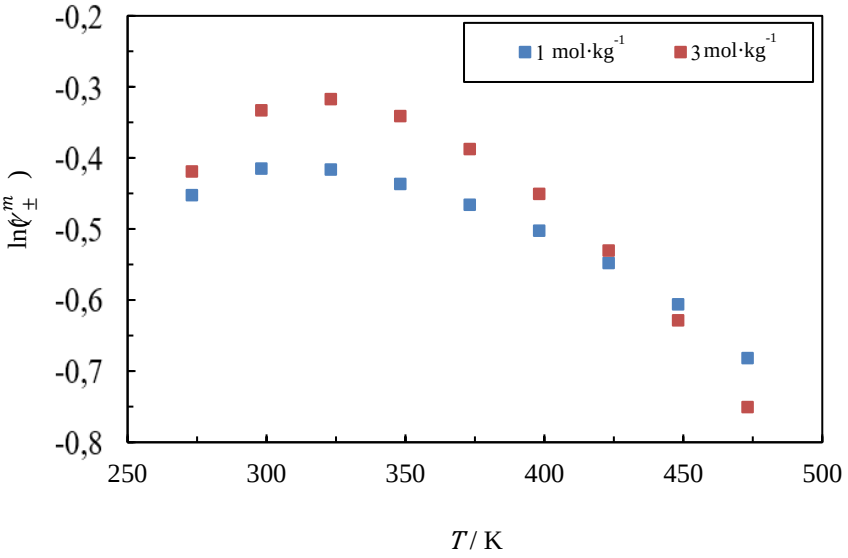

Figure 16 : Variation of the natural logarithm of experimental mean ionic activity coefficient ($\ln(\gamma_{\pm}^{m})$) with temperature at fixed molality. Blue curve is 1 molal NaCl concentration; red curve is 3 molal NaCl concentration.

Figure 16 shows the variation of the natural logarithm of the mean ionic activity coefficient with respect to temperature at different concentrations. As can be observed in the figure, there is a maximum at 323.15 K. The same behaviour is observed at 1 and 3 molal. However, it is important to note that the increase is higher at 3 molal than at 1 molal. This behaviour has an impact on the calculation of the enthalpy of solution as will be discussed below (section 2.5.4).

Similar results were found by Vaque et all. [28] when studying the experimental data using the adjustable parameter *B* of the Bromley model. Figure 17 shows the results found by Vaque et al. [28]. As it can be seen, various types of behaviours for the 20 salts exist, and this

does not allow to make a general conclusion. It can nevertheless be noticed that a similar behaviour is found for the salts NaBr, KBr and CsCl, in which a maximum appears. Other salts such as LiCl, KF and LiBr exhibit a continuous decrease of the mean ionic activity coefficient with respect to temperature. This type of variation of the mean ionic activity coefficient can also be linked to solvation interactions. As the temperature increases, the solvation becomes weaker, leaving free ions, which may favour the appearance of ion pairs.

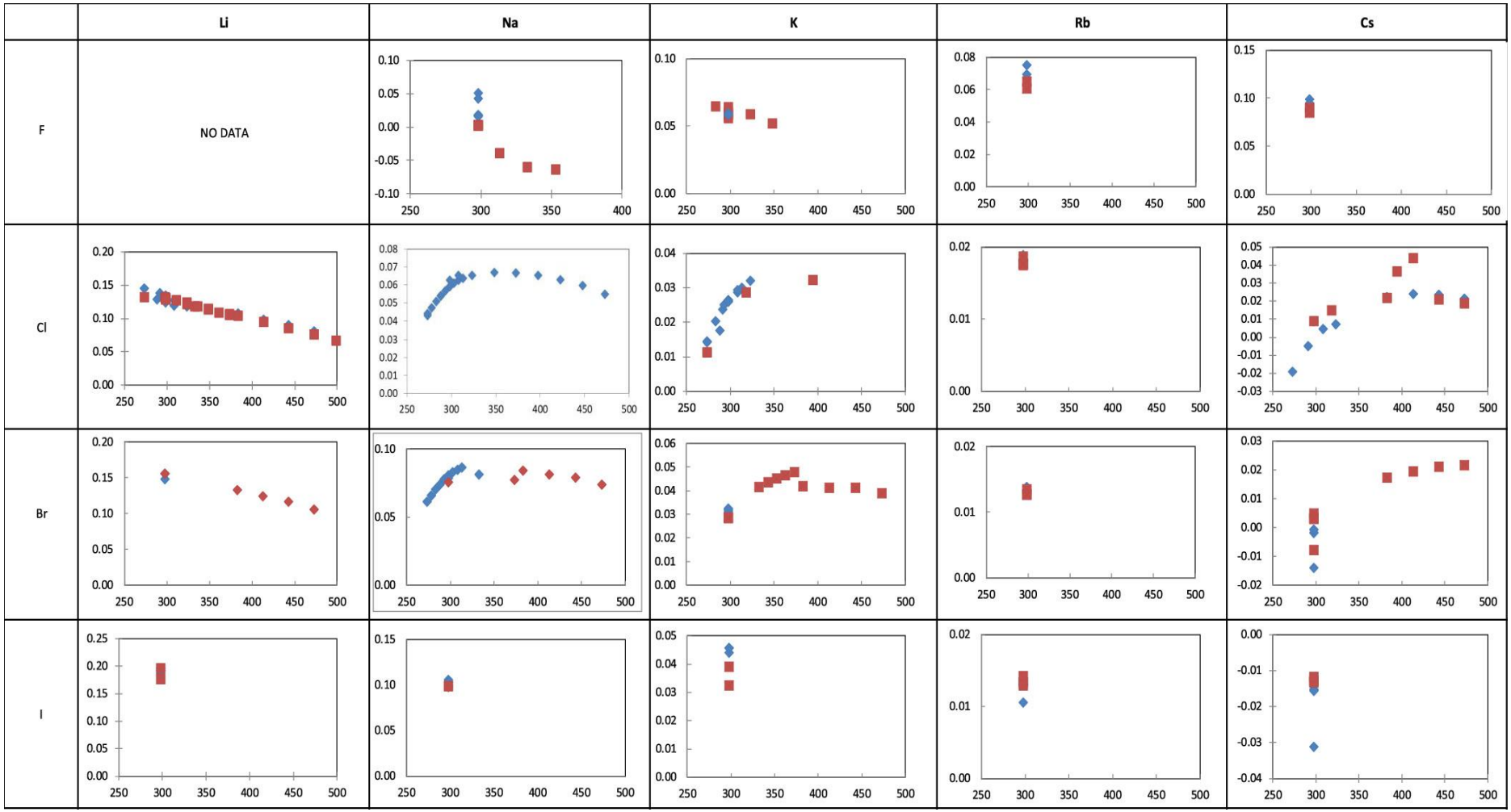

Figure 17 : Variation of parameter B of the Bromley model adjusted to the activity coefficient and the osmotic coefficient at different temperatures for different salts. The X axis shows the temperature (K), and the Y axis shows the value of B in kg/mol. The blue diamonds are obtained from mean ionic activity coefficients, and the red squares are from osmotic coefficients [28].

2.5.4 The enthalpy of solution and its relationship with the variation of mean ionic activity coefficient with temperature

As mentioned above, there is a relationship between the variation of the mean ionic activity coefficient with respect to temperature and the behaviour of the enthalpy of solution. To show the connection it is necessary to transform the expression of the enthalpy of solution (equation (2.27)), in terms of the mean ionic activity coefficient in molar basis (the form in which the experimental data are presented).

In order to transform the enthalpy of solution (equation (2.27)) in terms of the mean ionic activity coefficient $\left(\gamma_{\pm}^{m}\right)$ it is necessary to use equation (2.16), and to use the equivalence between the activity of the salt and that of the ions (i.e., $m_{XY}\,\gamma_{XY}^{m} = m_X\gamma_{\mathrm{X}}^{\mathrm{m}} \cdot m_Y\gamma_{\mathrm{Y}}^{\mathrm{m}}$ for a 1:1 salt) [49], which yields $\gamma_{XY}{}' = \frac{m_{XY}}{x_A}\left(\gamma_{\pm}^{m}\right)$. The enthalpy of solution is thus obtained as:

$$h^{sol} = -2RT^2\,\frac{m_{XY}}{x_A}\left.\frac{\partial ln\gamma_{\pm}^{m}}{\partial T}\right|_N + \left(h_{XY}^{\infty} - h_{XY}^{*,S}\right) \qquad (2.29)$$

or, in other words, the enthalpy of solution is the result of a sum of a constant term $\left(h_{XY}^{\infty} - h_{XY}^{*,S}\right)$ and a term related to the change in the MIAC with temperature ($\left.\frac{\partial ln\gamma_{\pm}^{m}}{\partial T}\right|_N$).

In Figure 18 the enthalpy of solution [54] as a function of salinity is shown. It can be seen that it is not zero in the limit of pure solvent:

$$\lim_{x_{XY}\to 0}\left(h^{sol}\right) = \lim_{x_{XY}\to 0}\left(\frac{h^{M'}}{x_{XY}}\right) + \left(h_{XY}^{\infty} - h_{XY}^{*,S}\right) \qquad (2.30)$$

In addition, this limit is not equal to the heat of solution $\left(h_{XY}^{\infty} - h_{XY}^{*,S}\right)$, because $\lim_{x_{XY}\to 0}\left(\frac{h^{M'}}{x_{XY}}\right) \neq 0$.

As suggested by Vaque Aura [28], an interpolation of the enthalpies at infinite dilution as a function of temperature was proposed:

$$\lim_{x_{XY}\to 0}\left(h^{sol}\right) = aT^2 + bT + c \qquad (2.31)$$

where *a*, *b* and *c* are empirical parameters.

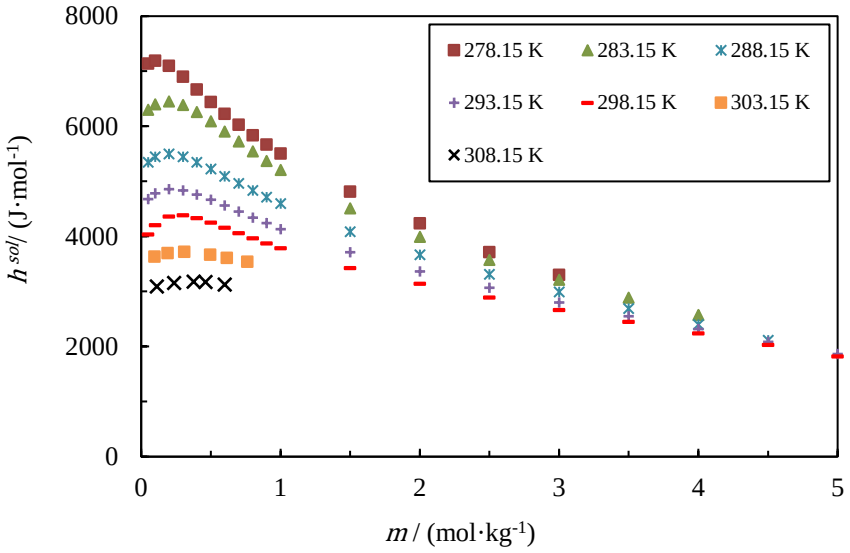

Figure 18 : Experimental molar enthalpy of solution of aqueous NaCl [54] at different temperatures.

Thus, when the enthalpy of solution decreases with composition, as observed in the largest part of the composition range above 0.2 molal (see Figure 18), the slope of the activity coefficient with temperature $\left(\frac{\partial ln\gamma_{\pm}^{m}}{\partial T}\Big|_{N}\right)$ is expected to increase. As can be seen in Figure 16, in the lower temperature range (below 308 K), the slope is slightly more positive in the case of 3 molal concentration than in the 1 molal case. This behavior is directly related to the behavior of the enthalpy of solution. The larger the slope (which is equal to the derivative of ln(MIAC) with respect to temperature) the lower the value of the enthalpy of solution. This shows that there is a correlation between these two properties.

Very few authors use this property since it is very difficult to catch the low temperature increasing trend of mean ionic activity coefficient correctly.

2.6 Conclusion

The main concepts for the calculation of phase equilibria, as well as the two main concentration units used in the study of electrolytic systems (molality and mole fraction), have been defined. The properties that we will use in this study have also been defined: mean ionic activity coefficient, osmotic coefficient, apparent molar volume, enthalpy of solution and saturation pressure. In addition, a summary of the database that was created for this study was presented. 20 different monovalent salts were included in the database. It was found that only NaCl is fully documented. For most salts the experimental data for the mean ionic activity

coefficient was found at 298 K. However, experimental data for the osmotic coefficient were found at higher temperatures and concentrations. Since both properties are related, the osmotic coefficient can be converted into the mean ionic activity coefficient.

The different trends of the mean ionic activity coefficient (MIAC) with respect to the variation of the salt concentration were presented. Two types of behaviour were observed. Firstly, salts for which the MIAC increases with concentration. Secondly, salts for which the MIAC remains almost constant after 1 molal. The differences are explained in literature by the competition between ion-water and cation-anion interactions. It was shown how the difference in ion diameters has an impact on the preference of the ions to be surrounded by water molecules (solvation), or to form dimers (ion pairs). Ions with similar sizes prefer to stay as dimers, while ions with different sizes prefer to interact with water molecules.

Concerning the behaviour of the MIAC of salts with respect to temperature, no clear trend can be observed, each salt having a particular behaviour. It was shown that the dependency of the MIAC with temperature is directly related to the enthalpy of solution.

These characteristic behaviours of each salt can be considered as a representation of the physics of the electrolytic solutions. These observations will be used later as a basis for comparison of different models. The aim will be to find out if the models studied are able to reproduce such behaviours. A connection can be made between the physics of the electrolyte solutions and the results of the models.

Chapter 3 Theoretical framework of statistical associating fluid theory (SAFT) equations of state

3.1 Introduction

The prediction or correlation of thermodynamic properties and phase equilibrium with equations of state remains an important goal in chemical and related industries. Although the use of equations of state has for a long time been restricted to systems of simple fluids, there is an increasing demand for models that are also suitable for complex and macromolecular compounds, and more recently for electrolyte systems. The electrolyte systems are characterized by having chemical species that dissociate spontaneously into ions [55]. These systems are strongly non-ideal. Ionic species feature electrostatic interactions that must be modelled with specific models, in addition to the usual short-range interactions.

Industrial approaches are most often based on activity coefficient models (Pitzer, eNRTL, eUNIQUAC, MSE – [32, 33, 35, 56]). None of these models is truly predictive. In contrast, using for example group contribution approaches, the SAFT family equations of state have shown to be well suited to predict properties of neutral molecules, including very polar ones [57, 58]. This is why we will focus on these types of equations in this work.

Several authors have developed equations of state capable of making calculations with electrolyte systems [59–62]. Among these equations, the most well-known ones are cubic [63, 64], but the more recent publications concern either CPA (Cubic Plus Association) [65] or SAFT (Statistical Associating Fluid Theory) [10]. All these equations are able to take into account the effects of pressure and non-ideality in the composition. However, their ability to model multi-solvent electrolyte systems is limited [38].

In the most fundamental form, an equation of state can be constructed using a minimum of two terms. One that describes the molecular repulsion and contains a parameter that reflects the molecular volume. The second describes attraction and contains a parameter that reflects the intermolecular potential [27]. In the case of the CPA and SAFT equations of state other

terms have been added to these two, in order to have an equation of state that can represent and make predictions of thermodynamic properties of complex systems. When ionic species are present in a solution, the positive and negative ions will interact electrostatically. Increasing the salt concentration increases the ion interactions in a way that depends on the dielectric constant of the solution. Several models used for modeling electrolytic systems depend on the dielectric constant, therefore special attention must be paid to this property. When the dielectric constant is large, the effect of the ions is smaller because of the screening effect of the solvent molecules.

In this section the construction of a SAFT type equation of state is presented. To this end, it will start by introducing the main intermolecular interactions. Then the perturbation theory and the construction of an equation of state will be discussed. In chapters 3.4, 3.5 and 3.6 the main theories used to describe each of the interactions present in an electrolytic system will be presented. In chapter 3.7 the models that will be used to compute the dielectric constant of the electrolyte solutions will be also presented. Finally, in chapter 3.8 the state of the art of the equations of state for electrolytic systems will be discussed.

3.2 Intermolecular interactions

The behaviour of fluid systems is the result of forces that act on the molecules. For example, a liquid boils when enough thermal energy is supplied to the system to overcome the energy of the attractive interactions in the liquid, forming vapour bubbles. When the molecules separate, they move into the vapour phase, where the attractive interactions between the molecules are much smaller (unless the pressure in the system becomes very high). These forces are the result of potentials. In general, intermolecular forces can be divided into several categories. Figure 19 illustrates the most important ones.

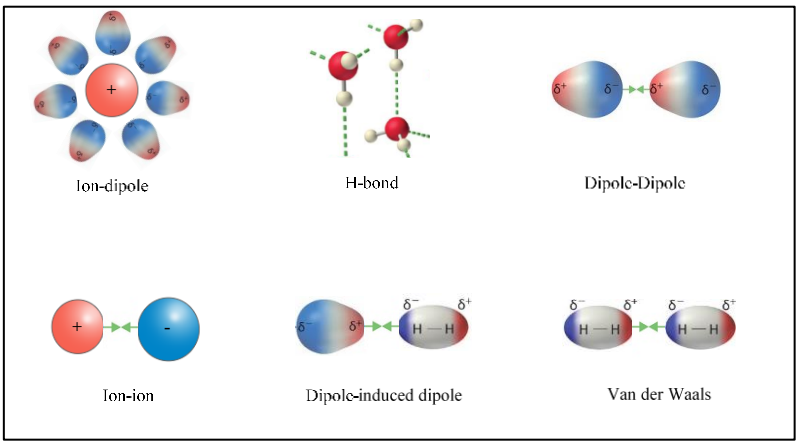

Figure 19 : Summary of the main interactions between the molecules.

The principal types of attractive interaction are:

Van der Waal's (London dispersion) forces: Are driven by induced electrical interactions between two or more atoms or molecules that are very close to each other. Van der Waals interaction is the weakest intermolecular attractions. These forces always operate in any substance.

Dipole-induced dipole Interactions: A dipole-induced dipole attraction is a weak attraction that results when a polar molecule induces a dipole in an atom or in a nonpolar molecule by disturbing the arrangement of electrons in the nonpolar species.

Dipole-dipole Interactions: Dipole-Dipole interactions result when two dipolar molecules interact with each other through space. When this occurs, the partially negative portion of one of the polar molecules is attracted to the partially positive portion of the second polar molecule. Substances whose molecules have dipole moment have a higher boiling point temperature than those of similar molecular mass, but whose molecules have no dipole moment.

Hydrogen bonds: It results from the attractive force between an electron donor atom such as N, O, or F and electron acceptors sites (H atom). Certain substances such as H_2O, HF, and NH_3 are well known to form hydrogen bonds, which affect the properties of the substance like solubility for example.

Ion-dipole Interactions: An ion-dipole interaction is the result of an electrostatic interaction between a charged ion and a molecule that has a dipole. It is an attractive force that is commonly found in solutions, especially ionic compounds dissolved in polar liquids.

Ion-Ion Interactions: Ion-ion interactions are electrostatic forces between ions. If the charges are opposite, then they may form ion pairs. In contrast, like charges repel each other. These forces (also called Coulombic) operate over long distances.

In a real fluid all these types of interactions can be present. Both attractive and repulsive forces act simultaneously. When ions are added to such fluids the structure of the solution changes because in addition to attraction and repulsion, ion-dipole and ion-ion long range interactions are present. This mixture of forces is the reason for the high complexity of modeling electrolyte systems.

As will be shown in the next chapter, the equations of state are derived from an expression of the Helmholtz free energy as a function of temperature, phase volume and phase composition [27]. Through statistical mechanics, it is possible to compute the Helmholtz free energy as a sum of two terms. One that represents the ideal gas that contains all kinetic and internal contributions to the energy, and one that contains only the potential energy and is called residual contribution.

3.3 Construction of an equation of state using the perturbation theory

An equation of state is constructed based on the Helmholtz energy which is a natural function of temperature, volume and number of particles. Through derivatives, all other properties can be obtained.

In general terms, the energy of the system is the sum of the kinetic and potential energy of all the components of the system at both the molecular and atomic levels. However, statistical thermodynamics focuses on the study of these energies at the molecular level. Therefore, only intermolecular interactions (presented above) and intramolecular interactions (extension, torsion, vibration, etc.) are taken into account. The main concepts of statistical thermodynamics and perturbation theory are presented below.

3.3.1 The partition function

The aim of an equation of state is to calculate thermodynamic properties from molecular properties. At the microscopic level, even at equilibrium, molecules continue to move, which is why multiple states are possible. Since there are multiple states, the probability of each one occurring must be included, hence the name statistical thermodynamics.

The calculation of thermodynamic properties is done on a canonical ensemble, which is the ensemble of N molecules at a known volume (V) and temperature (T). To calculate the internal energy (U) of a system it is necessary to calculate the average of the energy of all possible canonical ensembles, taking into account the probability that each one exists, as follows [66]:

$$U = \langle E \rangle = \sum_{i_{CE}} p_{i_{CE}}(E_{i_{CE}}) \cdot E_{i_{CE}} \qquad (3.1)$$

Where ⟨E⟩ is the mean of the total energy (E), $p_{i_{CE}}$ is the probability of finding the energy of the i_{CE} canonical ensemble and $E_{i_{CE}}$ is the energy of the i_{CE} canonical ensemble.

The probability is proportional to the energy of each ensemble, as follows:

$$p_{iCE} \ \alpha \ exp\left(-\frac{E_{i_{CE}}}{k_B T}\right) \tag{3.2}$$

Where k_B is the Boltzmann constant. To transform equation (3.2) into an equality the canonical partition function ($\mathcal{Q}$) is added. Furthermore, knowing that the sum of all probabilities is equal to one, we have:

$$\sum_{i_{CE}} p_{i_{CE}}(E_{i_{CE}}) = 1 = \frac{1}{\mathcal{Q}} \sum_{i_{CE}} exp\left(-\frac{E_{i_{CE}}}{k_B T}\right) \tag{3.3}$$

Thanks to equation (3.3) it is possible to know the canonical partition equation.

$$\mathcal{Q}(N,V,T) = \sum_{i_{CE}} exp\left(-\frac{E_{i_{CE}}(N,V)}{k_B T}\right) \tag{3.4}$$

Using equations (3.1), (3.3) and (3.4) it is possible to derive an equation for the internal energy in terms of the canonical partition [66]:

$$U = k_B T^2 \frac{\partial ln\mathcal{Q}}{\partial T}\bigg|_{V,N} \tag{3.5}$$

Entropy can also be calculated as a function of canonical partitioning, as follows [66]:

$$S = k_B ln\mathcal{Q} + \frac{U}{T} \tag{3.6}$$

From Equations 3.5 and 3.6 it is possible to derive an equation for Helmholtz free energy (A). Knowing that $A = U - TS$ we have:

$$A(N,V,T) = -k_B T ln\mathcal{Q}(N,V,T) \tag{3.7}$$

With equations 3.5, 3.6 and 3.7, it is possible to derive all the classical thermodynamic functions as a function of the canonical partition (calculated from microscopic information).

Note that A is proportional to the canonical partition function $\mathcal{Q}(N,V,T)$, and at the same time the variables on which A depends are the same as those on which $\mathcal{Q}$ depends. The canonical partition function is the central function of the statistical thermodynamics. While A can be

considered as the most important connection between thermodynamics and the canonical partition function. Thanks to the form of the $\mathcal{Q}$ function (equation (3.4)), the Helmholtz free energy can be calculated as the sum of the contributions of the different intermolecular interactions.

The energy of each ensemble $E_{i_{CE}}$, is obtained from the sum of the energies (ε) provided by each particle (j) in the i_{CE} canonical state, then:

$$E_{i_{CE}} = \sum_{j}^{N} \varepsilon_{i_{CE}j} \tag{3.8}$$

If several canonical states (i_{CE}, j_{CE} , k_{CE} , ...) are taken into account and equation (3.8) is used, equation (3.4) can be rewritten as follows [66]:

$$\mathcal{Q}(N,V,T) = \sum_{i_{CE}\cdots} exp\left(-\frac{\sum_{j}^{N} \varepsilon_{i_{CE}j}}{k_B T}\right) = \prod_{j}^{N}\left(\sum_{i_{CE}} exp\left(\frac{\varepsilon_{i_{CE}j}}{k_B T}\right)\right) = \prod_{j}^{N}(q_j) \tag{3.9}$$

Where

$$q_j(V,T) = \sum_{i_{CE}} exp\left(\frac{\varepsilon_{i_{CE}j}}{k_B T}\right) \tag{3.10}$$

Equation (3.9) shows that the canonical partition function can be calculated as the sum of independent terms. If the particles are distinguishable the calculation of $\mathcal{Q}$ reduces to the calculation of $q_j(V,T)$. Since $q_j(V,T)$ requires a knowledge only of the energy values of an individual particle.

If the energy states of all the particles are the same, equation (3.9) can be written as [66]:

$$\mathcal{Q}(N,V,T) = \left[q_j(V,T)\right]^N \tag{3.11}$$

Equation (3.11) can be used on the condition that all particles are distinguishable. However, in most cases the molecules are indistinguishable, this is taken into account by dividing by the number of possible permutations between these molecules. Thus, for indistinguishable molecules equation (3.11) can be written as:

$$\mathcal{Q}(N,V,T) = \frac{[q\,(V,T)]^N}{N!} \tag{3.12}$$

The function $q_j(V,T)$ is called molecular partition function. In most cases the energy of a state is a set of molecular energy states [ref]. In perturbation theory it is assumed that the energy of a molecule is the sum of independent contributions of the different energy forms that the particle possesses. For example, the translational (ε_t), rotational (ε_r), vibrational (ε_v), repulsive (ε_{rep}) and attractive (ε_{att}). From this hypothesis equation (3.11) can be written as:

$$\mathcal{Q}(N,V,T) = \frac{\left[q_t\, q_r q_v q_{rep} q_{att} \dots\right]^N}{N!} \tag{3.13}$$

If we write equation (3.13) in logarithmic form, we have:

$$ln\,\mathcal{Q}(N,V,T) = ln\,\mathcal{Q}_t + ln\,\mathcal{Q}_r + ln\,\mathcal{Q}_v + ln\,\mathcal{Q}_{rep} + ln\,\mathcal{Q}_{att} + \cdots$$

$$with \tag{3.14}$$

$$\mathcal{Q}_t = \frac{{q_t}^N}{N!}\ ;\ \mathcal{Q}_r = {q_r}^N\ ;\ \mathcal{Q}_v = {q_v}^N\ ;\ \mathcal{Q}_{rep} = {q_{rep}}^N\ ;\ \mathcal{Q}_{att} = {q_{att}}^N$$

Now that the expression for $ln\,\mathcal{Q}(N,V,T)$ is known, equation (3.7) can be rewritten as follows:

$$\frac{A}{Nk_BT} = \frac{A^t}{Nk_BT} + \frac{A^r}{Nk_BT} + \frac{A^v}{Nk_BT} + \frac{A^{rep}}{Nk_BT} + \frac{A^{att}}{Nk_BT} \tag{3.15}$$

3.3.2 The energy contributions

We now see that the energy can be written as a sum of energy contributions. The first three terms refer to the ideal gas, and the subsequent ones to what is called the 'residual' contribution

$$\frac{A}{Nk_BT} = \frac{A^{\#}}{Nk_BT} + \frac{A^{res}}{Nk_BT} \tag{3.16}$$

where $A^{\#}$ is the contribution to the Helmholtz free energy of the ideal gas (translational), A^{res} is the residual contribution to the Helmholtz free energy.

3.3.2.1 Ideal gas and internal energy contributions

It appears that in using equations of state, the most important properties are pressure (volume derivative of A) and chemical potential (mole number derivative of A). Neither the rotational nor the vibrational partition function contribute to these derivatives. They are therefore often neglected (they do have a temperature derivative, thus contributing to the thermal properties).

According to McQuarrie [66] the translational partition function (ideal gas) can be written as:

$$q_t = \left(\frac{2\pi \cdot mass \cdot k_B T}{h^2}\right)^{3/2} \cdot V = \frac{V}{\Lambda^3} \qquad (3.17)$$

Where mass is the molecular mass, h is the Planck's constant and Λ is the thermal De Broglie wavelength. The condition for the applicability of classical statistics is that Λ must be small compared to the dimensions of the container.

3.3.2.2 Other contributions: potential energies

For the calculation of the potential energy (intermolecular repulsion and attraction interactions), it is assumed that the total potential energy (U_P) is the sum of the potential energies derived from the interactions between pairs of molecules (u_{ij}).

$$U_P = \frac{N}{2}\sum_i \sum_j u_{ij} \qquad (3.18)$$

Note that the sum is multiplied by the number of molecules divided by two, since the same molecule is taken into account twice (once as a reference and once as a perturbation). Now the problem is reduced to the calculation of the potential energy between pairs of molecules.

According to McQuarrie [66], the potential energy can be calculated as follows:

$$u_{ij} = \int_0^\infty u(r_{ij})\rho(r_{ij}) 4\pi {r_{ij}}^2 \, dr_{ij} \qquad (3.19)$$

Where $u(r_{ij})$ is intermolecular potential, $\rho(r_{ij})$ is the probability that a molecule j can be found at the distance r_{ij} from molecule i.

Intermolecular potentials

The potential energy contributed by the intermolecular interactions between two molecules can be obtained through different functions called intermolecular potentials. The best known are: ideal gas, hard spheres, square well and Lenard Jones. Each of these potentials represents intermolecular interactions in a different way. Figure 20 shows each of these potentials.

Ideal gas potential:

$$u(r_{ij}) = \begin{cases} \infty & r_{ij} = 0 \\ 0 & r_{ij} > 0 \end{cases} \qquad (3.20)$$

In the perfect gas potential, the potential energy is infinite when the distance between the molecules is zero. In contrast, the potential energy is zero if there is a distance between the molecules.

Hard sphere potential:

The hard sphere potential is similar to the perfect gas potential, but in this case a volume is associated with the molecules. Therefore, the potential energy is infinite when the intermolecular distance (r_{ij}) is equal to σ_{ij}.

$$u(r_{ij}) = \begin{cases} \infty & r_{ij} < \sigma_{ij} \\ 0 & r_{ij} > \sigma_{ij} \end{cases} \qquad (3.21)$$

Where σ_{ij} closest distance between the centers of the molecules i and j, represented as hard spheres (mean diameter).

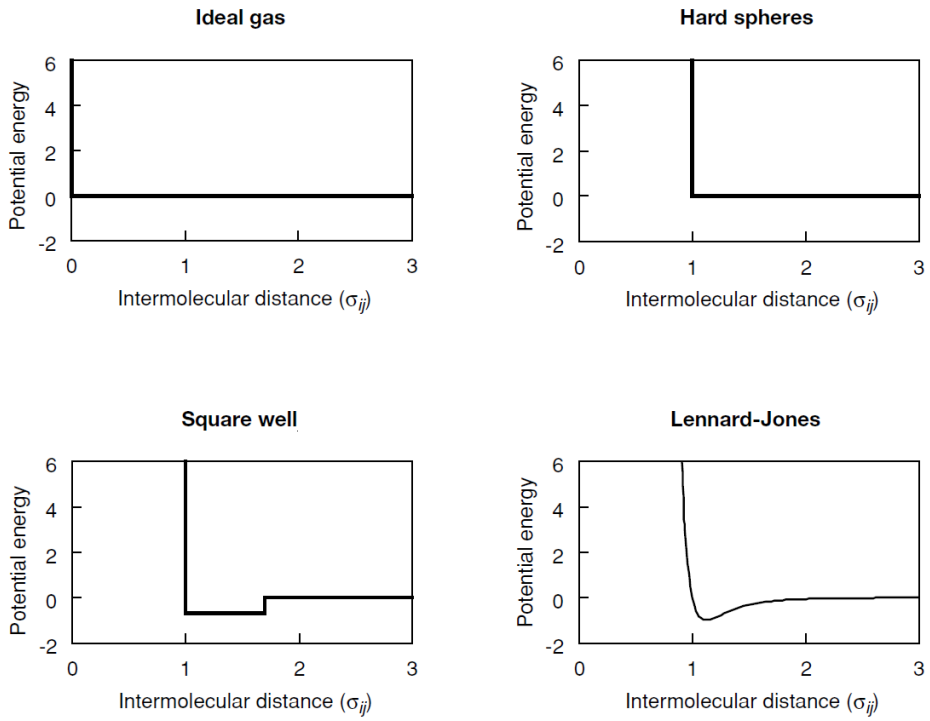

Figure 20 Molecular interactions (attraction and repulsion) of different models [27].

Finally, the Square Well and Lennard Jones potentials take into account the attraction energy generated by the interaction between two molecules, over a distance range. In the Lennard Jones potential, the potential energy varies as the molecules move away, while in the Square Well potential the potential energy is constant over the range (σ_{ij} to $\lambda\sigma_{ij}$).

Square Well potential:

$$u(r_{ij}) = \begin{cases} \infty & r_{ij} < \sigma_{ij} \\ -\varepsilon_{ij} & \sigma_{ij} < r_{ij} < \lambda\sigma_{ij} \\ 0 & r_{ij} > \lambda\sigma_{ij} \end{cases} \qquad (3.22)$$

Where λ is the reduced range of the attractive well, is usually taken to be between 1.5 and 2.0.

Lennard Jones potential:

$$u(r_{ij}) = 4\varepsilon_{ij}\left[\left(\frac{\sigma_{ij}}{r_{ij}}\right)^{12} - \left(\frac{\sigma_{ij}}{r_{ij}}\right)^{6}\right] \qquad (3.23)$$

Radial distribution functions

The second factor of the equation (3.19) is the probability function $\rho(r_{ij})$ which represents the local density of molecule j around molecule i. It can be calculated as:

$$\rho(r_{ij}) = \rho_j g_{ij}(r_{ij}) = \frac{N_j}{V} g_{ij}(r_{ij}) \qquad (3.24)$$

Where ρ_j is the density of the molecule j and $g_{ij}(r_{ij})$ is the radial distribution function of j surrounding i.

The radial distribution function represents the probability of finding a molecule j around molecule i at a distance r_{ij}. As an example, Figure 21 shows the radial distribution function for the Lenard Jones potential. As can be seen in the figure when the distance between the molecules approaches value slightly above σ_{ij}, the probability of the molecules interacting is maximal. In contrast, as the distance increases the probability of the molecules meeting decreases. Note that for $r_{ij}/\sigma_{ij} < 1$ the probability of finding another molecule is zero, this is because each molecule has an excluded volume. This type of distribution is calculated from molecular dynamics calculations [66].

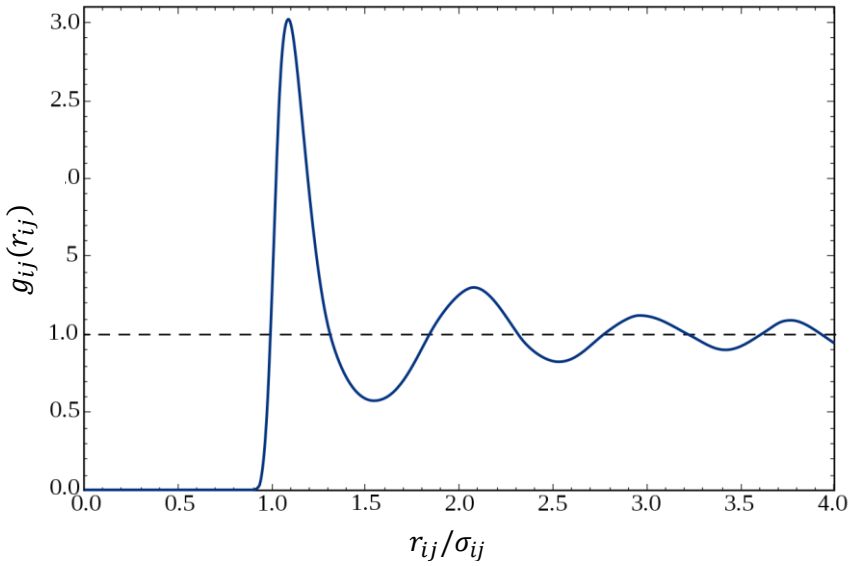

Figure 21 : Radial distribution function for the Lennard-Jones potential [66].

If equations (3.24) and (3.19) are replaced in equation (3.18) we obtain:

$$U = \frac{1}{2}\sum_i N_i \sum_j 4\pi \frac{N_j}{V} \int_0^\infty u(r_{ij}) g_{ij}(r_{ij})\, {r_{ij}}^2\, dr_{ij} \qquad (3.25)$$

Equation (3.25) is the basis for the calculation of the potential energies of the equations of state, to be used in the fundamental equation (3.7).

3.3.3 Perturbation expansion

Unfortunately, no model is capable of describing a real fluid. Only simplified fluids are known and can be approached through molecular simulation techniques. However, the thermodynamic perturbation theory proposes a way to correct a simple fluid in order to approach the behaviour of a more complex one. The principle of this theory is to divide the potential energy is divided in two parts. The first part is the reference (or simple) fluid for which an equation is available, and the second is the perturbation that approaches the real fluid.

$$u(r_{ij}) = u(r_{ij})^{(0)} + u(r_{ij})^{(1)} \tag{3.26}$$

Where $u(r_{ij})^{(0)}$denotes the reference potential energy (usually the hard sphere) and $u(r_{ij})^{(1)}$ is the potential energy of the perturbation. Using the Barker and Henderson high temperature expansion (based on a Square Well potential) it is found that [66]:

$$\frac{A}{Nk_BT} = \frac{A^{(0)}}{Nk_BT} + \frac{2\pi N}{Vk_BT}\int_0^\infty u^{(1)}(r_{ij})g_{ij}{}^{(0)}(r_{ij})\,r_{ij}{}^2\,dr_{ij} - \frac{\pi N}{Vk_BT}\int_0^\infty \left[u^{(1)}(r_{ij})\right]^2 g_{ij}{}^{(0)}(r_{ij})\left(\frac{\partial\rho}{\partial P}\bigg|_T\right)^{(0)} r_{ij}{}^2\,dr_{ij} + O(\beta^3) \tag{3.27}$$

Where the first term $A^{(0)}$ is the Helmholtz free energy of the reference fluid. The other terms are the perturbations that add to the reference. Note that the radial distribution is that of the reference state (0) and not that of the perturbed system (1). Equation 3.27 is the fundamental basis of the perturbation theory and is truncated in the fourth term. However, to calculate the true behavior of the solution it is necessary to go to an infinite number of terms. In practice, the expansion converges quickly and only the first order and sometimes the second order is considered. For polar terms, the convergence is very low, and a different type of expansion is used (Stell).

3.3.4 Construction of an equation of state (an example)

In the simplest form an equation of state expresses the residual free Helmholtz energy as a sum of two terms: one that describes the hard spheres or more generally the repulsion, and a perturbation that takes into account attractive interactions. Cubic equations of state [63, 64] are well known examples of this type of equation. However, the perturbation theory makes it possible to further elaborate, and consider a specific perturbation for each type of molecular

interaction, assuming that these types are independent. The theory is often a bit loosened for this purpose, because it would mean that for any additional perturbation the exact solution of the previous (reference) is known. This is how the SAFT (Statistical associating fluid theory) models are often taken as a sum of contributions equation of state is based on the perturbation theory and in addition to the perturbations presented in equation (3.27) includes the perturbations due to the association interactions. These interactions are taken into account through Wertheim's association theory [67–69] (see section 3.4.1.3).

The generally accepted approach for constructing electrolyte equations of state is based on the same logic: terms are added to the Helmholtz free energy expression as if the various interactions could be handled independently of each other, using the perturbation theory. In order to illustrate this, Rozmus [70] proposed a thermodynamic cycle (Figure 22) for the construction of an electrolytic equation of state. This example will be used to show how one of the different versions of the SAFT family EoS (ePPC-SAFT, which is the one that is investigated in this work) is built.

The objective is to describe the difference between the liquid solution and the ideal gas. Hence, the starting point is the mixture containing all species in its ideal gas state. This means that the species have no volume and no interactions, they only have kinetic energy. In the first step, the Born term (generally used for this purpose) describes the discharge of the ions to produce the initial mixture but this time without charge. In a second step, a volume is attributed and van der Waals interactions (repulsion and attraction) are activated. These interactions can be described for example with the hard sphere (repulsion interactions), dispersion (Van der Waals interactions), and polar (dipole-dipole interactions) terms.

In the third step the ions continue to be present within the system with a neutral charge. This means that the only interactions that the ions have until now are repulsive interactions and short-range attraction, therefore no structure has yet been created between the molecules (dispersed liquid). To go from a dispersed liquid to a structured liquid, the association term is used. This term can be used to model the solvent-solvent, ion-solvent and ion-ion interactions.

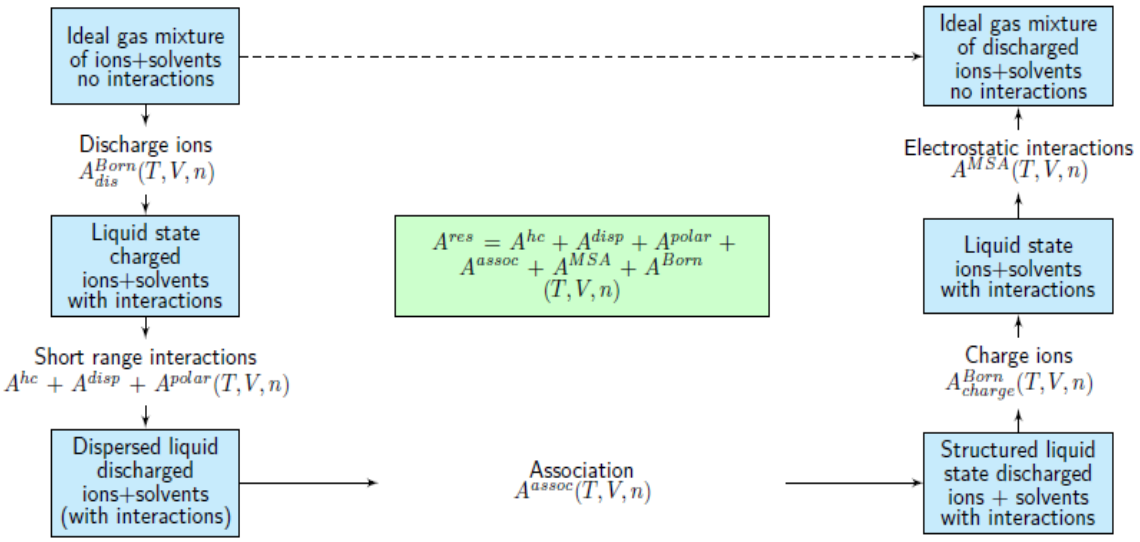

Figure 22: Thermodynamic cycle representing steps in forming an electrolyte thermodynamic equation of state. Example from Rozmus [70].

From the physical point of view, the ions interact with each other and with the water molecules. In step four the Born term generates the "activation of the ions charges", from this point the formation of the ion structures with the water is considered. The water molecules will cluster around the ions to form the so-called "solvation shell" or "hydration shell". Water, being a polar molecule, tends to orient its negative part around a cation, or its positive part around an anion, this generates the formation of a solvation shell as shown in Figure 23. Many molecular simulation studies [71, 72] have shown that water molecules generate a structure around ions. Fauve showed [71] that the number of oxygen atoms around the Na^+ ion in an aqueous NaCl solution is between 6 and 7. They also indicates that around a sodium cation, 6 to 7 water molecules can be placed.

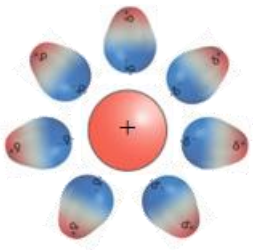

Figure 23: Cation solvation shell.

The structure of ion-water mixtures will be discussed in the next chapters. The opinions regarding which model should be used to describe this phenomenon are divided. For example, Fürst & Renon [73] used a specific short range term (dispersion term) to describe the solvation

phenomenon inspired by the theory of Blum [74]. Inchekel [61] as well as Rozmus et al. [60] and Herzog et al. [75] use the Wertheim association term combined with Born term for describing this phenomenon.

The last step of the cycle illustrated in Figure 22 is related to the presence of the charge in the ions. When the ions are charged, they generate long-range electrostatic interactions (coulombic interactions). There are some theories [76–78] that take into account the coulombic interactions, but also the ion-solvent interactions at the same time. However, these theories are very complex and difficult to include in the context of process simulation.

The final equation of state is then a sum of the perturbations:

$$A^{res} = A^{\,repulsion\ interactions} + A^{Van\ der\ Waals\ interactions} + A^{Polar} + A^{Association\ interactions} + A^{Charging} + A^{Electrostatic} \quad (3.28)$$

Where A is the total Helmholtz free energy and A^{X} is the Helmholtz free energy for each contribution.

Many SAFT variants exist nowadays. The several choices made by authors in the literature are discussed in section 3.5.

The following section will explain in detail how the model that is used in this work is constructed. The equations that will be used in this study for each of the terms will be also presented.

3.4 Construction of ePPC-SAFT

The PPC-SAFT equation is state is used as a basis in this work because this equation has been investigated in the past by members of our IFPEN group, more specifically in view of constructing a group contribution model able to describe a wide variety of molecular mixtures [79]. It has also been used as a basis for describing electrolyte systems in other previous work [70, 80, 81]. This work will propose a benchmark of different approaches, but all based on PPC-SAFT.

3.4.1 Physical interactions

In this first part called *physical interactions,* theories describing short-range interactions such as repulsion, dispersion, association and polar will be presented.

3.4.1.1 Hard sphere term (Repulsion interactions)

Repulsive interactions in general are represented by models that describe the molecules as hard spheres. The model of the hard sphere has been used by several authors to describe the repulsive forces between molecules. As mentioned above, this term is taken as the reference for SAFT EoS. Probably the best known equation, and one of the most used for this purpose, is that obtained by Carnahan and Starling [82]. This model was later expanded to be used in mixtures by Mansoori et al. [83]. Authors such as Huang et al. [84] have used the Carnahan and Starling model in the study of systems with small, large and polydisperse molecules. The Mansoori model has been used by Adidharma et al. [85] to study systems with heterosegmented polymers.

The equation that will be used in PPC-SAFT to calculate the perturbation of repulsive interactions to Helmholtz free energy is [82, 83]:

$$\frac{A^{HS}}{RT} = \frac{6V}{\pi N_{Av}}\left[\left(\frac{\zeta_2^3}{\zeta_3^2} - \zeta_0\right) ln(1-\zeta_3) + \frac{3\zeta_1\zeta_2}{1-\zeta_3} + \frac{\zeta_2^3}{\zeta_3(1-\zeta_3)^2}\right] \qquad (3.29)$$

With:

$$\xi_k = \frac{\pi N_{Av}\rho}{6}\sum_{i=1}^{n} x_i\left(d_i(T)\right)^k \text{ and } d_i(T) = \sigma_i^{HS}\left[1 - \lambda_i e^{-3\frac{\varepsilon_i}{RT}}\right] \qquad (3.30)$$

Where, ρ is the molar density of the fluid, σ_i^{HS} is the hard sphere diameter, ε_i is the dispersive energy parameter, λ_i is the softness parameter which is equal to 0.12 (except for water in the model used in this work: λ_i= 0.203). For water, the temperature dependence of $d_i(T)$ was modified by Ahmed [80]. Further, N_A is Avogadro's number (6.02214x10^{23} mol^{-1}), $d_i(T)$ is the segment diameter proposed by [86], x_i is the molar fraction of the component i, V is the volume and R is the universal gas constant.

The hard sphere term is characterised by the hard sphere diameter (σ_i^{HS}), which is specific for each ion. It should be noted that although the water molecule is composed of several atoms, in this study the water molecule is taken as a single hard sphere.

3.4.1.2 Dispersion term (Van der Waals interactions)

To describe the attractive part there are several theories that are much more complex. Some authors use cubic equations of state to model the short-range attractions between molecules. Others like Müller et al. [87], use the COSMO-RS model. This model assumes that short-range interactions can be described by pairwise interactions of molecular surfaces. The main parameter determining the strength of molecular interactions in the model is the screening charge density. Monoatomic ions exhibit very high screening charge densities compared to most neutral compounds. To account for the short range interaction strength between the ions and the solvent, an additional energy contribution is introduced [88].

Many authors [59, 89–91] present the dispersion free energy together with repulsion, as a single term that is sometimes called A^{MONO} or A^{Seg} (interactions between monomers or segments). This term is then approximated using the high temperature expansion of the Barker-Henderson perturbation theory (equation (3.27)), where the reference fluid (Hard sphere) is calculated using equation (3.29). Pamies et al. [92] used the Lennard Jones potential to describe both attraction and repulsion interactions in a single term.

The main variation between the different dispersion terms is the way in which the intermolecular potential is described. For example references [59, 93] used the Square-Well potential to describe the attraction interactions. Eriksen et al. [89] used the Mie potential, Anvari et al. [90] used the Yukawa potential, Shahriari et al. [91] used the Morse potential and Najafloo et al. [94] used a potential proposed by Chen and Kreglewski.

In this study the square-well potential with a radial distribution function is assumed. Based on the high temperature expansion of the Barker-Henderson perturbation theory (equation (3.27)), the Helmholtz free energy is given as [10]:

$$\frac{A^{Disp}}{RT} = \frac{A_1}{RT} + \frac{A_2}{RT} \tag{3.31}$$

Where:

$$\frac{A_1}{RT} = -2\pi\rho\,\overline{\varepsilon\sigma^3}\int_1^{\infty} g_{ij}^{hs}(x_i,\rho)x^2 dx \tag{3.32}$$

$$\frac{A_2}{RT} = -\pi\rho\left(Z^{hc} + \rho\frac{\partial Z^{hc}}{\partial\rho}\right)^{-1}\overline{\varepsilon^2\sigma^3}\,\frac{\partial}{\partial\rho}\left[\rho\int_1^{\infty} g_{ij}^{hs}(x_i,\rho)x^2dx\right] \tag{3.33}$$

$$g_{ij}^{HS} = \frac{1}{1-\xi_3} + 3\frac{d_{ij}\xi_2}{\left(1-\xi_3\right)^2} + 2\frac{\left(d_{ij}\xi_2\right)^2}{\left(1-\xi_3\right)^3} \tag{3.34}$$

Where $x = \frac{r}{\sigma}$ is the reduced radial distance around a segment, Z^{hc} is the compressibility factor, g_{ij}^{HS} is the radial distribution function at contact in the hard sphere system for component i [83, 95] and ξ_k is calculated by equation (3.30).

$\overline{\varepsilon\sigma^3}$ and $\overline{\varepsilon^2\sigma^3}$ represent average values obtained by a mixing rule based on the Van der Waals one fluid theory [52]. Equation *(3.35)* and equation *(3.36)* are the mathematical expressions for these two parameters:

$$\overline{\varepsilon\sigma^3} = \sum_i^n\sum_j^n x_i\,x_j\left(\frac{\varepsilon_{ij}}{kT}\right)\left(\sigma_{ij}^{HS}\right)^3 \tag{3.35}$$

$$\overline{\varepsilon^2\sigma^3} = \sum_i^n\sum_j^n x_i\,x_j\left(\frac{\varepsilon_{ij}}{kT}\right)^2\left(\sigma_{ij}^{HS}\right)^3 \tag{3.36}$$

The dispersion term requires two parameters: the distance of closest approach (σ_{ij}^{HS}) and the binary dispersion energy (ε_{ij}). The distance of closest approach is computed directly from the hard sphere diameters:

$$\sigma_{ij}^{HS} = \frac{\sigma_i^{HS} + \sigma_j^{HS}}{2} \tag{3.37}$$

Where σ_i^{HS} is the hard sphere diameter.

The dispersion energy parameter between the species i and j is (ε_{ij}) is calculated using the modified Lorentz-Berthelot combining rules. For this, it is necessary to set a pseudo-unitary dispersion energy (ε_i) (specific for each ion or for the solvent), and pseudo-binary parameter (k_{ij}) as shown in the equation *(3.38)*.

$$\varepsilon_{ij} = \left(1-k_{ij}\right)\sqrt{\varepsilon_i\varepsilon_j} \tag{3.38}$$

The pseudo-binary parameter k_{ij} is useful to correct the amount of interactions that occur between two species.

3.4.1.3 Association term (hydrogen bonding interactions)

Interactions between the molecules can in some cases be much stronger and directional than indicated by the dispersive term. When these interactions are strong enough, the formation of multimers occurs within the mixture (typically in the case of hydrogen bonds). Association interactions strongly affect the fluid structure, and the thermodynamic properties of solutions. Their inclusion improves the equation strongly.

Several approaches have been developed to describe association [96]. However, the model described by Chapman et al. [97] is the most used within engineering models such as SAFT [27], this model is based on Wertheim's association theory [67–69]. The association term considers the short-range directional interactions. It can be considered as a pseudo-chemical term that describes the formation of a chemical bond between sites. Hence, the first step when using this term is to define the number of sites and their charge, for each species. The association term contribution to the Helmholtz energy is given as [97]:

$$\frac{A^{Assoc}}{RT} = \sum_i n_i \sum_{A_i} \left[\left(lnX^{A_i} - \frac{X^{A_i}}{2} \right) + \frac{1}{2} M_i \right] \qquad (3.39)$$

Where M_i is the number of association sites in a molecule i and X^{Ai} is the fraction of un-bonded associations sites of A on molecule i, computed as:

$$X^{A_i} = \left[1 + N_{Av} \sum_{B_j} \left(\rho X^{B_j} \Delta^{A_i B_j} \right) \right]^{-1} \qquad (3.40)$$

The equilibrium constant is expressed as $\Delta^{A_i B_j}$ between the A site of molecule i and the B site of molecule j. The equation used to calculate the this constant is [77]:

$$\Delta^{A_i B_j} = d_{ij}^3 g_{ij}^{HS} k^{A_i B_j} \left[exp\left(\frac{\varepsilon^{A_i B_j}}{kT} \right) - 1 \right] \quad \text{with} \quad d_{ij} = \frac{\sigma_i^{HS} \sigma_j^{HS}}{\sigma_i^{HS} + \sigma_j^{HS}} \qquad (3.41)$$

Where $g_{\mathrm{ij}}^{\mathrm{HS}}$ is the radial distribution function at contact in the hard sphere system for component i given by Boublik and Mansoori [83, 95] and given in equation (3.34).

In the context of electrolyte equations of state, the association term is generally used only to describe the association between the solvent molecules (usually water) [59, 94, 98–100], but there are also models [101–103] in which it is proposed to describe the solvation, a

highly directional interaction, and even ion-pairing, using this association term [60, 80]. In the work by Ahmed [10], the cations are described with 7 interaction sites and anions with 6. Thanks to the way in which this theory has been formulated, it is possible to distinguish between the association of molecules of the same type (solvent-solvent or ion-ion) or different types (ion-solvent) [67–69].

The site-site association interactions (equation (3.41)) are characterized by two binary parameters, the association energy ($\varepsilon^{A_iB_j}$) and the association volume ($k^{A_iB_j}$). Note that these are not species-species, but rather site-site interaction parameters. To simplify the approach, for ions all sites are considered equivalent, which means that at the end, the parameters may be considered as relating two species.

Since both ions and water molecules are considered to be associative species, the cross-association can be taken into account. For this purpose, the so called combining rule (CR-1) [81] can be used.

$$\varepsilon^{A_iB_j} = \frac{\varepsilon^{A_i} + \varepsilon^{B_j}}{2}\left(1 - w_{ij}\right) \qquad (3.42)$$

$$k^{A_iB_j} = \sqrt{k^{A_i}k^{B_j}}\left(1 - u_{ij}\right) \qquad (3.43)$$

Like the dispersion term, both the association energy and the association volume depend on pseudo-unary parameters ($\varepsilon^{A_i}, \varepsilon^{B_j}, k^{A_i}$ and k^{B_j}) and include pseudo-binary parameters (w_{ij}, u_{ij}). This gives a larger number of possible combinations compared to the dispersion term, when optimising using this term. However, it should be noted that not all parameters are independent of each other (as can be seen in equations (3.42) and *(3.43)*). For both association energy and association volume there are a pseudo-binary parameter (w_{ij} and u_{ij} respectively). Like in the dispersion term these parameters are useful to correct the amount of interactions that occur between two species.

3.4.1.4 Polar term (polar interactions)

Some molecules by their nature possess native dipole or quadrupole (such as water and CO_2 respectively). These molecules interact with each other within the system but, the interactions between the electron donor and receptor sites are not strong enough to consider that an association exists. The Padé approximation proposed by Stell [104], has been used as a basis to propose several equations that describe this phenomenon. The best known are: Gubbins and

Twu [105], Kraska and Gubbins [106, 107], Jog and Chapman [108, 109], Karakatsani and Economou [110]. The use of this term can be very powerful as it makes the theory predictive for polar mixtures. However, it should be used with great caution, as the additional parameters are highly correlated with the dispersion parameters [27]. An improved representation of the behaviour of the water solutions when taking into account the polar term was demonstrated by Nguyen-Huynh and Ahmed [57, 58, 81].

The model proposed by Jog and Chapman [109] to describe the polar interactions will be used in this study. The contribution of Helmholtz free energy describing these interactions are given as:

$$\frac{A^{polar}}{RT} = \frac{A_2^{polar}}{1 - \frac{A_3^{polar}}{A_2^{polar}}} \tag{3.44}$$

$$A_2^{polar} = -\frac{2\pi\rho}{9(kT)^2}\sum_i^n\sum_i^n x_i\, x_j m_i m_j x_{pi} x_{pj} \frac{\mu_i^2\mu_j^2}{d_{ij}^3} I_{2,ij} \tag{3.45}$$

$$A_3^{polar} = -\frac{15\pi^2\rho^2}{9(kT)^3}\sum_i^n\sum_j^n\sum_k^n x_i\, x_j x_k m_i m_j m_k x_{pi} x_{pj} x_{pk} \frac{\mu_i^2\mu_j^2\mu_k^2}{d_{ij}d_{jk}d_{ik}} I_{3,ijk} \tag{3.46}$$

Here μ_i is the dipole moment and x_{pi} the fraction of the polar hard spheres of molecule i. $I_{2,ij}$ and $I_{3,ijk}$ are correlations representing integrals over statistical properties, x_i is the mole fraction of molecule i and m_i the chain length.

3.4.2 Ion-Ion (Coulombic) interactions

Long-range interactions (coulombic interactions) govern various properties and phenomena of salt systems, since ions are species that possess electrostatic charges. There are two theories that are most often used to describe these interactions, the Mean Spherical Approximation (MSA) and the Debye Hückel (DH) theory. MSA and DH models can be divided into two types: Primitive and non-primitive. Primitive means that the solvent is described as a continuum with fixed dielectric constant. While in non-primitive theories, all species are considered explicitly. Debye-Hückel is a primitive theory. For MSA, both versions

exist. As will be shown below, primitive MSA and Debye Hückel have been compared and it has been shown that very close mathematical results can be obtained under similar conditions.

3.4.2.1 Debye Hückel (DH) theory

One of the first theoretical works on electrolytes was developed by P. Debye and E. Hückel in 1923 [111], the Debye-Hückel theory is one of the most recognized and oldest of its kind. This model explains the deviation from the ideality of a solution due to the presence of ions.

In the DH theory it is assumed that there are no ion-solvent interactions, this theory considers only the long-range interactions between ions of different charges. In this model the solvent is taken as a dielectric continuum and is characterized by the dielectric constant, which has led people to describe this model as a "dielectric continuum model". This model only represents perturbations from electrostatic interactions and must be combined with other terms representing short- and medium-range interactions to fully describe the properties of concentrated electrolyte solutions.

In the Debye-Hückel theory, the Coulomb law is used to represent the electrostatic force that a positive ion exerts on a negative ion through the solvent medium:

$$u(r_{ij})^{Coulomb} = \frac{z_i z_j e^2}{4\pi\varepsilon_o \varepsilon_r r_{ij}} \qquad (3.47)$$

where z_i and z_j are the valency of the ion i and j respectively, e is the electronic charge ($1{,}6 \cdot 10^{-19}$ C), ε_o is the dielectric constant in the vacuum (8.85418×10^{-12} C mol^{-1}), ε_r is the dielectric constant (relative permittivity) of the fluid (unitless), the value of the relative permittivity of water is 78.4 at 298.15K and r_{ij} is the distance between the ion i and the ion j.

DH theory uses Poisson's equation to describe the potential resulting from the presence of a point charge (ion) in a cloud of opposite charge. This equation gives a relationship between the charge density (ρ_{C_i}Cm^{-3}) around the ion i and the electrical potential (ψ_i J/C) for a sphere with radius r_{ij} around ion i [40]:

$$\frac{1}{{r_{ij}}^2}\frac{d}{dr_{ij}}\left(r_{ij}\frac{d\psi_i(r_{ij})}{dr_{ij}}\right) = -\frac{\rho_{C_i}(r_{ij})}{\varepsilon_0 \varepsilon_r} \qquad (3.48)$$

Due to the charges of the ions their distribution in the solution is uniform. For example, near a cation, anions tend to be in excess, while near an anion, cations tend to be in excess. Thanks to this it can be assumed that the distribution of the ions in the solution follows the form of a Boltzmann distribution. This assumption gives another relation between the charge density and the electrical potential [40]:

$$\rho_{C_i}(r_{ij}) = \sum_{j}^{N} z_j e \rho_j g_{ij}(r_{ij}) \tag{3.49}$$

Where ρ_j is the number density of the ion j and $g_{ij}(r_{ij})$ is the radial distribution function known from statistical mechanics [66]. Equation (3.49) may only be solved when $g_{ij}(r_{ij})$ is a known function of the potential $\psi_i(\mathrm{r_{ij}})$. An ion j has an electric potential energy of $z_j e \psi_i$ if it is in distance r_{ij} from ion i, then [40]:

$$g_{ij}(r_{ij}) = exp\left(-\frac{z_j e \psi_i(r_{ij})}{k_B T}\right) \tag{3.50}$$

Combining equations (3.49) and (3.50) gives an equation for the charge density as a function of electric potential:

$$\rho_{C_i}(r_{ij}) = \sum_{j}^{N} z_j e \rho_j exp\left(-\frac{z_j e \psi_i(r_{ij})}{k_B T}\right) \tag{3.51}$$

Debye and Hückel combined the Poisson equation (equation (3.48)) and the Boltzmann equation (equation (3.51)) thereby eliminating the charge density. The resulting Poisson-Boltzmann equation looks as follows:

$$\nabla^2 \psi_i = -\frac{1}{\varepsilon_0 \varepsilon_r} \sum_{j}^{N} z_j e \rho_j exp\left(-\frac{z_j e \psi_i(r_{ij})}{k_B T}\right) \tag{3.52}$$

Where $\nabla^2 \psi_i(r_{ij})$ is the Poisson equation in spherical coordinates.

Linearizing equation (3.52), applying the electroneutrality condition ($\sum_i \rho_i z_i e = 0$) and introducing the Debye Length (κ^{-1}) we arrive at:

$$\nabla^2 \psi_i = \kappa^2 \psi_i(r_{ij}) \tag{3.53}$$

with

$$\kappa = \sqrt{\left(\frac{1}{k_B T \varepsilon_0 \varepsilon_r} \sum_i \rho_i (z_i e)^2 \right)}$$

In electrolyte models the Debye screening length (κ^{-1}), is a key property. This property has an important physical importance, since it is the limit range of electrostatic interactions, because at that distance the charge in the liquid balances out the charge in the central ion, beyond this range the Coulombic interactions are very small or null and can be neglected.

Finally, the electric potential ψ_i can be derived by solving equation (3.53) and from the Coulomb potential (equation (3.47)) of the ion as presented in the derivation shown in McQuarrie [66]. The final expression for the Helmholtz free energy at $r_{ij} = d_{ij}$ is:

$$\frac{A^{DH}}{RT} = -\frac{k_B T V}{4\pi N_{Av} \sum_i n_i (z_i)^2} \sum_i n_i (z_i)^2 \chi_i \qquad (3.54)$$

Where

$$\chi_i = \frac{1}{d_{ij}^3} \left[ln(1 + \kappa d_{ij}) - \kappa d_{ij} + \frac{1}{2} (\kappa d_{ij})^2 \right] \qquad (3.55)$$

The Debye-Hückel theory [111] matches very nicely the initial slope of the activity coefficients: it is widely recognized as a good theory for highly diluted ionic solutions. This model is not valid at high concentration of salt. It is normally applicable up to a concentration of 0.002 molal [40], otherwise the behavior of the model becomes very distant from the real behavior of the solution. However, there are several versions of this model that can be used to study electrolyte systems at high salt concentrations.

Extended Debye-Hückel as its name mentions it is an extension of the DH model in which a new constant is included. This constant considers the maximum approach distance that any other ion can approach the central ion. This distance is close to the hydrated ion diameter [40]. The Hückel model [112] improves the Debye-Hückel model by the addition of a parameter that is proportional to the ionic strength to make it possible to extend the application range of the model. The addition of the parameter allows to calculate activity coefficients up to higher concentrations with good accuracy. Finally, the Pitzer Debye-Hückel model [35] is an empirical activity model based on the extended Debye-Hückel model. This model is composed of the sum of three functions. The first is a modification of the Debye-Hückel Gibbs excess

function, which depends on ionic strength. The second term is a function of the binary interaction coefficient, that take into account the short-range interactions between pairs of ions, it depends also on the ionic strength. The third function represent a ternary interaction between the components. The dependence of this function respect to the ionic strength is neglected.

3.4.2.2 Mean Spherical Approximation (MSA) theory

The fundamental difference between the MSA and Debye-Hückel derivations is that in MSA the ions are treated as hard spheres with diameter σ_i^{MSA} and not as point charges with a distance d_{ij} between charges. Since the ions now have a defined volume, they generate spaces inaccessible to other ions, this results in different expressions for the Helmholtz free energy and the screening length compared to the Debye-Hückel theory. Figure 24 shows graphically the difference between the p-MSA and DH models.

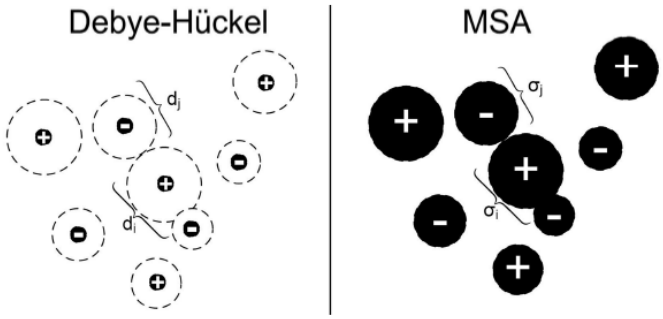

Figure 24: Illustration of the differences between the assumptions of the Debye−Hückel and of the MSA model [113].

The Mean Spherical Approximation theory describes the interactions between ion-ion, ion-dipoles, and dipoles-dipoles. In other words, it is a rather complete theory that may be used to describe simultaneously several types of interactions of interest in electrolytes solutions. The MSA theory [74, 114–118] is based on the perturbation of polar fluids, where the reference system is the Percus-Yevick approximation using the Ornstein-Zernike equation as the specific closure. This theory has two versions, primitive and non-primitive.

Like in DH models, primitive MSA models [74, 111, 115] assume that the ions are surrounded by a solvent which is represented as a dielectric continuum. In MSA models the ions are treated as charged hard spheres with a diameter σ_i^{MSA} . The restricted (explicit) version [119] is simple and uses a common diameter for all ions, whereas the unrestricted (implicit) version [80] has a specific diameter for each ion [120].

In this study the unrestricted primitive mean spherical approximation (p-MSA) [118] will be used to describes long-range cation-anion interactions (coulombic interactions). The final expression of the Helmholtz energy is:

$$\frac{A^{MSA}}{RT} = -\frac{N_{Av}e^2}{4\pi\,\varepsilon_o\varepsilon_r RT}\sum_i^{ions}\frac{n_i {Z_i}^2\Gamma}{1+\Gamma\sigma_i^{MSA}} + \frac{V\Gamma^3}{3\pi}k_B T \qquad (3.56)$$

where ε_r is the dielectric constant of the fluid, ε_o is the dielectric constant in the vacuum (8.85418x10^{-12} C mol^{-1}), n_i is the number of moles of ion i, V represents a total volume, σ_i^{MSA} is a solvated ion diameter and Γ the shielding parameter that is calculated as follows:

$$4\Gamma^2 = \frac{N_A e^2}{\varepsilon_o\varepsilon_r RT}\sum_i^{ions}\frac{n_i}{V}\left(\frac{{Z_i}^2}{1+\Gamma\sigma_i^{MSA}}\right) \qquad (3.57)$$

The distance $(2\Gamma)^{-1}$ is the MSA equivalent of the screening length in the Debye–Hückel theory κ^{-1}.

3.4.2.3 Ion paring

The formation of dimers is another way in which ions can interact, this type of interaction is not frequently mentioned in the studies of electrolytic systems (as will be shown below in Table 2). It is well known that ion pair formation is present in salt solutions with asymmetric, multivalent, multiatomic salts [49, 50, 121] and also in solutions with mixed solvents [80, 122, 123]. In contrast, in most studies with 1:1 aqueous solutions of strong electrolytes, complete ionic dissociation is assumed [9, 124, 125]. However, there are experimental [126] data and reports from molecular dynamics simulations [127] that provide evidence of ion pairing formation in a 1:1 aqueous solution of strong electrolytes. This type of solution demonstrates the appearance and influence of ion pairs at concentrations higher than 1M [121], This is because as the salt concentration increases the amount of ions increases and the amount of water available to solvate the ions decreases. As there are more free ions, the formation of ion pairs is favored. Another factor that promotes the appearance of ion pairs is the increase in temperature, this is due to the fact that increasing the temperature causes a decrease in the dielectric constant. Figure 25 shows the experimental data [126] of the association constant of the aqueous NaCl solution as a function of temperature. As can be seen in the figure, as the temperature increases, the association constant also increases, thus promoting the increase of ion pairing.

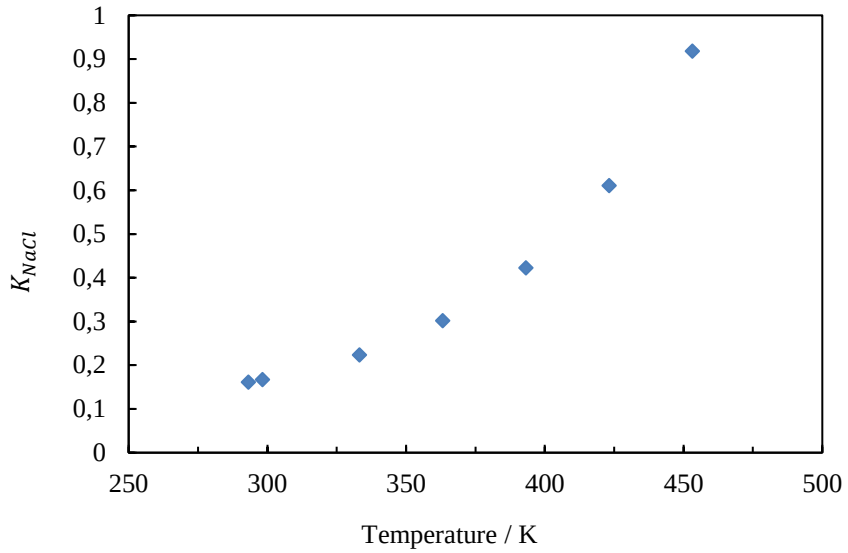

Figure 25 Experimental association constant of aqueous NaCl in function of temperature [126].

There are theories that include the formation of ion pairs. For example, in the non-primitive MSA theory [114, 116–118] it is assumed that ions are surrounded by a solvent, which is represented as dipolar hard spheres and not as a dielectric continuum. Non-primitive models have the advantage of describing all species explicitly: they combine both ion-ion and ion-solvent interactions and are both electrochemical and structural in nature. However, they require much more complex computations, and the authors who have published such models have never succeeded to reach a high degree of accuracy. In contrast, primitive models are simpler and allow for a similar if not higher accuracy.

The Binding Mean Spherical Approximation (BiMSA) [128–130], is a modified primitive-MSA model in which ion pair formation is included. In BiMSA a contribution is added to the model not only to count for the long-range electrostatic interactions between the unlike free ions, but also to account the ions associations (ion pairs). In this theory it is considered that each ion has one sticky spot which allows to associate with other unlike ion and form ion pairs. Moreover, the long-range electrostatic interactions between the ion pairs and free ions are considered as well. BIMSA uses Wertheim's theory [67–69] to include the association interactions between ion pairs.

Bülow et al. [131] took into account the formation of ion pairs by applying an association-dissociation equilibrium based on the law of mass action, where the ion pair is in

equilibrium with its respective free ions. For this they used Bjerrum theory (this theory will be reviewed in detail in chapter 5) which allows to calculate in a predictive way an equilibrium constant for the cation-anion interaction. Bülow et al. [131] used the Bjerrum treatment to calculate the degree of dissociation of the salts. From the degree of dissociation, the Debye-Hückel term was modified and then the thermodynamic properties were revaluated to account for ion pairing in the framework of a PC-SAFT equation of state.

3.4.3 Ion-solvent interactions "solvation"

While the Debye-Hückel theory deals with the interaction between charged ions, Born [132] and Planche [133] derived an equation for the interaction between an ion and the surrounding solvent. The presence of an ion in a solvent will disturb the solvent structure. Water, because of its high polarity, will re-orient its dipoles in such a way as to point its positive side towards the anions and its negative side towards the cation. As mentioned above, this phenomenon is known as solvation. The second short range model (see below) and the Born model can both be used to include these types of perturbation in the equations of state.

3.4.3.1 SR2

The second short range term (SR2), is a model proposed by Planche and Renon [133]. This model is specific to include the short-range interactions involving ions, both ion-solvent and ion-ion interactions. SR2 is derived from a non-primitive model and is used for electrolytic systems. In this term, the hard sphere and an electrostatic term are associated through the corresponding pair potential. It also associates a specific short-range interaction, as explained in the work of Planche and Renon. Some authors [73, 134] have used this term to take into account the ion-solvent interactions within their studies. However, in most of the articles reviewed in section 3.5 this term is not widely used.

3.4.3.2 Born term

A solvent consisting of polar molecules is polarizable and is also referred to as a dielectric medium. Highly polarizable solvents have high relative permittivities (dielectric constants). According to Coulomb's law (equation (3.47)), solvents with high relative permittivities decrease electrostatic interactions. In a vacuum, salts do not dissociate spontaneously since the electrostatic interactions between the ions are too strong. On the contrary, in strongly polarizable solvents the ions dissociate, and the solvent molecules protect the ions from each other and allow them to be separated.

The Born term describes the energy required to bring an ion from vacuum into a given dielectric constant medium [51]. According to the Born equation, it is essentially correlated with the inverse of the solvent dielectric constant. It is known that the presence of ions in a solvent results in a change in the dielectric constant. As a consequence, when an ion is added in a solution that already contains some salt, the electrostatic contribution to this ion will not be the same as that of the very first ion that came into the pure solvent. This difference can be described using the Born term, on the condition that the dielectric constant functionality is chosen adequately. If the definition of the activity coefficient is taken as an example (equation (3.59)), it can be seen that if the dielectric constant is considered as independent of the salt content ($\varepsilon_r = \varepsilon_r{}^{\infty}$ and $\frac{\partial(\varepsilon_r)}{\partial n_i} = 0$), the contribution of the Born term on the activity coefficient is null:

$$\left(\frac{\partial\left(A^{res}(T,V)\right)}{\partial n_i} - \frac{\partial\left(A^{res,*}(T,V)\right)}{\partial n_i}\right)^{Born} = \frac{N_{Av}e^2}{4\pi\,\varepsilon_o k_B T}\left(\frac{1}{\varepsilon_r} - \frac{1}{\varepsilon_r{}^{\infty}}\right)\frac{Z_i{}^2}{\sigma_i^{Born}} - \sum_i^{ions}\frac{n_i Z_i{}^2}{\sigma_i^{Born}}\frac{1}{\varepsilon_r{}^2}\frac{\partial(\varepsilon_r)}{\partial n_i}\bigg|_{V,T,n_i\neq i} \quad (3.58)$$

This term was first introduced by Born [132], but now very often used in electrolyte models [60, 80, 135]. It is given by:

$$\frac{A^{Born}}{RT} = \frac{N_{Av}e^2}{4\pi\,\varepsilon_o RT}\left(1 - \frac{1}{\varepsilon_r}\right)\sum_i^{ions}\frac{n_i Z_i{}^2}{\sigma_i^{Born}} \quad (3.59)$$

where σ_i^{Born} is the Born (covalent) diameter for each ion.

In equation (3.60) an effective radius corresponding to the radius of the spherical cavity in the solvent created by an ion (covalent radius) [22, 23] must be used instead of the ionic radius of the ion. The covalent radius of the metal corresponds to the radius of the cation plus that of the empty orbital around the cation, this empty orbital is assumed to be part of the cavity formed by the ion in the solvent. For example, the atomic radius of sodium is 190 pm, while the covalent radius is 154 pm and the ionic radius is 102 pm.

3.4.4 The dielectric constant

The dielectric constant or relative permittivity can be measured by exposing the solvent to a disturbing external electromagnetic field of small intensity. The solvent is placed between two conducting plates of a capacitor. The response to this field is measured and, from this response, the relative permittivity of the medium can be deduced.

Three models for the dielectric constant are considered in this work: the model of Schreckenberg et al. [136], which describes the property as a function temperature and of the solvent density, in addition to two other models based on the Schreckenberg et al. model but explicit accounting for salt concentration.

3.4.4.1 Schreckenberg's Model

The correlation proposed by Schreckenberg et al. [136] for the calculation of the dielectric constant is:

$$\varepsilon_r = \varepsilon_{r,Solvent} = 1 + \frac{n_{solvent}}{V} d_v \left(\frac{d_T}{T} - 1\right) \tag{3.60}$$

where $n_{solvent}$ is the number of moles of solvent V is the volume of system, T is the temperature, d_v and d_T are constants with a value for water of 0.3777 dm^3/mol and 1403 K respectively. Although this model does not consider explicitly the effect of the presence of salts in the solution, there is an implicit dependence through the use of $\frac{n_{solvent}}{V}$.

3.4.4.2 Pottel's model

This model of Pottel [137] is one of the most widely used to evaluate salt concentration effect on dielectric constant of electrolyte solutions. It is derived from the Onsager equations, linking the dielectric constant of the solution to the ionic compactness of the saturated solution which represents the cavities surrounding each ion [137] , as:

$$\varepsilon_r - 1 = \left(\varepsilon_{r,Solvent} - 1\right) \frac{1 - \xi_3''}{1 + \frac{\xi_3''}{2}} \tag{3.61}$$

The ion concentration intervenes through the theoretical compactness of the ions (ξ_3''):

$$\xi_3'' = \frac{N_{AV}\pi}{6} \sum_i^{ions} \frac{n_i \left(\sigma_i^{HS}\right)^3}{V} \tag{3.62}$$

where $\varepsilon_{r,Solvent}$ is the dielectric constant of the solvent (for which the model of Schreckenberg is used), σ_i^{HS} is the hard sphere diameter and V is the volume of the system. This model is purely predictive, as it does not require any additional empirical parameter.

3.4.4.3 Simonin's model

Simonin's model [138] has a more empirical structure and uses an adjustable parameter α_{ion} (one per ion pair). Thanks to this adjustable parameter, the concentration dependence of the dielectric constant can be better considered.

$$\varepsilon_r = \frac{\varepsilon_{r,Solvent}}{1 + \sum_i^{ions}(\alpha_{ion}\, x_i)} \tag{3.63}$$

where α_{ion} is the adjustable parameter and x_i is the molar fraction of the ions. Roa Pinto et al. [12] report that the variation of the parameter (α_{ion}) with respect to the temperature follows a linear trend for the aqueous NaCl solution. Based on this observation, Roa Pinto proposed to include two new parameters within Simonin's model. For this, the parameter (α_{ion}) was transformed into.

$$\alpha_{ion}(T) = \alpha_{T,ion}(T - 298.15) + \alpha_{o,ion} \tag{3.64}$$

Therefore, equation (3.63) can be rewritten as:

$$\varepsilon_r = \frac{\varepsilon_{r,Solvent}}{1 + \sum_i^{ions}\left(\left(\alpha_{T,ion}(T - 298.15) + \alpha_{o,ion}\right)x_i\right)} \tag{3.65}$$

where $\alpha_{T,ion}$ and $\alpha_{o,ion}$ are adjustable parameters.

3.5 Review of the existing electrolyte EoS

From the various theories described in the previous chapters, some research groups developed specific electrolyte equations of state. This chapter aims at reviewing such models.

There are several publications in which the thermodynamics of electrolyte solutions have been reviewed. Some of these publications are: Donohue et al. [139] that summarizes the models from 1985 to 1997, Pinsky and Takano [140] who present details about the calculation with activity coefficient models. There are also some publications [141],[125] in which electrolyte theories and equations of state are reviewed. In addition to these publications Michelsen and Mollerup [39] presented a discussion in which they included the derivation of theories for dipolar ions and the modern Debye-Hückel theory.

Held in 2020 published a short review [142] of the main excess Gibbs energy models and equations of state, his study focused on advances in the modeling of water-poor electrolytic systems and non-aqueous systems. Held shows that there is a variety of electrolyte models, and exposes the main problems associated with the modeling of water-free electrolyte systems. He highlights that none of the models presented in his study (with the exception of COSMO-RS-ES) meet the criterion for an advanced electrolyte model to be applicable over the full range of conditions from water-rich to water-poor with low to ultra-high salt concentrations. Another very interesting review made in the last years is the one made by Kontogeorgis et al. [143]. They have reviewed the state of the art of modeling electrolytic systems, highlighting the open questions regarding this challenge: the formation of ion pairs, the importance of the Born term, the best way to parameterize the models, how the dielectric constant should be modelled, and which model should be used to take into account the electrostatic interactions, are discussed in their review. These questions give an idea of the most important current issues in the study of electrolyte systems.

Authors like Maribo-Mogensen [65] and Ahmed [10] have made extensive reviews in which they summarize the different models used by many other authors for the thermodynamic study of electrolyte solutions. An extension of these reviews is presented in Table 2. This summary attempts to group the different models according to the research group they originate from. It appears clearly that each research group has its preferred physical model: for some, it is the CPA EoS, for others, one of the SAFT versions. It also appears that a given research group may have tested several theories for ion-ion or ion-solvent interactions. In what follows we will focus on both ion-ion and ion-solvent (or solvation) modelling. The solvation will be further focused on during this thesis.

The EoS models for the study of electrolytic systems are composed of a base model that takes into account the short-range interactions (*physical model*) in addition to terms that take into account the long-range interactions. Table 2 has been divided into several groups and presents the most relevant information from the different studies found on equations of state for electrolytes. The Table distinguishes, for each reference, the actual model used for the various types of interactions of interest here: physical model, ion-ion interaction model, ion-solvent interaction model, dependence of the dielectric constant, properties used for the regression and validation of the parameters and finally the system investigated.

	Authors	Publication year	Physical model	Ion-Ion	Ion-solvent	Dielectric constant	Property studied						Systems studied
							MIAC	VLE	ρ	SLE	Φ	Others	
Equation of state	**Jin et al.[124, 139, 144]**	1988	PACT	nrP-MSA	Perturbation-Expansion	D(T)	+	+	-	+	-	-	Strong and weak electrolytes
		1988					-	+	-	+	-	Ionic radius polarizability	Aqueous systems containing single volatile weak electrolytes
		1991					+	-	-	+	-	-	Systems containing multiple salts
	Prausnitz et al.[63, 64]	1991	SRK	DH	Born	D(T,V,ns)	+	+	-	-	-	-	NaCl/$MgCl_2$ and methanol-water-NaCl.
		1998	PR-Association	nrP-MSA	Born + Association	D(T)	-	+	-	-	-	-	Water hydrocarbons and salts
	Furst et al.[73]]	1993	Modified SRK	nrP-MSA	SR2	D(T,V)	-	-	-	-	+	-	Alkaline and alkaline-earth halide
	Zuo et al.[134]	1997	Modified SRK	nrP-MSA	SR2	D(T)	-	+	-	-	-	-	Single no aqueous electrolytes
	Myers et al [145].	2002	PR -Volume translation	rP-MSA	Born	D(T,V)	+	-	-	-	+	-	138 electrolytes
	Li et al. [76–78]	1999	SAFT	nP-MSA	-	D=cte	+	-	+	-	-	-	Aqueous electrolytes including 1:1, 2:1 and 1:2 electrolytes.
		2002			-	-	+	-	+	-	+	-	Aqueous NaCl
		2005		nP-MSA + Association	Association	D(T,ns)	+	-	+	-	+	-	Aqueous Alkali halide
	Galindo et al.[59, 89, 136]	1999	SAFT-VR	rP-MSA	Dispersion	D(T)	-	+	+	-	-	-	Aqueous Alkali halide
		2014		nrP-MSA	Born + Dispersion	D(T,V,ns)	+	+	+	-	+	LLE	Water, representative alcohols and carbon dioxide with Alkali halide family
		2016					+	+	+	-	+	Solubility limits	Aqueous salt systems
	Sadowski et al.[146–152]	2005	PC-SAFT	DH	Dispersion	D(T)	+	+	+	-	-	-	Aqueous Alkali halide + Li_2SO_4, Na_2SO_4, and K_2SO_4
		2013					+	-	+	+	+	-	Aqueous Alkali halide solutions + (NH_4)+ mixed solvent
		2014					-	-	-	-	-	LLE	Aqueous two-phase systems containing polyethylene glycol and one of 16 different inorganic salts
		2015					+	-	+	-	-	LLE	Copolymers in combination with 12 different inorganic salts water + alcohol
		2016					-	-	-	-	-	LLE	MIBK/water and ternary systems salt/MIBK/water
	Bulow et al. [131, 153, 154]	2021	PC-SAFT	DH + Bjerrum	Dispersion	D(T,V,ni)	+	-	-	-	-	Gibbs energy of solvation	alkali halides from water to alcoholic solvents

	Authors	Publication year	Physical model	Ion-Ion	Ion-solvent	Dielectric constant	Property studied						Systems studied
							MIAC	VLE	ρ	SLE	Φ	Others	
Equation of state	Tan et al. [98, 125, 125, 125, 155, 156]	2005	SAFT1	rP-MSA	Dispersion	D(T)	+	+	+	-	-	-	Aqueous alkali halide solutions
							+	+	+	-	+	-	Binary Aqueous Alkali halide
		2006	SAFT2				+	+	+	-	+	-	Single Aqueous Alkali halide $+ (Ca)^{2+}$, $(Mg)^{2+}$, $(NO3)^{-}$, $(SO4)^{2-}$,$(HCO3)^{-}$
	Lee et al.[101]	2009	PC-SAFT	rP-MSA	Born + Association	D(T)	+	-	+	-	+	-	Single aqueous salt systems
	De Hemptinne et al.[60, 80, 157]	2008	CPA+	P-MSA	SR2+ Born	D(T,V,ni)	+	-	+	-	-	-	Strong electrolytes
		2013	PPC-SAFT	P-MSA + Association	Born* + Association		+	+	+	-	-	Gas solubility	Aqueous Alkali halide + CO_2 and CH_4
		2018					+	-	+	-	-	-	Strong electrolytes + mixed-solvent
	Anvari et al.[90]	2013	SAFT-VR	MSA	Dispersion	D(T)	+	+	-	-	+	-	Aqueous electrolyte solutions of amino acids
	Najafloo et al.[94, 100]	2014	SAFT-HR	rP-MSA	Dispersion	D(T)	+	-	+	-	+	-	61 single electrolyte solutions with mono and multivalent ions
		2016			Dispersion + Born		+	+	+	-	+	-	Strong electrolytes
	Shadloo et al.[102, 103]	2016	PC-SAFT	DH	Dispersion + Association	D(T)	-	+	+	-	-	-	80 binary aqueous electrolyte solutions including 31 common ions
		2017					+	-	+	-	+	-	78 binary electrolyte solutions + mixed solvent
	Hajeb et al.[119]	2017	PC-SAFT	rP-MSA	Dispersion	D(T)	+	-	+	-	-	-	Strong aqueous electrolytes
	Shahriari et al.[91, 158]	2017	PC-SAFT	DH	Dispersion + Born	D(T,P,ni)	+	-	+	-	-	-	Aqueous electrolyte solutions
		2018	SAFT-VR		Dispersion + Born	D(T)	+	+	+	+	+	-	Aqueous electrolyte solutions contained seven ions
	Selam et al.[53]	2018	SAFT-VR		Dispersion + Born	D(T)	+	+	+	-	+	ΔGsolv	Strong aqueous electrolytes
	Lin et al.[159]	2007	CPA	MSA	Born	D(T,V)	+	-	-	+	+	AMV	Electrolyte solution +mixed solvent
	Haghighi et al.[160]	2008	CPA	DH	-	D(T,V)	-	-	-	-	-	Freezing point depression	Binary and ternary aqueous salt systems

	Authors	Publication year	Physical model	Ion-Ion	Ion-solvent	Dielectric constant	Property studied						Systems studied
							MIAC	VLE	ρ	SLE	Φ	Others	
Equation of state	**Carvalho et al.[161]**	2015	CPA	DH	-	D(T)	-	+	-	-	-	-	H_2O+CO_2 and H_2O+CO_2 + NaCl
	Mogensen et al.[135]	2015	CPA	DH	Born	D(T,V)	+	-	-	-	+	Freezing point depression	Aqueous single salt systems and mixed solvent
	Kontogeorgis et al.[62, 159, 162]	2017	CPA	DH	Born	D(T,V)	+	-	-	-	+	-	Aqueous salt systems and mixed solvent
		2019				D(T)	+	-	-	-	+	-	Tetra-n-butyl ammonium + halides aqueous solutions
		2020		DH			+	-	-	-	+	-	$H_2O+C_2H_6$, H_2O+tetra-n-methyl ammonium bromide (TMAB), H_2O+tetra-n-ethyl-ammonium bromide (TEAB), H_2O+tetra-npropyl- ammonium bromide (TPAB)
	Chababa et al.[163]	2019	CPA	P-MSA	Born	D(T)	-	+	-	-	+	-	CO_2 – H_2O – NaCl system; CO_2 solubility
	Afsharpour et al.[164]	2019	CPA	nr-MSA	Born	D(T)	-	+	-	-	-		CO_2 in aqueous MDEA

Table 2: Overview of electrolytes EoS published in literature. (e=electrolyte; n=non; r=restricted; P=primitive). The dielectric constant is shown with the variables on which it depends (T= temperature, V= volume, ni=moles of ion, ns=moles of solvent). D=cte means that the dielectric constant has been set to a constant value obtained from the literature. Born* means that the Born term depends explicitly on the salt concentration.

3.5.1 Ion-Ion modelling

The most popular models for the electrostatic interactions are based on the Debye Hückel (DH) and primitive mean spherical approximation (P-MSA) theories (we exclude here the non-primitive approaches). Some authors [59, 89, 124, 136, 139, 144, 145] prefer the use of the MSA model over the Debye-Hückel model arguing that DH model is valid only at infinite dilution. As mentioned above, the fundamental difference between these two theories is the way in which the diameters of the ions are considered (see section 3.4.2). Both theories are comparable and may yield similar results (depends on which versions are compared) [113]. Lin et al. [141] made an expansion of Taylor's series and the comparison of the mathematical form of both theories and concluded that there are very few differences when the same conditions are assumed.

Maribo Mogensen et al. [113] have demonstrated that the Debye-Hückel and MSA approaches are practically equivalent, in their ability to provide accurate descriptions of the experimental phase behaviour of electrolyte solutions (subject to the characterisation of the model parameters in each approach). According to some conclusions, the MSA theory has an advantage over the DH theory. Galindo et al. [59] compared these two theories to describe long-range interactions and reported that at high salt concentration of NaCl, densities were more accurately represented by P-MSA than by DH. However, for the representation of vapour pressure, the performance was almost the same. Thanks to these studies, it can be stated that the community that studies electrolyte systems generally agrees that the P-MSA and DH theories are equivalent.

3.5.1.1 Ion pairing

It is important to point out that none of the models (P-MSA and DH) consider ion-pair interactions. It is known from statistical mechanics and experimental measurements, that ion pair formation may occur [50]. The condition for pair formation is related to the ionic density: when the Debye screening lengths becomes smaller than the Bjerrum length (distance at which the electrostatic force is equivalent to the thermal energy) [165–167]. It is for this reason that some publications [60, 76, 77, 80, 146], include the concept of ion-ion association. Except by Bulow et al. [131] none of the authors (in Table 2) who included the concept of ion association have taken into account the effect that the ion pairs will have on electrostatics (i.e. the decrease of the ionic strength).

An innovative approach was proposed by Bülow et al. [131, 154]. They used the DH model to account for long-range interactions between ions and included the Bjerrum model to account for ion pair formation within their model. Thanks to this they were able to successfully predict the dissociation of salts in organic solvents, however the model they used did not match the dissociation behavior of ionic liquids, perhaps due to the lack of short-range physical contributions in the model.

3.5.2 Ion-solvent modelling

The dispersion term as mentioned above takes into account the short-range attraction interactions between the molecules. Many authors [59, 93, 94] use this term to describe interactions between solvent molecules and between solvent molecules and ions. Shadloo et al. [102, 103] used the dispersion term and the association term at the same time to describe the ion-solvent interactions. Other authors [53, 91, 158] have used the dispersion term in combination with the Born term and the dielectric constant to take into account the contribution of these types of interactions.

There is little consensus on how ion-solvent interactions should be modelled and especially on the use of the Born term for this purpose. To analyse how the different publications present in Table 2 describe the ion-solvent interactions, we can make a distinction between four types of publications.

The first group are publications that use **only the dispersion term**. In general, these models are able to correlate the experimental data for electrolytic systems by optimizing 2, 3 or even 4 parameters. Najafloo et al. [94] made a comparison between different models of this type (group 1) to compare which one had better results in correlating properties such as density and mean ionic activity coefficient (MIAC). They concluded that the best model is e-SAFT 1 which has three temperature dependent parameters, however they also showed that the e-SAFT HR model has very close results but for this model only two parameters need to be optimized which is an advantage.

In group two we classify the models that take into account the ion-solvent interaction with the **dispersion and Born** terms. In these models the dispersion term is used to model the

short-range interactions between the molecules, while the Born term is used in different ways. Galindo et al. [59, 136] use a dielectric constant that depends indirectly on salt concentration, using the Schreckenberg model. Shahriari et al. [158] used a dielectric constant that depends directly on the salt concentration. Both authors reported a good correlation of their models with the experimental data for properties such as MIAC and osmotic coefficient. It should be noted that having a dielectric constant that depends on the salt concentration (directly or indirectly), results on a large contribution of the Born term on the MIAC. Finally, other authors [53, 91, 94, 100] used a dielectric constant that depends only on the temperature, these authors justify the inclusion of the Born term, in order to take into account the energy of solvation. Galindo et al. [89] used the physical model SAFT VR to which they added the Born and P-MSA terms. With this model they only needed to optimize one parameter to obtain a good correlation of the experimental data for properties like MIAC, osmotic coefficient and density. But this model did not yield very good results on the MIAC with respect to temperature [89].

Models that describe ion-solvent interaction with **dispersion and association** terms are classified in group three. Shaldloo et al. [102, 103] made a study in which they compared two models. The first model they used was one in which the ion-solvent interaction was taken into account only with the dispersion term (group 1) and the second model is one from group 3 (both dispersion and association). In the two publications made on this subject, they concluded that the addition of the association term represents an improvement in the quality of the model, since it decreases the overall ARDs of liquid densities, MIACs, osmotic coefficients, and water activity. However, this also represents an increase in the number of parameters within the model.

Finally, in group four we include the models that use the **association plus the Born term** to describe the ion-solvent interactions. Wu et al. [64] state that the Born term contribution expresses only part of the change in Helmholtz energy due to charging of neutral particles, but the interaction between water and charged particles also generates a contribution due to the structure formed. Therefore, it becomes necessary to add an association interaction between ions and solvent to account for the short-range solvation interactions. Using this same argument Ahmed et al. [80] used e-PPC-SAFT EoS to study a electrolytic system with multi-solvent.

In both groups 2 and 3, the use of the Born term represented an improvement of the models to describe the electrolytic systems, however, opinions are divided as to the use of this

term. Some authors [60, 75, 80, 89, 136] defend the use of the Born term stating that it describes ion-solvent interactions in models where the solvent polarity is not accounted for otherwise, and in primitive models [136]. Other authors such as Simonin et al. [168] suggest that this term should not be included in models for electrolytes, as its magnitude greatly overestimates the ion-dipole contribution for aqueous systems. It is important to mention, however, that the correct sign of the solvation energy of ionic species, and the partitioning of ionic species among two liquid phases [142], cannot be modelled naturally without the inclusion of this term in models that do not otherwise account for solvent-ion electrostatic interactions.

3.5.3 The dielectric constant

When using a primitive model, an empirical correlation for the dielectric constant is required. Maribo-Mogensen [65] reported in his review of electrolytic models, that the majority of studies ignore the volumetric dependence of the dielectric constant (using a correlation of the static permittivity of water as a function of temperature at the saturation line), and the compositional dependence (unless the model is applied to mixed solvents). There are some exceptions [60, 145, 157], in which the authors have used empirical correlations that are function of water density. Inchekel [157] made a comparison of how well NaCl activity coefficients can be matched using two empirical models for the dielectric constant. On the other hand, Ahmed et al. [80] showed that the mean ionic activity coefficient calculations are improved when using the correlation proposed by Schreckenberg [136] for pure compounds (solvent), and adding the Pottel model [137] to take into account the effect of ion species concentration within the system.

Industrial electrolyte models consider usually that the dielectric constant is independent of the ionic concentration, which is not true in practice. They argue that the models used to make these calculations (MSA, Debye-Hückel and Born) are developed at infinite dilution conditions [2]. These models provide a corrective energy related to the charging of one ion or the ion-ion interactions. However, considering a thermodynamic cycle explained by Rozmus [70], the composition, temperature, and volume are constant throughout the cycle. The only thing that varies are the interactions between the different species of the system. This means that when considering the interactions involving the ions, the composition of the system is not at infinite dilution, but at the true concentration of the system. This is why a number of authors [60, 80, 157] suggest using a salt concentration-dependent dielectric constant. Maribo-

Mogensen [65, 169, 170] has shown that the use of such dependency provides a non-negligible change on the behaviour of the compositional derivative of the Helmholtz energy.

As mentioned above, there is no consensus on the use of the Born term and how the dielectric constant should be included in this term. It is important to note that the way in which the dielectric constant is modelled affects the impact of this term especially in the MIAC calculation (see section 3.4.3.2). The influence of the Born term becomes especially important at higher salt concentration, when the restructuring of the solvent perturbed by the ions is observed [70]. Therefore, the variation of the dielectric constant with salt concentration seems reasonable.

Some authors like de Hemptinne et al. [60, 61, 80] included a dielectric constant dependent on the salt concentration which resulted in the increasing contribution of the Born term to the residual energy of Helmholtz. Recently [60, 80] showed that including the effect of ion species within the dielectric constant makes that the Born term have an opposite contribution on the MIAC, compared to the MSA term (see Figure 26). This generates a better MIAC calculation. It is however questionable if this trend is due to a correct representation of the physical phenomenon by the Born term, or only a simple consequence of an adequate parametrization. Another very important conclusion that can be drawn from this figure is that at least for the model used in this study the contributions of the physical model is small in comparison with those of the Born and MSA terms that take into account the long range interactions involving the ions.

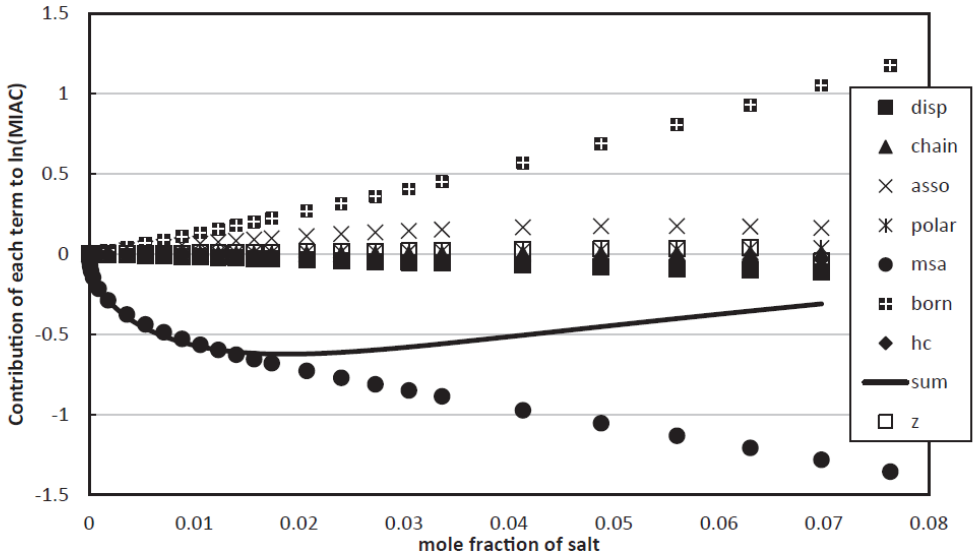

Figure 26: Effect of the various terms on the logarithm of the mean ionic activity coefficient (MIAC) for NaCl at 298.15 K [80].

3.5.4 Properties and systems

Most of the authors cited in Table 2 use MIAC (Mean ionic activity coefficient) or properties related to water activity such as osmotic coefficient, saturation pressure or freezing point depression to make the parameter correlation. Both the water activity and the ion activity are a representation of excess Gibbs energy. The measurement of ion activity is often performed using electrochemical cells [40]. Thanks to the Gibbs-Duhem equation and the osmotic coefficient, water activity coefficients and ion activity coefficients (MIAC) can be related [171]. Any (consistent) thermodynamic model that captures the osmotic coefficient will therefore also capture the mean ionic activity coefficient (and vice versa). Some authors [28, 125, 172] suggest using MIAC for electrolyte studies because it is more sensitive to the parameters of the equation of state.

The parameters used within the models can be ionic or salt specific. The first type concern parameters that are specific to each ion. Using this type of parameters makes it possible to study multiple-salt systems with a single set of parameters. The disadvantage of this approach is that it requires a simultaneous regression of many salts. The second type of parameters are those that are specific to each salt, the main advantage of the salt-specific parameters is that the parameterization is significantly less complicated [65]. However these parameters are specific to each system and this compromises the predictive ability of the model [173]. Maribo-Mogensen [65] and Ahmed [10] report that most authors use ion-specific parameters and only Radosz et al. [98, 125, 155] have ever used a combination of salt and ion-specific parameters. The vast majority of authors derive ion-specific parameters by studying the behaviour of aqueous halide systems.

In the literature there are not many publications of studies in which mixed-solvent systems have been modelled. However, some versions of CPA [135, 159] and SAFT [80, 103, 136, 149, 174] have been extended to model this type of system. Most of them are based on the adjustment of specific binary parameters of the salt, as mentioned above this compromises the predictive ability of the model [86]. So far, the models that have been studied to model multi-solvent electrolytic systems have a limited capacity.

Having a model that is able to correctly predict the temperature dependence of different thermodynamic properties is desirable. Most of the models we have found use a narrow range

of temperatures. However [10, 70, 80] attempted to correlate the temperature dependence in wide ranges of temperatures. For example, the model used by Ahmed et al. [80] is able to correctly reproduce the behaviour of the activity coefficient with respect to temperature above 25°C, however after 100 °C the deviation become more important. This behaviour was also reported by Rozmus [70], it should be noted that these two authors do not show the full range of temperatures discussed above in section 2.4.1. This shows the importance of validating the models for temperatures higher than 100 °C, since validating the models between 25 and 100 °C does not automatically make them capable of making an extrapolation to higher temperatures. In order to describe the behaviour of the mixtures with respect to temperature, several authors [101, 160, 175] correlated parameters as a function of temperature. In general, thanks to these parameters, they were able to improve the correlations of the experimental data, but this did not mean an important improvement in the predictive capacity of the models.

3.6 Conclusion

A summary of the main interactions present within the electrolyte solutions was presented. The perturbation theory on which the SAFT equations of state are based was described, as well as the construction of a thermodynamic model using an example of the application of the thermodynamic cycle. The theories used to calculate the interactions that can be found within an electrolyte system were also presented. Finally, the state of the art of the equations of state used for the study of electrolytic systems was discussed.

Thanks to Maribo-Mogensen's work, there seems to be an agreement that the primitive MSA and Debye Hückel models, which are used to describe the long-range interactions between ions, are equivalent. The vast majority of authors neglect ion pair formation. Ion pairs are fundamental when modeling electrolytic systems at high temperatures, high salt concentrations and for electrolytic systems with mixed solvents. However, it is known that even in strong salts and in solutions with low salt concentrations, ion pairs can be present in the solution [50]. Therefore, special attention must be paid to this type of interactions if a suitable thermodynamic model is to be developed, to make correlations and extrapolations of the thermodynamic properties of electrolytic systems.

The Born term and the influence of the dielectric constant on it, have been discussed in several articles but it is not yet possible to conclude which is the best way to use this term, and

which should be the model for the dielectric constant, when modelling electrolytic systems. There are different ways in which the ion-solvent interactions have been modelled (dispersion, association and Born term), but there is no consensus regarding the best method for considering these interactions within a thermodynamic model. As a final conclusion, it can be stated that all authors have shown that their model is able to obtain satisfactory results by correlating the experimental data. However, there has not yet been a discussion questioning whether the combination (model + parameters) makes physical sense.

That is why we think it is very important to deepen the study of ion-solvent and ion-ion interactions and find a model that is both accurate and physically consistent.

Chapter 4 Temperature dependence and short-range electrolytic interactions within the e-PPC-SAFT framework

4.1 Introduction

The formation of ion-pairs is rarely accounted for in equation of state models of strong electrolytes, as complete dissociation of the salt is assumed from the outset. At high temperatures and in non-aqueous solvents however, the formation of ion-pairs can have an important effect on the thermodynamics of the system. Held [142] for example points out that ion pairing does not only occur in systems with low water content or with mixed solvents, but also in aqueous systems, even at moderate salt concentrations. As mentioned above, the formation of ion pairs occurs largely because there are not enough water molecules to solvate the ions. The formation of ion pairs is inversely linked to the solvation of the ions, since the more ions are solvated, the less chance of ion pair formation, and vice versa. For this reason, it is of interest to consider ion-pairing and solvation together.

In SAFT frameworks, attractive ion-solvent and ion-ion interactions can be included through dispersion [59, 131, 154] (although not strictly pairing) and association [60, 80] terms. These terms are account for attractive interactions between neutral molecules but can be used to mimic the very strong ion-ion or ion-solvent interactions. Many models – approaches exist for describing electrolyte mixtures (see chapter 3). We want to evaluate their respective quality by benchmarking them using the same data.

Furthermore, the quality of a given thermodynamic model highly depends on the experimental data used in its parameterisation. Key experimental properties typically used in the study of electrolyte systems are mean ionic activity coefficient, osmotic coefficient, liquid (single phase or saturated) density, and vapour pressure. Properties such as the enthalpy, and Gibbs-free energy of solution can also be used. The enthalpy is related to the temperature

derivative of the Gibbs energy, and as such constitutes a stringent test of the global quality of the model.

In the current work, several modelling approaches are compared in their ability to reproduce experimental equilibrium properties of aqueous electrolyte solutions. We focus in a first time on NaCl solution, before testing these approaches on other 1:1 alkali halides. The mean ionic activity coefficient, the osmotic coefficient, the enthalpy of solution and the apparent molar volume are used in the comparison. A special emphasis is placed on reproducing the temperature dependence of the ionic activity coefficient. In carrying out careful parametrisation of the models proposed, an effort is made to keep the number of molecular model parameters to a minimum, and to ensure that their values are physically meaningful. In section 4.2 the models proposed are presented, as well as the parameterization strategies that have been used. In sections 4.3 to 4.5 a discussion of the results and conclusions is presented.

4.2 Model parameterization for NaCl

Several options in the choice of the ePPC-SAFT terms to mimic ion-ion, ion-solvent and solvent-solvent interaction are evaluated and discussed in this section. These combinations are shown in Table 3 . The proposed models are divided into two groups: The first group (dispersive models) contains models that use the dispersion term to describe the short-range interactions involving ions. The second group (associative models) contains models that use the association term to model the short-range interactions between ions. All other terms are identical. The distinction is implemented through a priory assumptions on the values of the model parameters. In dispersive models, ion-ion association energies are set to zero, while in associative models, the ion-ion dispersive energies are set to zero. A further subdivision is made based on the way the dielectric constant is used. Three models for the calculation of the dielectric constant are considered. They are discussed in section 3.7.

Table 3 : PPC-SAFT EoS models for compared in the current work ¤.

Interaction	*Model*					
	Dispersive models (Models 1)			Associative models (Models 2)		
	1.0	1.1	1.2	2.0	2.1	2.2
Hard sphere	all molecules	all molecules	all molecules	all molecules	all molecules	all molecules
Dispersion	solv-solv ion-solv ion-ion	solv-solv ion-solv ion-ion	solv-solv ion-solv ion-ion	solv-solv	solv-solv	solv-solv

Association	solv-solv	solv-solv	solv-solv	solv-solv ion-solv cat-ani	solv-solv ion-solv cat-ani	solv-solv ion-solv cat-ani
Polar	solv-solv	solv-solv	solv-solv	solv-solv	solv-solv	solv-solv
Born	ion-solv	ion-solv	ion-solv	ion-solv	ion-solv	ion-solv
MSA	cat-ani	cat-ani	cat-ani	cat-ani	cat-ani	cat-ani
Dielectric constant	Schreckenberg	Pottel	Simonin	Schreckenberg	Pottel	Simonin

[a]. The meaning of the abbreviations presented in the table are: solv-solv = solvent-solvent, ion-solv = ion-solvent, ion-ion = all the ion-ion interactions and cat-ani = cation-anion interactions. In the current work the solvent is always water.

4.2.1 Objective function

The objective function (OF) used is given as:

$$OF = \frac{1}{2}\sum_{j=1}^{n_{ser}} W_s^j \sum_{i=1}^{Npt^j} w_j^i \left(D_{calc}^{i,j} - D_{exp}^{i,j}\right)^2 \qquad (4.1)$$

where n_{ser} is the number of data series, Npt^j is the number of values for the data series j, W_s^j is global weight for each data series j, w_j^i is the local weight for the i^{th} value of data series j,_$D_{calc}^{i,j}$ are the calculated data and $D_{exp}^{i,j}$ the experimental data. In practice, the experimental uncertainties may be considered proportional to the experimental value, yielding

$$w_j^i = \left(\frac{1}{err(\%) \cdot D_{calc}^{i,j}}\right)^2 \qquad (4.2)$$

In some cases, the uncertainty is given in absolute terms:

$$w_j^i = \left(\frac{1}{e^j}\right)^2 \qquad (4.3)$$

The global weight of the property may be taken as inversely proportional to the number of points, which is why we have:

$$W_s^j = \left(\frac{w_s^j}{Npt_j}\right)^2 \qquad (4.4)$$

where w_s^j should be adapted to the relative importance of the property in the objective function for each property j.

4.2.2 Database

A selection among the large amount of data was made according to the criteria presented in chapter 2. In Table 4 temperature and concentration ranges used and corresponding references for aqueous NaCl are given.

Table 4 : Number of experimental data points (Npt^j), uncertainty ($err(\%)$ or e^j), data serial weight (w_s^j), temperature and concentration range of each properties used for the optimizations of aqueous NaCl. $\gamma_{\pm}^{m}$ is the mean ionic activity coefficient, ϕ is the osmotic coefficient, h^{sol} is the enthalpy of solution and $v_{\pm}$ is the apparent molar volume.

	$\gamma_{\pm}^{m}$	ϕ	h^{sol}	$v_{\pm}$	Reference
Npt^j	220	115	106	73	[46, 48, 54, 176–180]
$err(\%)$ or e^j	2%	5%	50 J/mol	10%	
w_s^j	1	1	0.01	1	
Temperature range / K	273.15-473.15	298.15-573.15	278.15-308.15	278.15-318.15	
Molality range (mol.kg^{-1})	0 - 6	0 - 10	0 - 5	0 - 6	

The four properties described in section 2 are used for model parameterization (mean ionic activity coefficient, osmotic coefficient, apparent molar volume, and enthalpy of solution). These properties vary in different ways with temperature and salt concentration, making the optimizations challenging. The uncertainties and the weight factors ($err(\%)$ - e^j and w_s^j) used in this work are presented in Table 4. They are selected as follows: the individual uncertainties, $err(\%)$ or e^j are determined based on knowledge from the experimental uncertainties [28]. The weight on each series is estimated in such a way that all four of properties carry a similar weight in the optimal value of the objective function. In Table 5 an example of the contribution of each sub-function to the total objective function is given, based on the data of Table 4.

Table 5 : Contribution of the different sub-objective functions (sOF) to the total objective function (OF) in the regression of the NaCl aqueous solution using model 1.2. $\gamma_{\pm}^{m}$ is the mean ionic activity coefficient, ϕ is the osmotic coefficient, h^{sol} is the enthalpy of solution and $v_{\pm}$ is the apparent molar volume.

Optimisation point	$\gamma_{\pm}^{m}$ sOF	ϕ sOF	h^{sol} sOF	$v_{\pm}$sOF	Total OF
Optimisation starting model	7.54	1.56	4.08	4.22	17.40
Optimum model	1.97	0.44	4.70	0.25	7.35

As can be seen in Table 5, at the initial model of optimisation, the contribution of the enthalpy of solution is lower than that of the mean ionic activity coefficient and apparent molar volume, but maintains the same order of magnitude. On the other hand, when we focus on the optimal model, it can be seen that even though the weight of the enthalpy of solution series is much lower than that of the mean ionic activity coefficient, this property ends up being the one that generates the largest contribution to the total objective function. Its value is in fact higher than it was at the starting point, illustrating that it is very difficult to minimize all properties simultaneously. This unexpected behaviour could point to inaccuracies in the model. As discussed below, it appears that the reason for this increase in the objective function is that the enthalpy of solution data are at low temperature (278-308 K) whereas the other data (mean ionic activity coefficient, and especially osmotic coefficients) are in a very different temperature range (up to 573 K). The model is unable to capture simultaneously the upward going slope at low temperature and the downward slope at high temperature (see Figure 13 and Figure 16). In what follows, we will also use the average absolute relative deviation (AARD) of each data series (j), defined as:

$$AARD_j(\%) = \frac{1}{Npt_j} \sum_{i=1}^{Npt_j} \left(\frac{\left| D_{calc}^{i,j} - D_{exp}^{i,j} \right|}{D_{exp}^{i,j}} \right) \cdot 100\% \qquad (4.5)$$

4.2.3 Optimisation strategies

The number of possible parameters in the models presented is rather large. In a first step, it is decided to investigate all of them. A number of criteria are considered to investigate the quality of the results. Firstly, the deviations (AARD) must be small (< 10%) for each property. This first criterion imposes a stringent test as we use four different types of properties, each one providing a different sensitivity to the model. The second criterion is based on the physical meaning of the parameters. In contrast with empirical models, the SAFT family of models are based on statistical thermodynamics that imply some restrictions on the parameter values. Finally, the sensitivity of the global objective function, and of each individual property within the objective function towards the parameter values is investigated. This sensitivity analysis will allow us to reduce the number of parameters.

Two strategies are used to carry out the optimisations. The parameters and their possible restrictions are presented in Table 6. In strategy “a” all available parameters are adjusted. For

the dispersive models, the interactions between the ions and the solvent, as well as the interactions between the ions (cation-cation, anion-anion and cation-anion) are taken into account. For associative models, interactions between ions of same charge are not allowed in the framework. In strategy "b", only 3 parameters are used for both dispersive and associative models. The discussion of why these parameters have been set in strategy "b" is presented below.

Table 6 : Unitary and binary parameters used for the optimisation strategies "a" and "b" ¤. Both strategies are applied for both dispersive and associative models. σ_i^{HS}, σ_i^{MSA} and σ_i^{Born} are the hard sphere, MSA and Born diameters, respectively, $\alpha_{0,\mathrm{ion}}$ and $\alpha_{T,ion}$ are the adjustable parameters of the Simonin dielectric constant, ε_{ij} is the dispersion energy, ε_{ij}^{AB} is the association energy and k_{ij}^{AB} is the association volume.

Strategy	"a"	"b"
Unary parameters (both types of model)		
σ_i^{HS}	Variable	Variable
σ_i^{MSA}	Variable	Fixed**
σ_i^{Born}	Fixed (see equation (4.6))	
${\alpha_{0,ion}}^*$	Variable see section 3.7*	0
${\alpha_{T,ion}}^*$		
Binary parameters for dispersive models (models type 1)		
$\varepsilon_{water-water}$	Fixed	201.75 / k_B/ K
$\varepsilon_{Na-water}$	Variable	201.75 / k_B/ K
$\varepsilon_{Cl-water}$	Variable	201.75 / k_B/ K
ε_{Na-Na}	Variable	0
ε_{Cl-Cl}	Variable	0
ε_{Na-Cl}	Variable	Variable
Binary parameters for associative models (models type 2)		
$\varepsilon_{water-water}^{AB}$	Fixed	1813.00 / k_B/ K
$\varepsilon_{Na-water}^{AB}$	Variable	Variable
$\varepsilon_{Cl-water}^{AB}$	Variable	1813.00 / k_B/ K
ε_{Na-Cl}^{AB}	Variable	Variable
ε_{Na-Na}^{AB}	0	0
ε_{Cl-Cl}^{AB}	0	0
$k_{Na-water}^{AB}$	Variable	0.044
$k_{Cl-water}^{AB}$	Variable	0.044
k_{Na-Cl}^{AB}	Variable	0.044

k^{AB}_{Na-Na}	0	0
k^{AB}_{Cl-Cl}	0	0
Number of adjustable parameters		
Model 1.0, 1.1	9	3
Model 1.2	11	
Model 2.0, 2.1	10	3
Model 2.2	12	

*Used only for models 1.2 and 2.2
** See equation *(4.11)*.
▫ In the dispersive models only the association energy between water molecules is taken into account, the other association interactions are equal to 0. For the associative models only the dispersion energy between water molecules is considered, all other dispersion interactions are set to zero.

In addition to the parameters that characterize the interactions of the ions, it is also necessary to use parameters to characterize the interactions between the solvent molecules (water in our case). The parameters used for water in this work are presented in Table 7.

Table 7 : Pure component parameters of water used in the current work, taken from [80]. $\boldsymbol{m}$ is the chain length, $\boldsymbol{\sigma_w^{HS}}$ is the hard sphere diameter, $\boldsymbol{\varepsilon_w}$ is the dispersion energy, $\boldsymbol{\varepsilon_w^{AB}}$ is the association energy, $\boldsymbol{\kappa_w^{AB}}$ is the association volume, M is the association sites, $\boldsymbol{\mu}$ is the dipole moment and $\boldsymbol{x_p}$ is the dipole fraction.

Parameter	Value	Parameter	Value
$\boldsymbol{\sigma_w^{HS}}$ /Å	See Note	ε_w^{AB}/k_B /K	1813
$\boldsymbol{m_w}$	1.02122	κ_w^{AB}	0.044394
$\boldsymbol{\varepsilon_w/k_B}$/ **K**	201.747	M	4
$\boldsymbol{\mu}$ /D	1.85	x_p	0.276

Note: A temperature-dependent diameter is used only for water molecules in this study. The segment diameter of pure water is given by [81] (in Å): $\sigma_w^{HS} = 2.2423 + 0.51212\exp(0.001126 \cdot T) + \frac{9904.13}{T^2}$, with T the temperature in K. With these parameters the mean absolute deviation for density is 0.72% and for vapour pressure is 2.32% [80].

Born diameter

In this work, we have set the Born diameter of each ion to the value corresponding to its experimental Gibbs energy of solvation, as suggested by Fawcett *et al.* [51]. Equation (4.6) is used, and the resulting Born diameters are shown in. The validity of this approach will be discussed further in section 4.4.2.

$$\Delta_s G_i = -\frac{N_A Z_i^2 e^2}{4\pi\varepsilon_o \sigma_i^{Born}}\left(1 - \frac{1}{\varepsilon_{solvent}}\right) \qquad (4.6)$$

Table 8 : Experimental Gibbs energy of Solvation [51] and Born diameters for each ion. $\Delta_s G_i$ is the Gibbs energy of solvation and σ_i^{Born} is the Born diameter.

Cation	$\Delta_s G_i$ /kJ / mol [51]	σ_i^{Born} / Å	Anion	$\Delta_s G_i$ /kJ / mol [51]	σ_i^{Born} / Å
Na^+	-424	3.23	Cl^-	-304	4.51
K^+	-352	3.89	Br^-	-278	4.93

4.3 Results

4.3.1 Models type 1 (dispersive models)

a. **Strategy "a"**

In Table 9 the AARD (%) obtained with the optimisation strategy "a" applied to dispersive models are presented. It can be observed that the deviations for the different properties are not of the same order of magnitude. The deviations on the enthalpy of solution are often much larger than those for the other properties. None of the dispersive models investigated in this work are able to reproduce quantitatively the downward trend of the enthalpy of solution with molality (see Figure 18). This is related to the fact that none of the models can reproduce accurately the low temperature increasing behaviour of the mean ionic activity coefficient with temperature. Indeed, as shown further, the only model that yields qualitatively good results for the enthalpy of solution, also shows a correct behaviour of the mean ionic activity coefficient with respect to temperature.

Table 9 : Average absolute relative deviation (AARD) of the optimisations of dispersive models using optimisation strategy "a" (model 1.2' is discussed in section 4.3.1-III). $\gamma_{\pm}^m$ is the mean ionic activity coefficient, ϕ is the osmotic coefficient, h^{sol} is the enthalpy of solution and $v_{\pm}$ is the apparent molar volume. In bold the results of the model with the lowest AARD.

	Model 1.0 $AARD_j$ / %	Model 1.1 $AARD_j$ / %	Model 1.2 $AARD_j$ / %	*Model 1.2' $AARD_j$ / %*
$\gamma_{\pm}^m$	3.53	3.36	**3.10**	3.33
ϕ	5.72	5.15	**4.82**	5.70
h^{sol}	37.94	38.22	**37.44**	36.37
$v_{\pm}$	6.61	5.44	**5.72**	5.43

Osmotic coefficients and mean ionic activity coefficients are related through the Gibbs-Duhem relationship. Yet, the data on osmotic coefficients are available at much higher temperature and concentration (see table 4). Therefore, the deviations on the osmotic coefficients are an indication of the capacity of the model to extrapolate both towards high

temperatures and concentrations. The apparent molar volumes provide a detailed view on the quality for the molar density of the models. For this property, deviations below 10% can be considered acceptable. In Table 9, the model 1.2 which leads to the lowest deviations is highlighted in bold.

As shown in Figure 27, model 1.2 represents accurately the mean ionic activity coefficient with respect to the salt concentration. However, the model results in a continuous decrease of the MIAC with respect to temperature. Therefore, a positive slope of the enthalpy of solution is observed (see Figure 28). The osmotic coefficients and apparent molar volume are both well represented qualitatively and quantitatively (see Annex A). Graphs showing the detailed contribution of each term to the natural logarithm of mean ionic activity coefficient at 298 K, and the behaviour of the different dielectric constants models with respect to temperature and salt concentration are provided in Annex B and C.

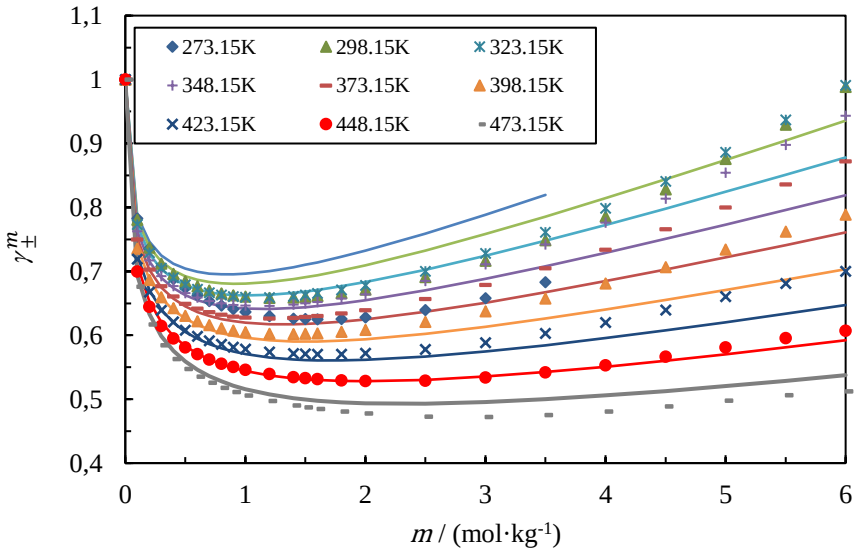

Figure 27 : NaCl mean ionic activity coefficient ($\gamma_{\pm}^{m}$) as a function of salt concentration obtained from the optimisation of model 1.2 using optimisation strategy "a". The symbols represent the experimental data and the curves show the results obtained with the model. The calculations were made at 1 bar for temperatures up to 373.15 K, the saturation pressure of the solvent was used for temperatures above 373.15 K.

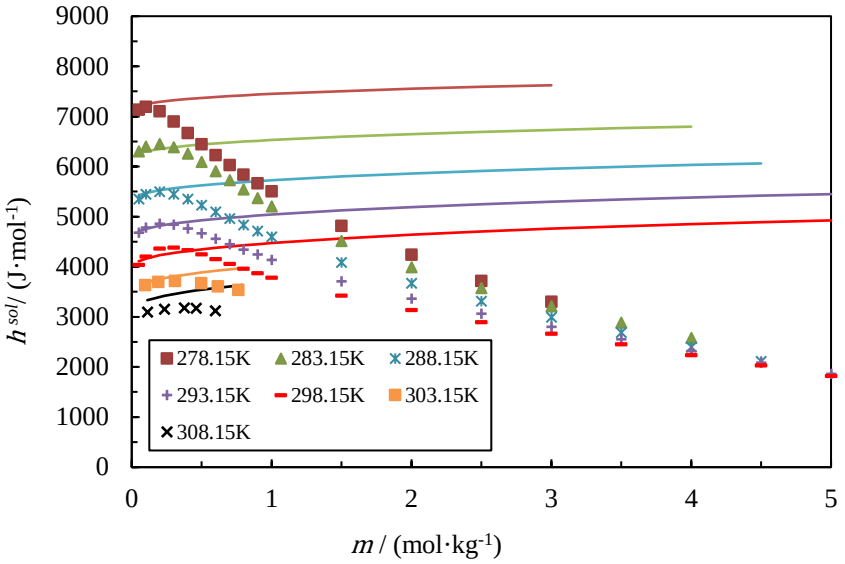

Figure 28 : NaCl enthalpy of solution as a function of salt concentration obtained from the optimisation of model 1.2 using optimisation strategy "a". The symbols represent the experimental data and the curves represent the results obtained with the model. The calculations were made at 1 bar.

Since the final objective of this study is to obtain a model that is consistent with the physics of the electrolytic solutions, it is important to verify that the adjusted parameters make sense from a physical point of view. In Table 10 the parameters obtained for the different models with optimisation strategy "a" are shown.

Three different criteria are used to analyse parameter consistency:

I. The first criterion is based on the comparison between MSA diameter and hard sphere diameter.

As MSA diameter (σ_i^{MSA}) can be seen as a hydrated ion diameter, it must be bigger or equal to the hard sphere diameter (σ_i^{HS}). In addition, the hard sphere diameter of the cation ($\sigma_{\mathrm{Na^+}}^{HS}$) must be smaller than the hard sphere diameter of the anion ($\sigma_{\mathrm{Cl^-}}^{HS}$), following the conclusion of several fundamental studies [181, 182].

Table 10 : Parameters obtained of the optimisation of dispersive models using the optimisation strategy "a". In bold, inconsistencies regarding diameters and energy parameters (discussed below). $\boldsymbol{\varepsilon_{ij}}$ is the dispersion energy, $\boldsymbol{\sigma_i^{HS}}$, $\boldsymbol{\sigma_i^{MSA}}$ and $\boldsymbol{\sigma_i^{Born}}$ are the hard sphere, MSA and Born diameters respectively, $\boldsymbol{\alpha_{0,ion}}$ and $\boldsymbol{\alpha_{T,ion}}$ are the adjustable parameters of the Simonin dielectric constant.

Parameters	Model 1.0	Model 1.1	Model 1.2	Model 1.2'
$\varepsilon_{water-Water}/k_B$/ K	201.75			
$\varepsilon_{Na-Water}/k_B$/ K	392.25	370.79	570.16	590.59

$\varepsilon_{Cl-water}/k_B$/ K	379.82	427.55	257.40	287.46
ε_{Na-Cl}/k_B/ K	332.29	721.46	709.67	794.42
ε_{Na-Na}/k_B/ K	477.09	148.57	**651.02**	**763.48**
ε_{Cl-Cl}/k_B/ K	720.61	492.07	343.50	366.24
$\varepsilon^{AB}_{water-Water}/k_B$ / K	1813.00			
σ^{HS}_{Na} / Å	3.22	3.42	3.59	3.76
σ^{HS}_{Cl} / Å	**2.81**(1)	**2.64**(1)	**2.53**(1)	**2.31**(1)
σ^{MSA}_{Na} / Å	**1.59**(2)	**1.40**(2)	**3.34** (2)	4.03
σ^{MSA}_{Cl} / Å	7.49	5.11	4.09	3.50
σ^{Born}_{Na}/ Å	3.23			
σ^{Born}_{Cl}/ Å	4.51			
$\alpha_{0,ion}$	-	-	0.013	0
$\alpha_{T,ion}$	-	-	-0.001	0

[a] In dispersive models only water-water association interactions are taken into account. The Born diameter has been fixed for all models using the values presented in Table 8. Water-water dispersion and association energies are also fixed with values from [80].

(1) $\sigma^{HS}_{Cl}<\sigma^{HS}_{Na}$
(2) $\sigma^{MSA}_{Na}<\sigma^{HS}_{Na}$

In Table 10, the diameters that do not meet the above conditions are highlighted in bold. As can be seen in the table, none of the models have physically consistent diameters. However, with model 1.2' only one diameter is inconsistent. This may suggest firstly that there are several local minima, and secondly that using the salt concentration explicitly within the dielectric constant, may lead to problems of consistency between the parameters.

II. The second criterion is based on the interaction energies:

As a second consistency test, it is checked whether the attractive interaction parameters between the like charge ions are physically consistent. The potential energy as a function of the distance may be evaluated as the sum of a square well (SW) and a coulombic (Coulomb) interaction:

$$u(r_{ij}) = u(r_{ij})^{SW} + u(r_{ij})^{Coulomb} \tag{4.7}$$

The square-well ($u(r_{ij})^{SW}$) and the Coulomb ($u(r_{ij})^{Coulomb}$) potential are given by [2, 27] as follows:

$$u(r_{ij})^{SW} = -\varepsilon_{ij} \quad when \quad \sigma^{HS}_{ij} < r_{ij} < \lambda\sigma^{HS}_{ij} \tag{4.8}$$

$$u(r_{ij})^{Coulomb} = \frac{z_i z_j e^2}{4\pi\varepsilon_o\varepsilon_r r_{ij}} \tag{4.9}$$

A negative (attractive) interaction energy can only be observed when the intermolecular distance lies between σ_{ij}^{HS} and $\lambda\sigma_{ij}^{HS}$. The parameter λ is the well width and can be taken at 1.2 or 1.5 depending on the authors [59, 183]. For two ions of the same charge not to attract each other, the potential energy must be always greater than or equal to 0. Applying these conditions and combining equations (4.7), (4.8) and *(4.9)* yields:

$$\varepsilon_{ij} \leq \frac{z_i z_j e^2}{4\pi\varepsilon_o\varepsilon_r\lambda\sigma_{ij}^{HS}} \qquad (4.10)$$

Equation (4.10) can be used to assess whether the parameters obtained for the dispersion energies would not lead to an unphysical attraction of ions of the same charge. If the ion-ion dispersion energy is bigger than the one obtained from equation (4.10), the parameters are rejected. By applying this analysis to the results obtained in Table 10, it was observed that none of the dispersive models present consistent parameters. In all cases at least one attractive interaction between ions of equal charge is obtained (bold parameters in Table 10). Therefore, no dispersive model presented here is physically consistent. This proves that even if a model can represent experimental data accurately, it does not mean that it is physically correct.

As the main limitation for the dispersive models to be physically consistent is that there is no attraction between ions of equal charge, some authors such as Held et al. [172, 184] have used optimisation strategies in which they cancel this type of interaction. This way, the consistency problem presented above is solved.

III. The third criterion is based on the dielectric constant

In Figure 29 the water dielectric constant calculated by each of the three models as a function of salt concentration is shown. For the calculation of the Simonin dielectric constant, the parameters presented in Table 10 were used. As can be seen in Figure 29, both the Schreckenberg and Simonin models generate very similar results. This is because the parameter values of the Simonin model are very small, which may indicate that the system tends to eliminate the impact of salt concentration within the Simonin dielectric constant. On the other hand, the Pottel model is more sensitive to the variation of the salt concentration and differs significantly from the two other models. Note that the Schreckenberg model shows a decreasing trend of the dielectric constant with molality, even though the salt mole fraction does not appear in equation *(3.60)*. It is related to the decrease of the ratio $n_{solvent}/V$. As will be

shown later (in section 4.3.2) this tendency is repeated for the associative models, where the best results are obtained with the model 2.0 (Schreckenberg model for dielectric constant). The behaviour of the different dielectric constants with respect to salt concentration and at different temperatures is presented in Annex C.

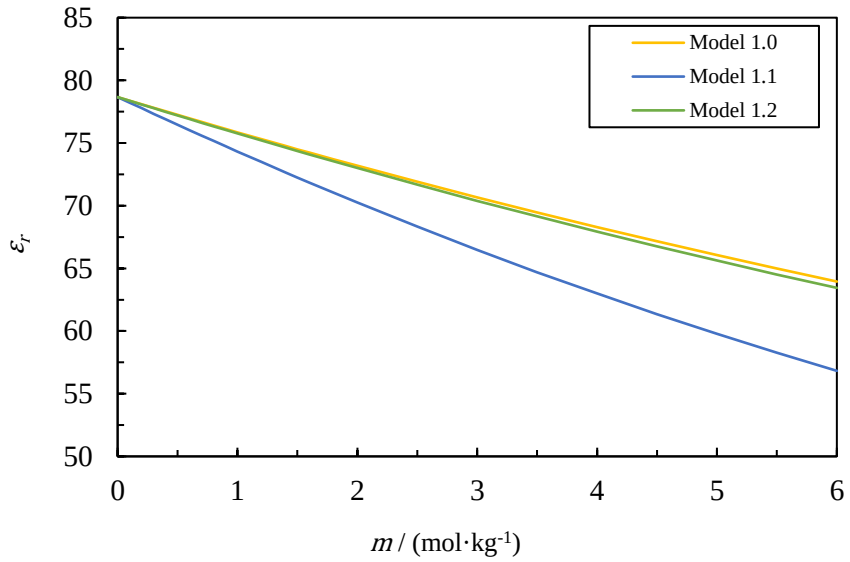

Figure 29 : Dielectric constant as a function of NaCl concentration at 298.15 K, using the parameters presented in Table 9 for the three dispersive models 1.0 (Schreckenberg), 1.1 (Pottel) and 1.2 (Simonin).

It is interesting to consider that, considering that the only difference between the models is the dielectric constant, and that this property is almost identical in models 1.0 and 1.2, the parameters values and the AARD % should also be very similar. In Table 9 the deviations shown are of the same order for the two models, except for the apparent molar volume. Yet the parameters values are very different (see Table 10). This is most probably because local minima have been reached resulting from parameter degeneracy. When regressing the parameters again (using the parameters of model 1.2 as a starting point for optimisation, and setting $\alpha_{0,ion} = 0$ and $\alpha_{T,ion} = 0$, which is equivalent to model 1.0), new parameters are obtained with values close to the parameters of model 1.2 (see Table 10). The deviations are shown in Table 9 (model 1.2'). It appears that the deviations are similar, but even smaller than those obtained with model 1.2, confirming that (1) there are local minima, and that (2) this approach is the one to be recommended.

b. Sensitivity analysis

The goal of strategy "b" is to reduce the number of adjustable parameters. A global sensitivity analysis (GSA) was performed on the optimal solution of strategy "a" (model 1.2). It allows visualizing how much the objective function is affected by a variation on any given input parameter. The GSA evaluates the impact of the variation of a given parameter on the objective function. This analysis is performed by analysis of variance. For this purpose, response surfaces first generated, and the GSA is performed on these surfaces.

The, response surfaces were created using the Kriging method, which consists of interpolating using a Gaussian process (a probability distribution over random functions), characterized by a mean and a covariance structure. The advantage of this method is that it performs an interpolation that goes through the whole experimental design [185]. For this, a Latin Hypercube experimental design method is used for generating 1000 parameter sets within the range that has been imposed (see Table 11). After obtaining the response surfaces, the global sensitivity analysis was performed. For this, the Monte-Carlo sampling technique was used.

The definition of Monte-Carlo sampling consists in attributing a probabilistic law to each parameter, in the investigated domain. The inputs of a Monte-Carlo sampling are therefore: a probabilistic law for each parameter and a sample size [185]. The probability law provides a sampling density within the range under study. In the present study the uniform law was used, which gives the same probability of finding the parameter in all the studied range. The use of this law implies that the range for each parameter is known. The result of this type of analysis depends strongly on the range chosen for each parameter. For the present study, it has been decided to use a range of +/- 10% of the optimal parameters obtained. Below in Table 11, the range for each parameter is shown.

Table 11 Range used for the global sensitivity analysis of model 1.2. ε_{ij} is the dispersion energy, σ_i^{HS} and σ_i^{MSA} are the hard sphere and MSA diameters respectively, $\alpha_{0,ion}$ and $\alpha_{T,ion}$ are the adjustable parameters of the Simonin dielectric constant.

Parameters	minimum	maximum
$\varepsilon_{Na-Water}/k_B$/ K	382.95	468.05
$\varepsilon_{Cl-water}/k_B$/ K	386.31	472.16
ε_{Na-Cl}/k_B/ K	254.95	311.61
ε_{Na-Na}/k_B/ K	1194.03	1459.37
ε_{Cl-Cl}/k_B/ K	850.73	1039.79

σ_{Na}^{HS} / Å	2.80	3.42
σ_{Cl}^{HS} / Å	3.13	3.83
σ_{Na}^{MSA} / Å	2.49	3.04
σ_{Cl}^{MSA} / Å	6.92	8.45
$\alpha_{0,ion}$	-0.05	-0.04
$\alpha_{T,ion}$	-0.0024	-0.0020

As a result of the global sensitivity analysis, the total effect of each parameter on the different objective functions are obtained. *"The total effects measure the part of the response variance explained by all the effects in which a given parameter plays a role. The sum of all the total effects can be higher than one because the same interaction terms are counted several times*" [185]. The larger the total effect of a parameter, the more sensitive the objective function is to a variation of this parameter. In Table 12 the total effect of the parameters used in the optimisation of model 1.2, for both the total objective function and each of the sub-functions (MIAC, Osmo, Hsol and AMV).

Table 12 Results from the sensitivity analysis of model 1.2 [a]. ε_{ij} is the dispersion energy, σ_i^{HS} and σ_i^{MSA} are the hard sphere and MSA diameters respectively, $\alpha_{0,ion}$ and $\alpha_{T,ion}$ are the adjustable parameters of the Simonin dielectric constant. The most sensitive parameters are highlighted in bold.

Parameters	Total effect (%)				
	Total OF	$\gamma_{\pm}^{m}$ sOF	h^{sol} sOF	ϕ sOF	$v_{\pm}$ sOF
$\varepsilon_{Na-Water}/k_B$/ K	6.24	6.19	5.22	7.6	0.53
$\varepsilon_{Cl-water}/k_B$/ K	2.94	2.83	2.54	3.5	0.79
$\boldsymbol{\varepsilon_{Na-Cl}/k_B}$**/ K**	**36.65**	**34.98**	**25.58**	**34.1**	0.17
ε_{Na-Na}/k_B/ K	3. 53	3.44	2.4	3.1	0.16
ε_{Cl-Cl}/k_B/ K	0.07	0.12	0.1	0.1	0.11
$\boldsymbol{\sigma_{Na}^{HS}}$ / Å	**37.64**	**37.42**	**5.9**	**31.2**	**62.47**
$\boldsymbol{\sigma_{Cl}^{HS}}$ / Å	**72.07**	**69.06**	**58.73**	**81.1**	**86.55**
σ_{Na}^{MSA} / Å	1.08	1.2	0.23	1	0.16
σ_{Cl}^{MSA} / Å	1.27	1.28	0.17	0.6	0.11
$\alpha_{0,ion}$	0.13	0.15	0.1	0.1	0.1
$\alpha_{T,ion}$	0.17	0.18	0.43	0.8	0.13

[a] OF means Objective Function. The Total OF is that which is used for the parameter regression; It is the sum of four contributions: the mean ionic activity coefficient ($\gamma_{\pm}^{m}$), the enthalpy of solution (h^{sol}), the osmotic coefficient (ϕ) and the apparent molar volume ($v_{\pm}$).

Table 12 shows that the largest effect is that of the anion hard sphere diameter, and this is true for all sub-functions. The cation hard sphere diameter (smaller) has the second largest

effect almost equivalent with the cation-anion interaction parameter. For the AMV, only the hard sphere diameters are truly important.

As it can be seen in Table 12, both the dispersion energies between ions of equal charge, as well as the parameters $\alpha_{0,ion}$ and $\alpha_{T,ion}$ (explicit salt effect on dielectric constant), have a very low influence on all objective functions. Therefore, these parameters can be set to a value equal to zero. In contrast, it is observed that the influence of the hard sphere diameters has the greatest impact on the objective functions, especially the hard sphere diameter of chlorine. The influence of these diameters becomes especially important for the AMV. This result was expected since this property is volumetric, in the same way as the hard sphere diameters. Regarding the dispersive energy parameters, the dispersion between cation-anion is important for all sOF, except AMV. The effect is significant on the total objective function and in the mean ionic activity coefficient, enthalpy of solution and osmotic coefficient sub-objective functions.

As an example of response surfaces, Figure 30 shows graphically the effect of the hard sphere diameters on the sub-functions (sOF) and the total objective function (OF).

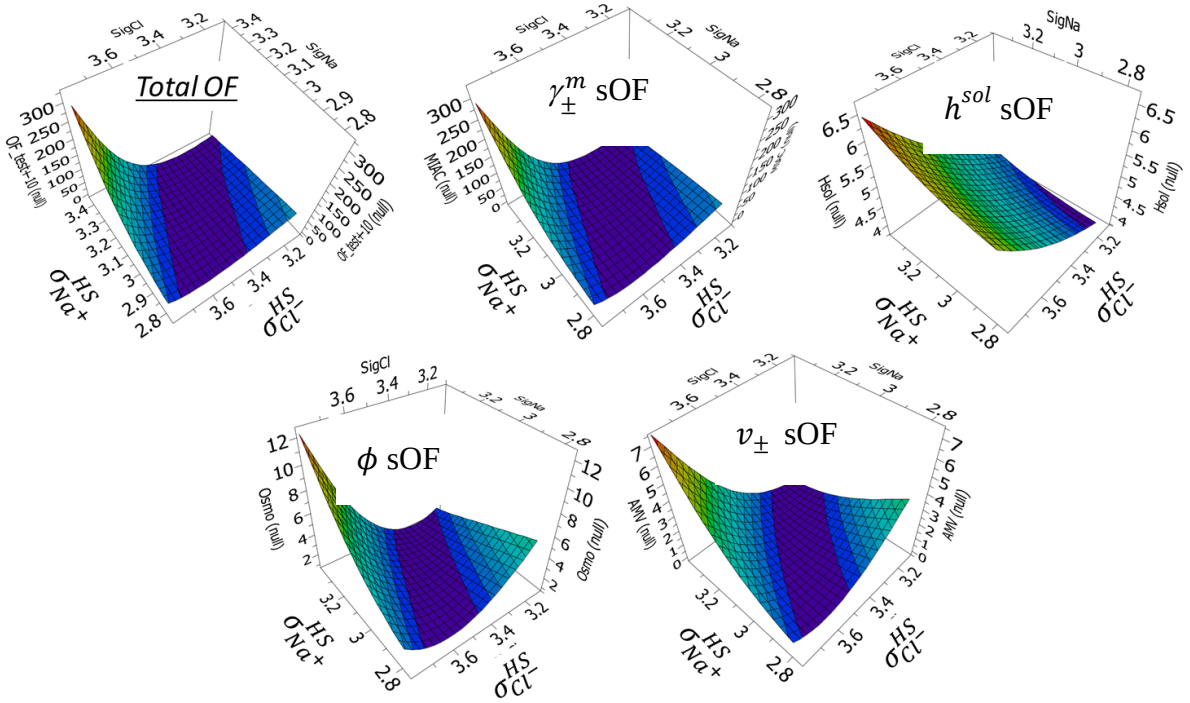

Figure 30 : Model 1.2 response surface of the hard sphere diameters for the total objective function and the mean ionic activity coefficient ($\gamma_{\pm}^{m}$), enthalpy of solution (h^{sol}), osmotic coefficient (ϕ) and apparent

molar volume ($\mathbf{v}_{\pm}$) sub-objective functions. All other parameters are taken at their optimal value (Table 10).

From Figure 30, the response surfaces are valley-like except for the enthalpy of solution, which shows a minimum at low values of chlorine hard sphere diameter. In fact, it seems that the valley is simply shifted to higher values of the anion diameter. This is an indication that the model is not suitable for studying this property. Temperature-dependent parameters may have been needed to improve this. The valleys in the other objective functions indicate that there is a correlation between the diameters of the two ions. The valley is located in the same position for the remaining properties, which points to the capacity of the model to represent the considered properties in a consistent way.

c. Strategy "b"

From the sensitivity analysis, the three most important parameters for the dispersive models are found to be the hard sphere diameters of both ions (but they are correlated) and the dispersion energy between the cation and the anion. Therefore, these three parameters are the only ones used in regression strategy "b". Taking advantage of the fact that the MSA diameters are not as sensitive and to reduce the number of adjustable parameters, a proportionality parameter between the hard sphere and the MSA diameters is introduced as:

$$\sigma_i^{MSA} = \sigma_i^{HS} \cdot 1.5 \qquad (4.11)$$

The value of 1.5 is imposed based on the results of multiple optimizations performed in this study.

Using the arguments developed above, a second optimization is performed with a reduced number of parameters (strategy "b" in Table 6). As shown in Table 13, after reducing the number of parameters from 11 to 3 the results have not worsened greatly. An increase in the deviation of no more than 3% is obtained, except for the case of the apparent molar volume, for which it increases by almost 3.5%. The deviation increases in the osmotic coefficient and in the enthalpy of solution are larger than in the mean ionic activity coefficient. This is a consequence of a deterioration of low enthalpy of solution and high temperature osmotic coefficient.

Table 13 : Comparison between the best results obtained using optimisation strategy “a” (model 1.2 - 11 parameters), and the results obtained using optimisation strategy “b” (model 1.0 – 3 parameters).

Strategy	AARD$_j$ / %			
	$\gamma_{\pm}^{m}$	ϕ	h^{sol}	$v_{\pm}$
a (Model 1.2)	3.53	5.72	37.94	6.61
b (Model 1.0)	4.02	6.52	41.47	8.90

Figure 31. Shows that the model can reproduce the mean ionic activity coefficient with respect to salt concentration, but unfortunately not the trend with respect to temperature. This is expected considering that the original model, with all parameters was also unable to reproduce the temperature dependence of the MIAC. A large deviation at low (273.15 K) and high (473.15 K) temperature is observed. The graphs for the other properties are presented in Annex A.

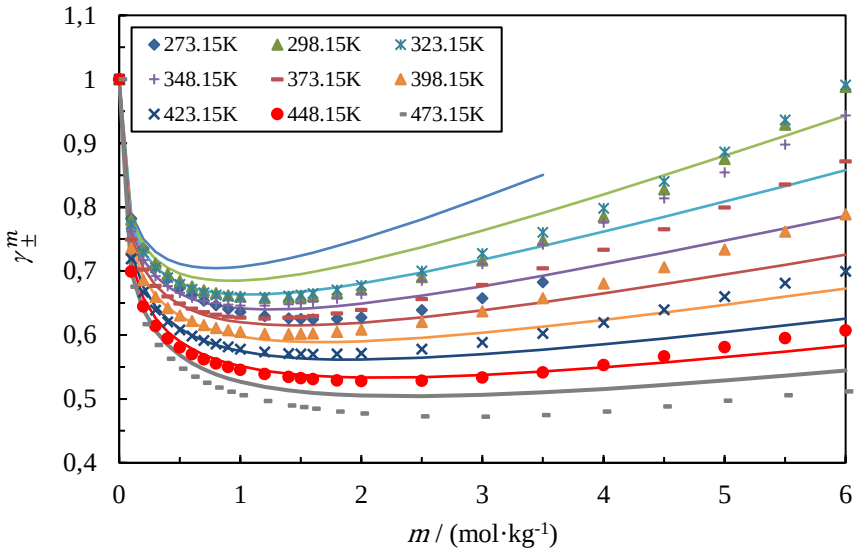

Figure 31 : NaCl mean ionic activity coefficient as a function of salt concentration obtained from the optimisation of model 1.0 using optimisation strategy “b”. The symbols represent the experimental data and the curves the results obtained with the model. The calculations were made at 1 bar for temperatures up to 373.15 K, then the saturation pressure of the solvent was used for temperatures above 373.15 K.

The parameters obtained for model 1.0 using strategy “b” are shown in Table 14. The parameters used to optimise the model are in bold. In dispersive models only water-water association interactions are taken into account. Ion-water dispersion energies are fixed with a value equal to the water-water dispersion energy. Cation-cation and anion-anion dispersion energies are set to 0. The MSA diameter is calculated using equation 54. Born diameter has been fixed using the values presented in Table 4 (see section 3.6). Water-water dispersion and association energies are also fixed [80].

Table 14 : Parameters obtained from the optimisation of model 1.0 using optimisation strategy "b" [a]. Regressed parameters are in bold. ε_{ij} is the dispersion energy, ε_{ij}^{AB} is the association energy, σ_i^{HS}, σ_i^{MSA} and σ_i^{Born} are the hard sphere, MSA and Born diameters respectively.

Parameter	value	Parameter	value
$\varepsilon_{water-Water}/k_B$/ K	201.75	$\boldsymbol{\sigma_{Na}^{HS}}$ / Å	**2.09**
$\varepsilon_{Na-Water}/k_B$/ K	201.75	$\boldsymbol{\sigma_{Cl}^{HS}}$ / Å	**3.45**
$\varepsilon_{Cl-water}/k_B$/ K	201.75	σ_{Na}^{MSA} / Å	3.14
$\boldsymbol{\varepsilon_{Na-Cl}/k_B}$/ **K**	**318.35**	σ_{Cl}^{MSA} / Å	5.17
ε_{Na-Na}/k_B/ K	0.00	σ_{Na}^{Born}/ Å	3.23
ε_{Cl-Cl}/k_B/ K	0.00	σ_{Cl}^{Born}/ Å	4.51
$\varepsilon_{water-Water}^{AB}/k_B$ / K	1813.00		

[a] In dispersive models only water-water association interactions are taken into account. Ion-water dispersion energies are fixed with a value equal to the water-water dispersion energy. Cation-cation and anion-anion dispersion energies are set to 0. The MSA diameter is calculated using equation *(4.11)*. Born diameter has been fixed using the values presented in Table 8.

Table 8. Water-water dispersion and association energies are also fixed [80].

As a conclusion for the dispersive models, it is possible to reach reasonable accuracy on the investigated properties, with the exception of the temperature-dependence of mean ionic activity coefficient (and consequently on enthalpy of solution). It is thus shown that the number of parameters can be reduced without greatly affecting the quality of the model.

4.3.2 Models type 2 (Associative models)

For the case of the associative-type models, the same procedure as described in the previous section is applied.

a. Strategy "a"

Using this strategy, the number of parameters is very large (see Table 6: 10 to 12 parameters).

Table 15 : Absolute relative deviation (ARD) from the optimisations of associative models using optimisation strategy "a". $\gamma_{\pm}^{m}$ is the mean ionic activity coefficient, ϕ is the osmotic coefficient, h^{sol} is the enthalpy of solution and $v_{\pm}$ is the apparent molar volume. In bold the results of the model with the lowest ARD.

	Model 2.0 $AARD_j$ / %	Model 2.1 $AARD_j$ / %	Model 2.2 $AARD_j$ / %
$\gamma_{\pm}^{m}$	**1.02**	2.07	1.63
ϕ	**2.97**	2.49	1.60
h^{sol}	**16.99**	31.54	23.15
$v_{\pm}$	**4.96**	8.58	5.70

In Table 15 the AARD (%) obtained with optimisation strategy "a" applied to the associative models are shown, and in Table 16 the corresponding parameters are presented. As shown in Figure 32, model 2.0 leads to a very accurate representation of the mean ionic activity coefficient with respect to not only salt concentration, but also temperature, in contrast to dispersive models. This same type of behaviour is found in model 2.2, but with lower accuracy. This may be the result of the fact that there are several minima and with the model 2.2 (which is almost equivalent to the model 2.0, see section 4.3.1.a.III) a local minimum was reached. In contrast, model 2.1 only reproduces the behaviour of the mean ionic activity coefficient and osmotic coefficient with respect to the salt concentration. As can be seen in Table 15, the deviation of the enthalpy of solution of model 2.1 is almost twice the deviation of model 2.0.

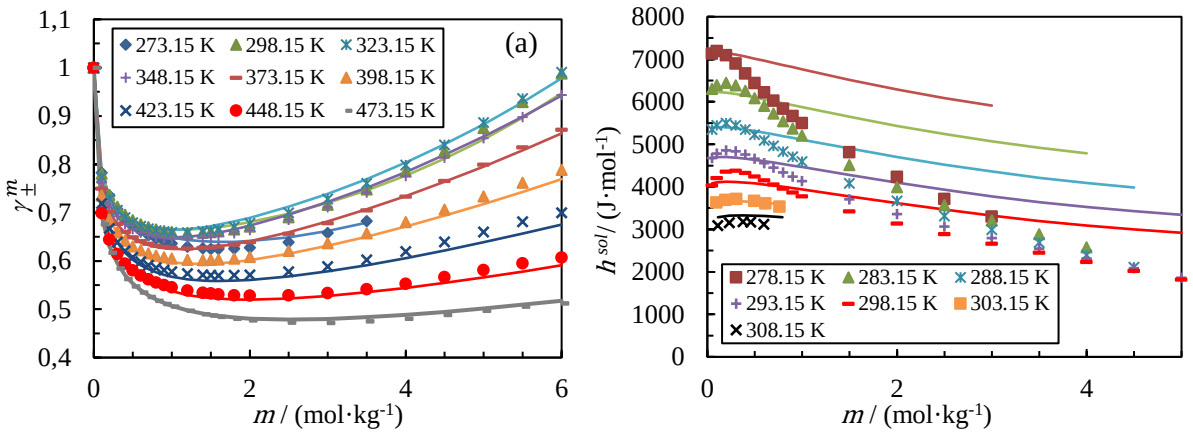

Figure 32 : (a) NaCl mean ionic activity coefficient and (b) enthalpy of solution as a function of the salt concentration obtained from the optimisation of model 2.0 using optimisation strategy "a". The symbols represent the experimental data and the curves represent the results obtained with the model. The calculations were made at 1 bar for temperatures up to 373.15 K, then the saturation pressure of the solvent was used for temperatures above 373.15 K.

Figure 32 and Figure 33 show the mean ionic activity coefficient and enthalpy of solution results for models 2.0 and 2.1, respectively. In Figure 32, it can be observed that model 2.0 can reproduce qualitatively the behaviour of the enthalpy of solution with respect to the salt concentration. In contrast, model 2.1 does not reproduce this behaviour (see Figure 33). The relationship between the slope of enthalpy of solution curve and the temperature behaviour of the mean ionic activity coefficient was pointed out theoretically in section 2.6.4. Here, it can be seen that the model correctly follows the theory: only model 2.0, that has the correct enthalpy of solution slope is able to follow the mean ionic activity coefficient trend with a maximum value close to 323 K.

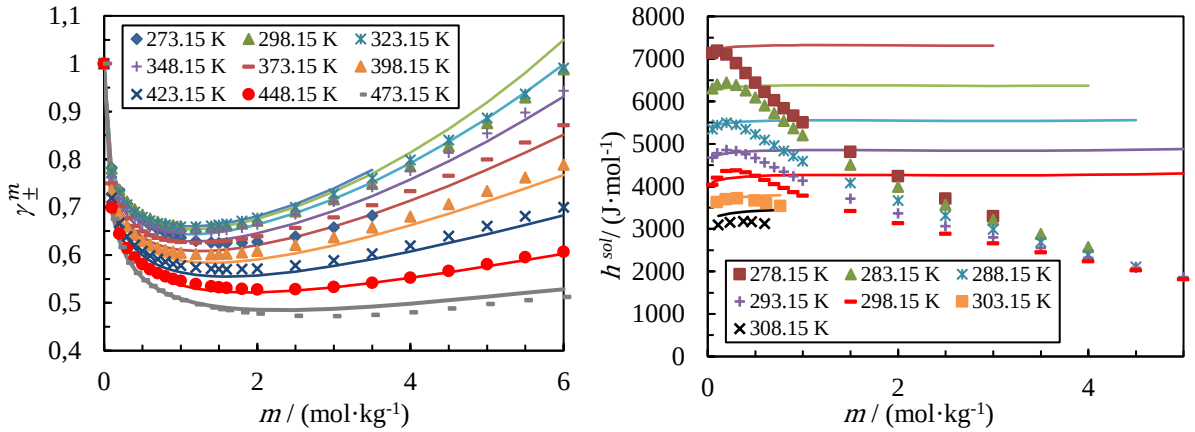

Figure 33 : (a) NaCl mean ionic activity coefficient and (b) enthalpy of solution as a function of salt concentration obtained from the optimisation of model 2.1 using optimisation strategy "a". The symbols represent the experimental data and the curves represent the results obtained with the model. The calculations were made at 1 bar for temperatures up to 373.15 K, then the saturation pressure of the solvent was used for temperatures above 373.15 K.

As with the dispersive models, the parameters are checked for their physical consistency. Table 16 shows a summary of the parameters obtained for the associative models with the optimisation strategy "a". Due to the association scheme, the interaction between two ions is only possible if they are of different charges. Thus, in contrast to dispersive models, associative models do not consider short range cation-cation and anion-anion interactions. Hence, the physical consistency analysis focuses only on adjusted diameters, with the same criterion as for dispersive model.

Table 16 : Parameters obtained from the optimisation of associative models using the optimisation strategy "a" a. In bold, inconsistencies regarding diameters. ε_{ij}^{AB} is the association energy, $k_{Na-Water}^{AB}$ is the association volume, σ_i^{HS}, σ_i^{MSA} and σ_i^{Born} are the hard sphere, MSA and Born diameters respectively, $\alpha_0 ion$ and $\alpha_T ion$ are the adjustable parameters of the Simonin dielectric constant.

Parameters	Model 2.0	Model 2.1	Model 2.2
$\varepsilon_{water-Water}/k_B$ / K		201.61	
$\varepsilon_{Na-Water}^{AB}/k_B$ / K		1813.00	
$\varepsilon_{Na-Water}^{AB}/k_B$ / K	2132.21	2450.28	1762.99
$\varepsilon_{Cl-Water}^{AB}/k_B$ / K	2319.02	1994.12	2981.09
$\varepsilon_{Na-Cl}^{AB}/k_B$ / K	2410.64	2100.38	871.87
$k_{Na-Water}^{AB}$	0.005	0.064	0.003
$k_{Cl-water}^{AB}$	0.02	0.003	0.016
k_{Na-Cl}^{AB}	0.002	0.002	0.001
σ_{Na}^{HS} / Å	1.00	1.42	4.08
σ_{Cl}^{HS} / Å	4.17	4.32	**2.01**[3]

σ_{Na}^{MSA} / Å	5.86	**1.00**[(2)]	3.97
σ_{Cl}^{MSA} / Å	**2.00** [(1)]	6.24	6.64
σ_{Na}^{Born} / Å		3.23	
σ_{Cl}^{Born} / Å		4.51	
$\alpha_0 ion$	-	-	-0.047
$\alpha_T ion$	-	-	-0.003

[a] In associative models only water-water dispersion interactions are taken into account. Born diameter has been fixed for all models using the values presented in Table 8 (see section 4.2.3.1). Water-water dispersion and association energies are also fixed [80].

(1) $\sigma_{Cl}^{MSA} < \sigma_{Cl}^{HS}$

(2) $\sigma_{Na}^{MSA} < \sigma_{Na}^{HS}$

(3) $\sigma_{Cl}^{HS} < \sigma_{Na}^{HS}$

In Table 16 the diameters that do not meet the consistency criterion are highlighted. None of the models have physically consistent parameters. It should be noted that all parameters that are not physically consistent reach the lower limit imposed in the optimisations. This may be an indicator that the models are over-parameterised. Sensitivity analysis has therefore been used to verify the impact of the parameters on the objective function, and to reduce the number of parameters used for optimisation in strategy "b".

b. **Sensitivity analysis**

Table 17 shows the result of the GSA for model 2.0, which leads to the best results in strategy "a". The procedure is identical as that which was used for the dispersive models presented in section 4.3.1 (b).

A similar conclusion is reached as for dispersive models: the most influential parameters are the hard sphere diameters and the interaction energy between cation and anion ($\varepsilon_{\mathrm{Na-Cl}}^{AB}$). In contrast to the dispersive models, the cation-water association energy ($\varepsilon_{\mathrm{Na-water}}^{AB}$) and the cation-anion association volume (κ_{Na-Cl}^{AB}) are also found to have an important impact on the objective function. However, there are two elements that can be used to reduce the number of parameters. Firstly, as can be seen in Table 17 the effect of the association energy is significantly larger compared to that of the association volume. Therefore, the association volume between cation and anion can be set to any arbitrary value (value of water in this work).

Table 17 Results from the sensitivity analysis of model 2.0. [a]. ε_{ij} is the dispersion energy, σ_i^{HS} and σ_i^{MSA} are the hard sphere and MSA diameters respectively. The most sensitive parameters are highlighted in bold

Parameters	Total effect (%)				
	Total OF	$\gamma_{\pm}^{m}$ sOF	h^{sol} sOF	ϕ sOF	$v_{\pm}$ sOF
$\boldsymbol{\varepsilon_{Na-Water}^{AB}/k_B}$ / K	**13.742**	**29.362**	**21.892**	**4.582**	0.13
$\varepsilon_{Cl-Water}^{AB}/k_B$ / K	6.361	11.29	12.435	4.414	0.179
$\varepsilon_{Na-Cl}^{AB}/k_B$ / K	**76.754**	**59.273**	**93.517**	**83.981**	0.106
$\kappa_{Na-Water}^{AB}$	2.036	4.357	3.81	0.399	0.117
$\kappa_{Cl-water}^{AB}$	0.794	0.921	3.787	0.408	0.116
$\boldsymbol{\kappa_{Na-Cl}^{AB}}$	**13.182**	**12.099**	**15.162**	**14.879**	0.103
$\boldsymbol{\sigma_{Na}^{HS}}$ / Å	**10.945**	**18.577**	**3.839**	**6.82**	**76.44**
$\boldsymbol{\sigma_{Cl}^{HS}}$ / Å	**11.244**	**22.572**	**3.598**	**7.605**	**63.54**
σ_{Na}^{MSA} / Å	4.375	11.544	3.62	0.478	0.103
σ_{Cl}^{MSA} / Å	2.099	3.691	3.691	0.507	0.168

[a] OF means Objective Function. The Total OF is that which is used for the parameter regression; It is the sum of four contributions: the mean ionic activity coefficient ($\gamma_{\pm}^{m}$), the enthalpy of solution (h^{sol}), the osmotic coefficient (ϕ) and the apparent molar volume ($v_{\pm}$).

Secondly, the response surface of the hard sphere diameters (Figure 34) shows that there is a correlation between the two ions in the same way as for dispersive models (Figure 30). Figure 34 also shows that the experimental Pauling diameter of the cation (1.9 Å) is located in a reasonably flat zone. For this reason, the value of the cation hard sphere diameter is set equal to the Pauling diameter.

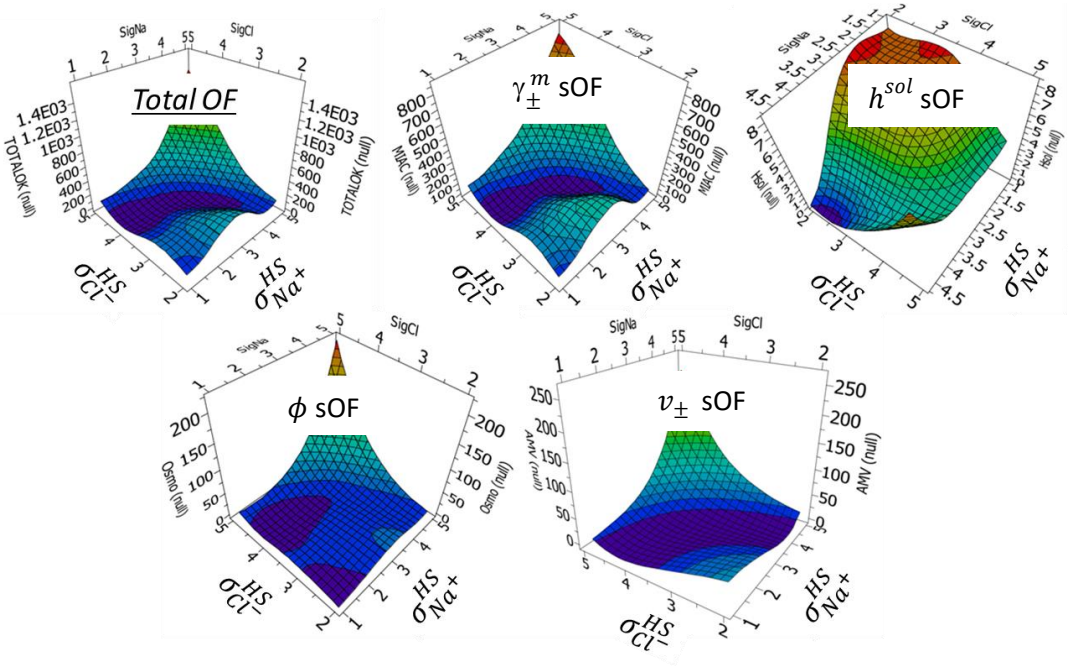

Figure 34 : Model 2.0 response surface of the hard sphere diameters for the total objective function and the mean ionic activity coefficient ($\gamma_{\pm}^{m}$), enthalpy of solution (h^{sol}l), osmotic coefficient (ϕ) and apparent molar volume ($v_{\pm}$) sub-objective functions. All other parameters are taken at their optimal value (Table 16).

Finally, as for dispersive model, the parameters $\alpha_{0,ion}$ and $\alpha_{T,ion}$ are close to zero, indicating again that taking explicitly into account salt effect in dielectric constant has no real effect on the results. Cation-water and anion-water association volumes are observed to have a poor impact on the objective function, compared to other parameters. To reduce the number of adjustable parameters, their values are fixed to that of water, as was done in previous studies [60, 80]. The MSA diameter does not have a high impact on the objective function and is fixed using equation (4.11).

c. **Strategy "b"**

From the sensitivity analysis and taking into account the discussion presented above, the three parameters that will be used for the regression with strategy "b" are, cation-solvent association energy ($\varepsilon^{AB}_{Na-Water}/k_B$), cation-anion association energy ($\varepsilon^{AB}_{Na-Cl}/k_B$) and anion hard sphere diameter (σ^{HS}_{Cl}).

Table 18 : Comparison of the best results obtained using optimisation strategy "a" (model 2.0 - 10 parameters), with the results obtained using optimisation strategy "b" (model 2.0 – 3 parameters). $\gamma_{\pm}^{m}$ is the mean ionic activity coefficient, ϕ is the osmotic coefficient, h^{sol} is the enthalpy of solution and $v_{\pm}$ is the apparent molar volume.

Strategy	AARD$_j$ / %			
	$\gamma_{\pm}^{m}$	ϕ	h^{sol}	$v_{\pm}$
a (Model 2.0)	1.02	2.97	16.99	4.96
b (Model 2.0)	3.56	5.61	34.58	14.01

In Table 18 the comparison of the AARD results of model 2.0 using optimisation strategy "a" and "b" are presented. The deviations are similar for the mean ionic activity coefficient and osmotic coefficient (difference less than 3% in both cases). However, the AARD for enthalpy of solution is more than double and almost triple for apparent molar volume. In Figure 35 the quality of this new model is seen. The model can describe the mean ionic activity coefficient as a function of concentration, but only at intermediate temperatures, and incapable to capture the slope of enthalpy of solution. The increase in the deviation of the apparent molar volume can be attributed to the fact that in strategy "b", only the hard sphere diameter of the

anion has been optimised, while this property is strongly dependent on the hard sphere diameter of both ions.

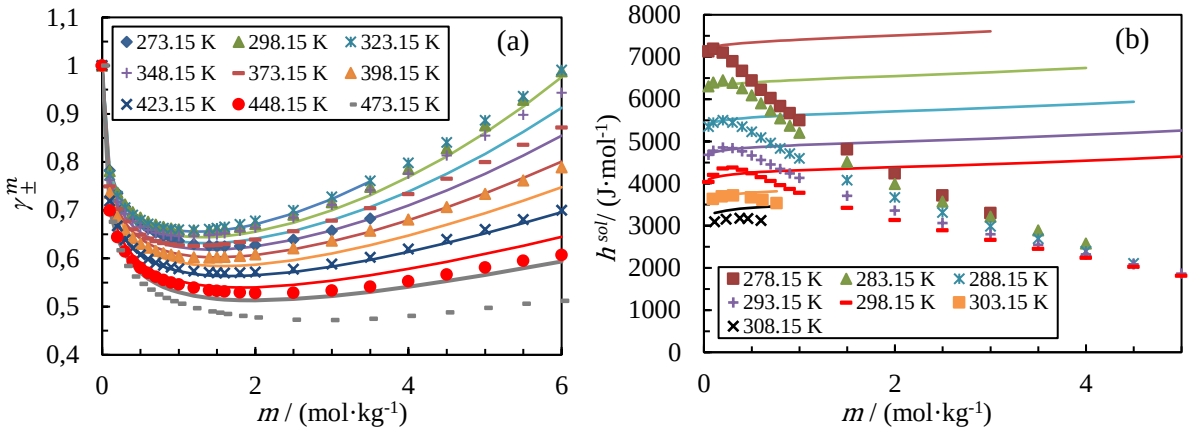

Figure 35 : (a) Mean ionic activity coefficient and (b) enthalpy of solution as a function of salt concentration obtained from the optimisation of model 2.0 using optimisation strategy "b". The symbols represent the experimental data and the curves represent the results obtained with the model. The calculations were made at 1 bar for temperatures up to 373.15 K, then the saturation pressure of the solvent was used for temperatures above 373.15 K.

Table 19 presents the parameter values obtained for model 2.0 using strategy "b". In bold the parameters used to optimise the model.

Table 19 : Parameters obtained from the optimisation of model 1.0 using optimisation strategy "b" [¤]. Only bold parameters are regressed. ε_{ij}^{AB} is the association energy, $k_{Na-Water}^{AB}$ is the association volume, σ_i^{HS}, σ_i^{MSA} and σ_i^{Born} are the hard sphere, MSA and Born diameters respectively.

Parameter	value	Parameter	value
$\varepsilon_{water-Water}^{AB}/k_B$ / K	1813.00	$\varepsilon_{water-Water}/k_B$ / K	201.61
$\varepsilon_{Na-Water}^{AB}/k_B$ / K	**2617.86**	σ_{Na}^{HS} / Å	1.9
$\varepsilon_{Cl-Water}^{AB}/k_B$ / K	1813.00	σ_{Cl}^{HS} / Å	**3.96**
$\varepsilon_{Na-Cl}^{AB}/k_B$ / K	**2047.78**	σ_{Na}^{MSA} / Å	2.85
$k_{Na-Water}^{AB}$	0.044	σ_{Cl}^{MSA} / Å	5.94
$k_{Cl-water}^{AB}$	0.044	σ_{Na}^{Born} / Å	3.23
k_{Na-Cl}^{AB}	0.044	σ_{Cl}^{Born} / Å	4.51

[¤] In associative models only water-water dispersion interactions are taken into account. Anion-water association energy, ion-water association volume and cation-anion association volume are fixed with a value equal to the water-water association energy and water-water association volume respectively. The cation hard sphere diameter is fixed with the Pauling diameter. The MSA diameter is calculated using equation *(4.11)*. Born diameter has been fixed using the values presented in Table 8. Water-water dispersion and association energies are also fixed [80].

As a conclusion on the use of associative models, it appears that the large number of parameters makes it possible to reach a very nice representation of the data, but at the price of non-physical parameters. The most important parameters are the cation-anion interaction

energy. It is observed that when the number of parameters is reduced in such a way as to make the order of the diameters physically meaningful, it becomes impossible to represent correctly the enthalpy of solution and the temperature trend of the mean ionic activity coefficient.

4.4 Discussion

Having settled on two modelling approaches that provide equivalent results, we can now evaluate their behavior on various salts and properties. In this section, we first evaluate how the model can be extrapolated to other salts. We then present how the use of the full model impacts the Gibbs energy of solvation and finally, a discussion is proposed on single ionic activity coefficients. The salts considered are NaCl, KCl, NaBr and KBr. In Table 20 the temperature and concentration range of the experimental data used for each salt are presented.

Table 20 : Number of experimental data points (Npt^j), temperature and concentration range of each property used for the optimizations of models 1.0 and 2.0 [a]. $\gamma_{\pm}^{m}$ is the mean ionic activity coefficient, ϕ is the osmotic coefficient, h^{sol} is the enthalpy of solution and $v_{\pm}$ is the apparent molar volume.

Salt		$\gamma_{\pm}^{m}$	ϕ	h^{sol}	$v_{\pm}$	Reference
KCl	Npt^j	82	120	64	75	[186–193]
	Temperature range / K	273.15-323.15	273.15-413.15	298.15-348.15	273.15-323.15	
	Molality range / mol.kg^{-1}	0 - 4.5	0 - 5.2	0 - 0.6	0.3 - 1	
NaBr	Npt^j	133	233	17	24	[179, 194–197]
	Temperature range / K	273.15-333.15	298.15-498.15	298.15-333.15	298.15	
	Molality range / mol.kg^{-1}	0 - 9.5	0 - 10.6	0 - 0.2	0 - 8.3	
KBr	Npt^j	29	286	52	52	[179, 195, 197–200]
	Temperature range / K	298.15	298.15-498.15	283.15-313.15	313.15-553.15	
	Molality range / mol.kg^{-1}	0 - 5.5	0 - 7.5	0 - 6	0.1 - 1.5	

[a] Uncertainty ($err(\%) - e^j$) and data serial weight (w_s^j) are the same for all salts and are presented in Table 4.

4.4.1 Model extension to 4 salts

Using the approaches chosen in the previous section, an extension has been made to model the same properties in aqueous solution of 4 salts, using the strategy “b” previously described (3 adjustable parameters per salt). The deviations with respect to the data whose references and those provided in Table 4 and Table 20 are given in Table 21. The resulting parameters from the model optimisation are shown in Table 22. Note that the parameters for NaCl have been re-optimised. This was done to find parameters that work well for salts that share the same ions (NaCl, KCl, NaBr).

Table 21 : Absolute relative deviations (ARD) from optimisation of models 1.0 and 2.0 using optimisation strategy "b". $\gamma_{\pm}^{m}$ is the mean ionic activity coefficient, ϕ is the osmotic coefficient, h^{sol} is the enthalpy of solution and $v_{\pm}$ is the apparent molar volume.

	Model 1.0 (Dispersive model)				Model 2.0 (Associative model)			
	NaCl	KCl	NaBr	KBr	NaCl	KCl	NaBr	KBr
	AARD$_j$ / %							
$\gamma_{\pm}^{m}$	3.98	3.56	6.17	3.53	3.90	1.54	5.53	1.16
ϕ	6.18	4.14	7.60	6.03	7.19	1.42	7.70	2.19
h^{sol}	42.16	1.16	2.95	7.54	40.46	1.06	2.83	5.53
$v_{\pm}$	6.86	6.23	22.26	6.06	10.90	36.23	39.22	4.06

Table 22 : Parameters obtained from the optimisation of model 1.0 and 2.0 using optimisation strategy "b", for aqueous NaCl, KCl, NaBr and KBr [a]. Only bold parameters are regressed. $\boldsymbol{\sigma_i^{HS}}$, $\boldsymbol{\sigma_i^{MSA}}$ and $\boldsymbol{\sigma_i^{Born}}$ are the hard sphere, MSA and Born diameters respectively. $\boldsymbol{\varepsilon_{ij}}$ is the dispersion energy, $\boldsymbol{\varepsilon_{ij}^{AB}}$ is the association energy, $\boldsymbol{k_{Na-Water}^{AB}}$ is the association volume.

	Model 1.0 (Dispersive model)				Model 2 (Associative model)			
Parameters	NaCl	KCl	NaBr	KBr	NaCl	KCl	NaBr	KBr
$\boldsymbol{\sigma_{cation}^{HS}}$ / Å	**2.11**	**3.46**	**2.11**	**3.46**	1.90	2.66	1.90	2.66
$\boldsymbol{\sigma_{anion}^{HS}}$ / Å	**3.32**	**3.32**	**3.48**	**3.48**	**3.84**	**3.84**	**3.69**	**3.69**
σ_{cation}^{MSA} / Å	4.34	4.15	4.34	4.15	2.85	3.99	2.85	3.99
σ_{anion}^{MSA} / Å	4.53	4.53	5.21	5.21	5.76	5.76	5.54	5.54
σ_{Na}^{Born} / Å	3.23							
σ_{Cl}^{Born} / Å	4.51							
$\varepsilon_{water-Water}/k_B$ / K	201.61							
$\varepsilon_{cat-Water}/k_B$ / K	201.61	201.61	201.61	201.61	-	-	-	-
$\varepsilon_{ani-water}/k_B$ / K	201.61	201.61	201.61	201.61	-	-	-	-
$\boldsymbol{\varepsilon_{cat-ani}/k_B}$ / K	**26.76**	**238.61**	**5.43**	**198.18**	-	-	-	-
$\varepsilon_{cat-cat}/k_B$ / K	0.00	0.00	0.00	0.00	-	-	-	-
$\varepsilon_{ani-ani}/k_B$ / K	0.00	0.00	0.00	0.00	-	-	-	-
$\boldsymbol{\varepsilon_{water-Water}^{AB}/k_B}$ / K	1813.00							
$\boldsymbol{\varepsilon_{cat-Water}^{AB}/k_B}$ / K	-	-	-	-	**1270.11**	**1531.28**	**1270.11**	**1531.28**
$\varepsilon_{ani-Water}^{AB}/k_B$ / K	-	-	-	-	1813.00	1813.00	1813.00	1813.00
$\boldsymbol{\varepsilon_{cat-ani}^{AB}/k_B}$ / K	-	-	-	-	**0.00**	**0.00**	**0.00**	**201.16**
$k_{cat-Water}^{AB}$	-	-	-	-	0.04	0.04	0.04	0.04
$k_{ani-water}^{AB}$	-	-	-	-	0.04	0.04	0.04	0.04

$k_{cat-ani}^{AB}$	-	-	-	-	0.04	0.04	0.04	0.04

[a] In dispersive model 1.0 only water-water association interactions are taken into account. In associative model 2.0 only water-water dispersion interactions are considered Ion-water dispersion energies are fixed with a value equal to the water-water dispersion energy. Cation-cation and anion-anion dispersion energies are set to 0. Anion-water association energy, ion-water association volume and cation-anion association volume are fixed with a value equal to the water-water association energy and water-water association volume respectively. The cation hard sphere diameter is fixed with the Pauling diameter. The MSA diameter is calculated using equation 54. Born diameter has been fixed using the values presented in Table 8 (see section 4.2.3.1). Water-water dispersion and association energies are also fixed [80].

Several observations can be made.

4.4.1.1 Regarding the comparison between the two models

The global observation is that the two models are equally able to represent the four salts considered: the deviations are generally of the same order of magnitude (up to 6% for mean ionic activity coefficient and up to 8% for osmotic coefficient). Regarding the enthalpy of solution, only the NaCl deviations are significant, which is easily explained by the fact that only for this salt, high concentration enthalpies of solution are available. Concerning apparent molar volume, those of KCl and NaBr seem particularly difficult to capture correctly. It is important to remember that the apparent molar volume expresses the change in the volume of the solution when salt is added, this property is very sensitive and generates very small values, so it is difficult to obtain low deviations. The sensitivity analysis performed for the NaCl aqueous solution showed that the apparent molar volume is particularly sensitive to the variation of the hard sphere diameter. This explains why higher ARDs are obtained with the 2.0 model, as in this model only the HS diameter of the anions was optimised.

4.4.1.2 Regarding the parameter values.

Vaque Aura *et al.* [28] discussed how the shape of the mean ionic activity coefficient curve illustrates the competing tendency of ion solvation (curve leans upward) and ion pairing (curve leans downward). In the SAFT models, this competition can be made visible by comparing respectively the ion-water and ion-ion interaction parameters. According to Vaque Aura et al., the order of most solvating (least pairing) to least solvating (most pairing) salts is as follows: NaBr > NaCl > KBr > KCl, this same trend can be seen in the experimental data at 298.15 K in Figure 36. Looking at the magnitude of the model 1.0 parameters, where only ion-pairing parameters have been allowed to change, it appears indeed that NaBr has the lowest ion-pair interaction energy, while KBr and KCl have the highest values, KCl showing the highest value. The trend of these parameters agrees with the conclusions of Vaque Aura et al. [28]. For model 2.0, the association parameters are fitted. Almost all ion pair parameters are zero, pointing to full dissociation, except for KBr. For this last salt, it is true that 201 K is extremely small, and can therefore be considered zero as well. Hence, for this model, the

solvation (ion-water) parameters should be used as a guide. Yet, here the trend seems opposite: the salts that are expected to "solvate" more have a smaller cation-water interaction energy. This may be caused by the imposed value of the association energy of the anion with water, that is larger than the one that is found between cation and water. It is known that cations are more solvated than anions [49].

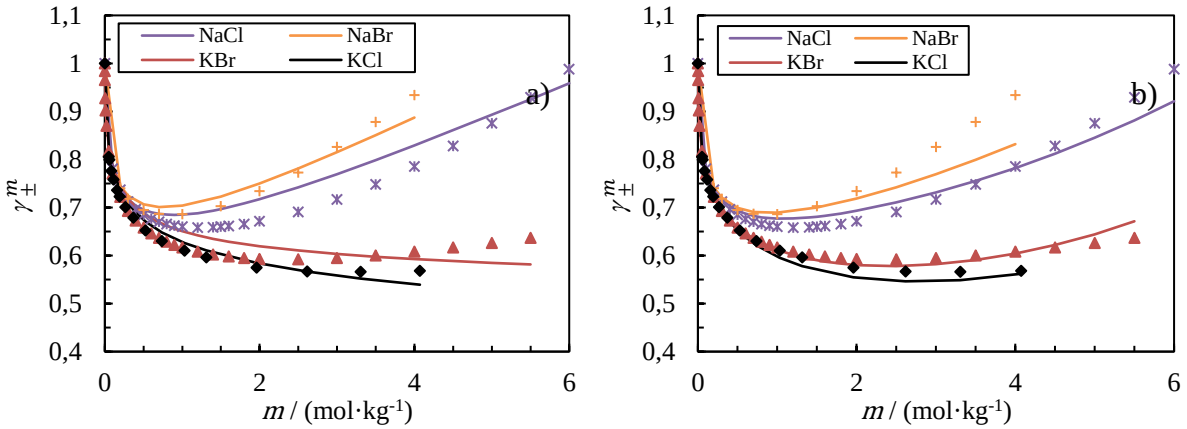

Figure 36 : Comparison of the mean ionic activity coefficient calculation for NaBr, NaCl, KBr and KCl salts at 298 K. (a) using model 1.0 and (b) using model 2.0. The symbols are the experimental data and the curves represent the model. Calculations were made at 1 bar.

As can be seen in Figure 36, both models follow the trend of the experimental data. Model 2.0 generates better results, especially for KBr and KCl salts.

The trend of the hard sphere ionic parameters is shown in Figure 37. The MSA diameters are systematically obtained by multiplying the hard sphere diameter by 1.5 (see equation (4.11)). It appears that for the model 2.0, the fitted parameters are very close to those of Pauling, except for the diameter of the ion Br^- which is smaller than the Pauling diameter. For model 1.0, a small inversion is observed, the diameter of the potassium is larger than the diameter of the chlorine.

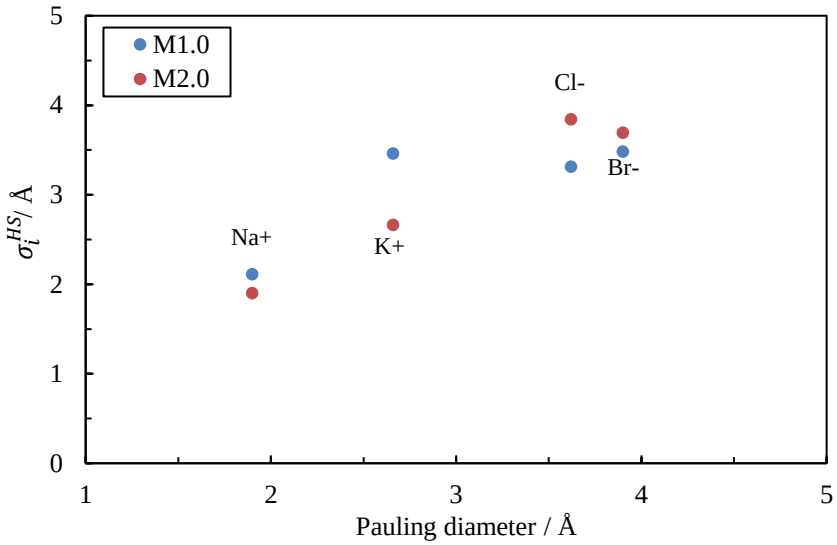

Figure 37 : Comparison of the hard sphere diameters obtained for the models 1.0 (M1.0) and 2.0 (M2.0), with the Pauling diameter. Blue points are dispersive model 1.0 and red points are associative model 2.0.

4.4.1.3 Regarding the maximum of mean ionic activity coefficient with temperature

As shown by Vaque Aura et al. [28], the dependence of the mean ionic activity coefficient with temperature for the 4 salts considered presents an increase and in some cases a maximum, as can be seen in Figure 38. As mentioned above, this type of behaviour is difficult to capture, even for NaCl, where the enthalpy of solution values that are included in the objective function reach large molalities (up to 5 molal as shown for example in Figure 32(b)). For all other salts, the deviations on the enthalpy of solution are very small because the data are insignificant (concentration below 0.6 molal), and as a consequence, the mean ionic activity coefficient continually decreases with temperature.

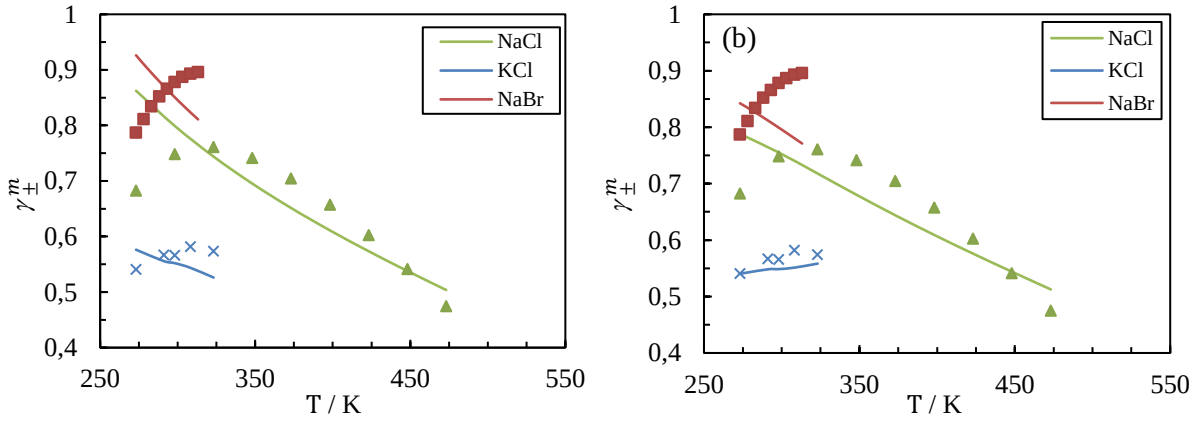

Figure 38 : Variation of mean ionic activity coefficient with respect to temperature at 3.5 molal. The dots represent the experimental data and the curves the model. (a) Model 1.0 and (b) Model 2.0.

A possible way to correct the model is to include temperature-dependent interaction parameters. Using dispersive models, this has been done in the past [201]. For model 2.0, the framework of the association term leads to a decrease of association force when temperature increases. It is not designed to allow for changing this dependence.

4.4.2 Representation of the Gibbs energy of solvation

Even though the Born radius is calculated from the Gibbs energy of solvation, it is worth assessing if this property can be described accurately. Using the SAFT framework, the Gibbs energy of solvation of an ion is directly related to the fugacity coefficient of that ion at infinite dilution in water:

$$\frac{\Delta_s G_i}{RT} = ln(\varphi_i^{\infty}) = \frac{1}{RT}\left(\sum \frac{\partial A^{\infty}}{\partial n_{ion}}\right) - ln\left(\frac{Z}{Z^{\infty}}\right) \qquad (4.12)$$

In Table 23 the experimental values of the Gibbs energy of solvation and the calculated values for all the ions used in this work are shown. The calculated values were obtained using the parameters presented in Table 22. The AARD (%) of the calculated values does not exceed 5% with either model 1.0 or model 2.0.

Table 23 : Comparison between the experimental and calculated Gibbs energy of solvation for Na+, K+, Cl- and Br- ions, using dispersive and associative models [a]. $\Delta_s G_i Exp.$ is the experimental Gibbs energy of solvation and $\Delta_s G_i$ Calc is the Gibbs energy of solvation calculated with each model.

Cation	$\Delta_s G_i$ Exp. / kJ/mol [51]	$\Delta_s G_i$ Calc. / kJ/mol M1.0	$\Delta_s G_i$Calc. / kJ/mol M2.0	Anion	$\Delta_s G_i$Exp. / kJ/mol [51]	$\Delta_s G_i$Calc. / kJ/mol M1.0	$\Delta_s G_i$Calc. / kJ/mol M2.0
Na^+	-424.00	-429.44	-423.75	Cl^-	-304.00	-308.29	-313.69
K^+	-352.00	-358.16	-360.85	Br^-	-278.00	-281.88	-289.33

[a] The calculation of the Gibbs energy of solvation was done using the parameters presented in Table 22. M1.0 refers to the dispersive model 1.0 and M2.0 refers to the associative model 2.0.

4.4.3 Single ionic activity coefficients (SIAC)

A number of authors [41, 42] have tried to obtain data for the individual activity coefficient of the ions. For the NaCl salt, their results show that the activity coefficient of the cation is higher than the activity coefficient of the anion. This may indicate that the cation is more solvated than the anion. To compare models 1.0 and 2.0 with these results, the individual activity coefficient for NaCl was calculated using the parameters presented in Table 22.

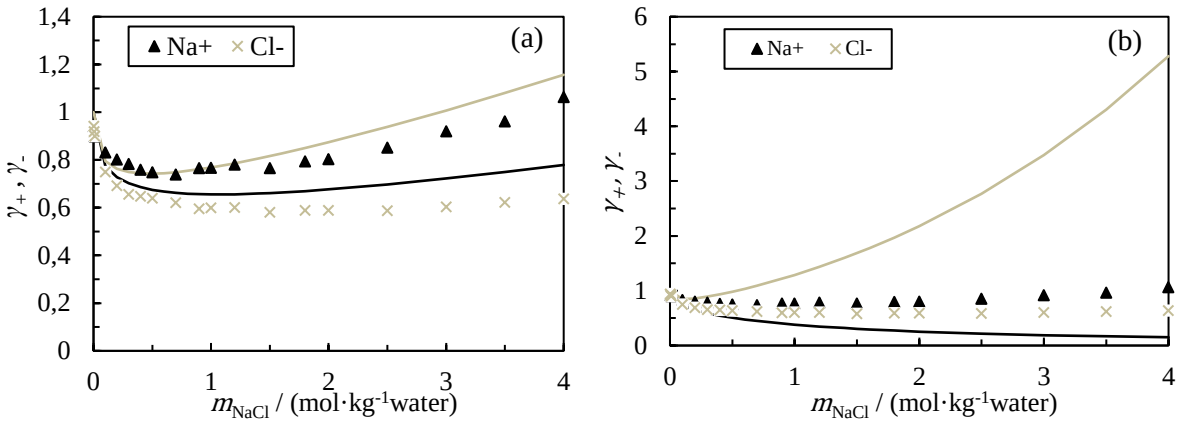

Figure 39 Individual activity coefficient (γ_+, γ_-) of chloride and sodium as a function of salt concentration at 298.15 K. (a) using model 1.0, (b) using model 2.0. The dots represent the experimental data [42] and curves the model. Calculations were made at 1 bar.

In Figure 39(a) model 1.0 shows an inverse behavior compared to the experimental data. Although the parameters appear to be physically consistent, the model is not able to reproduce this property correctly. This may be because the two dispersion energies are equal. In Figure 39(b) the trend is also inverse. This behaviour may be due to the very high value of the association energy of the anion (chlorine). For model 2.0 the association energy of the cation (sodium) was used as an adjustable parameter. Therefore, it may be assumed that this parameter compensates for the excess solvation of the anion, by decreasing the association energy of the cation. This would explain why the association energies of both ions in model 2.0 show an inverse behaviour to the expected one.

4.4.4 Comments on the contribution to the natural logarithm of mean ionic activity coefficient

Extracting conclusions by analysing the contribution of each term to the natural logarithm of the MIAC is quite complex. However, some observations have been made by comparing the contribution of terms for dispersive and associative models. In Figure 40 the two models that have been selected as the most accurate ones (in strategy “a”) are compared (the corresponding plots for all models are available in supplementary information B).

In Figure 40(a) the dispersive approach is considered. In this case, both the dispersion and MSA terms generate a negative contribution. They are counterbalanced by the hard sphere, Born and association terms (water-water associations exist in this model, and they have an impact on the ionic activity coefficients). In contrast, the contributions using the association

model, shown in Figure 40(b), the hard sphere term has a negative effect, in addition to MSA, and the association, much larger in magnitude, is the only significant positive contribution. The large, and opposite, contributions of the Hard Sphere term need to be further understood but explain why the ionic hard sphere diameters have a large impact on the result.

The same trends are observed for all sub-models (i.e., using various types of dielectric constant functionalities). The Born contribution is obviously larger when using the Pottel correction, because the dielectric constant decreases much faster, but it does not change the global picture.

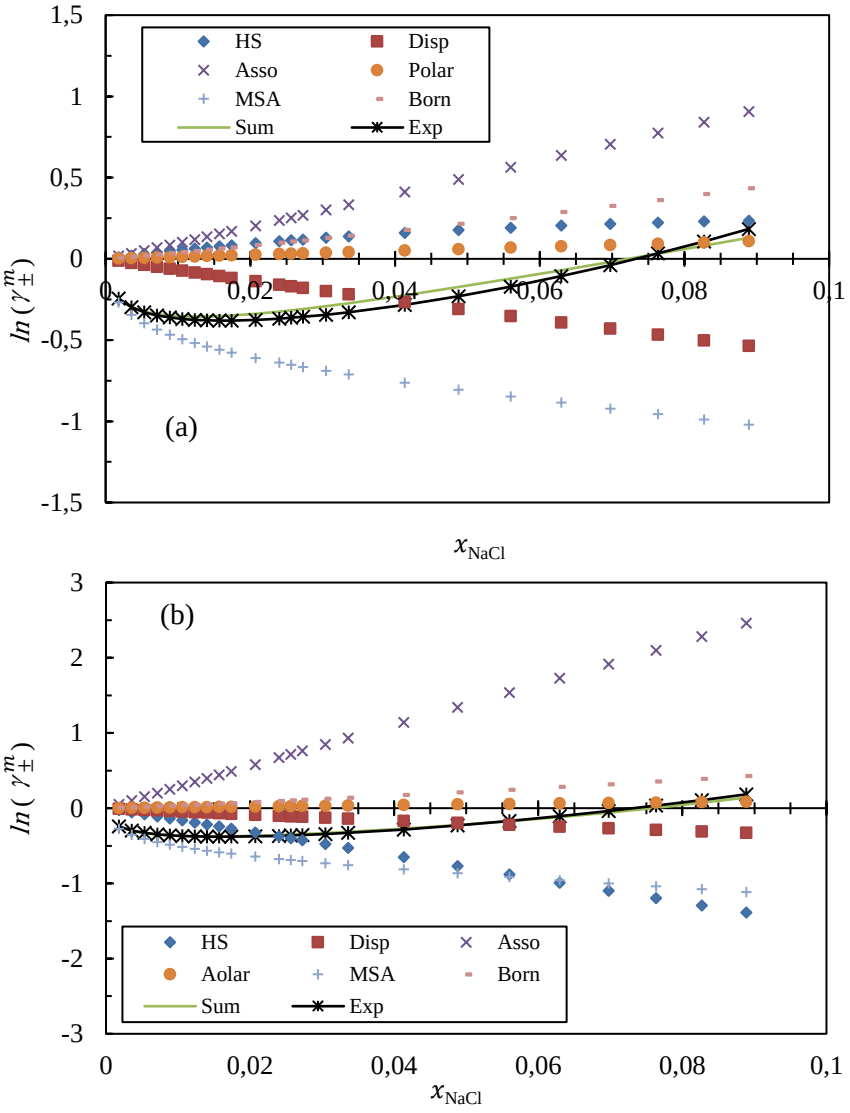

Figure 40 : Effect of the various terms on the natural logarithm of mean ionic activity coefficient for aqueous NaCl as a function of salt concentration at 298 K (a) using model 1.2 and (b) using model 2.0. Where HS=hard sphere, Disp=dispersion, Asso=association, Polar=polar, MSA= MSA and Born=Born terms, Sum = sum of all terms and Exp= experimental mean ionic activity coefficient data.

4.5 Conclusion

The objective of this chapter was to benchmark various PPC-SAFT-based equations of state for describing the concentration and temperature trend of mean ionic activity coefficient, and more particularly at the low temperature, where an anomalous behaviour is observed. To this end, four important properties for NaCl aqueous solutions have been used (mean ionic activity coefficient, osmotic coefficient, enthalpy of solution and apparent molar volume). Three other salts (KBr, KCl, NaBr) have been investigated as extensions in the discussion section.

The use of enthalpy of solution data that cover a large concentration range and a low temperature range (below 323 K) is found to be consistent with a rising value of mean ionic activity coefficient at fixed molality in this low temperature range, resulting effectively in a maximum in the temperature trend close to 320 K (see section 2.6.4). This trend has rarely been pointed out, and it appears that, to the best of our knowledge, no author has attempted to describe it. Our attempts to do so show that it is very difficult to model it for a model with physically consistent parameters. We believe that the only way to reach this goal would be to use temperature-dependent parameters.

Two modelling approaches have been compared. The main difference between the models is the way in which short-range interactions involving ions are considered (solvation interactions and ion pair formation), in addition to the different models used to describe the dielectric constant. The first approach (dispersive models) consists in using a dispersion term, while the second approach (associative models) consists in using the Wertheim association term. In both approaches the MSA term was used to account for long-range electrostatic interactions and the Born term to model electrostatic interactions between ions and solvent. No major difference in the capacity of modelling the target properties was found.

Three different sub-models have been used to calculate the dielectric constant of the solutions. In the present study it is observed that the addition of an explicit salt concentration dependence on top of the implicit Schreckenberg model [136] is not needed for the description of the activity coefficient for the system NaCl + water. The parameters that take into account the salt concentration ($\alpha_{0,ion}$ and $\alpha_{T,ion}$) for the Simonin correction tend to zero. Furthermore, a sensitivity analysis showed that these Simonin parameters have a negligible influence on the

objective function. In most cases, the models in which the Pottel dielectric constant was used gave the worst results. These results may indicate that it is not necessary to use an explicit salt concentration-dependent dielectric constant for the study of electrolytic systems. However, a more detailed study may help further clarifying these observations.

The use of the Born term remains essential, though, for representing Gibbs energies of solvation. For this property, the Born term has the largest impact, as was also shown by Fawcett [51].

This study has also identified the most sensitive parameters in modelling electrolyte solutions with PPC-SAFT, allowing a reduction of the number of adjustable parameters without significantly affecting the quality of the model. Some consistency constraints were also applied to obtain adequate results with physically consistent parameters. For the dispersive model, the hard sphere diameter (σ_i^{HS}) of both ions and the cation-anion dispersion energy ($\varepsilon_{\mathrm{Cat-}Ani}$) were identified as the most influential parameters. For associative model, the most influential parameters were the cation-water association energy $\left(\varepsilon_{Cat-Water}^{AB}\right)$, the cation-anion association energy ($\varepsilon_{Cat-ani}^{AB}$) and the hard sphere diameter of the anion (σ_{anion}^{HS}). In both cases the parameters that consider the interactions between the cation and anion, were found to be quite influential in the model.

Chapter 5 An equation of state for highly concentrated solutions

5.1 Introduction

For any theoretical study of electrolyte solutions, correctly describing the interactions between ions and between ions and solvent is a key point. In the study of strong electrolyte systems, it is usual to assume that the salts are completely dissociated. In aqueous solutions of strong electrolytes at low salt concentrations and room temperature, ion pairing is not significant, because the dielectric constant of the solvent very effectively screens ion-ion interactions [174]. But as the molality of the salt increases, the interactions between the ions become more significant. This is because the average distance between the ions decreases and the ions can form ion pairs or even contact groups separated by the solvent in solution [202].

The success of the Debye-Hückel theory [111] in the 1920s, in which dilute electrolyte solutions were modeled as fully dissociated ions perturbed by long-range Coulombic interactions, led to the almost total eclipse of the ion association models until a few years ago. In the article by Marcus et al. [50] one can read *"[the idea of complete dissociation] was not proposed as a universally valid rule. However…complete dissociation was so attractively simple and harmonized so happily with [other] knowledge that it [passed as such] into popular science.....fomented, no doubt, by the suspicion that deviations from Debye-Onsager theories would find a physical explanation [that did not involve association"]."* According to Marcus, these opinions were favored since most studies focused their attention on aqueous solutions in which the high dielectric constant of water favors ion separation. Even today, many studies still use the assumption that salts dissociate completely, although there are studies [50, 121, 202] indicating the opposite. However, the lack of theories that satisfactorily explain the experimental data (even at modest concentrations), without recourse to empirical parameters, together with the constant accumulation of direct evidence for the existence of ion pairs, is resulting in continued support for the concept of ion pairing.

When talking about ion pair formation, the phenomenon of solvation must also be taken into account. These two types of interactions involving ions are complementary. When solvation interactions decrease the number of ion pairs increases. There are several factors that favor the appearance of ion pairs. The first is the increase in salt concentration. As the salt concentration increases, the number of ions in solution increases, and the amount of solvent molecules available to interact with the ions decreases. Furthermore, at a higher salt concentration the probability of finding an ion close enough to form an ion pair increases.

Some studies [52, 202, 203] show that the difference between the diameters of the salt ions is another determining factor in the formation of ion pairs. According to Collins [52], the combination of two small or two large ions results in an increased trend of ion pairing (see chapter 2.5.2), while the combination of a large ion with a small ion results in an increase in solvation interactions. Collins called this phenomenon the Law of Matching Water Affinities (LMWA). A study by Fennell et al. [202] using molecular simulation, showed that size-symmetric ions compared to size-asymmetric ions associate more easily and form contact ion pairs, which validates the LMWA proposed by Collins. Niazi et al. [203] investigated the effect of ion pairs in strongly concentrated salt solutions. In their study Niazi et al. found that the LiCl salt preferred to form ion pairs, whereas the LiBr salt remained completely dissociated, even at concentrations above 12m, these results being consistent with those of Collins and Fennell. In addition, that study showed that the Br ion interacted strongly with water molecules at high salt concentrations. This suggests that even when the salt concentration is very high, the amount of ion pairs depends strongly on the difference between the diameters.

Das et al. [174] studied the behavior of the mean ionic activity coefficient (MIAC) of 19 alkali-halide salts at high salt concentrations. For this study, the authors used a non-primitive SAFT-VR type equation of state, for which they first optimized the solvent parameters and then optimized the ion-ion association energy, and the cation-solvent dispersion energy. The anion-solvent dispersion energy was not optimized. Although they found that the model could correctly describe the MIAC behavior for salts such as LiCl, and KF (salts with a tendency to form ion pairs), they also found that the model underestimated the MIAC value for salts such as LiBr, where solvation interactions are more present. The problems with the model were attributed to the fact that the anion-solvent dispersion energy was not optimized, and therefore solvation interactions were underestimated. These results highlight the importance of correctly including solvation interactions and ion pair formation, within the models for the study of

highly concentrated electrolyte solutions. It should be noted that to the best of our knowledge, besides the studies performed by Das et al. [174] and Liu et al. [78] (using non-primitive SAFT type equations of state), no other studies have been found with SAFT type equations of state, in which electrolyte solutions at very high salt concentrations (> 6m) are studied.

As discussed several times in this work (see section 2.5.3 and Chapter 4), temperature is another factor that affects the way in which ions interact with each other and with the solvent, and thus the behavior of properties such as MIAC. The increase in temperature causes a decrease in the dielectric constant and consequently an increase in ion pairs. Experimental data show that an increase in temperature generates an increase in the association constant between ions (see Figure 25). In the previous chapter, we presented a study in which we tried to describe the behavior of MIAC with respect to temperature for aqueous NaCl solution. The results showed that the best way to describe this behavior was to use the associative model (using Wertheim's association theory to describe ion-solvent and ion-ion interactions), by adjusting 11 parameters (see section 4.3.2). However, by reducing the number of parameters the associative model lost the ability to describe this behavior. This is because by construction of the quasi-chemical association model (see equation (3.41)), the association constant ($\Delta^{A_iB_j}$) always decreases with the increase of temperature. This behavior is expected for ion-solvent and solvent-solvent interactions but is opposite to the behavior of ion-ion interactions.

In this section we present a modification of the association term for SAFT type equations of state for the study of electrolytic systems at very high salt concentrations. In this chapter, a special attention has been paid to model salts containing the cation Li^+ whose maximum concentration in water can be up to 20m at 298 K. To this end, this section will begin by introducing Bjerrum's theory. Then in chapter 5.3 the modifications to the association term will be discussed. Section 5.4 presents the experimental data as well as the parameterization strategies used. Finally, sections 5.5 and 5.6 present the discussion of the results and conclusions.

5.2 Bjerrum theory

Based on some concepts of the Debye-Hückel theory, Bjerrum [204] was the first to introduce the concept of ion pairs for strong electrolytes [50]. In this model the ions are considered as hard spheres with a diameter σ_i^{HS} and a closest approach σ_{ij}^{HS} (see equation

(3.37)). The ions are also considered to be within a dielectric continuum characterized by the dielectric constant ε_r, and only pairwise interactions are taken into account. The Debye-Hückel theory assumes that the ions are completely dissociated. However, the assumption that the electrostatic energy ($z_j e\psi_i(r_{ij})$) between any two ions i and j at distance (r_{ij}), is much smaller than the average thermal energy ($k_B T$) is not valid for small r_{ij} [131]. Bjerrum's treatment was developed with the aim of compensating for this problem.

The electrostatic work W_{ij} required to separate two ions, i and j, with charges $z_i e$ and $z_j e$, from a distance r_{ij} to infinity is (for $r_{ij} \geq \sigma_{ij}^{HS}$):

$$W_{ij}(r_{ij}) = \frac{|z_i z_j| e^2}{4\pi\varepsilon_o \varepsilon_r r_{ij}} \qquad (5.1)$$

For $r_{ij} < \sigma_{ij}^{HS}$ $W_{ij}(r_{ij}) = -\infty$.

Bjerrum then calculated the probability ($H(r_{ij})$) for an ion i to be at a distance r_{ij} from the ion j.

$$H(r_{ij}) = 4\pi N_A c_i \, exp\left(\frac{W_{ij}(r_{ij})}{k_B T}\right) {r_{ij}}^2 = 4\pi N_A c_i \, exp\left(\frac{|z_i z_j| e^2}{4\pi\varepsilon_o \varepsilon_r k_B T}\frac{1}{r_{ij}}\right) {r_{ij}}^2 \qquad (5.2)$$

Where c_i is the molar concentration of the ion i. Figure 41 shows the probability $H(r_{ij})$ as a function of the distance between the ions (r_{ij}).

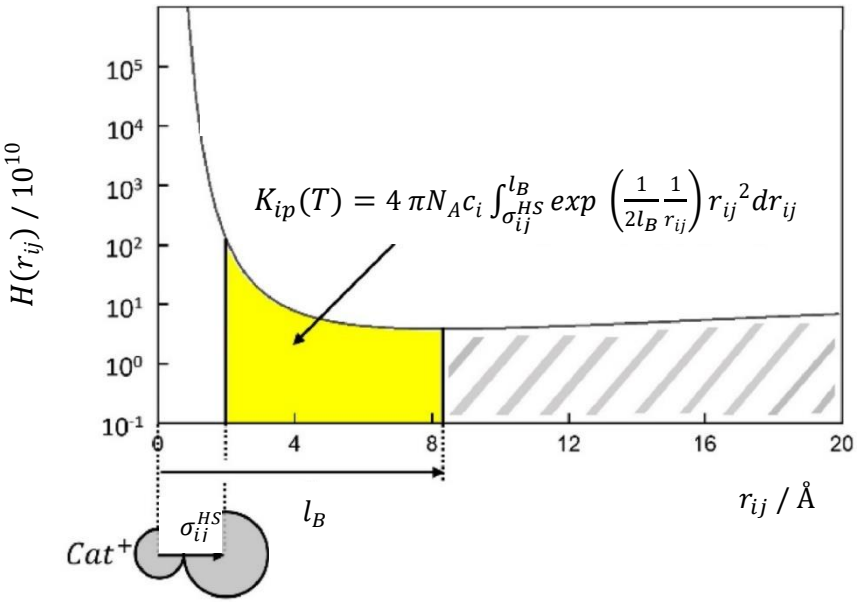

Figure 41 : Graphical representation of the distinction between free ions and ion pairs. The yellow portion represents the area where ion pairing occurs, while the shaded domain represents the area where only free ions are present. [131].

As it can be seen in the Figure 41 the probability $H(r_{ij})$ has a minimum at a distance $r_{ij} = l_B$, the Bjerrum length:

$$l_B = \frac{|z_i z_j| e^2}{8\,\pi \varepsilon_o \varepsilon_r k_B T} \tag{5.3}$$

Bjerrum suggested that up to this distance (from σ_{ij}^{HS} to l_B) all oppositely charged ions form ion pairs, while ions at a greater distance ($r_{ij} > l_B$) should be treated as free ions. Although this distance is arbitrary, Bjerrum argues that choosing it as the cut-off point is reasonable since the work required to separate two ions is then at least twice the thermal energy [50].

The ion pairs are dipolar, and since the charge of the ions is different, it is generally considered that they do not contribute to the conductivity of the electrolyte solution. Free ions participate in the ionic force of the medium and are subject to the resulting electrostatic effects, which must be taken into account through the Debye-Hückel theory or the primitive MSA. Bjerrum also considered that ion pairs and free ions are in chemical and thermodynamic equilibrium. Using the law of mass action, for the reaction

$$C^+ + A^- \rightleftarrows CA \tag{5.4}$$

Were C^+ is the cation and A^- is the anion. The ion pairing chemical equilibrium constant is [50]:

$$K_{ip} = \frac{a_{AC}}{a_A a_C} \tag{5.5}$$

Where the activity, a_i, is computed from the molality as:

$$a_i = \frac{m_i \gamma_i}{m_i{}^0} = \frac{n_i \gamma_i}{n_w} \tag{5.6}$$

Where n_w is the number of moles of water in 1 kg (= 1/Mw = 55.5 moles/kg), n_i is the number of moles of ion i. The activity coefficient, γ_i, is often taken to be unit when no other information is available. According to the stoichiometry, the number of moles of reactive species, for n_w moles of water, is:

$$n_A = \alpha\, n^0 \;\; ; \;\; n_C = \alpha\, n^0 \;\; ; \;\; n_{AC} = (1-\alpha)\, n^0 \tag{5.7}$$

α is the dissociation degree and n^0 is the number of moles of salt added to the system. Then, equation (5.5) becomes:

$$K_{ip} = \frac{(1-\alpha)}{\alpha^2 \, {}^{n^0}/_{n_w}} \qquad (5.8)$$

Where ${}^{n^0}/_{n_w}$ is the molality of the salt.

In practice, the models are often constructed per unit volume, i.e. based on the molar concentration, $c^0 = {}^{n^0}/_{\mathrm{V}}$, hence, ${}^{n^0}/_{n_w} = c^0 V \, /n_w$

According to Bjerrum at high salt concentrations, the final expression for the association constant is obtained by integrating equation (5.2) from σ_{ij}^{HS} to l_B as shown below:

$$K_{ip} = 4\,\pi c^0 N_A \int_{\sigma_{ij}^{HS}}^{l_B} exp\left(\frac{2l_B}{r_{ij}}\right) {r_{ij}}^2 dr_{ij} \qquad (5.9)$$

As shown in equation *(5.9)* the overall mass action law is then described with an expression that contains temperature, density and the apparent dielectric constant of the medium. This equilibrium constant can be understood as the partition function of two ions i and j. In the spatial domains ($\sigma_{ij}^{HS} \leq r_{ij} \leq l_B$) the ions will be considered as ion pairs, while for ($l_B \leq r_{ij} \leq \infty$) the ions will be considered as free ions. This holds at low ion concentration [131]. Figure 41 explains graphically the areas where the distinction between free ions and ion pairs is made from the probability $H(r_{ij})$.

The Bjerrum model is a fully predictive model, which is highly dependent on the value of the Bjerrum length. As mentioned above, this length is an arbitrary value, and it is the one that defines the length up to which ion pairs are considered to exist. In the present study a modification was made to the Bjerrum model, to which an adjustable parameter (λ_{ij}^{BJ}) was added. The purpose of this parameter is to vary the length up to which the number of ion pairs are considered, and thus allow the model to adjust the number of ion pairs that are taken into account for each salt. The new association constant is calculated as shown below.

$$K_{ip} = 4\,\pi c^0 N_A \int_{\sigma_{ij}^{HS}}^{\lambda_{ij}^{BJ} \cdot l_B} exp\left(\frac{2l_B}{r_{ij}}\right) {r_{ij}}^2 dr_{ij} \qquad (5.10)$$

Where λ_{ij}^{BJ} is the adjustable parameter for the Bjerrum model.

5.3 Association term and the Bjerrum theory

The association theory [67–69], calculates the association between associative sites *M* and not between molecules. In this study the water molecule has 4 associative sites: two are positive and two are negative. The positive sites allow the water molecule to associate with the anions or with the negative sites of the other water molecules. In the case of ions, we have so far used 7 positive associative sites on cations and 6 negative sites on anions. This means that 7 water molecules can associate around a cation, but, with the framework, it also means that a cation could associate with 7 anions. Furthermore, the anions in contact with this cation could associate with other cations, which means that in the associative term there is the possibility of forming ion clusters (as illustrated on Figure 42, right). Consequently, two modifications are proposed to the association term as originally described in section 3.4.1.3, to avoid such as ion cluster formation These modifications are described below.

5.3.1 Labelling of the associative sites of the ions

Two types of sites have been assigned to each ion; one that allows interactions with water molecules only (ion-water site), and another that allows interactions with another ion of opposite charge only (cation-anion site). This means that for the cations 7 cation-solvent associative sites are conserved, and in addition a single cation-anion associative site is included. The same modification is made for the anions for which 6 anion-solvent associative sites are conserved, plus a single anion-cation associative site. The purpose of this modification is to allow the ions to interact with several water molecules (solvation), but only to form ion pairs and not ion clusters.

5.3.2 New cation-anion association constant ($\Delta^{A_iB_j}$)

The second modification focuses on changing the way the association constant ($\Delta^{A_iB_j}$) between ions is calculated. Although in this chapter calculations will be made only at 298.15 K, it is planned to extend the model to make calculations at higher temperatures. As mentioned above by the construction of the associative term, the association constant decreases with temperature independently of the type of interaction calculated. This trend is correct for solvent-solvent and ion-solvent interactions. However, experimental data show that the association constant increases for cation-anion interactions (see Figure 25). To correctly calculate the cation-anion association constant, the Bjerrum association constant is introduced into the

associative model. In the new modified associative model (which we will call M 2.0Bj) the $\Delta^{A_iB_j}$ for the cation-anion interactions is calculated as follows.

In the association theory [67–69] $\Delta^{A_iB_j}$ is considered as a quasi-chemical association constant. As explained above, in this theory the interactions are between sites of each molecule and not between molecules. Therefore, it is considered that the formation of an ion pair (A_iB_j) is given by the interaction of site A of ion i (A_i) with site B of ion j (B_j). Thus, the equilibrium between ionic sites can be expressed as:

$$A_i + B_j \rightleftarrows A_iB_j \tag{5.11}$$

From Equation (5.11) the association constant ($\Delta^{A_iB_j}$) is given as:

$$\Delta^{A_iB_j} = \frac{[A_iB_j]}{[A_i][B_j]} \tag{5.12}$$

Where $[A_iB_j]$ is the concentration of associated sites A_iB_j and $[A_i], [B_j]$ are the concentration of free sites of ions i and j , respectively. The concentration of the sites can be written as a function of the extent of the non-bonded fraction (α) as follows:

$$[A_iB_j] = \frac{n^0}{V}(1-\alpha) \quad ; \quad [A_i] = \frac{\alpha \cdot n^0}{V} \quad ; \quad [B_j] = \frac{\alpha \cdot n^0}{V} \tag{5.13}$$

If equations (5.13) are substituted into equation (5.12), we obtain:

$$\Delta^{A_iB_j} = \frac{(1-\alpha)}{\alpha^2 c^0} \tag{5.14}$$

If equation (5.14) is compared with equations (5.5) and (5.10), we obtain:

$$\Delta^{A_iB_j} = \frac{K_{ip}}{c^0} = 4\pi N_A \int_{\sigma_{ij}^{HS}}^{\lambda_{ij}^{BJ} \cdot l_B} exp\left(\frac{2l_B}{r_{ij}}\right) {r_{ij}}^2 dr_{ij} \tag{5.15}$$

Equation (5.15) is the new equation that will be used to calculate the association constant between the cation and the anion. Figure 42 shows a representation of the modifications made to the associative term.

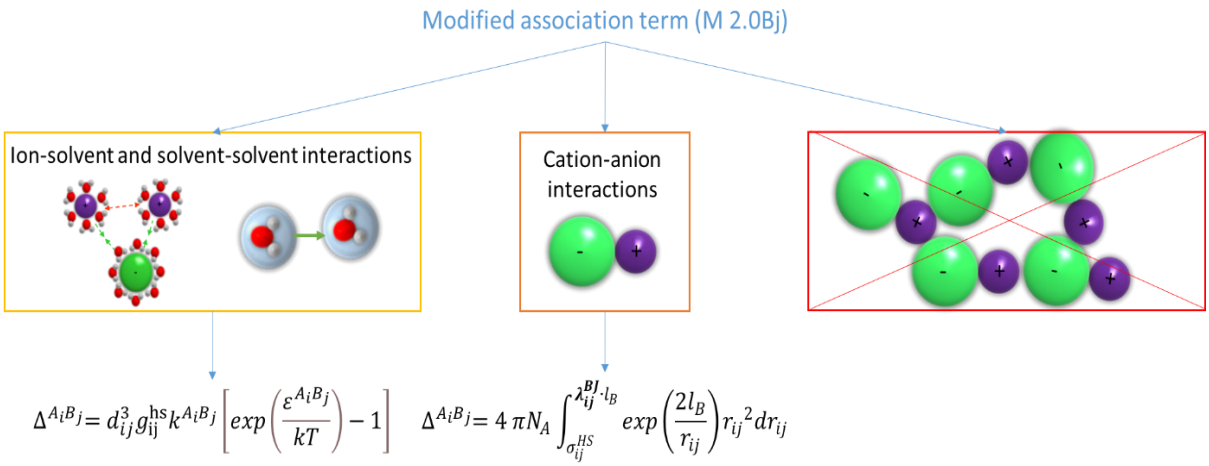

Figure 42 : Graphical representation of the modifications made to the associative term. For solvent-solvent and solvent-ion association, the Wertheim theory is used. For ion-ion association, the Bjerrum theory is used.

5.4 Model parametrization for LiBr

This section describes the model parameterization to reproduce MIAC of the LiBr salt with this new approach. This salt is chosen since it is very soluble in water (maximum solubility of 20 mol/kg at 298.15K). Furthermore, as can be seen in Figure 43, as the salt concentration increases the MIAC value increases rapidly reaching values of 400 at 20 m, which represents a challenge for any model.

Several options in the choice of the ePPC-SAFT terms to mimic ion-ion, ion-solvent and solvent-solvent interaction were evaluated and discussed in the previous section. It was found that both types of models (dispersive and associative) provided good results to describe the behavior of the mean ionic activity coefficient and the osmotic coefficient with respect to salt concentration. However, with the associative model, lower deviations were obtained (see Chapter 4.4.1). In addition, the associative model was the only model (using 11 parameters) that was able to describe the behavior of MIAC with respect to temperature.

In this chapter we will use the associative ePPC-SAFT equation of state (Model 2.0 in Table 3) to calculate the residual Helmholtz free energy from six contributions that now include the modified association term as presented in previous section.

$$A = A^{Hard\ sphere} + A^{Dispersion} + A^{Association-Bj} + A^{Polar} + A^{Born} + A^{MSA} \quad (5.16)$$

Here the dispersion term is used only to take into account the dispersive interactions between the solvent molecules. The model that will be used for dielectric constant is the Schreckenberg model (see section 3.4.4.1).

5.4.1 Objective function and database

The objective function (OF) that will be used in this chapter has been presented in detail in section 4.2.1. A selection among the large amount of data was made according to the criteria presented in Chapter 2. The first part of this chapter will focus on the description of the mean ionic activity coefficient and the osmotic coefficient of the aqueous solution of LiBr.

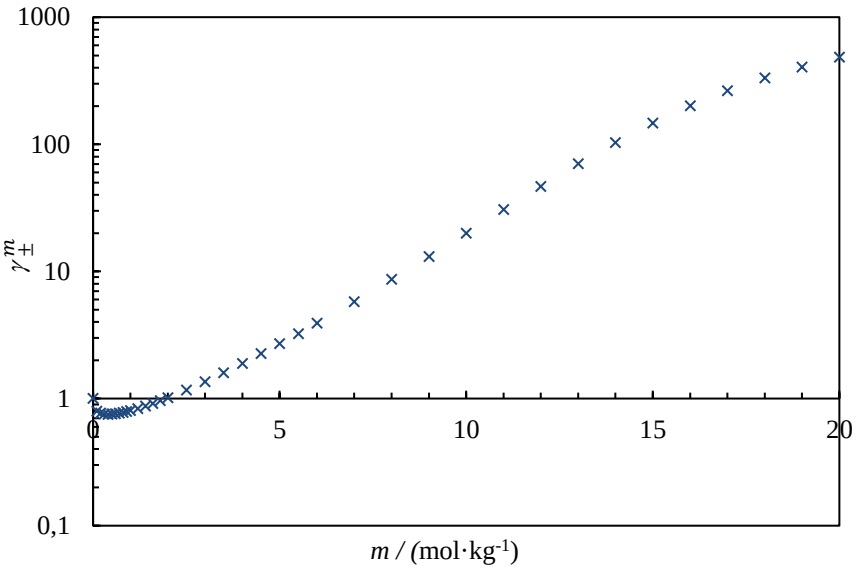

Figure 43 : Experimental mean ionic activity coefficient data for LiBr at 298.15K [179].

Temperature and concentration ranges used and corresponding references for aqueous LiBr are given in Table 24.

Table 24 : Number of experimental data points (Npt^j), uncertainty (err(%)), data serial weight (w_s^j), temperature and concentration range of each properties used for the optimizations of aqueous LiBr [a]. $\gamma_{\pm}^{m}$ is the mean ionic activity coefficient and ϕ is the osmotic coefficient.

	$\gamma_{\pm}^{m}$	ϕ	Reference
Npt^j	38	43	
err(%)	2%	5%	
w_s^j	1	1	[179]
Temperature range / K	298.15	298.15	
Molality range (mol.kg^{-1})	0 - 20	0 - 20	

[a] The objective function is the same as described in section 4.2.1.

The uncertainties and the weight factors ($err(\%)$ and w_s^j) used in this work are also presented in Table 24. They are selected as follows: the individual uncertainties, $err(\%)$ are determined based on knowledge from the experimental uncertainties [28]. As in the previous chapter, the average absolute relative deviation (AARD) of each data series (j) (see equation *(4.5)*) will be used.

5.4.2 Optimisation strategies

In the previous chapter the most important parameters were identified to perform the optimization of four alkali-halide salts. Thanks to the sensitivity analysis presented in section 4.3.2, it was found that the most important parameters for modelling alkali-halide salts (using the associative model) are the ion-solvent and ion-ion association energies, in addition to the hard sphere diameters. It was also observed that the hard sphere diameters present a minimum in the zone corresponding to the Pauling diameter values (see Figure 34). In addition, when extending the model to four salts, it was found that the hard-sphere diameter values for the ions were very close to the Pauling diameter, which shows that using these values to set the hard-sphere diameter could reduce the number of adjustable parameters and also help to preserve the physical consistency of the model.

The first step of this optimization is to evaluate if the modifications introduced in section 5.3 improve the ability of the associative model to describe salts at very high salt concentrations. The comparison will be made with respect to models 1.0 (dispersive) and 2.0 (associative) and the combination of these two models (M 1-2). It was decided to optimize 3 parameters for models 1.0, 2.0 and 2.0Bj. For model 1-2, 6 parameters are optimized (the combination of the parameters of M 1.0 and M 2.0). This is done to evaluate the performance of models 1.0 and 2.0 combined. For model 1.0 the ion-solvent dispersion energies plus the cation-anion dispersion energy will be used, the dispersion energy between like charged ions is equal to 0. For model 2.0 the ion-solvent association energies and the cation-anion association energy will be used. Finally for model 2.0Bj the ion-solvent association energy plus the parameter $\lambda^{Bj}_{Li^+-Br^-}$ (which varies the association constant between the cation and the anion), will be used.

Concerning the other SAFT parameters, the hard sphere diameters will be set to the Pauling diameter value. MSA and Born diameters have been set using the criteria presented in

section 4.2.3. The parameters and their restrictions are presented in Table 25. For associative models, interactions between ions of same charge are not allowed in the framework.

Table 25 : Unitary and binary parameters used for the optimisation of the models 1.0, 2.0, 1-2 and modified associative model 2.0Bj [a]. σ_i^{HS}, σ_i^{MSA} and σ_i^{Born} are the hard sphere, MSA and Born diameters, respectively, ε_{ij} is the dispersion energy, ε_{ij}^{AB} is the association energy, λ_{Li-Br}^{BJ} is the adjustable parameter of the Bjerrum model and k_{ij}^{AB} is the association volume.

Parameters	Dispersive M 1.0	Associative M 2.0	Dispersive + Associative M 1-2	Associative M 2.0Bj
σ_{Li}^{HS} / Å	1.2	1.2	1.2	1.2
σ_{Br}^{HS} / Å	3.90	3.90	3.90	3.90
σ_{Li}^{MSA} / Å*	1.8	1.8	1.8	1.8
σ_{Br}^{MSA} / Å*	5.85	5.85	5.85	5.85
σ_{Li}^{Born} / Å**	2.59	2.59	2.59	2.59
σ_{Br}^{Born} / Å**	4.93	4.93	4.93	4.93
$\varepsilon_{water-Water}/k_B$ / K	201.61	201.61	201.61	201.61
$\varepsilon_{Li-Water}/k_B$ / K	**variable**	0	**variable**	0
$\varepsilon_{Br-water}/k_B$ / K	**variable**	0	**variable**	0
ε_{Li-Br}/k_B / K	**variable**	0	**variable**	0
ε_{Li-Li}/k_B / K	0	0	0	0
ε_{Br-Br}/k_B / K	0	0	0	0
$\varepsilon_{water-Water}^{AB}/k_B$ / K	1813.00	1813.00	1813.00	1813.00
$\varepsilon_{Li-Water}^{AB}/k_B$ / K	0	**variable**	**variable**	**variable**
$\varepsilon_{Br-Water}^{AB}/k_B$ / K	0	**variable**	**variable**	**variable**
$\varepsilon_{Li-Br}^{AB}/k_B$ / K	0	**variable**	**variable**	-
λ_{Li-Br}^{BJ}	-	-	-	**variable**
$k_{Li-Water}^{AB}$	0	0.044	0.044	0.044
$k_{Br-water}^{AB}$	0	0.044	0.044	0.044
k_{Li-Br}^{AB}	0	0.044	0.044	0.044

* see section 4.2.3.
** See equation *(4.11)*.
[a] For the associative models only the dispersion energy between water molecules is considered, all other dispersion interactions are set to zero. Water-water dispersion and association energies are fixed [80].

In addition to the parameters that characterize the interactions of the ions, it is also necessary to use parameters to characterize the interactions between the solvent molecules (water in our case). The parameters used for water in this work are presented in Table 7.

5.4.3 Results of the comparison between the models 1.0, 2.0, 1-2 and 2.0Bj for LiBr

Table 26 shows the results of the optimizations with models 1.0, 2.0, 1-2 and 2.0Bj, and Table 27 provides the optimized parameter values. Thanks to the modifications made to model 2.0Bj, the deviation was reduced from 62.29% (with model 2.0) to 13.25% (with model 2.0Bj) for the MIAC. A similar result was found for the osmotic coefficient calculations, where the deviation was reduced from 16.33% to 5.43% (see Table 26). The combination of models 1.0 and 2.0 (M 1-2) generated a deviation of 16% with respect to the MIAC and 4.43% with respect to the osmotic coefficient. Although 6 adjustable parameters were used for model 1-2, the modifications made to the associative model (M 2.0Bj) allowed obtaining better results for MIAC and just 1% of additional deviation for the osmotic coefficient, using 3 adjustable parameters.

Table 26 : Average absolute relative deviation (AARD) from optimisation of models 1.0, 2.0 and modified 2.0. $\gamma_{\pm}^{m}$ is the mean ionic activity coefficient, ϕ is the osmotic coefficient.

	AARD %			
	M 1.0	M 2.0	M 1-2	M 2.0Bj
$\gamma_{\pm}^{m}$	58.42	34.88	16.00	13.25
ϕ	13.40	8.60	4.43	5.43

As can be seen in Figure 44, both model 1.0 and model 2.0 are unable to quantitatively reproduce the behavior of the MIAC with respect to salt concentration. With the dispersive model (M 1.0) the MIAC is overestimated up to 12 m, after that the model underestimates the MIAC. With model 2.0 the MIAC is underestimated up to 18 m. However, with this model it is possible to reproduce the MIAC behavior in a qualitative way.

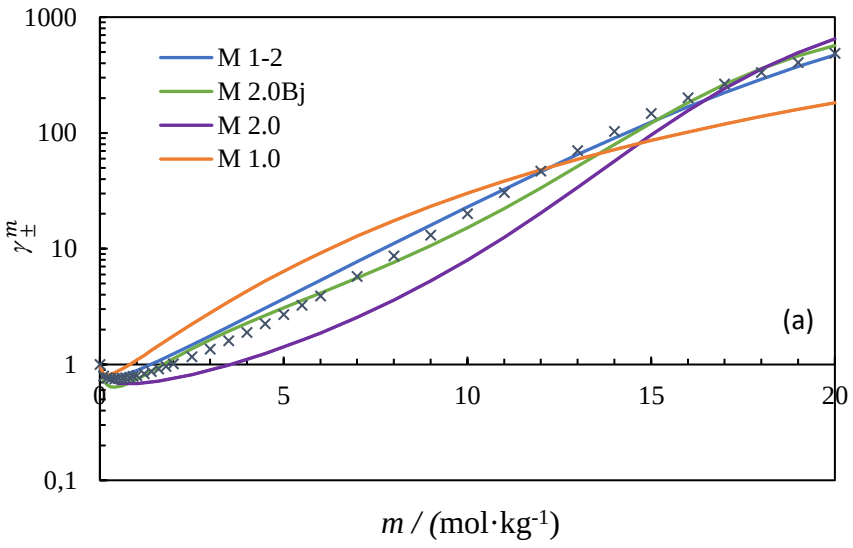

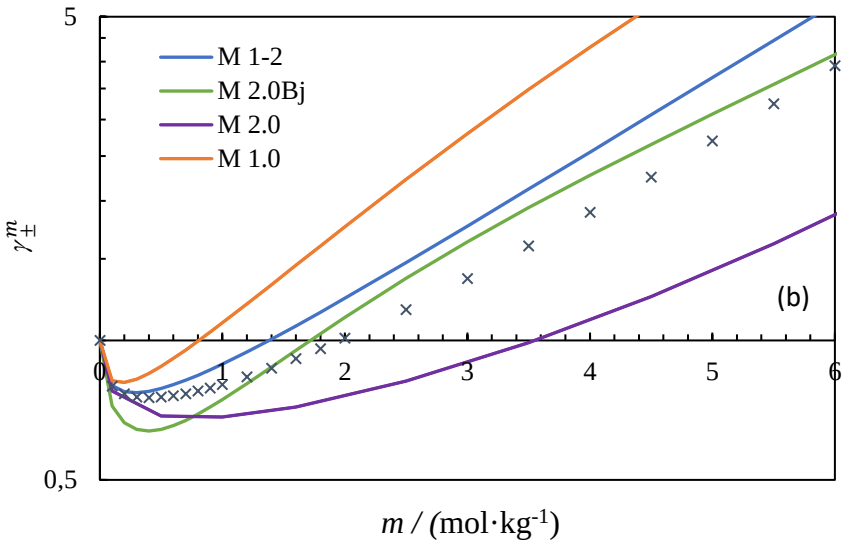

Figure 44 : Comparison of the mean ionic activity coefficient calculation for aqueous LiBr at 298 K using models 1.0 (orange curve), 2.0 (violet curve), 1-2 (blue curve) and modified associative model (green curve). (a) full concentration range and (b) zoom to concentrations between 0 and 6m. The symbols are the experimental data and the curves represent the models. Calculations were made at 1 bar.

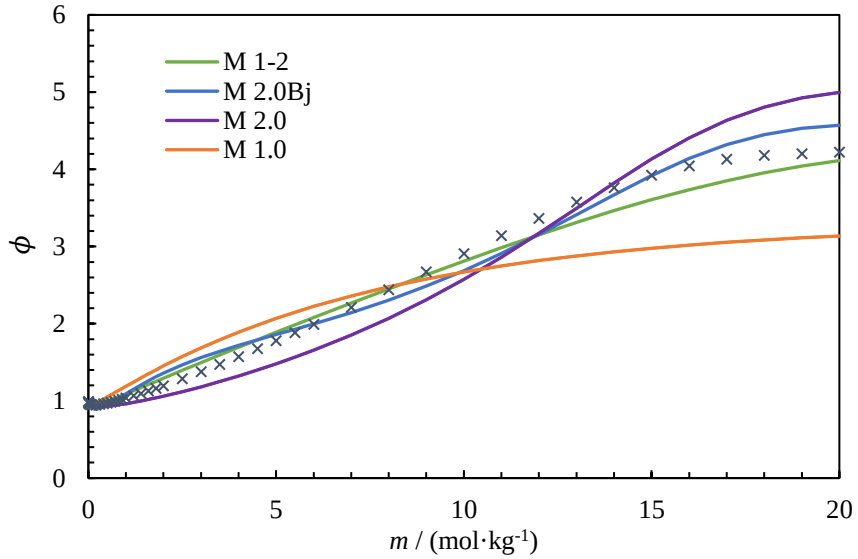

Figure 45 : Comparison of the osmotic coefficient calculation for aqueous LiBr at 298 K using models 1.0 (orange curve), 2.0 (violet curve), 1-2 (green curve) and modified associative model 2.0Bj (blue curve). The symbols are the experimental data and the curves represent the models. Calculations were made at 1 bar.

The models 1.0 and 2.0 have opposite behaviors and seem to compensate for each other. The behavior of model 1-2 shows that this model can reproduce the trend of the MIAC with respect to salt concentration over the range of salt concentration. Comparing the results of models 1-2 and 2.0Bj, it can be seen that: first, model 1-2 manages to reproduce better the MIAC behavior at low salt concentrations (up to 1m, see Figure 44b). Second, the model 2.0Bj does a better correlation of the MIAC when the salt concentration increases (m > 1). However, there are areas where the model 2.0Bj fails (e.g., between 9 and 13 m). This may be due to two

factors. On the one hand, the parameters presented in Table 27 show that in this model the cation-water association energy is very high, while the anion-water association energy is at least 7 times lower. On the other hand, the parameter λ_{Li-Br}^{BJ} is equal to 1.23. This may indicate that the model has the tendency to favor the formation of ion pairs. With these results it could be considered that the model 2.0Bj favors cation solvation and ion pair formation, but that it may also be underestimating anion solvation. In the study performed by Niazi et al. [203] it was shown that the LiBr salt remains in its ionic form even at concentrations higher than 12m, which could confirm that the parameters found are not consistent with the expected behavior.

Table 27 : Parameters obtained from the optimisation of model 1.0, 2.0 and 2.0 modified for aqueous LiBr [a]. Only bold parameters are regressed. $\boldsymbol{\sigma_i^{HS}}$, $\boldsymbol{\sigma_i^{MSA}}$ and $\boldsymbol{\sigma_i^{Born}}$ are the hard sphere, MSA and Born diameters respectively. $\boldsymbol{\varepsilon_{ij}}$ is the dispersion energy, $\boldsymbol{\varepsilon_{ij}^{AB}}$ is the association energy, $\boldsymbol{k_{Na-Water}^{AB}}$ is the association volume.

Parameters	M 1.0	M 2.0	Dispersive + Associative M 1-2	M 2.0Bj
σ_{Li}^{HS} / Å	1.2	1.2	1.2	1.2
σ_{Br}^{HS} / Å	3.90	3.90	3.90	3.90
σ_{Li}^{MSA} / Å*	1.8	1.8	1.8	1.8
σ_{Br}^{MSA} / Å*	5.85	5.85	5.85	5.85
σ_{Li}^{Born} / Å**	2.59	2.59	2.59	2.59
σ_{Br}^{Born} / Å**	4.93	4.93	4.93	4.93
$\varepsilon_{water-Water}/k_B$ / K	201.61	201.61	201.61	201.61
$\varepsilon_{Li-Water}/k_B$ / K	**375.05**	0	**295.71**	0
$\varepsilon_{Br-water}/k_B$ / K	**66.75**	0	**141.99**	0
ε_{Li-Br}/k_B / K	**109.08**	0	**88.35**	0
ε_{Li-Li}/k_B / K	0	0	0	0
ε_{Br-Br}/k_B / K	0	0	0	0
$\varepsilon_{water-Water}^{AB}/k_B$ / K	1813.00	1813.00	1813.00	1813.00
$\varepsilon_{Li-Water}^{AB}/k_B$ / K	0	**3384.01**	**2186.31**	**3186.51**
$\varepsilon_{Br-Water}^{AB}/k_B$ / K	0	**1813.00**	**3330.43**	**436.67**
$\varepsilon_{Li-Br}^{AB}/k_B$ / K	0	**2295.87**	**2887.57**	-
λ_{Li-Br}^{BJ}	-	-	-	**1.23**
$k_{Li-Water}^{AB}$	0	0.044	0.044	0.044
$k_{Br-water}^{AB}$	0	0.044	0.044	0.044
k_{Li-Br}^{AB}	0	0.044	0.044	0.044

* see section **Erreur ! Source du renvoi introuvable.**.
** See equation *(4.11)*.
[a] In dispersive model 1.0 only water-water association interactions are taken into account. In associative model 2.0 and 2.0Bj only water-water dispersion interactions are considered. Hard sphere diameters are fixed with the Pauling diameter. Cation-cation and anion-anion dispersion energies are set to 0. Ion-water association volume and cation-anion association volume are fixed with a value equal to water-water association volume. Water-water dispersion and association energies are also fixed [80].

Since the model 2.0Bj has been shown to have potential to describe the LiBr aqueous solution up to 20m using only three adjustable parameters, we will focus the discussion on this model only.

5.4.4 Number of associated sites

To see how the model is considering the interactions within the system, the number and the nature of bonds per molecule (water, cation, anion) is analysed. From equation *(5.8)* the concentration of associated sites is equal to the association constant multiplied by the concentration of free sites.

$$[A_iB_j] = \Delta^{A_iB_j}[A_i][B_j] \qquad (5.17)$$

The concentration of sites can also be calculated as moles of sites (associated or free) over volume:

$$[A_iB_j] = \frac{n_{A_iB_j}}{V} \quad ; \quad [A_i] = \frac{n_{A_i}}{V} \quad ; \quad [B_j] = \frac{n_{B_j}}{V} \qquad (5.18)$$

Where $n_{A_iB_j}$ are the moles of the associated sites A and B of molecule i and j. n_{A_i} and n_{B_j} are the moles of the free sites of A and B of molecules i and j respectively.

If equation (5.18) is replaced in equation (5.17) we have:

$$n_{A_iB_j} = \frac{\Delta^{A_iB_j}}{V} n_{A_i} n_{B_j} \qquad (5.19)$$

The number of moles of the free sites n_{A_i} can be calculated as the number of moles of molecule i (n_i) multiplied by the fraction of free sites A of molecule i (X^{A_i}) as follows:

$$n_{A_i} = n_i X^{A_i} \; ; \; n_{B_j} = n_j X^{B_j} \qquad (5.20)$$

Rewriting equation (5.19) we have:

$$n_{A_iB_j} = \frac{\Delta^{A_iB_j}}{V} n_i X^{A_i} n_j X^{B_j} \qquad (5.21)$$

Finally, to calculate the number of bonds between two types of sites ($NB_{A_iB_j}$), it is necessary to multiply equation (5.20) by the number of occurrences of a given site type within each molecule (M_{A_i} and M_{B_j}) and divide by the mole fraction of the molecule to be taken as a reference. In our case we will take as reference the mole fraction of the ions for cation-anion

(cat-ani), cation-water (cat-water) and anion-water (ani-water) interactions. For the water-water interaction, the water mole fraction will be taken as reference. The final equation to calculate the number of bonds (NB_{ij}) is:

$$NB_{A_iB_j} = \frac{\Delta^{A_iB_j}}{V} n_i X^{A_i} M_{A_i}\, n_j X^{B_j} M_{B_j} \qquad (5.22)$$

It should be noted that in the case of water-water interactions, the number of bonds must be multiplied by 2, since the same water molecule must be taken into account twice, once as the reference molecule, and once as the molecule interacting with the reference molecule.

Figure 46 shows the number of bonds of the different interactions that are taken into account in the modified association term. The calculation was made using the parameters presented in Table 27.

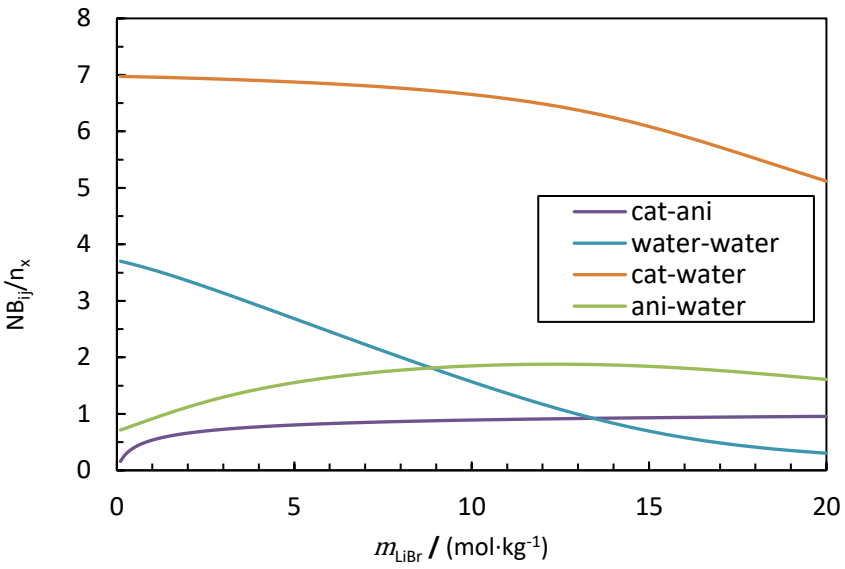

Figure 46 : Number of bonds as a function of salt concentration for aqueous LiBr at 298 K using modified associative model 2.0BJ. Cat-ani are the number of bonds between cation and anion, per ion ($n_X = n_{ion}$), water-water are the number of water-water bonds per water molecule ($n_X = n_{water}$), cat-water and ani-water are the number of bonds between cation and anion with water respectively, per ion molecule ($n_X = n_{ion}$).

Several observations can be made from this plot:

- The number water-water bonds decrease when salt is added to the solution. It starts at close to four, which is the number of available bonds, and decreases to less than one, indicating that a large majority of the water molecules take part in a solvation shell.

- The number of ion pairs increases quickly at first, then less quickly, up to a value of 1, meaning that all ions participate in a pair. This is probably overestimated.

- The cations are fully hydrated (surrounded by water molecules) at infinite dilution: all the sites are bound to water. The number decreases with increasing salinity as a consequence of less water being available.

- The anions have on the average only one water molecule in their solvation shell at infinite dilution. The solvation shell then increases with the salinity, up to a maximum, then decreases. This behavior is not intuitive, since at infinite dilution all the ions are expected to be solvated by the water molecules.

We may conclude that Figure 46 confirms through the infinite dilution consideration that the model is probably not correctly considering the interactions between the anion and the water molecules.

5.4.5 Sensitivity analysis

A global sensitivity analysis (GSA) was performed on the optimal solution of the model 2.0Bj.

Table 28 shows the result of the GSA. The procedure is identical as that which was used in previous chapter (see section 4.3.1(b)).

Table 28 Results from the sensitivity analysis of model 2.0Bj [¤]. ε_{ij}^{AB} is the association energy and λ_{Li-Br}^{BJ} is the adjustable parameter of the Bjerrum model. The most sensitive parameter is highlighted in bold.

Parameters	Total effect %		
	Total OF	$\gamma_{\pm}^{m}$ sOF	ϕ sOF
$\boldsymbol{\varepsilon_{Li-water}^{AB}/k_B}$ **/ K**	**98.43**	**98.03**	**98.80**
$\varepsilon_{Br-water}^{AB}/k_B$ / K	5.26	5.82	7.92
λ_{Li-Br}^{BJ}	1.44	1.67	4.75

[¤] OF means Objective Function. The Total OF is that which is used for the parameter regression; It is the sum of two contributions: the mean ionic activity coefficient ($\gamma_{\pm}^{m}$) and the osmotic coefficient (ϕ).

By comparing the sensitivity of the parameters, it is evident that the association model depends almost exclusively on the Li-water association energy. As can be seen in Table 28 the most sensitive parameter for both the total objective function and the sub-objective functions is

the Li-water association energy, with a total effect of 98% in all cases. With a total effect between 5 and 8% the Br-water association energy is the next most sensitive parameter. Finally, the least sensitive parameter is the adjustable parameter λ_{Li-Br}^{BJ}.

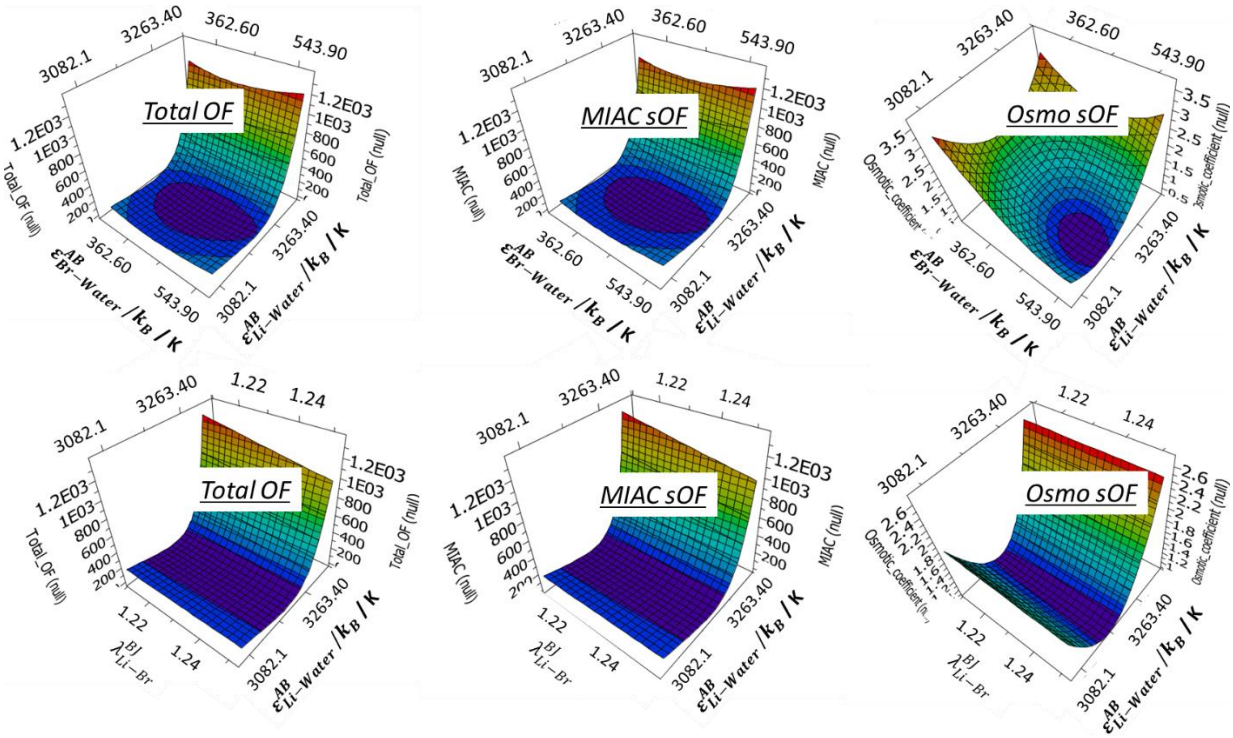

Figure 47 : Model 2.0Bj response surface of the association energies and the parameter λ_{Li-Br}^{BJ} for the total objective function, the mean ionic activity coefficient ($\gamma_{\pm}^{m}$) and the osmotic coefficient (ϕ) sub-objective functions. All other parameters are taken at their optimal value (Table 27).

Figure 47 shows the response surfaces of the association energies and the parameter λ_{Li-Br}^{BJ}. With this figure it can be corroborated that the cation-solvent association energy is the most sensitive parameter. It can also be seen that for both the total objective function and the MIAC subobjective function, there is an area where the cation-solvent and anion-solvent association energies are correlated (purple area at the top of Figure 47). Thanks to this correlation it would be possible to change the values of the association energies without affecting the results. However, the values of the association energy where this minimum exists are still very small, so the problem of underestimation of anion solvation would still be present. When looking the sensitivity of λ_{Li-Br}^{BJ} , it can be seen that this parameter does not have a major impact on the model. This parameter can be varied over the entire range of values without affecting the results. The objective subfunction of the osmotic coefficient presents more defined minima but this is because this objective function varies very little in comparison to the

variation of the MIAC objective function. This may be because the MIAC values vary between 1 and 400, while the osmotic coefficient values vary between 1 and 4 (see Figure 44 and Figure 45).

5.4.6 Impact of the number of associative sites per ion

In the previous section, it was shown that although the model 2.0Bj seems to work well for describing the MIAC and the osmotic coefficient of the aqueous LiBr, the optimized parameters result in physical inconsistencies making the model questionable.

As discussed throughout this work, a correct balance in the calculation of solvation interactions (ion-solvent) and ion-pair interactions (cation-anion) is required to correctly describe electrolyte solutions. Multiple optimizations have been attempted with the parameters discussed in Table 25 without finding satisfactory results (deviations below 10%). So far, the associative sites are the only parameter that had remained fixed for all the associative models; 7 positive sites for the cations and 6 negative sites for the anions.

The impact of the number of solvation sites of the ions on the model 2.0Bj is investigated here. For this purpose, the number of ion-solvent associative sites was varied between 7 and 9 for the cation, and between 6 and 8 for the anion. For every combination, the same optimization strategy as shown in Table 25 was used. The same methodology was maintained for all optimizations (method, number of initial points, optimization limits and weights for each data series). The results obtained are presented in Table 29 and in Figure 48.

As can be seen in Figure 48, with most of the combinations evaluated, a very good correlation of MIAC with respect to salt concentration can be made. The main difference between the results obtained is found at low salt concentrations (between m=0.1 and m=1.2). Using the combination of sites $M_{Li} = 9$; $M_{Br} = 7$ the best correlation of the data at low salt concentrations is achieved (see Figure 48b).

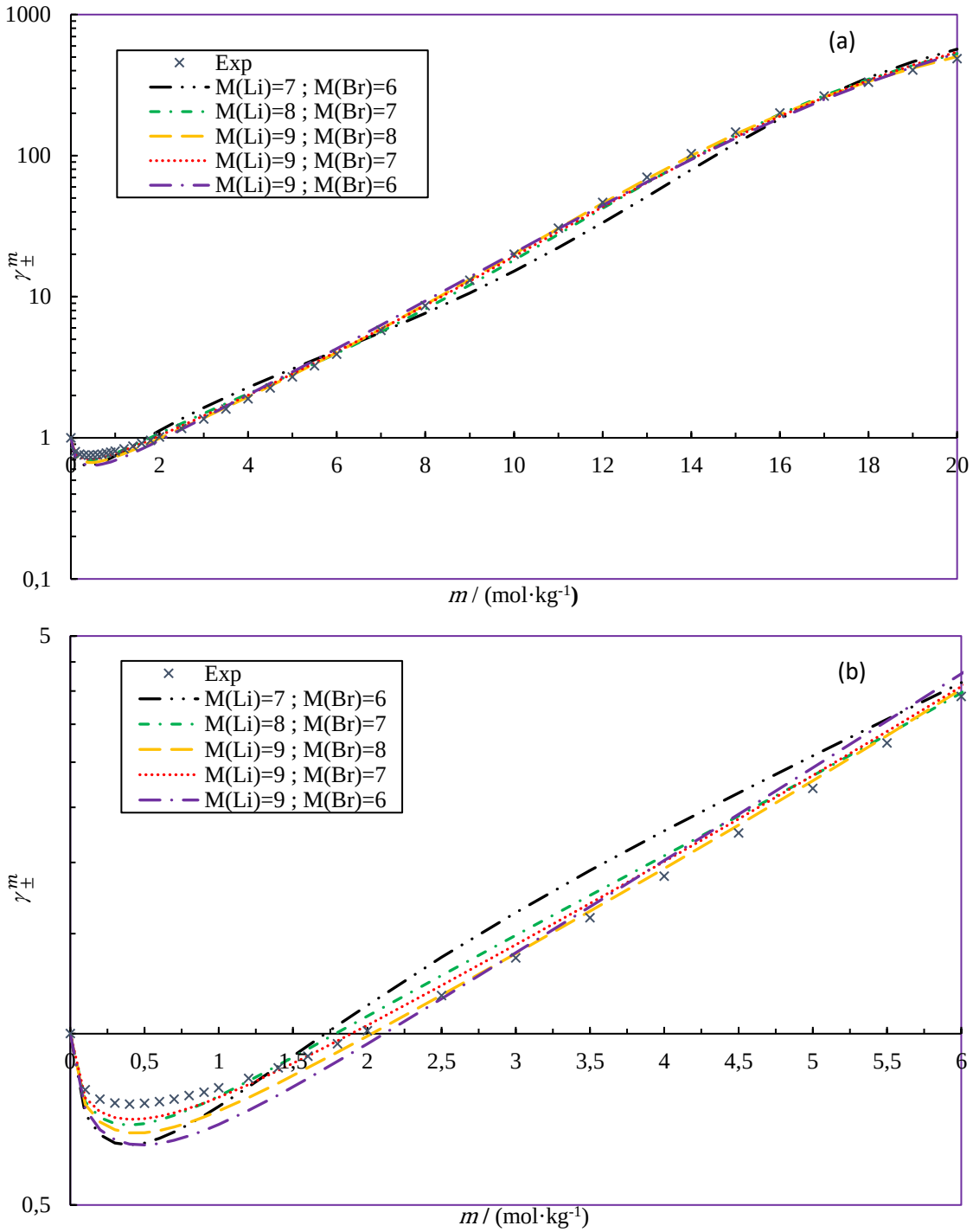

Figure 48 : Comparison of the mean ionic activity coefficient calculation for aqueous LiBr at 298 K using modified associative model. (a) full concentration range and (b) zoom to concentrations between 0 and 6m. The symbols are the experimental data and the curves represent the model. Calculations were made at 1 bar.

Several observations can be made from the results presented in Table 29. First, varying the number of associative sites of the ions has a considerable impact on the quality of the model. Increasing the number of associative sites improves the model. Second, the combination that allowed obtaining the lowest deviation for the MIAC is 9 associative sites for the cation (Li^+)

and 8 associative sites for the anion (Br^-). However, when using the combination $M_{Li} = 9$; $M_{Br} = 7$ the model was better at lower concentrations, and the deviations with respect to MIAC increased by less than 0.12% (see Table 29). In addition, with this site combination the deviation with respect to the osmotic coefficient was lower than when using $M_{Li} = 9$; $M_{Br} = 8$. This information agrees with the observations made by several authors [52, 203], who say that the smaller the ion the more interactions it will have with water, because the electron density is higher.

Table 29 : Average absolute relative deviation (AARD) from optimisation of models 2.0Bj using different ion-solvent associative sites ($\mathbf{M_i}$). $\gamma_{\pm}^{m}$ is the mean ionic activity coefficient, $\boldsymbol{\phi}$ is the osmotic coefficient.

	AARD % M 2.0Bj				
	$M_{Li} = 7$ $M_{Br} = 6$	$M_{Li} = 8$ $M_{Br} = 7$	$M_{Li} = 9$ $M_{Br} = 8$	$M_{Li} = 9$ $M_{Br} = 7$	$M_{Li} = 9$ $M_{Br} = 6$
$\gamma_{\pm}^{m}$	13.25	5.79	4.46	4.57	8.27
ϕ	5.43	2.49	2.15	1.73	3.36

Table 30 presents the parameters obtained from the optimizations with different associative sites. One of the first observations that can be made is that as the number of associative sites increases, the association energies vary inversely for the cation and for the anion. When the number of cation association sites is larger, the cation-water association energy is smaller. Yet, when the anion-water number of association sites is increased, the anion-water association energy also increases. A larger value of anion-water interaction energy helps increasing the number of solvating bonds at low concentrations. However, when the number of cation associative sites is maintained and the number of anion sites is increased, the anion-solvent association energy decreases.

Table 30 : Parameters obtained from the optimisation of model 2.0BJ for aqueous LiBr ▫. Only bold parameters are regressed. σ_i^{HS}, σ_i^{MSA} and σ_i^{Born} are the hard sphere, MSA and Born diameters respectively. ε_{ij} is the dispersion energy, ε_{ij}^{AB} is the association energy, $k_{Na-Water}^{AB}$ is the association volume.

Parameters	$M_{Li} = 7$ $M_{Br} = 6$	$M_{Li} = 8$ $M_{Br} = 7$	$M_{Li} = 9$ $M_{Br} = 8$	$M_{Li} = 9$ $M_{Br} = 7$	$M_{Li} = 9$ $M_{Br} = 6$
σ_{Li}^{HS} / Å	1.2	1.2	1.2	1.2	1.2
σ_{Br}^{HS} / Å	3.90	3.90	3.90	3.90	3.90
σ_{Li}^{MSA} / Å	1.8	1.8	1.8	1.8	1.8
σ_{Br}^{MSA} / Å	5.85	5.85	5.85	5.85	5.85
σ_{Li}^{Born} / Å	2.59	2.59	2.59	2.59	2.59
σ_{Br}^{Born} / Å	4.93	4.93	4.93	4.93	4.93
$\varepsilon_{water-Water}/k_B$ / K	201.61	201.61	201.61	201.61	201.61
$\varepsilon_{water-Water}^{AB}/k_B$ / K	1813.00	1813.00	1813.00	1813.00	1813.00

$\varepsilon^{AB}_{Li-Water}/k_B$ / K	**3186.51**	**2865.08**	**2634.39**	**2616.90**	**2643.89**
$\varepsilon^{AB}_{Br-Water}/k_B$ / K	**436.67**	**762.87**	**913.71**	**1046.45**	**1115.20**
λ^{BJ}_{Li-Br}	**1.23**	**1.10**	**1.11**	**1.02**	**1.13**
$k^{AB}_{Li-Water}$	0.044	0.044	0.044	0.044	0.044
$k^{AB}_{Br-water}$	0.044	0.044	0.044	0.044	0.044
k^{AB}_{Li-Br}	0.044	0.044	0.044	0.044	0.044

* see section 4.2.3.
** See equation *(4.11)*.
▫ In modified associative model 2.0Bj only water-water dispersion interactions are considered. Hard sphere diameters are fixed with the Pauling diameter. Ion-water association volume and cation-anion association volume are fixed with a value equal to water-water association volume. Water-water dispersion and association energies are also fixed [80].

When using $M_{\mathrm{Li}} = 9$ and $M_{Br} = 7$ the lowest deviations are obtained at low salt concentrations, and the AARD% are similar to the best model ($M_{\mathrm{Li}} = 9$ and $M_{Br} = 8$). Furthermore, the parameters of this model seem to be physically consistent. To check this, the number of bonds of each molecule is plotted again as a function of salt concentration (Figure 49).

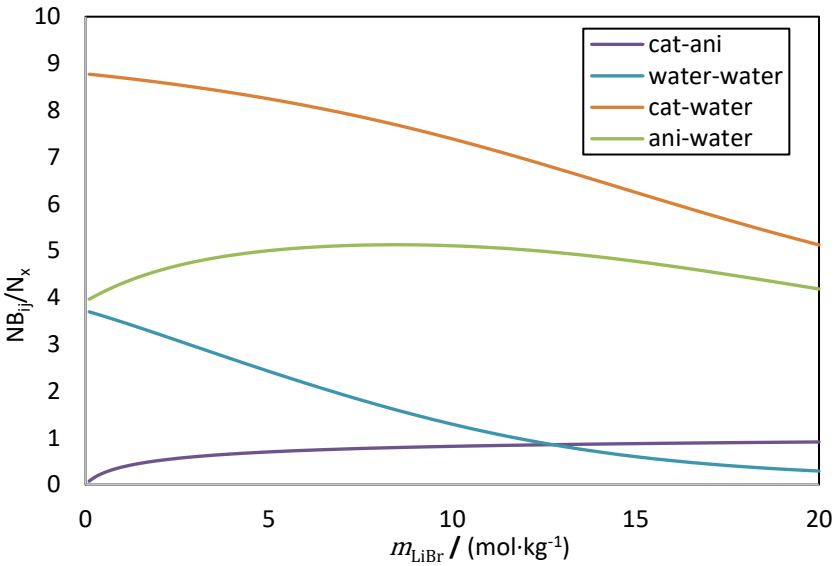

Figure 49 : Number of bonds as a function of salt concentration for aqueous LiBr at 298 K using modified associative model 2.0BJ with $M_{\mathrm{Li}} = 9$ and $M_{Br} = 7$. Cat-ani are the number of bonds between cation and anion, per ion ($n_{\mathrm{X}} = n_{\mathrm{ion}}$), water-water are the number of water-water bonds per water molecule ($n_{\mathrm{X}} = n_{\mathrm{water}}$), cat-water and ani-water are the number of bonds between cation and anion with water respectively, per ion molecule ($n_{\mathrm{X}} = n_{\mathrm{ion}}$).

As can be seen in Figure 49, at infinite dilution the cation is completely solvated, while the anion starts with 4 bonds with water molecules. As the salt concentration increases, the number of water-water and cation-water bonds decrease. This is the expected behaviour since the water molecules separate to interact with the ions, and the ions form ion pairs. Less expected, but similar to what was seen in figure 46, are the number of anion-water interactions

that show a maximum close to $m_{LiBr} = 7$. Water prefers to interact with the cation than with the anion. As the salt concentration increases, the formation of ion pairs also increases.

The contribution of the SAFT terms to the logarithm of the activity coefficient, for the 2.0BJ model with the combination of associative sites $M_{Li} = 9$ and $M_{Br} = 7$ is presented in Figure 50. It shows that the most important terms within the equation of state are the association term (ion-solvent, solvent-solvent and cation-anion attraction interactions), the MSA term (coulombic cation-anion interactions) and the hard sphere term (repulsive interactions between all molecules).

At low concentrations the MSA term generates the highest contribution. This behavior is expected since at low concentrations the ions are completely dissociated and generate mainly coulombic interactions. As the salt concentration increases the contribution of the association term also becomes more important. This is again the expected behavior, since this term takes into account the main short-range interactions within the solution. Finally, at very high salt concentration ($m_{LiBr} > 10$) the hard sphere term starts becoming more important.

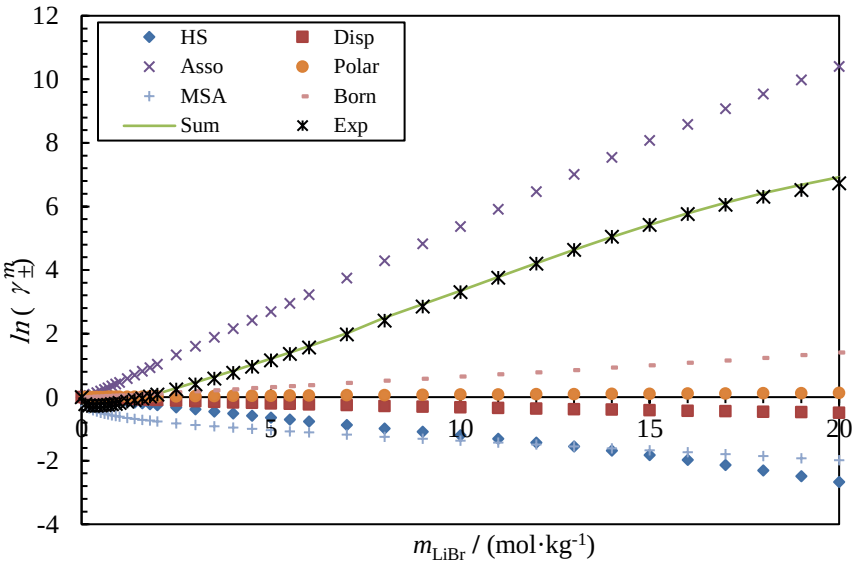

Figure 50 : Effect of the various terms on the logarithm of mean ionic activity coefficient, for aqueous LiBr in function of the salt concentration at 298 K using model 2.0Bj with the combination of associative sites $M_{Li} = 9$ and $M_{Br} = 7$. Where Hs=Hard sphere, Disp=dispersion, Asso=association, Polar=polar, MSA= MSA and Born=Born terms, sum = sum of all terms and Exp= experimental data. The calculations were made at 1 bar.

The results presented above demonstrate that the number of solvating sites that are assigned to an ion has an impact on the value of the parameters, and thus influence the

consistency of the parameters obtained. It was found that 9 associative sites for the cation and 7 associative sites for the anion are the best combination to describe the aqueous LiBr solution up to 20 molal using the modified associative model (2.0Bj). However, when 7 associative sites (ion-solvent) for the anion were used, a better correlation was obtained at low salt concentrations.

5.5 EXTENSION TO LiCl, LiBr and LiI

Now that we have verified that the modified associative model provides results with less than 5% deviation with respect to the MIAC and the osmotic coefficient, we can evaluate its behavior in other salts at high concentrations. In this section, we first evaluate how the model behaves when extrapolating to other salts using ion-specific and salt-specific parameters. Next, we present how the use the new model affects the bonds between the molecules.

5.5.1 Ion-specific parameterization

Using the approximations chosen in the previous section dealing with LiBr, an extension has been carried out to model the same properties in aqueous solution of two new lithium salt (LiCl and LiI), using the strategy described above (3 adjustable parameters per salt). Table 31 presents the temperature and concentration range as well as the number of experimental points used for each salt.

Table 31 : Number of experimental data points (Npt^j), temperature and concentration range of each property used for the optimizations of model 2.0Bj[¤]. $\gamma_{\pm}^{m}$ is the mean ionic activity coefficient and ϕ is the osmotic coefficient.

Salt	Property	Temperature range / K	Molality range / mol.kg^{-1}	Npt^j	Reference
LiCl	$\gamma_{\pm}^{m}$	298.15	0.001-19	43	[179]
	ϕ	298.15	0.001-19	43	
LiI	$\gamma_{\pm}^{m}$	298.15	0-12.05	44	[179, 205]
	ϕ	298.15	0-12.05	44	

[¤] Uncertainty ($err(\%)$) and data serial weight (w_s^j) are the same for all salts and are presented in Table 24.

Considering that the number of associative sites has an important impact on the model, it was chosen to keep the number of associative sites for Li^+ and Br^- as 9 and 7 respectively, and to impose the number of associative sites for Cl^- and I^- to 8 and 6 respectively. This choice is based on the postulate that the smaller the ion size the higher the electronic density, and therefore the higher the solvation.

The deviations from the data whose references are provided in Table 24 and Table 31 are given in Table 32. The parameters resulting from the model optimization are shown in Table 33. Note that the parameters for LiBr have been reoptimized compared to the work presented in section 5.4.5. Indeed, to reduce the number of adjustable parameters, all lithium salts have been adjusted simultaneously, in order to find a set of parameters working well for all salts sharing the same cation.

Table 32 : Average absolute relative deviation (AARD) from optimisation of modified associative model 2.0BJ for aqueous LiCl, LiBr and LiI. $\gamma_{\pm}^{m}$ is the mean ionic activity coefficient, $\boldsymbol{\phi}$ is the osmotic coefficient.

	AARD %		
	LiCl	LiBr	LiI
$\gamma_{\pm}^{m}$	11.64	36.42	36.35
ϕ	3.78	17.20	21.85

Table 33 : Parameters obtained from the optimisation of modified associative model for aqueous LiCl, LiBr and LiI a. Only bold parameters are regressed. σ_i^{HS}, σ_i^{MSA} and σ_i^{Born} are the hard sphere, MSA and Born diameters respectively. M_i is the associative sites, ε_{ij} is the dispersion energy, ε_{ij}^{AB} is the association energy, $k_{Na-Water}^{AB}$ is the association volume.

Parameters	LiCl	LiBr	LiI
σ_{Li}^{HS} / Å	1.2	1.2	1.2
σ_{ani}^{HS} / Å	3.62	3.90	4.32
σ_{Li}^{MSA} / Å	**1.8**	**1.8**	**1.8**
σ_{ani}^{MSA} / Å	**5.43**	**5.85**	**6.48**
σ_{Li}^{Born} / Å	2.59	2.59	2.59
σ_{ani}^{Born} / Å	4.51	4.93	5.64
M_{Li}	9	9	9
M_{ani}	8	7	6
$\varepsilon_{water-water}/k_B$ / K	201.61	201.61	201.61
$\varepsilon_{water-water}^{AB}/k_B$ / K	1813.00	1813.00	1813.00
$\varepsilon_{Li-water}^{AB}/k_B$ / K	**2382.41**	**2382.41**	**2382.41**
$\varepsilon_{Ani-water}^{AB}/k_B$ / K	**1048.89**	**747.21**	**723.09**
λ_{Li-ani}^{BJ}	**0.84**	**1.21**	**0.97**
$k_{Li-water}^{AB}$	0.044	0.044	0.044
$k_{ani-water}^{AB}$	0.044	0.044	0.044
k_{Li-ani}^{AB}	0.044	0.044	0.044

▫ In modified associative model 2.0Bj only water-water dispersion interactions are considered. Hard sphere diameters are fixed with the Pauling diameter. Ion-water association volume and cation-anion association volume are fixed with a value equal to water-water association volume. Water-water dispersion and association energies are also fixed [80].

In section 5.4.5, we saw that when adjusting parameters only on LiBr, the modified associative model showed a very good ability to model the LiBr aqueous solution with only three parameters, over the whole concentration range (0 to 20 m). Nevertheless, when simultaneously modeling LiCl, LiBr and LiI salts (using the same cation parameters), this model is not able to generate results with a similar accuracy. As it can be seen in Table 32 none of the salts has a deviation of less than 10%. Furthermore, as shown in Figure 51, the model is able to reproduce the MIAC trend with respect to salt concentration for LiCl, but in the case of LiBr and LiI the model fails, especially at high salt concentrations. The generated values were significantly below the experimental values. Consequently, it appears very challenging to adjust ion parameters simultaneously on various salt sharing the same ions. The error in the model may be because it depends heavily on the cation-solvent association energy, and since the behavior between salts is so different the same value for all salts is not sufficient.

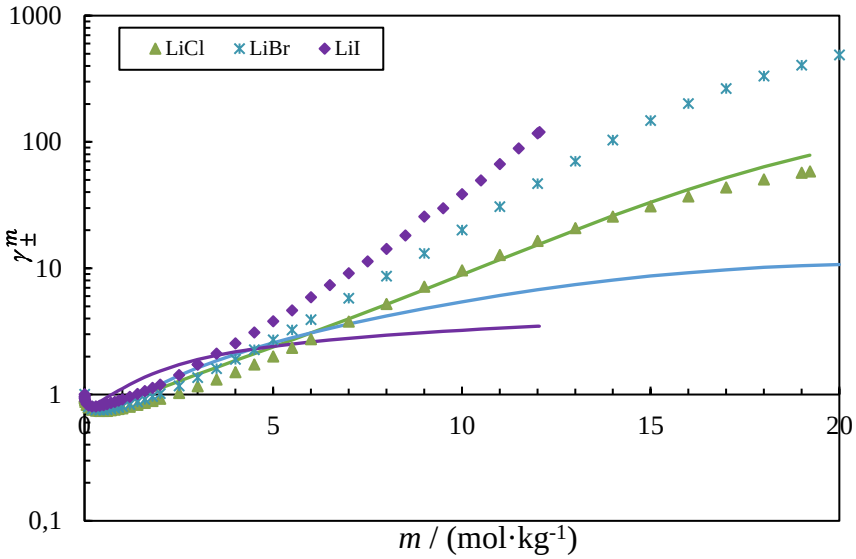

Figure 51 : Mean ionic activity coefficient in function of the salt concentration for aqueous LiCl, LiBr and LiI at 298 K using modified associative model and a global optimization on all salts. (a) full concentration range and (b) zoom to concentrations between 0 and 6m. The symbols are the experimental data and the curves represent the models. Calculations were made at 1 bar.

As can be seen in Figure 51, the three salts have different behavior. LiI is the salt with the largest difference between the hard sphere diameters and is the salt for which the MIAC increases the most when increasing salt concentration. The behavior of LiBr has already been discussed in the previous section, and we know that the ions of this salt are solvated even at

strong salt concentrations and that the occurrence of ion pairs is stronger at very high salt concentrations. Finally, LiCl is a salt with the lowest MIAC values (58 at 19m), and it is also the salt whose ions have most similar diameters. Following the theory of the Law of Matching Water Affinities (LWMA) [52], it would be expected that LiCl would present more cation-anion interactions relative to the ion-solvent interactions. Looking at the parameter values (Table 33) the trend of the parameters is opposite to that expected.

As can be seen in Figure 52 the anion-water association energy decreases with the increase in the difference in hard sphere diameters. One would expect the energies to increase in order to account for more solvation interactions. The low values for the anion-solvent association energy cause the model to underestimate the solvation interactions for LiBr and LiI, and therefore cannot generate sufficiently high values for MIAC, especially at very high salt concentrations. The number of bonds for the three salts is presented in Annex E - E.

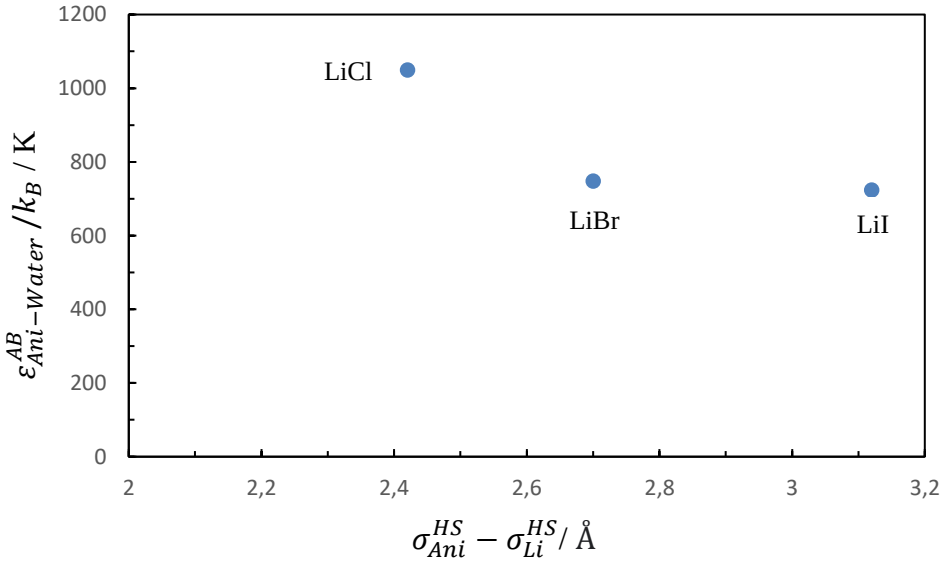

Figure 52 : Anion-solvent association energy in function of the difference between the hard sphere diameters of the ion.

Finally, it can be seen that the trend of the cation-anion interaction parameter, λ^{BJ}_{Li-ani}, is also reversed. Indeed, LiCl is the salt expected to have a higher amount of ion pairs but is also the salt with the smallest value of the parameter λ^{BJ}_{Li-ani}. This means that the model would be disfavoring the occurrence of ion pairs, since it is considering fewer ion pairs than the Bjerrum model predicts. On the contrary, the salt expected to have fewer ion pairs (LiI) has a high λ^{BJ}_{Li-ani} value.

Finally, the above results show that as the new proposed model is not suitable to optimize several salts at the same time.

5.5.2 Salt-specific parameterization.

Having seen that the model fails to optimize all three salts at the same time, in this section the model will be optimized for the LiCl and LiI salts separately. The first objective is to evaluate whether the model can correctly represent each of the salts. The second objective is to verify that the assumption on the number of associative sites for the ions works correctly.

The same optimization strategy presented above is used. Eight associative sites for Cl^- and six associative sites for I^- are retained. The results obtained are presented in Table 34. Although only LiCl and LiI were optimized, the results obtained in Section 5.4.4 for LiBr are also presented to compare the model results for the three salts.

Table 34 : Average absolute relative deviation (AARD) from optimisation of model modified 2.0. $\gamma_{\pm}^{m}$ is the mean ionic activity coefficient, ϕ is the osmotic coefficient. The LiBr is the same as that discussed in section 5.4.5.

	AARD %		
	LiCl	LiBr	LiI
$\gamma_{\pm}^{m}$	5.81	4.57	2.12
ϕ	2.70	1.73	1.10

As can be seen in Table 34, using the modified associative model it is possible to calculate the MIAC and the osmotic coefficient of LiCl, LiBr and LiI with a very good accuracy. By optimizing each salt separately, the deviations are less than 6% for the MIAC and less than 3% for the osmotic coefficient for all the salts. It should be noted that for LiI the deviations do not exceed 2.12%. Figure 53 shows the results of the model for the three salts. As can be seen, the model 2.0Bj can make an accurate correlation of the experimental data in the whole concentration range, even at low concentrations the model is able to generate values very close to the experimental values (see Figure 53b).

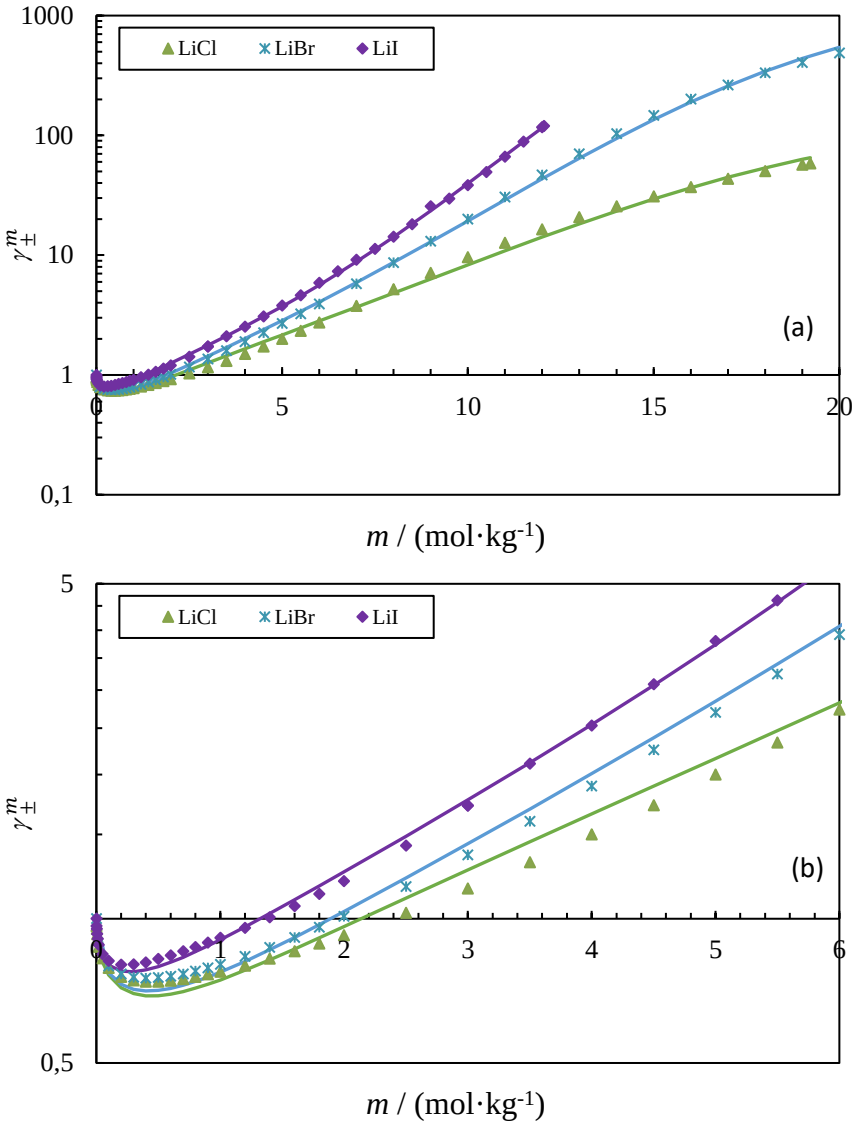

Figure 53 : Mean ionic activity coefficient in function of the salt concentration for aqueous LiCl, LiBr and LiI at 298 K using modified associative model 2.0BJ, and an optimization on each salt individually. (a) full concentration range and (b) zoom to concentrations between 0 and 6m. The symbols are the experimental data and the curves represent the model. Calculations were made at 1 bar.

Table 35 shows that the parameters follow a similar trend to that the expected one. LiCl (the salt expected to present more ion pairs and less solvation interactions) is the salt with the highest value of the parameter λ_{Li-ani}^{BJ} and at the same time the salt with the lowest ion-solvent association energies. If the LiBr parameters are compared with those of LiI it can be seen that the cation-solvent association energy is higher for LiI. This result is expected since according to LMWA, this salt should be more solvated. The anion-solvent association energy seems not to vary much compared to the cation-solvent association energy. This behavior is expected, since in the sensitivity analysis, the anion-solvent association energy did not show to be as sensitive as the cation-solvent association energy (see section 5.4.5).

Table 35 : Parameters obtained from the optimisation of model 2.0 modified for aqueous LiCl, LiBr and LiI [¤]. Only bold parameters are regressed. σ_i^{HS}, σ_i^{MSA} and σ_i^{Born} are the hard sphere, MSA and Born diameters respectively. M_i is the associative sites, ε_{ij} is the dispersion energy, ε_{ij}^{AB} is the association energy, $k_{Na-Water}^{AB}$ is the association volume.

Parameters	LiCl	LiBr	LiI
σ_{Li}^{HS} / Å	1.2	1.2	1.2
σ_{Ani}^{HS} / Å	3.62	3.90	4.32
σ_{Li}^{MSA} / Å	1.8	1.8	1.8
σ_{Ani}^{MSA} / Å	5.43	5.85	6.48
σ_{Li}^{Born} / Å	2.59	2.59	2.59
σ_{Ani}^{Born} / Å	4.51	4.93	5.64
M_{Li}	9	9	9
M_{ani}	8	7	6
$\varepsilon_{water-Water}/k_B$ / K	201.61	201.61	201.61
$\varepsilon_{water-Water}^{AB}/k_B$ / K	1813.00	1813.00	1813.00
$\varepsilon_{Li-Water}^{AB}/k_B$ / K	**2411.93**	**2616.90**	**2842.24**
$\varepsilon_{Ani-Water}^{AB}/k_B$ / K	**974.29**	**1046.45**	**1013.77**
λ_{Li-ani}^{BJ}	**1.02**	**1.02**	**0.98**
$k_{Li-Water}^{AB}$	0.044	0.044	0.044
$k_{Ani-water}^{AB}$	0.044	0.044	0.044
k_{Li-Ani}^{AB}	0.044	0.044	0.044

[¤] In associative model 2.0 modified only water-water dispersion interactions are considered. Hard sphere diameters are fixed with the Pauling diameter. Ion-water association volume and cation-anion association volume are fixed with a value equal to water-water association volume. Water-water dispersion and association energies are also fixed [80].

Figure 54 shows that there is a linear relationship between the cation association energy, and the difference between the hard sphere diameters of the ions. Finally, Table 35 shows that the values of the parameter λ_{Li-ani}^{BJ} are close to 1. This added to the fact that the sensitivity analysis showed that this parameter is not influential in the model, shows that using the purely predictive Bjerrum model is a good approximation for this type of systems. To test this hypothesis, a new optimization was performed where the parameter λ_{Li-ani}^{BJ} was set to a value equal to 1. Table 36 and Table 37 show the results obtained.

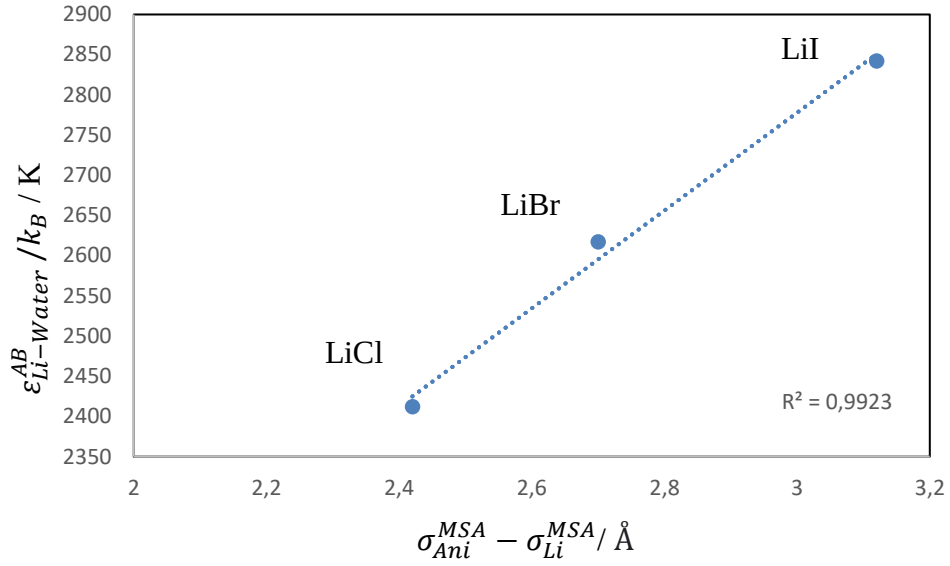

Figure 54 : Li-solvent association energy in function of the difference between the hard sphere diameters of the ions.

When imposing a value of 1 for the parameter λ^{BJ}_{Li-ani}, the deviations were not affected, even for LiCl and LiBr the deviations were reduced. These results confirm that the purely predictive Bjerrum model works adequately for this type of systems.

Table 36 : Average absolute relative deviation (AARD) from optimisation of model modified 2.0. $\gamma^{m}_{\pm}$ is the mean ionic activity coefficient, ϕ is the osmotic coefficient. The LiBr is the same as that discussed in section 5.4.5.

	AARD %		
	LiCl	LiBr	LiI
$\gamma^{m}_{\pm}$	5.72	4.54	2.25
ϕ	2.61	1.66	1.11

The values of the reoptimized parameters are presented in Table 37. As expected, there is only slight variations in the parameters, but the trends remained the same as those presented in Table 35.

Table 37 : Parameters obtained from the optimisation of model 2.0 modified for aqueous LiCl, LiBr and LiI [a]. Only bold parameters are regressed. σ^{HS}_{i}, σ^{MSA}_{i} and σ^{Born}_{i} are the hard sphere, MSA and Born diameters respectively. M_i is the associative sites, ε_{ij} is the dispersion energy, ε^{AB}_{ij} is the association energy, $k^{AB}_{Na-Water}$ is the association volume.

Parameters	LiCl	LiBr	LiI
σ^{HS}_{Li} / Å	1.2	1.2	1.2
σ^{HS}_{Ani} / Å	3.62	3.90	4.32
σ^{MSA}_{Li} / Å	1.8	1.8	1.8

σ_{Ani}^{MSA} / Å	5.43	5.85	6.48
σ_{Li}^{Born} / Å	2.59	2.59	2.59
σ_{Ani}^{Born} / Å	4.51	4.93	5.64
M_{Li}	9	9	9
M_{ani}	8	7	6
$\varepsilon_{water-Water}/k_B$ / K	201.61	201.61	201.61
$\varepsilon_{water-Water}^{AB}/k_B$ / K	1813.00	1813.00	1813.00
$\varepsilon_{Li-Water}^{AB}/k_B$ / K	**2406.41**	**2611.73**	**2842.85**
$\varepsilon_{Ani-Water}^{AB}/k_B$ / K	**985.88**	**1058.83**	**996.32**
λ_{Li-ani}^{BJ}	1.0	1.0	1.0
$k_{Li-Water}^{AB}$	0.044	0.044	0.044
$k_{Ani-water}^{AB}$	0.044	0.044	0.044
k_{Li-Ani}^{AB}	0.044	0.044	0.044

[a] In associative model 2.0 modified only water-water dispersion interactions are considered. Hard sphere diameters are fixed with the Pauling diameter. Ion-water association volume and cation-anion association volume are fixed with a value equal to water-water association volume. Water-water dispersion and association energies are also fixed [80].

As can be seen by using the model 2.0Bj with two salt-specific parameters, an excellent correlation of the experimental data can be made for both the MIAC and the osmotic coefficient over the entire concentration range (see Figure 55and Figure 56). Figure 56 shows that the model is also able to reproduce the non-monotonic behavior of the osmotic coefficient at very high salt concentrations ($m > 15$).

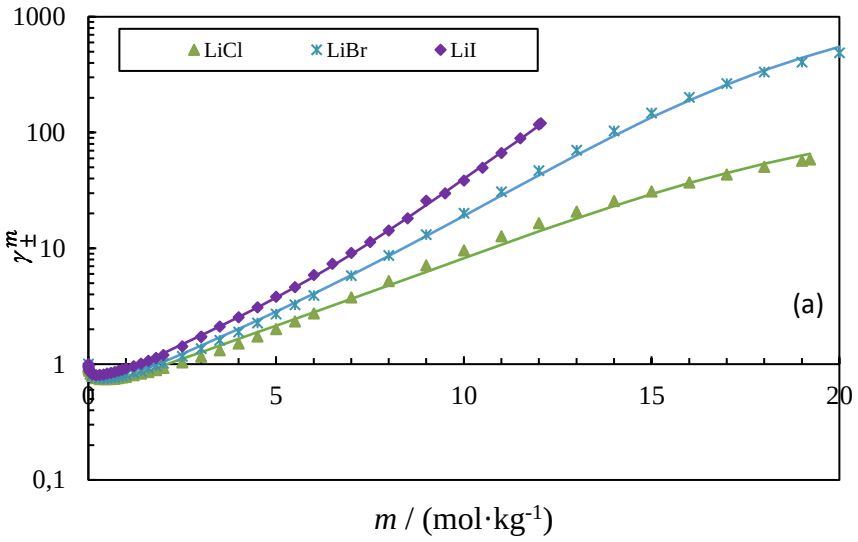

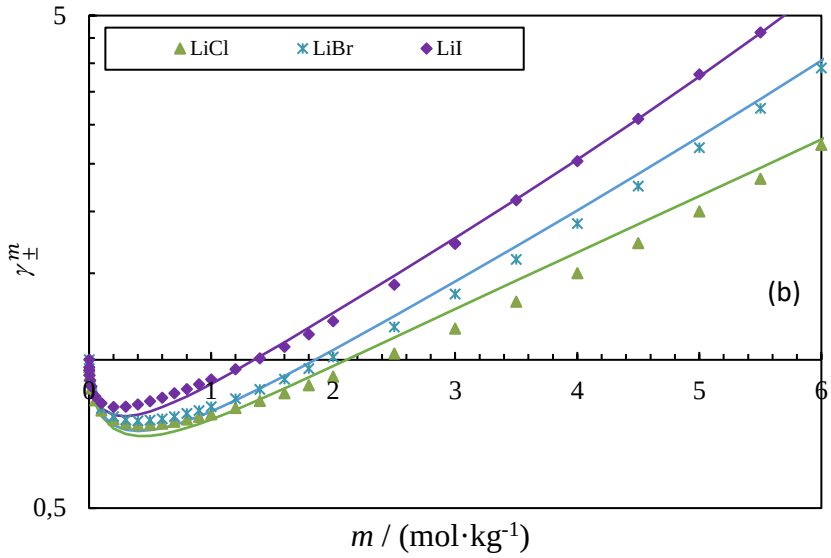

Figure 55 : Mean ionic activity coefficient in function of the salt concentration for aqueous LiCl, LiBr and LiI at 298 K using modified associative model 2.0BJ using two salt-specific parameters. (a) full concentration range and (b) zoom to concentrations between 0 and 6m. The symbols are the experimental data and the curves represent the model. Calculations were made at 1 bar

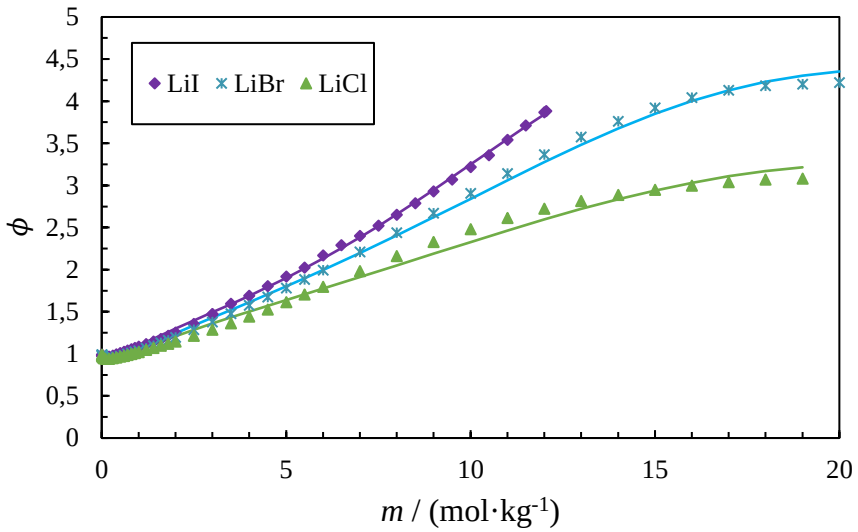

Figure 56 : Osmotic coefficient calculation in function of the salt concentration for aqueous LiCl, LiBr and LiI at 298 K using modified associative model 2.0BJ using two salt-specific parameters. The symbols are the experimental data and the curves represent the models. Calculations were made at 1 bar.

5.5.2.1 Number of associated sites per molecule

As a complement to Figure 49 that showed the number of bonds for the LiBr system, Figure 57 illustrates the number of bonds per molecule as a function of salt concentration for LiCl and Figure 58 for LiI. LiCl is the salt expected to give the highest number of ion pairs. According to LMWA theory, LiI should present a higher amount of ion-solvent interactions.

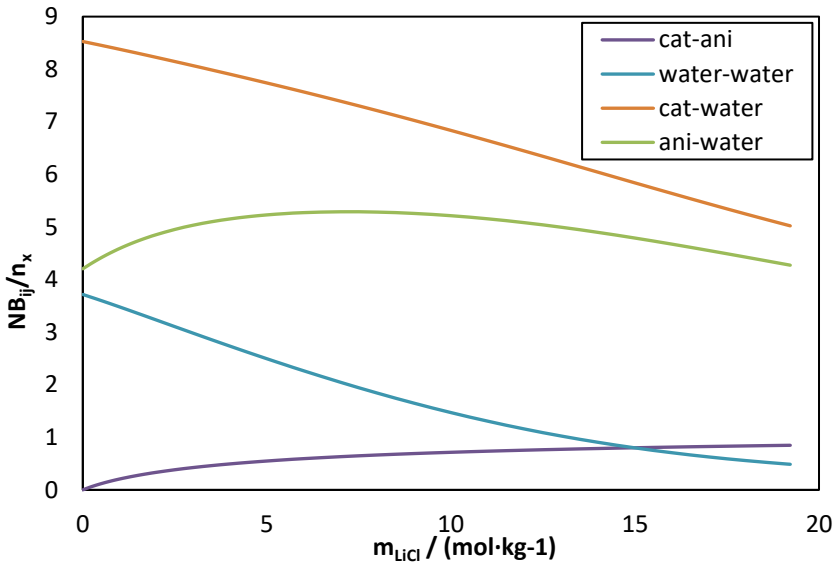

Figure 57 : Number of bonds per molecule as a function of salt concentration for aqueous LiCl at 298 K using modified associative model 2.0BJ with $M_{Li} = 9$ and $M_{Cl} = 8$. Cat-ani are the number of bonds between cation and anion, per ion ($n_X = n_{ion}$), water-water are the number of water-water bonds per water molecule ($n_X = n_{water}$), cat-water and ani-water are the number of bonds between cation and anion with water respectively, per ion molecule ($n_X = n_{ion}$).

One of the most important observations when comparing the number of anion-water bonds is that for all three salts, the number of anion-water bonds starts around 4. For LiCl and LiBr, when increasing salt concentration, the number of anion-water bonds increases, and then at very high salt concentrations it starts to decrease. In contrast, for LiI, the number of anion-water bonds always increases whatever the concentration. When looking at the cation-solvent interactions, for all salts the number of bonds decreases as the concentration increases, especially at high concentrations. However, the number of cation-water bonds for LiI decreases more slowly, remaining almost constant up to $m_{LiI} = 6$.

These results demonstrate the potential of the modified associative model, which can generate results with a low deviation in concentration ranges from 0 to 20 m, with only 3 parameters per salt. The parameters obtained are physically consistent. However, further studies are needed to improve the model and to perform calculations with several salts at the same time.

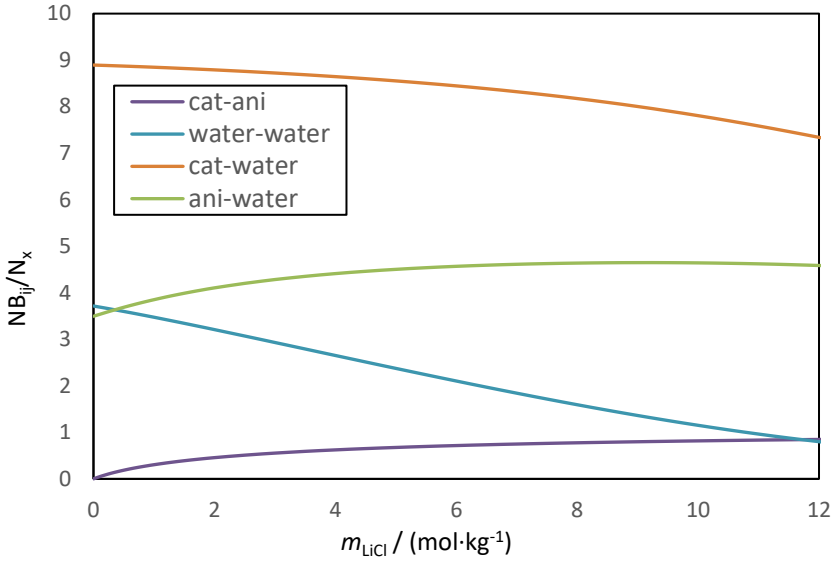

Figure 58 : Number of bonds as a function of salt concentration for aqueous LiI at 298 K using modified associative model 2.0BJ with $M_{Li} = 9$ and $M_{Br} = 6$. Cat-ani are the number of bonds between cation and anion, per ion ($n_X = n_{ion}$), water-water are the number of water-water bonds per water molecule ($n_X = n_{water}$), cat-water and ani-water are the number of bonds between cation and anion with water respectively, per ion molecule ($n_X = n_{ion}$).

5.6 Conclusions

The objective of this chapter was to create a new SAFT-type equation of state for the study of electrolyte systems at very high salt concentrations. For this purpose, the Wertheim association model was modified. Two types of associative sites were imposed for each ion. One that allows it to have multiple interactions with the solvent, and another that allows it to interact only with an oppositely charged ion. The second modification to the association model was to introduce the Bjerrum model to calculate the cation-anion association constant. The model was first evaluated for the aqueous solution of LiBr, between 0 and 20 m at 298.15K. Then two other salts (LiCl and LiI) were included.

The use of aqueous solutions of lithium salts is a real challenge for any model, since these salts can reach concentrations up to 20 molal at 298.15 K. For example, the MIAC for LiBr can reach values of over 400 at 20 m. Although the osmotic coefficient does not lead to such high values, it also has a particular behavior, with a curvature at contractions higher than 15m. This trend has rarely been pointed out, and it appears that, to the best of our knowledge, no author has attempted to describe it with a primitive equation of state. Initially four models were compared. The models were: a dispersive model (model 1.0; use of the dispersion term to

account for short range interactions), an associative model (model 2.0; use of the association term to account for solvent-solvent, ion-solvent and cation-anion interactions), a combination of the dispersive and associative models (model 1-2) and finally the modified associative model (model 2.0Bj). For all models 3 parameters were regressed, except for model 1-2 for which 6 parameters were regressed. From this comparison it was found that model 2.0Bj was the most accurate. The models 1.0 and 2.0 produced very high deviations. The combination of models 1.0 and 2.0 produced a deviation of 16% with respect to the MIAC, but this model was discarded because even using 6 parameters (twice as many as for model 2.0Bj), it produced a higher error in comparison with model 2.0Bj. Our attempts to reproduce the behavior of LiBr show that it is possible to model them using the associative model 2.0Bj. Furthermore, the parameters obtained are found to be physically consistent.

The impact of the number of associative (ion-solvent) sites within the model was investigated. It was found that increasing the number of sites improves the quality of the model, and also helps to obtain physically coherent parameters. Both the ion-solvent association energy and the ion-solvent associative sites are correlated. Increasing the number of sites decreases the association energy. But when the number of sites of both ions are increased simultaneously, the energy of the cation decreases while that of the anion increases. This inverse behavior may suggest that the association energies of both ions are also correlated with each other. When using $M_{\mathrm{L}i} = 9$ and $M_{Br} = 7$, 0.12% more error was obtained with respect to the MIAC compared to when using $M_{\mathrm{L}i} = 9$ and $M_{Br} = 8$, but the error with respect to the osmotic coefficient was also found to be lower. In addition, with $M_{\mathrm{L}i} = 9$ and $M_{Br} = 7$ the model correlated better the MIAC at low salt concentrations.

A sensitivity analysis was performed in which it was found that the associative model 2.0Bj depends almost exclusively on the association energy of the cation. Then, when performing the extension for several salts it was found that using ion-specific parameters, it is not possible to correlate all salts at the same time. This can be attributed to the dependence of the model on the cation association energy. If the model is able to fit one salt, the parameter will be far away from the value needed for the other salts. When the model was fitted for the three salts using salt-specific parameters, it was shown that both the anion-solvent association energy and the parameter λ^{BJ}_{Li-ani} did not vary much between the three salts. On the contrary, the cation-solvent association energy varied considerably resulting in deviations of less than

5% for all salts. Although the thermodynamic model appears to be symmetric, it can distinguish between ions through the hard sphere diameter. The influence of this parameter is found both in the calculation of the ion-solvent association constant and in the calculation of the repulsion term. Including the hard sphere diameter in the parameters could help to improve the model, to make calculations with ion-specific parameters. For this it would also be necessary to include a volume-dependent property in the regression.

With the parameters obtained from the regressions with salt-specific parameters, the number of bonds of each molecule was calculated for the three salts. It was found that with these parameters the model presents a physically consistent behavior. At infinite dilution the cation is completely solvated, ion pair formation is zero, the anion interacts with approximately four water molecules and the water molecules are bonded to four other water molecules. As the salt concentration increases the cation-solvent and solvent-solvent interactions decrease, in addition ion pair formation starts to be present. However, the anion-solvent interactions exhibit a particular behavior as they increase with salt concentration up to a maximum and then decrease. This behavior is seen for both LiBr and LiCl. In the case of LiI the cation-solvent interactions decrease more slowly, and the anion-solvent interactions increase and then remain constant. These behaviors are physically consistent in that for LiBr and LiCl solvation is expected to decrease and ion pair formation to increase, while for LiI more solvation interactions are expected.

Chapter 6 Conclusions and perspectives

The objective of this work was to analyze in depth the differences and similarities between various electrolyte modeling approaches using an equation of state, in order to identify the best way to reconcile the theoretical foundation of the model and the expected experimental behavior, up to saturation concentrations and high temperatures of aqueous alkali-halide solutions. The EoS e-PPC-SAFT was adapted and improved to model thermodynamic properties such as mean ionic activity coefficient (MIAC), osmotic coefficient, enthalpy of solution and apparent molar volume (AMV) of strong electrolyte systems. This objective was achieved by studying and understanding the experimental data, then analyzing and benchmarking the main theories for the study of electrolytes, then by evaluating model parameterizations, and finally proposing an adaptation of the association term of the e-PPC-SAFT model in order to of describe salts up to a concentration of 20m.

The e-PPC-SAFT equation of state, in which the Helmholtz residual energy is calculated as a sum of contributions, allows to quantify the contribution of each kind of interaction in the system. Thus, this model is a powerful tool to understand the balance of forces that are present within an electrolytic system, and to check the consistency of adjusted parameters.

Although the modeling of aqueous alkali-halide solutions is not new and is being studied by many research groups, the present investigation stands out for the following reasons:

1. First, a database with more than 5800 data for 20 alkali-halide salts was created and analyzed, including properties such as the mean ionic activity coefficient, the osmotic coefficient, the enthalpy of solution and the apparent molar volume. The first two are rightly considered essential in the study of electrolyte systems by all authors. The apparent molar volume is less used since it has very small values and is rather difficult to correlate. The enthalpy of solution is rarely considered in this type of studies, but it was included in our study as it helps to improve the temperature dependence of the model. From the data analysis, several salt-specific trends were found with respect to temperature, salt concentration and the difference between ion diameters. These trends

were then used to evaluate the ability of the different models to describe the electrolyte solutions with physical consistency.

2. Secondly, a study was made on the main theories used to model electrolytic systems with equations of state, and how they are used. Although electrolytes are a subject that has been studied for many years, the use of equations of state to model this type of systems is something relatively new. It is for this reason that in the scientific world there are more questions than certainties around this subject. Thanks to the bibliographic study made throughout this work, it was possible to identify the main differences and agreements when modeling electrolytic systems with equations of state. Prior works done by several authors [59, 113, 159] showed that the primitive-MSA (Mean Spherical Approximation) and Debye-Hückel theories generate similar results for modelling the long-range cation-anion interactions (coulombic interactions). In this work, we systematically used the primitive-MSA. MSA diameters were calculated using the ratio of 1.5 times the hard sphere diameter. Due to the low sensitivity of the model to this parameter, the results found using this ratio were satisfactory. Moreover, it was found that very few authors include short-range (non-coulombic) ion-ion interactions within the models, despite data show that ion-ion pair formation is present even in aqueous solutions with strong salts. Furthermore, four ways of modeling ion-solvent interactions were identified: using only the dispersive term, using the dispersive term and the Born term, using the associative term and the dispersion term, and finally using the association term and the Born term. The use of the Born term is a hotly debated issue in the literature. Some authors defend the use of the Born term by claiming that it describes ion-solvent interactions in models where the polarity of the solvent is not otherwise taken into account, and in primitive models. Other authors suggest that this term should not be included in models for electrolytes, since its magnitude greatly overestimates the ion-dipole contribution for aqueous systems. Finally, it was found that there is also an open discussion on the modelling of the dielectric constant, and more specifically whether it should or should not be dependent on the salt concentration. In this study, the Born term has been systematically included in the model using a dielectric constant that does not explicitly depend on the salt concentration. This ensures that the Gibbs energy of solvation is correctly described, without overestimating the solvation interactions.

3. Thirdly, a comparison of several PPC-SAFT equations of state was made to describe the trend of MIAC as a function of both concentration and temperature, and more specifically at low temperature, where a particular behavior is observed. For this purpose, the study was based on NaCl aqueous solutions. In addition, we extended the best approaches found to model 4 salts with ion-specific parameters. Based on the observations from the literature review, it was decided to compare two types of approaches. The first one considers short range ion-solvent and solvent-solvent interactions through the dispersion term. The second one takes into account the short-range ion-solvent and cation-anion interactions through the association term. Thanks to the theoretical foundations of the association model, it is possible to control the amount of interactions between molecules through the associative sites. This advantage helps to give a more solid physical consistency to the model.

   For both approaches, the repulsion, polar, MSA and Born terms were also included. A subdivision of the approaches was made since three different dielectric constants were used, two explicitly depending on the salt concentration and one implicitly depending on the salt concentration. All models are compared using the same conditions (database, objective function, series weights and properties). The use of the enthalpy of solution was a challenge in this study since this property is related to the variation with respect to the MIAC temperature, which has a maximum near 320 K. This trend has rarely been studied, and it appears that, as far as we know, no author has attempted to describe it. Our attempts to describe the enthalpy of solution show that it is very difficult to model it for a model with physically consistent parameters. We believe that the only way to achieve this goal would be to use temperature-dependent parameters or by modifying the Wertheim association constant. In the present study it was observed that it is not necessary to use a dielectric constant that explicitly depends on the salt concentration for the description of the activity coefficient for the NaCl + water system. The use of the Born term remains essential, though, for representing Gibbs energies of solvation. The most sensitive parameters were identified for each approach. For the dispersive model, the hard sphere diameter (σ_i^{HS}) of both ions and the cation-anion dispersion energy ($\varepsilon_{\mathrm{Cat}-Ani}$) were identified as the most influential parameters. For associative model, the most influential parameters were the cation-water association energy ($\varepsilon_{Cat-Water}^{AB}$), the cation-anion association energy ($\varepsilon_{Cat-ani}^{AB}$) and

the hard sphere diameter of the anion (σ_{anion}^{HS}). In both cases the parameters that consider the interactions between the cation and anion, were found to be quite influential in the model. No major differences were found between the two approaches for modeling the target properties.

4. Fourth, this study also focused on the modeling of aqueous solutions at very high salt concentration, with the example of aqueous solutions of lithium salts. Electrolyte systems at very high salt concentrations are difficult to model due to the presence of ion pairs. Even for systems with moderate salt concentrations, it is important to correctly calculate the balance between solvation interactions and ion pair formation. For this purpose, two modifications to the association model were introduced. The first modification consisted in labeling the associative sites of the ions (two types for each ion). The first type of site (ion-solvent) allows multiple interactions between the ions and the solvent. The second type of site (cation-anion), allows only one interaction between the cation and the anion. This provides the ability for the ions to interact with neighboring solvent molecules (polar hard spheres) and to form only ion pairs, and not ion chains. The second modification was to replace the Wertheim association constant by the Bjerrum association constant for cation-anion association. Within the Bjerrum model, an adjustable parameter was added that allows varying the number of ion pairs taken into account by the model. The impact of the number of associative sites (ion-solvent) within the model was investigated. Both the ion-solvent association energy and the ion-solvent association sites are correlated. Increasing the number of sites decreases the association energy. But when the number of sites of both ions increases simultaneously, the energy of the cation decreases while that of the anion increases. This inverse behavior may suggest that the association energies of both ions are also correlated with each other. Using 9 cation-solvent associative sites and 7 anion-solvent associative sites, it is possible to model the aqueous LiBr solution between 0 and 20 m with deviations of less than 5% for both the MIAC and the osmotic coefficient. From the sensitivity analysis performed for the model 2.0Bj, it was found that the parameter with the highest sensitivity is the cation-solvent association energy, followed by the anion-solvent association energy. The parameter with the least sensitivity is the adjustable parameter $\lambda_{cat-ani}^{BJ}$, showing that the use of the purely predicted Bjerrum model is a good approximation for this type of system. It was found that it is not possible

to model the three lithium salts using ion-specific parameters. However, using only two salt-specific parameters, the model was able to model all salts with deviations below 5% for both MIAC and osmotic coefficient. An analysis of the number of bonds between molecules showed that the model parameters are physically consistent.

Table 38 summarizes the main conclusions of this work.

Table 38 : Main conclusions of the work.

Interactions	ion-ion	ion-solvent
Short Range	**Association** can describe ion pairing. The number of ionic sites may be adapted, and a labelling makes it possible to use a different (Bjerrum type) association constant. **Dispersion** is often used in literature. It does not allow describing ion pairing but is sufficient in dilute conditions (below 5M). Care must be taken not to include like-ion dispersion which would result in attractive forces between like charged ions.	**Association** can describe short-range solvation. There is no experimental evidence that the description is correct, but the model is very sensitive to the solvation energy used in the Wertheim association expression. **Dispersion** can adequately be used to describe ion-solvent interactions. The model results are very sensitive to these parameters, and in order to improve temperature dependence, a temperature-dependence k_{ij} should be introduced.
Long Range	The **primitive MSA** model does an adequate job. It may be questioned whether the formation of ion pairs should affect this term.	**The Born term** is necessary for describing the solvation energy from vacuum. Its effect on the MIAC and phase equilibrium properties is depends extremely on the dielectric constant formulation.
Dielectric constant	The dielectric constant, important in Born and MSA terms should be salt-concentration dependent, but not as strongly as could be expected from the experimental data. The Schreckenberg model is most adequate.	

Based on all the observations presented throughout this work, an e-PPC-SAFT type equation of state was proposed, which takes advantage of a modified association term for short range cation-anion interactions. The final model is composed of the hard sphere term, the dispersion term (takes into account only solvent-solvent interactions), the modified association term (takes into account solvent-solvent, ion-solvent and cation-anion interactions), the Polar term, the Born term and the MSA term. The dielectric constant is calculated using the Schreckenberg model. Hard sphere diameters are imposed using Pauling diameters, Born diameters are calculated from the Gibbs energy of solvation and MSA diameters are imposed as 1.5 times the hard sphere diameter. This model can perform calculations for various salts at very high salt concentrations using physically consistent parameters. Nevertheless, we observed

that salt-dependant parameters are finally required to get an acceptable accuracy, making the model not so predictive as initially expected.

Perspectives

The model proposed in this work can be improved by making it more physically robust and more predictable. The following paths of research would be explored in future works:

- First, the primitive MSA model should be modified to include the formation of ion pairs. For this the BiMSA model [128, 129] could be included in replacement of the classical MSA term. The main advantage of the BiMSA term is to explicitly take into account the ion-pairing formation, and we can thus expect more predictability in the model.

- Although the use of Pauling diameters proved to be a good approximation, throughout this work these diameters were identified as key parameters. Including them in the optimization parameters could help to improve the quality of the model and it is consequently recommended to include a property that depends on the volume within the properties used to parameterize the model.

- The new associative approach using the Bjerrum theory for ion-ion short range interactions has been modified to correctly account for the influence of temperature on the ion pair formation. Nevertheless, at this step, only systems at room temperature have been investigated, and it could be very interesting to evaluate this approach on systems at higher temperatures, using the same parameterization methodology developed in this work.

Chapter 7 References

1 United Nations (2015) The Paris Agreement. Available at: https://www.un.org/en/climatechange/paris-agreement.

2 Kontogeorgis G.M., Folas G.K. (2009) *Thermodynamic Models for Industrial Applications: From Classical and Advanced Mixing Rules to Association Theories*, John Wiley & Sons.

3 Kontogeorgis G.M., Dohrn R., Economou I.G., Hemptinne J.-C. de, Kate A. ten, Kuitunen S., Mooijer M., Žilnik L.F., Vesovic V. (2021) Industrial Requirements for Thermodynamic and Transport Properties: 2020, *Industrial & engineering chemistry research* **60**, 13, 4987–5013. DOI: 10.1021/acs.iecr.0c05356.

4 Hemptinne J.-C. de, TSANAS C., MAGHSOODLOO S., NGO T.-D. (2022) *Best Practices for Electrolyte Thermodynamics: Main learnings from EleTher 1 Joint Industrial Project*, IFPEN.

5 (2020.000Z) EleTher - Home. Available at: http://www.elether.fr/Projet/jcms/c_3776305/fr/home.

6 Groysman A. (2017) Corrosion problems and solutions in oil, gas, refining and petrochemical industry, *Koroze a ochrana materialu* **61**, 3, 100–117. DOI: 10.1515/kom-2017-0013.

7 Groysman A., Erdman N. (1999) A Study of Corrosion of Mild Steel in Mixtures of Petroleum Distillates and Electrolytes, *NACE International* **56**, 1266–1271.

8 Du J., Wang X., Liu H., Guo P., Wang Z., Fan S. (2019) Experiments and prediction of phase equilibrium conditions for methane hydrate formation in the NaCl, CaCl2, MgCl2 electrolyte solutions, *Fluid Phase Equilibria* **479**, 1–8. DOI: 10.1016/j.fluid.2018.09.028.

9 Patel B.H., Paricaud P., Galindo A., Maitland G.C. (2003) Prediction of the Salting-Out Effect of Strong Electrolytes on Water + Alkane Solutions, *Ind. Eng. Chem. Res.* **42**, 16, 3809–3823. DOI: 10.1021/ie020918u.

10 Ahmed S. (2019) Thermodynamic modeling of mixed-solvent electrolytes for process simulators, *Thèse de doctorat*, Sorbonne Université.

11 Ghoreychi M. (2015) *Transition énergétique - Stockage souterrain de l'hydrogène*, Verneuil-en-Halatte. Available at: https://www.ineris.fr/sites/ineris.fr/files/contribution/Documents/stockage-souterrain-hydrog%C3%A8ne-1468824082.pdf.

12 Roa Pinto J.S., Bachaud P., Fargetton T., Ferrando N., Jeannin L., Louvet F. (2021) Modeling phase equilibrium of hydrogen and natural gas in brines: Application to storage in salt caverns, *International Journal of Hydrogen Energy* **46**, 5, 4229–4240. DOI: 10.1016/j.ijhydene.2020.10.242.

13 Béroud Q., Caron P., Chlieh R. (2018) *Stockage d'hydrogène en cavités salines*, Mines ParisTech, Paris.

14 Zhang Z., Liu B., Zhao Z. (2012) Efficient acid-catalyzed hydrolysis of cellulose in organic electrolyte solutions, *Polymer Degradation and Stability* **97**, 4, 573–577. DOI: 10.1016/j.polymdegradstab.2012.01.010.

15 Li Z.-G., Sun Y.-Q., Zheng W.-L., Teng H., Xiu Z.-L. (2013) A novel and environment-friendly bioprocess of 1,3-propanediol fermentation integrated with aqueous two-phase extraction by ethanol/sodium carbonate system, *Biochemical Engineering Journal* **80**, 68–75. DOI: 10.1016/j.bej.2013.09.014.

16 New E.K., Tnah S.K., Voon K.S., Yong K.J., Procentese A., Yee Shak K.P., Subramonian W., Cheng C.K., Wu T.Y. (2022) The application of green solvent in a biorefinery using lignocellulosic biomass as a feedstock, *Journal of environmental management* **307**, 114385. DOI: 10.1016/j.jenvman.2021.114385.

17 Li B., Xia D. (2017) Anionic Redox in Rechargeable Lithium Batteries, *Advanced materials (Deerfield Beach, Fla.)* **29**, 48. DOI: 10.1002/adma.201701054.

18 Neidhardt J.P., Fronczek D.N., Jahnke T., Danner T., Horstmann B., Bessler W.G. (2012) A Flexible Framework for Modeling Multiple Solid, Liquid and Gaseous Phases in Batteries and Fuel Cells, *J. Electrochem. Soc.* **159**, 9, A1528-A1542. DOI: 10.1149/2.023209jes.

19 Latham R.J., Linford R.G., Schlindwein W.S. (2003) Pharmaceutical and medical applications of polymer electrolytes, *Ionics* **9**, 41–46.

20 Helmy A.M. (2021) Overview of recent advancements in the iontophoretic drug delivery to various tissues and organs, *Journal of Drug Delivery Science and Technology* **61**, 102332. DOI: 10.1016/j.jddst.2021.102332.

21 Jouyban A. (2010) *Handbook of Solubility Data for Pharmaceuticals*, CRC Press, United States of America.

22 Liddell K. (2005) Thermodynamic models for liquid–liquid extraction of electrolytes, *Hydrometallurgy* **76**, 3-4, 181–192. DOI: 10.1016/j.hydromet.2004.10.005.

23 Hodjaoglu G.A., Ivanov I.S. (2014) Metal recovery of solid metallurgical wastes. Galvanostatic electroextraction of copper from sulphate electrolytes containing Zn2+ and Fe2+ ions, *Bulgarian Chemical Communications,* **46**, 1, 150–156.

24 Lefebvre O., Moletta R. (2006) Treatment of organic pollution in industrial saline wastewater: a literature review, *Water research* **40**, 20, 3671–3682. DOI: 10.1016/j.watres.2006.08.027.

25 Abou-Elela S.I., Kamel M.M., Fawzy M.E. (2010) Biological treatment of saline wastewater using a salt-tolerant microorganism, *Desalination* **250**, 1, 1–5. DOI: 10.1016/j.desal.2009.03.022.

26 Michelsen M. L. (1993) Phase equilibrium calculations. what is easy and what is difficult?, *Computers chem* **17**, 5/6, 431–439.

27 Hemptinne J.-C. de, Ledanois J.-M., Mougin P., Barreau A. (2012) *Select thermodynamic models for process simulation: A practical guide using a three steps methodology*, Editions Technip, Paris. ISBN: 9782710809494.

28 Vaque Aura S., Roa Pinto J.-S., Ferrando N., Hemptinne J.-C. de, Kate A. ten, Kuitunen S., Diamantonis N., Gerlach T., Heilig M., Becker G., Brehelin M. (2021) Data Analysis for Electrolyte Systems: A Method Illustrated on Alkali Halides in Water, *J. Chem. Eng. Data* **66**, 8, 2976–2990. DOI: 10.1021/acs.jced.1c00105.

29 Fosbøl P.L., Thomsen K., Stenby E.H. (2009) Modeling of the Mixed Solvent Electrolyte System CO 2 −Na 2 CO 3 −NaHCO 3 −Monoethylene Glycol−Water, *Ind. Eng. Chem. Res.* **48**, 9, 4565–4578. DOI: 10.1021/ie801168e.

30 Anil Rastogi and Dimitrios Tassios (1987) Thermodynamics of a single electrolyte in a mixture of two solvents, *Ind. Eng. Chem. Res.* **26**, 1344–1351.

31 Chen C., Bokis C. P., Mathias P. (2001) Segment-based excess Gibbs energy model for aqueous organic electrolytes, *AIChE J.* **47**, 11, 2593–2602.

32 Iliuta M. C., Thomsen K., Rasmussen P. (2000) Extended UNIQUAC model for correlation and prediction of vapour-liquid-solid equilibria in aqueous salt systems containing non-electrolytes: Part A. Methanol-water-salt systems, *Chemical Engineering Science* **55**, 2673–2686.

33 Thomsen K., Iliuta M.C., Rasmussen P. (2004) Extended UNIQUAC model for correlation and prediction of vapor–liquid–liquid–solid equilibria in aqueous salt systems containing

non-electrolytes. Part B. Alcohol (ethanol, propanols, butanols)–water–salt systems, *Chemical Engineering Science* **59**, 17, 3631–3647. DOI: 10.1016/j.ces.2004.05.024.

34 Anderko A., Pitzer K.S. (1993) Equation-of-state representation of phase equilibria and volumetric, properties of the system NaCl-Hz0 above 573 K, *Geochimica et Cosmochimica* **57**, 1657–1680.

35 Pitzer K.S. (1973) Thermodynamics of electrolytes. I. Theoretical basis and general equations, *The Journal of Physical Chemistry,* **77**, 2, 268–277.

36 Pitzer K.S. (1991) *Activity coefficients in electrolyte solutions*, CRC Press, Boca Raton. ISBN: 0849354153.

37 Kosinski J.J., Wang P., Springer R.D., Anderko A. (2007) Modeling acid–base equilibria and phase behavior in mixed-solvent electrolyte systems, *Fluid Phase Equilibria* **256**, 1-2, 34–41. DOI: 10.1016/j.fluid.2006.11.018.

38 Peiming Wang, Andrzej Anderko, Robert D. Young (2002) A speciation-based model for mixed-solvent electrolyte systems, *Fluid Phase Equilibria* **203**, 141–176.

39 Michael L. Michelsen & Jorgen Mollerup (2007) *Thermodynamic Models: Fundamentals and Computational Aspects*, TIE-LINE Publications, Denmark.

40 Thomsen K. (2009) Electrolyte Solutions: Thermodynamics, Crystallization, Separation Methods, *DTU Library* **1**, 1–111.

41 Rodil E., Vera J.H. (2001) Individual activity coefficients of chloride ions in aqueous solutions of MgCl2, CaCl2 and BaCl2 at 298.2 K, *Fluid Phase Equilibria* **15–27**, 187–188, 15–27.

42 Wilczek-Vera G., Rodil E., Vera J.H. (2004) On the activity of ions and the junction potential: Revised values for all data, *AIChE Journal* **50**, 2, 445–462.

43 Smith W.R., Moučka F., Nezbeda I. (2016) Osmotic pressure of aqueous electrolyte solutions via molecular simulations of chemical potentials: Application to NaCl, *Fluid Phase Equilibria* **407**, 76–83. DOI: 10.1016/j.fluid.2015.05.012.

44 Bousfield W.R., Bousfield C.E. (1918) Vapour pressure and density of sodium chloride solutions, *Trans. Faraday Soc.* **13**, 401.

45 Prausnitz, J. M., Lichtenthaler, R. N., & De Azevedo, E. G (1998) *Molecular thermodynamics of fluid-phase equilibria*, Pearson Education.

46 Vaslow F. (1966) The Apparent Molal Volumes of the Alkali Metal Chlorides in Aqueous Solution and Evidence for Salt-Induced Structure Transitions, *Journal of Physical Chemistry* **710**, 7, 2286–2294.

47 Zarembo V.I., Fedorov M. (1975) Density of sodium chloride solutions in the 25 - 350 degrees range and pressure up to 1000 kg-force/cm2., *Zh. Prikl. Khim.* **48**, 1949–1953.

48 H. Frank Gibbard Jr., George Scatchard, Raymond A. Rousseau, and Jefferson L. Creek Liquid-vapor equilibrium of aqueous sodium chloride, from 298 to 373.deg.K and from 1 to 6 mol kg-1, and related properties.

49 Robinson R.A., Stokes R.H. (2002) *Electrolyte solutions*, Courier Corporation.

50 Marcus Y., Hefter G. (2006) Ion pairing, *Chemical Reviews* **106**, 11, 4585–4621. DOI: 10.1021/cr040087x.

51 Fawcett W.R. (1999) Thermodynamic Parameters for the Solvation of Monatomic Ions in Water, *J. Phys. Chem. B* **103**, 50, 11181–11185. DOI: 10.1021/jp991802n.

52 Collins K.D. (2004) Ions from the Hofmeister series and osmolytes: Effects on proteins in solution and in the crystallization process, *Methods (San Diego, Calif.)* **34**, 3, 300–311. DOI: 10.1016/j.ymeth.2004.03.021.

53 Selam M.A., Economou I.G., Castier M. (2018) A thermodynamic model for strong aqueous electrolytes based on the eSAFT-VR Mie equation of state, *Fluid Phase Equilibria* **464**, 47–63. DOI: 10.1016/j.fluid.2018.02.018.

54 Taniewska-Osinska S., Logwinienko R. (1976) Calorimetric Investigations of Aqueous Solutions of Sodium Chloride and Cobalt(II) Chloride at Several Temperatures., *Acta Univ. Lodz. Ser* **2**, 69–75.

55 Pereira C.G. (ed.) (2019) *Thermodynamics of Phase Equilibria in Food Engineering: Chapter 13 - Equilibrium in Electrolyte Systems*, Academic Press, Brazil. ISBN: 978-0-12-811556-5.

56 Honarparvar S., Saravi S.H., Reible D., Chen C.-C. (2017) Comprehensive thermodynamic modeling of saline water with electrolyte NRTL model: A study on aqueous Ba 2+ -Na + -Cl − -SO 4 2− quaternary system, *Fluid Phase Equilibria* **447**, 29–38. DOI: 10.1016/j.fluid.2017.05.016.

57 NguyenHuynh D., Passarello J.-P., Tobaly P., Hemptinne J.-C. de (2008) Application of GC-SAFT EOS to polar systems using a segment approach, *Fluid Phase Equilibria* **264**, 1-2, 62–75. DOI: 10.1016/j.fluid.2007.10.019.

58 NguyenHuynh D., Passarello J.-P., Hemptinne J.-C. de, Tobaly P. (2011) Extension of polar GC-SAFT to systems containing some oxygenated compounds: Application to ethers, aldehydes and ketones, *Fluid Phase Equilibria* **307**, 2, 142–159. DOI: 10.1016/j.fluid.2011.04.009.

59 Galindo A., Gil-Villegas A., Jackson G., Burgess A.N. (1999) SAFT-VRE: Phase Behavior of Electrolyte Solutions with the Statistical Associating Fluid Theory for Potentials of Variable Range, *J. Phys. Chem. B* **103**, 46, 10272–10281. DOI: 10.1021/jp991959f.

60 Rozmus J., Hemptinne J.-C. de, Galindo A., Dufal S., Mougin P. (2013) Modeling of Strong Electrolytes with ePPC-SAFT up to High Temperatures, *Ind. Eng. Chem. Res.* **52**, 29, 9979–9994. DOI: 10.1021/ie303527j.

61 Inchekel R., Hemptinne J.-C. de, Fürst W. (2008) The simultaneous representation of dielectric constant, volume and activity coefficients using an electrolyte equation of state, *Fluid Phase Equilibria* **271**, 1-2, 19–27. DOI: 10.1016/j.fluid.2008.06.013.

62 Schlaikjer A., Thomsen K., Kontogeorgis G.M. (2017) Simultaneous Description of Activity Coefficients and Solubility with eCPA, *Ind. Eng. Chem. Res.* **56**, 4, 1074–1089. DOI: 10.1021/acs.iecr.6b03333.

63 Simon H. G., Kistenmacher H., Prausnitz J.M., Vortmeyer D. (1991) An Equation of State for Systems Containing Electrolytes and Nonelectrolytes, *Chem. Eng. Process.* **29**, 139–146.

64 Jianzhong Wu and and John M. Prausnitz* (1998) Phase Equilibria for Systems Containing Hydrocarbons, Water, and Salt: An Extended Peng−Robinson Equation of State, *Ind. Eng. Chem. Res.* **37**, 5, 1634–1643.

65 Maribo-Mogensen B. (2014) Development of an Electrolyte CPA Equation of state for Applications in the Petroleum and Chemical Industries, *PhD*, Technical University of Denmark.

66 McQuarrie D.A., Simon J.D. (1997) *Physical chemistry: a molecular approach.*, Sausalito, CA: University science books.

67 M. S. Wertheim (1984) Fluids with highly directional attractive forces.: I. Statistical thermodynamics, *Journal of Statistical Physics* **35**, 19–34.

68 M. S. Wertheim (1984) Fluids with highly directional attractive forces.: II. Thermodynamic perturbation theory and integral equations, *Journal of Statistical Physics* **35**, 35–47.

69 M. S. Wertheim (1986) Fluids with highly directional attractive forces.: III. Multiple attraction sites, *Journal of Statistical Physics* **42**, 459–476.

70 Rozmus J. (2012) Équation d'état électrolyte prédictive pour le captage du CO2 Predictive electrolyte equation of state for CO2 capture, *PhD*, UNIVERSITE PIERRE ET MARIE CURIE.

71 Fauve R., Guichet X., Lachet V., Ferrando N. (2017) Prediction of H2S solubility in aqueous NaCl solutions by molecular simulation, *Journal of Petroleum Science and Engineering* **157**, 94–106. DOI: 10.1016/j.petrol.2017.07.003.

72 Zhou J., Lu X., Wang Y., Shi J. (2002) Molecular dynamics study on ionic hydration, *Fluid Phase Equilibria*, 194–197, 257–270.

73 W. Furst, H. Renon (1993) Representation of excess properties of electrolyte solutions using a new equation of state, *AIChE J.* **39**, 2, 335–343.

74 Blum L., Hoye J. S. (1977) Mean spherical model for asymmetric electrolytes.: 2. Thermodynamic properties and the pair correlation function, *The Journal of Physical Chemistry*, **81**, 13, 1311–1316.

75 Herzog S., Gross J., Arlt W. (2010) Equation of state for aqueous electrolyte systems based on the semirestricted non-primitive mean spherical approximation, *Fluid Phase Equilibria* **297**, 1, 23–33. DOI: 10.1016/j.fluid.2010.05.024.

76 Liu W. B., Li Y.-G., Lu J.-F. (1999) A new equation of state for real aqueous ionic fluids based on electrolyte perturbation theory, mean spherical approximation and statistical associating fluid theory, *Fluid Phase Equilibria*, 158-160, 595–606.

77 Liu Z.-P., Li Y.-G., Lu J.-F. (2002) Low-Density Expansion of the Solution of Mean Spherical Approximation for Ion−Dipole Mixtures, *J. Phys. Chem. B* **106**, 20, 5266–5274. DOI: 10.1021/jp0140264.

78 Liu Z., Wang W., Li Y. (2005) An equation of state for electrolyte solutions by a combination of low-density expansion of non-primitive mean spherical approximation and statistical associating fluid theory, *Fluid Phase Equilibria* **227**, 2, 147–156. DOI: 10.1016/j.fluid.2004.11.007.

79 Rozmus J., Brunella I., Mougin P., Hemptinne J.-C. de (2012) Isobaric Vapor–Liquid Equilibria of Tertiary Amine and n -Alkane/Alkanol Binary Mixtures: Experimental Measurements and Modeling with GC-PPC-SAFT, *J. Chem. Eng. Data* **57**, 11, 2915–2922. DOI: 10.1021/je300568h.

80 Ahmed S., Ferrando N., Hemptinne J.-C. de, Simonin J.-P., Bernard O., Baudouin O. (2018) Modeling of mixed-solvent electrolyte systems, *Fluid Phase Equilibria* **459**, 138–157. DOI: 10.1016/j.fluid.2017.12.002.

81 Ahmed S., Ferrando N., Hemptinne J.-C. de, Simonin J.-P., Bernard O., Baudouin O. (2016) A New PC-SAFT Model for Pure Water, Water–Hydrocarbons, and Water–Oxygenates Systems and Subsequent Modeling of VLE, VLLE, and LLE, *J. Chem. Eng. Data* **61**, 12, 4178–4190. DOI: 10.1021/acs.jced.6b00565.

82 Carnahan N.F., Starling K.E. (1972) Intermolecular repulsions and the equation of state for fluids, *AIChE J.* **18**, 6, 1184–1189.

83 Mansoori G.A., Carnahan N.F., Starling K.E., Leland T.W. (1971) Equilibrium Thermodynamic Properties of the Mixture of Hard Spheres, *The Journal of Chemical Physics* **54**, 4, 1523–1525. DOI: 10.1063/1.1675048.

84 Stanley H. Huang/Maciej Radosz (1991) Equation of state for small, large, polydisperse, and associating molecules: extension to fluid mixtures, *Ind. Eng. Chem. Res.* **30**, 1994-2005.

85 Adidharma H., Radosz M. (1998) Prototype of an Engineering Equation of State for Heterosegmented Polymers, *Ind. Eng. Chem. Res.* **37**, 11, 4453–4462. DOI: 10.1021/ie980345e.

86 Gross J., Sadowski G. (2001) Perturbed-Chain SAFT: An Equation of State Based on a Perturbation Theory for Chain Molecules, *Ind. Eng. Chem. Res.* **40**, 4, 1244–1260. DOI: 10.1021/ie0003887.

87 Müller S., González de Castilla A., Taeschler C., Klein A., Smirnova I. (2020) Calculation of thermodynamic equilibria with the predictive electrolyte model COSMO-RS-ES: Improvements for low permittivity systems, *Fluid Phase Equilibria* **506**, 112368. DOI: 10.1016/j.fluid.2019.112368.

88 Ingram T., Gerlach T., Mehling T., Smirnova I. (2012) Extension of COSMO-RS for monoatomic electrolytes: Modeling of liquid–liquid equilibria in presence of salts, *Fluid Phase Equilibria* **314**, 29–37. DOI: 10.1016/j.fluid.2011.09.021.

89 Eriksen D.K., Lazarou G., Galindo A., Jackson G., Adjiman C.S., Haslam A.J. (2016) Development of intermolecular potential models for electrolyte solutions using an electrolyte SAFT-VR Mie equation of state, *Molecular Physics* **114**, 18, 2724–2749. DOI: 10.1080/00268976.2016.1236221.

90 Anvari M.H., Pazuki G., Kakhki S.S., Bonakdarpour B. (2013) Application of the SAFT-VR equation of state in estimation of physiochemical properties of amino acid solutions, *Journal of Molecular Liquids* **184**, 24–32. DOI: 10.1016/j.molliq.2013.04.024.

91 Shahriari R., Dehghani M.R. (2018) New electrolyte SAFT-VR Morse EOS for prediction of solid-liquid equilibrium in aqueous electrolyte solutions, *Fluid Phase Equilibria* **463**, 128–141. DOI: 10.1016/j.fluid.2018.02.006.

92 Pàmies J.C., Vega L.F. (2001) Vapor−Liquid Equilibria and Critical Behavior of Heavy n -Alkanes Using Transferable Parameters from the Soft-SAFT Equation of State, *Ind. Eng. Chem. Res.* **40**, 11, 2532–2543. DOI: 10.1021/ie000944x.

93 Ji X., Tan S.P., Adidharma H., Radosz M. (2005) SAFT1-RPM Approximation Extended to Phase Equilibria and Densities of CO 2 −H 2 O and CO 2 −H 2 O−NaCl Systems, *Ind. Eng. Chem. Res.* **44**, 22, 8419–8427. DOI: 10.1021/ie050725h.

94 Najafloo A., Feyzi F., Zoghi A.T. (2016) Modeling solubility of CO 2 in aqueous MDEA solution using electrolyte SAFT-HR EoS, *Journal of the Taiwan Institute of Chemical Engineers* **58**, 381–390. DOI: 10.1016/j.jtice.2015.06.016.

95 Boublik T. (2006) Perturbation theory of pure quadrupolar hard gaussian overlap fluids, *Molecular Physics* **69**, 3, 497–505. DOI: 10.1080/00268979000100361.

96 Ioannis G. Economou and Marc D. Donohue (1991) Chemical, quasi-chemical and perturbation theories for associating fluids, *AIChE J.* **37**, 12, 1875–1894.

97 Chapman W.G., Jackson G., Gubbins K.E. (1988) Phase equilibria of associating fluids: Chain molecules with multiple bonding sites, *Molecular Physics* **65**, 5, 1057–1079. DOI: 10.1080/00268978800101601.

98 Tan S.P., Ji X., Adidharma H., Radosz M. (2006) Statistical associating fluid theory coupled with restrictive primitive model extended to bivalent ions. SAFT2: 1. Single salt + water solutions, *The journal of physical chemistry. B* **110**, 33, 16694–16699. DOI: 10.1021/jp0625107.

99 Ji X., Adidharma H. (2008) Ion-based SAFT2 to represent aqueous multiple-salt solutions at ambient and elevated temperatures and pressures, *Chemical Engineering Science* **63**, 1, 131–140. DOI: 10.1016/j.ces.2007.09.010.

100 Najafloo A., Feyzi F., Zoghi A.T. (2014) Development of electrolyte SAFT-HR equation of state for single electrolyte solutions, *Korean J. Chem. Eng.* **31**, 12, 2251–2260. DOI: 10.1007/s11814-014-0185-1.

101 Lee B.-S., Kim K.-C. (2009) Modeling of aqueous electrolyte solutions based on perturbed-chain statistical associating fluid theory incorporated with primitive mean spherical approximation, *Korean J. Chem. Eng.* **26**, 6, 1733–1747. DOI: 10.1007/s11814-009-0286-4.

102 Shadloo A., Abolala M., Peyvandi K. (2016) Application of ion-based ePC-SAFT in prediction of density of aqueous electrolyte solutions, *Journal of Molecular Liquids* **221**, 904–913. DOI: 10.1016/j.molliq.2016.06.043.

103 Shadloo A., Peyvandi K. (2017) The implementation of ion-based ePC-SAFT EOS for calculation of the mean activity coefficient of single and mixed electrolyte solutions, *Fluid Phase Equilibria* **433**, 226–242. DOI: 10.1016/j.fluid.2016.11.008.

104 Stell G., Rasaiah J.C., Narang H. (1974) Thermodynamic perturbation theory for simple polar fluids. II, *Molecular Physics* **27**, 5, 1393–1414. DOI: 10.1080/00268977400101181.

105 Gubbns K. E., Twu C. H. (1978) Thermodinamics of polyatomic fluid mistures-I, *Chemical Engineering Science* **33**, 863–878.

106 Thomas Kraska and Keith E. Gubbins (1996) Phase Equilibria Calculations with a Modified SAFT Equation of State. 1. Pure Alkanes, Alkanols, and Water, *Ind. Eng. Chem. Res.* **35**, 4727–4737.

107 Thomas Kraska and Keith E. Gubbins Phase Equilibria Calculations with a Modified SAFT Equation of State. 2. Binary Mixtures of n-Alkanes, 1-Alkanols, and Water.

108 Jog P.K., Chapman W. G. (2009) Application of Wertheim's thermodynamic perturbation theory to dipolar hard sphere chains, *Molecular Physics* **97**, 3, 307–319. DOI: 10.1080/00268979909482832.

109 Jog P.K., Sauer S.G., Blaesing J., Chapman W. G. (2001) Application of Dipolar Chain Theory to the Phase Behavior of Polar Fluids and Mixtures, *Ind. Eng. Chem. Res.*, 40, 4641–4648.

110 Karakatsani E.K., Economou I.G. (2006) Perturbed chain-statistical associating fluid theory extended to dipolar and quadrupolar molecular fluids, *The journal of physical chemistry. B* **110**, 18, 9252–9261. DOI: 10.1021/jp056957b.

111 Debye P., Hückel E. (1923) Zur Theorie der Elektrolyte: I: Gefrierpunktserniedrigung und verwandte Erscheinungen., *Phys. Z.* **24**, 185–207.

112 Hückel E. (1925) Zur theorie konzentrierterer wässeriger Lösungen starker elektrolyte, *Phys. Z.* **26**, 93–147.

113 Maribo-Mogensen B., Kontogeorgis G.M., Thomsen K. (2012) Comparison of the Debye–Hückel and the Mean Spherical Approximation Theories for Electrolyte Solutions, *Ind. Eng. Chem. Res.* **51**, 14, 5353–5363. DOI: 10.1021/ie2029943.

114 Blum L. (1974) Solution of a model for the solvent-electrolyte interactions in the mean spherical approximation, *The Journal of Chemical Physics* **61**, 5, 2129–2133. DOI: 10.1063/1.1682224.

115 Blum L. (1975) Mean spherical model for asymmetric electrolytes: I. Method of solution., *Molecular Physics* **30**, 5, 1529–1535. DOI: 10.1080/00268977500103051.

116 Blum L., Wei D.Q. (1987) Analytical solution of the mean spherical approximation for an arbitrary mixture of ions in a dipolar solvent, *The Journal of Chemical Physics* **87**, 1, 555–565. DOI: 10.1063/1.453604.

117 Blum L. (1978) Solution of the mean spherical approximation for hard ions and dipoles of arbitrary size, *Journal of Statistical Physics* **18**, 5, 451–474.

118 Wei D., Blum L. (1987) The mean spherical approximation for an arbitrary mixture of ions in a dipolar solvent: Approximate solution, pair correlation functions, and thermodynamics, *The Journal of Chemical Physics* **87**, 5, 2999–3007. DOI: 10.1063/1.453036.

119 Y. Hajeb, A. A. Izadpanah, Sh. Osfouri (2017) Modeling thermodynamic properties of electrolytes: Inclusion of the mean spherical approximation (MSA) in the simplified SAFT equation of state, *Journal of Oil, Gas and Petrochemical Technology* **4**, 1, 69–84.

120 Mathias P.M. (2003) The Second Virial Coefficient and the Redlich−Kwong Equation, *Ind. Eng. Chem. Res.* **42**, 26, 7037–7044. DOI: 10.1021/ie0340037.

121 Chen A.A., Pappu R.V. (2007) Quantitative characterization of ion pairing and cluster formation in strong 1:1 electrolytes, *The journal of physical chemistry. B* **111**, 23, 6469–6478. DOI: 10.1021/jp0708547.

122 Das G., dos Ramos M.C., McCabe C. (2018) Predicting the thermodynamic properties of experimental mixed-solvent electrolyte systems using the SAFT-VR+DE equation of state, *Fluid Phase Equilibria* **460**, 105–118. DOI: 10.1016/j.fluid.2017.11.017.

123 Das G., Hlushak S., McCabe C. (2016) A SAFT-VR+DE equation of state based approach for the study of mixed dipolar solvent electrolytes, *Fluid Phase Equilibria* **416**, 72–82. DOI: 10.1016/j.fluid.2015.11.027.

124 Gang Jin and Marc D. Donohue (1988) An equation of state for electrolyte solutions.: 1. Aqueous systems containing strong electrolytes, *American Chemical Society* **27**, 6, 1073–1084.

125 Ji X., Tan S.P., Adidharma H., Radosz M. (2005) Statistical Associating Fluid Theory Coupled with Restricted Primitive Model to Represent Aqueous Strong Electrolytes: Multiple-Salt Solutions, *Ind. Eng. Chem. Res.* **44**, 19, 7584–7590. DOI: 10.1021/ie050488i.

126 Fournier P., Oelkers E.H., Gout R., Pokrovski G. (1998) Experimental determination of aqueous sodium-acetate dissociation constants at temperatures from 20 to 2408C, *Chemical geology* **151**, 69–84.

127 Uchida H., Matsuoka M. (2004) Molecular dynamics simulation of solution structure and dynamics of aqueous sodium chloride solutions from dilute to supersaturated concentration, *Fluid Phase Equilibria* **219**, 1, 49–54. DOI: 10.1016/j.fluid.2004.01.013.

128 Bernard O., Blum L. (1996) Binding mean spherical approximation for pairing ions: An exponential approximation and thermodynamics, *The Journal of Chemical Physics* **104**, 12, 4746–4754. DOI: 10.1063/1.471168.

129 Simonin J.-P., Bernard O., Blum L. (1999) Ionic Solutions in the Binding Mean Spherical Approximation: Thermodynamic Properties of Mixtures of Associating Electrolytes, *J. Phys. Chem. B* **103**, 4, 699–704. DOI: 10.1021/jp9833000.

130 Ruas A., Moisy P., Simonin J.-P., Bernard O., Dufrêche J.-F., Turq P. (2005) Lanthanide salts solutions: representation of osmotic coefficients within the binding mean spherical approximation, *The journal of physical chemistry. B* **109**, 11, 5243–5248. DOI: 10.1021/jp0450991.

131 Mark Bulow, Moreno Ascani, Christoph Held (2021) ePC-SAFT advanced - Part II: Application to Salt Solubility in Ionic and Organic Solvents and the Impact of Ion Pairing, *Fluid Phase Equilibria* **537**, 1–11.

132 Von M. Born (1920) Volumen und Hydratationswärme der Ionen, *Phys. Ges.* **21**, 13, 45–48.

133 Planche H., Renon H. (1981) Mean spherical approximation applied to a simple but nonprimitive model interaction for electrolyte solutions and polar substances, *J. Phys. Chem. B*, 85, 3924–3929.

134 You-Xiang Zuo W.F. (1997) Prediction of vapor pressure for nonaqueous electrolyte solutions using an electrolyte equation of state, *Fluid Phase Equilibria* **138**, 87–104.

135 Maribo-Mogensen B., Thomsen K., Kontogeorgis G.M. (2015) An electrolyte CPA equation of state for mixed solvent electrolytes, *AIChE J.* **61**, 9, 2933–2950. DOI: 10.1002/aic.14829.

136 Schreckenberg J.M., Dufal S., Haslam A.J., Adjiman C.S., Jackson G., Galindo A. (2014) Modelling of the thermodynamic and solvation properties of electrolyte solutions with the statistical associating fluid theory for potentials of variable range, *Molecular Physics* **112**, 17, 2339–2364. DOI: 10.1080/00268976.2014.910316.

137 Karl Giese/U. Kaatze/R. Pottel (1970) Permittivity and dielectric and proton magnetic relaxation of aqueous solutions of the alkali halides, *The Journal of Physical Chemistry*, **74**, 21.

138 Simonin J.-P., Bernard O., Blum L. (1998) Real Ionic Solutions in the Mean Spherical Approximation. 3. Osmotic and Activity Coefficients for Associating Electrolytes in the Primitive Model, *Journal of physics chemical*, 102, 4411–4417.

139 Gang Jin and Marc D. Donohue (1991) An equation of state for electrolyte solutions.: 3. Aqueous solutions containing multiple salts, *American Chemical Society* **30**, 1, 240–248.

140 Pinsky M.L., Takano K. (2004) Chater 8: Property Estimation for Electrolyte Systems, in *Computer Aided Property Estimation for Process and Product Design*, Elsevier, pp. 181–204.

141 Lin Y. (2007) Development of an equation of state for solution containing electrolytes, *Ph. D. Thesis*, Technical University of Denmark.

142 Held C. (2020) Thermodynamic gE Models and Equations of State for Electrolytes in a Water-Poor Medium: A Review, *J. Chem. Eng. Data* **65**, 2073–5082.

143 Kontogeorgis G.M., Maribo-Mogensen B., Thomsen K. (2018) The Debye-Hückel theory and its importance in modeling electrolyte solutions, *Fluid Phase Equilibria* **462**, 130–152. DOI: 10.1016/j.fluid.2018.01.004.

144 Gang Jin and Marc D. Donohue (1988) An equation of state for electrolyte solutions.: 2. Single volatile weak electrolytes in water, *American Chemical Society* **27**, 9, 1737–1743.

145 Myers J.A., Sandler S.I., Wood R.H. (2002) An Equation of State for Electrolyte Solutions Covering Wide Ranges of Temperature, Pressure, and Composition, *Ind. Eng. Chem. Res.* **41**, 13, 3282–3297. DOI: 10.1021/ie011016g.

146 Cameretti L.F., Sadowski G., Mollerup J.M. (2005) Modeling of Aqueous Electrolyte Solutions with Perturbed-Chain Statistical Associated Fluid Theory, *Ind. Eng. Chem. Res.* **44**, 9, 3355–3362. DOI: 10.1021/ie0488142.

147 Held C., Prinz A., Wallmeyer V., Sadowski G. (2012) Measuring and modeling alcohol/salt systems, *Chemical Engineering Science* **68**, 1, 328–339. DOI: 10.1016/j.ces.2011.09.040.

148 Held C., Sadowski G., Carneiro A., Rodríguez O., Macedo E.A. (2013) Modeling thermodynamic properties of aqueous single-solute and multi-solute sugar solutions with PC-SAFT, *AIChE J.* **59**, 12, 4794–4805. DOI: 10.1002/aic.14212.

149 Reschke T., Brandenbusch C., Sadowski G. (2015) Modeling aqueous two-phase systems: III. Polymers and organic salts as ATPS former, *Fluid Phase Equilibria* **387**, 178–189. DOI: 10.1016/j.fluid.2014.12.011.

150 Reschke T., Brandenbusch C., Sadowski G. (2014) Modeling aqueous two-phase systems: I. Polyethylene glycol and inorganic salts as ATPS former, *Fluid Phase Equilibria* **368**, 91–103. DOI: 10.1016/j.fluid.2014.02.016.

151 Reschke T., Brandenbusch C., Sadowski G. (2014) Modeling aqueous two-phase systems: II. Inorganic salts and polyether homo- and copolymers as ATPS former, *Fluid Phase Equilibria* **375**, 306–315. DOI: 10.1016/j.fluid.2014.04.040.

152 Mohammad S., Held C., Altuntepe E., Köse T., Gerlach T., Smirnova I., Sadowski G. (2016) Salt influence on MIBK/water liquid–liquid equilibrium: Measuring and modeling with ePC-SAFT and COSMO-RS, *Fluid Phase Equilibria* **416**, 83–93. DOI: 10.1016/j.fluid.2015.11.018.

153 Bülow M., Ji X., Held C. (2019) Incorporating a concentration-dependent dielectric constant into ePC-SAFT. An application to binary mixtures containing ionic liquids, *Fluid Phase Equilibria* **492**, 26–33. DOI: 10.1016/j.fluid.2019.03.010.

154 Mark Bulow, Moreno Ascani, Christoph Held (2021) ePC-SAFT advanced - Part I: Physical meaning of including a concentration-dependent dielectric constant in the born term and in the Debye-Hückel theory, *Fluid Phase Equilibria* **535**, 1–8.

155 Ji X., Tan S.P., Adidharma H., Radosz M. (2006) Statistical associating fluid theory coupled with restrictive primitive model extended to bivalent ions. SAFT2: 2. Brine/seawater properties predicted, *The journal of physical chemistry. B* **110**, 33, 16700–16706. DOI: 10.1021/jp062511z.

156 Tan S.P., Adidharma H., Radosz M. (2005) Statistical Associating Fluid Theory Coupled with Restricted Primitive Model To Represent Aqueous Strong Electrolytes, *Ind. Eng. Chem. Res.* **44**, 12, 4442–4452. DOI: 10.1021/ie048750v.

157 Inchekel R., Hemptinne J.-C. de, Fürst W. (2008) The simultaneous representation of dielectric constant, volume and activity coefficients using an electrolyte equation of state, *Fluid Phase Equilibria* **271**, 1-2, 19–27. DOI: 10.1016/j.fluid.2008.06.013.

158 Shahriari R., Dehghani M.R. (2017) Prediction of thermodynamic properties of aqueous electrolyte solutions using equation of state, *AIChE J.* **63**, 11, 5083–5097. DOI: 10.1002/aic.15827.

159 Lin Y., Thomsen K., Hemptinne J.-C. de (2007) Multicomponent equations of state for electrolytes, *AIChE J.* **53**, 4, 989–1005. DOI: 10.1002/aic.11128.

160 Haghighi H., Chapoy A., Tohidi B. (2008) Freezing Point Depression of Electrolyte Solutions: Experimental Measurements and Modeling Using the Cubic-Plus-Association Equation of State, *Ind. Eng. Chem. Res.* **47**, 11, 3983–3989. DOI: 10.1021/ie800017e.

161 Carvalho P.J., Pereira L.M., Gonçalves N.P., Queimada A.J., Coutinho J.A. (2015) Carbon dioxide solubility in aqueous solutions of NaCl: Measurements and modeling with electrolyte equations of state, *Fluid Phase Equilibria* **388**, 100–106. DOI: 10.1016/j.fluid.2014.12.043.

162 Sun L., Liang X., Solms N. von, Kontogeorgis G.M. (2020) Thermodynamic modeling of gas solubility in aqueous solutions of quaternary ammonium salts with the e-CPA equation of state, *Fluid Phase Equilibria* **507**, 112423. DOI: 10.1016/j.fluid.2019.112423.

163 Chabab S., Théveneau P., Corvisier J., Coquelet C., Paricaud P., Houriez C., Ahmar E.E. (2019) Thermodynamic study of the CO2 – H2O – NaCl system: Measurements of CO2 solubility and modeling of phase equilibria using Soreide and Whitson, electrolyte CPA and SIT models, *International Journal of Greenhouse Gas Control* **91**, 102825. DOI: 10.1016/j.ijggc.2019.102825.

164 Afsharpour A., Haghtalab A. (2019) Implementation of electrolyte CPA EoS to model solubility of CO2 and CO2 + H2S mixtures in aqueous MDEA solutions, *Chinese Journal of Chemical Engineering* **27**, 8, 1912–1920. DOI: 10.1016/j.cjche.2019.01.007.

165 Michael E. Fisher and Yan Levin (1993) Criticality in ionic fluids: Debye-Huckel theory, Bjerrum, and beyond, *Physical review* **71**, 23, 3826–3829.

166 Jiang J., Blum L., Bernard O., Prausnitz J.M., Sandler S.I. (2002) Criticality and phase behavior in the restricted-primitive model electrolyte: Description of ion association, *The Journal of Chemical Physics* **116**, 18, 7977–7982. DOI: 10.1063/1.1468638.

167 Aqua J.-N., Banerjee S., Fisher M.E. (2005) Criticality in Charge-asymmetric Hard-sphere Ionic Fluids, *Phys. Rev. E* **72**, 4, 183. DOI: 10.1103/PhysRevE.72.041501.

168 Simonin J.-P. (2019) On the "Born" term used in thermodynamic models for electrolytes, *The Journal of Chemical Physics* **150**, 24, 244503. DOI: 10.1063/1.5096598.

169 Maribo-Mogensen B., Kontogeorgis G.M., Thomsen K. (2013) Modeling of dielectric properties of aqueous salt solutions with an equation of state, *The journal of physical chemistry. B* **117**, 36, 10523–10533. DOI: 10.1021/jp403375t.

170 Maribo-Mogensen B., Kontogeorgis G.M., Thomsen K. (2013) Modeling of dielectric properties of complex fluids with an equation of state, *The journal of physical chemistry. B* **117**, 12, 3389–3397. DOI: 10.1021/jp310572q.

171 Kontogeorgis G.M., Folas G.K. (2010) *Thermodynamic models for industrial applications: From classical and advanced mixing rules to association theories*, Wiley, Chichester U.K. ISBN: 0470697261.

172 Held C., Cameretti L.F., Sadowski G. (2008) Modeling aqueous electrolyte solutions: Part 1. Fully dissociated electrolytes, *Fluid Phase Equilibria* **270**, 1-2, 87–96. DOI: 10.1016/j.fluid.2008.06.010.

173 Hernández-Garduzaa O., Garcia-Sánchez F, Neaub E., Rogalskic M. (2000) Equation of state associated with activity coefficient models to predict low and high pressure vapor–liquid equilibria, *Chemical Engineering Journal* **79**, 87–101.

174 Das G., Hlushak S., dos Ramos M.C., McCabe C. (2015) Predicting the thermodynamic properties and dielectric behavior of electrolyte solutions using the SAFT-VR+DE equation of state, *AIChE J.* **61**, 9, 3053–3072. DOI: 10.1002/aic.14909.

175 Ji X., Adidharma H. (2006) Ion-Based SAFT2 to Represent Aqueous Single- and Multiple-Salt Solutions at 298.15 K, *Ind. Eng. Chem. Res.* **45**, 22, 7719–7728. DOI: 10.1021/ie060649y.

176 Harned H.S., Nims L.F. (1932) The thermodynamic properties of aqueous sodium chloride solutions from 0 to 40°, *Journal of the American Chemical Society* **54**, 2, 423–432.

177 Chia-tsun L.2., W. T. Lindsay JR. (1972) Thermodynamics of sodium chloride solutions at high temperatures, *Journal of Solution Chemistry* **1**, 1, 45–69.

178 Rodney P. Smith/Donald S. Hirtle (1939) The Boiling Point Elevation. III. Sodium Chloride 1.0 to 4.0 <italic>M</italic> and 60 to 100°, *Department of Chemistry of Yale University* **61**, 1123–1126.

179 Hamer W.J., Wu Y.C. (1972) Osmotic Coefficients and Mean Activity Coefficients of Uni-Univalent Electrolytes in Water at 25 °C, *J. Phys. Chem. Ref. Data* **1**, 4, 1047–1099.

180 Gèrald Perron, Alain Roux, and Jacques E. Desnoyers (1981) Heat capacities and volumes of NaCl, MgCl2, CaCl2, and NiCl2 up to 6 molal in water, *CAN J. CHEM.* **59**, 3049–3054.

181 Pauling L. (1960) *The Nature of the Chemical Bond*, Cornell University Press.

182 R. D. SHANNON (1976) Revised effective ionic radii and systematic studies of interatomic distances in halides and chalcogenides, *Acta Cryst.* **32**, 751–767.

183 Trinh T.-K.-H., Passarello J.-P., Hemptinne J.-C. de, Lugo R., Lachet V. (2016) A non-additive repulsive contribution in an equation of state: The development for homonuclear square well chains equation of state validated against Monte Carlo simulation, *The Journal of Chemical Physics* **144**, 12, 124902. DOI: 10.1063/1.4944068.

184 Held C., Sadowski G. (2009) Modeling aqueous electrolyte solutions. Part 2. Weak electrolytes, *Fluid Phase Equilibria* **279**, 2, 141–148. DOI: 10.1016/j.fluid.2009.02.015.

185 Delphine S. (2017) *Advanced Tools for Optimization and Uncertainty Treatment: USER MANUAL*, IFPEN, Paris France.

186 Caramazza R. (1960) Measurement of the activity coefficients of potassium chloride in aqueous solution, *Gazz. Chim. Ital.* **90**, 1721–1729.

187 Hernández-Luis F., Rodríguez-Raposo R., Galleguillos H.R., Morales J.W. (2010) Activity coefficients of KCl in PEG 4000+water mixtures at 288.15, 298.15 and 308.15K, *Fluid Phase Equilibria* **295**, 2, 163–171. DOI: 10.1016/j.fluid.2010.04.012.

188 R. H. Stokes/Barbara J. Levien (1946) The Osmotic and Activity Coefficients of Zinc Nitrate, Zinc Perchlorate and Magnesium Perchlorate. Transference Numbers in Zinc Perchlorate Solutions, *J. Am. Chem. Soc.* **68**, 2, 333–337.

189 Platford R.F. (1973) Osmotic coefficients of aqueous solutions of seven compounds at 0.deg., *J. Chem. Eng. Data* **18**, 2, 215–217.

190 Thomas M. Davis/Lisa M. Duckett/Judith F. Owen/C. Stuart Patterson/Robert Saleeby (1985) Osmotic coefficients of aqueous lithium chloride and potassium chloride from their isopiestic ratios to sodium chloride at 45.degree.C, *J. Chem. Eng. Data* **30**, 4, 432–434.

191 John T. Moore/William T. Humphries/C. Stuart Patterson (1972) Isopiestic studies of some aqueous electrolyte solutions at 80.deg., *J. Chem. Eng. Data* **17**, 2, 180–182.

192 Patterson C.S., Gilpatrick L.O., Soldano B.A. (1960) The Osmotic Behaviour of Representative Aqueous Salt Solutions at 100°C, *J. Chem. Soc.* **37**, 2730–2734.

193 Soldano B.A., Meek M. (1963) Isopiestic Vapour-Pressure Measurements of Aqueous Salt Solutions at Elevated Temperatures. Part III., *J. Chem. Soc.* **1**, 4424–4426.

194 Herbert S. Harned/Chester C. Crawford (1937) The Thermodynamics of Aqueous Sodium Bromide Solutions from Electromotive Force Measurements[1], *J. Chem. Eng. Data* **1**, 1903–1905.

195 Christov C. (2007) An isopiestic study of aqueous NaBr and KBr at 50°C: Chemical equilibrium model of solution behavior and solubility in the NaBr–H2O, KBr–H2O and

Na–K–Br–H2O systems to high concentration and temperature, *Geochimica et Cosmochimica Acta* **71**, 14, 3557–3569. DOI: 10.1016/j.gca.2007.05.007.

196 Voigt W., Dittrich A., Haugsdal B., Grjotheim K. (1990) Thermodynamics of Aqueous Reciprocal Salt Systems. II. Isopiestic Determination of the Osmotic and Activity Coefficients in LiNO3 - NaBr - H2O and LiBr - NaNO3 - H2O at 100. °C, *Acta Chem. Scand.* **44**, 12–17.

197 Holmes, H. F. and Mesmer, R. E. (1998) An isopiestic study of aqueous solutions of the alkali metal bromides at elevated temperatures, *J. Chem. Thermodyn.* **30**, 723–741.

198 George C. Johnson/Rodney P. Smith (1941) The Boiling Point Elevation. IV. Potassium Bromide in Water[1], *J. Am. Chem. Soc.* **63**, 1351–1353.

199 Semin A.V., Klopov V.I. (1979) Thermochemistry of Potassium Bromide Dissolution in Mixtures of Water with tert-Butanol at 10 - 40 °C, *Izv. Vyssh. Uchebn. Zaved. Khim. Khim. Tekhnol.* **22**, 2, 248–250.

200 Gorbachev S.V., Kondratev V.P., Androsov V.I. (1974) Specific volumes of potassium bromide, iodide, and nitrate solutions in water., *Zh. Fiz. Khim.* **48**, 11, 2675–2677.

201 Pabsch D., Held C., Sadowski G. (2020) Modeling the CO 2 Solubility in Aqueous Electrolyte Solutions Using ePC-SAFT, *J. Chem. Eng. Data* **65**, 12, 5768–5777. DOI: 10.1021/acs.jced.0c00704.

202 Fennell C.J., Bizjak A., Vlachy V., Dill K.A. (2009) Ion pairing in molecular simulations of aqueous alkali halide solutions, *The journal of physical chemistry. B* **113**, 19, 6782–6791. DOI: 10.1021/jp809782z.

203 Niazi A., Olszowy N., Rabideau B., Ismail A. (2014) *Measurement of enthalpy and free energy changes for dissolution in concentrated electrolyte media using molecular simulations.*, AIChE Annual Conference, Atlanta.

204 Bjerrum N., Lunos B. (1926) Untersuchungen über Ionenassoziation.: I. Der Einfluss der Ione- nassoziation auf die Aktivität der Ionen bei Mittleren Assoziationsgraden., *Mathematisk-fysiske Meddelelser* **7**, 9, 1–48.

205 Filippov V.K., Vivcharik L.P., Gubanikhin E.A. (1975) Thermodynamic Study of the CdI2-LiI-H2O System at 25 °C, *Russ. J. Inorg. Chem.* **20**, 6, 941–943.

Annex A - Optimisation results for dispersive and associative models

1. Results from model 1.0 using strategy a

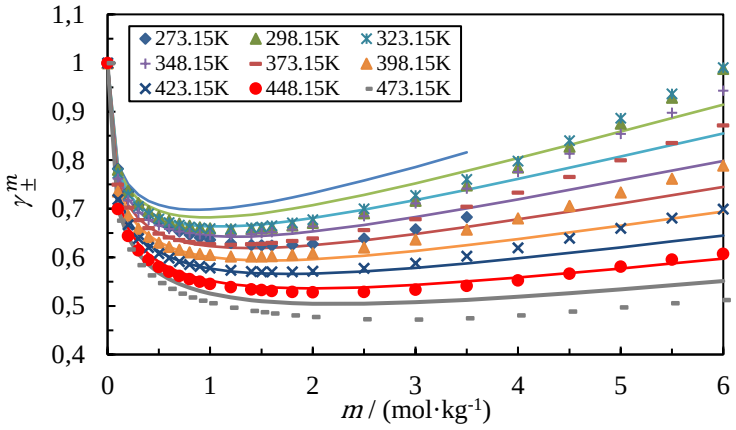

Figure 59 : Mean ionic activity coefficient in function of the salt concentration obtained from the optimisation of model 1.0 using optimisation strategy a. The symbols represent the experimental data and the lines represent the results obtained with the model. The calculations were made at 1 bar for temperatures up to 373.15 K, then the saturation pressure of the solvent was used for temperatures above 373.15 K.

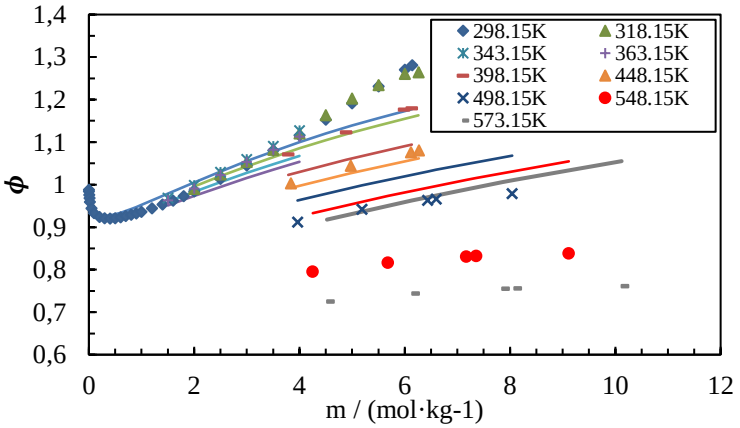

Figure 60 : Osmotic coefficient in function of the salt concentration obtained from the optimisation of model 1.0 using optimisation strategy a. The symbols represent the experimental data and the lines represent the results obtained with the model. The calculations were made at 1 bar for temperatures up to 373.15 K, then the saturation pressure of the solvent was used for temperatures above 373.15 K.

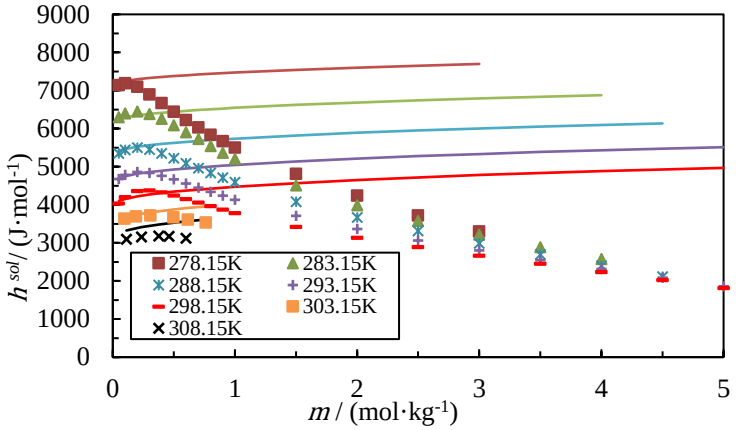

Figure 61 : Enthalpy of solution in function of the salt concentration obtained from the optimisation of model 1.0 using optimisation strategy a. The symbols represent the experimental data and the lines represent the results obtained with the model. The calculations were made at 1 bar.

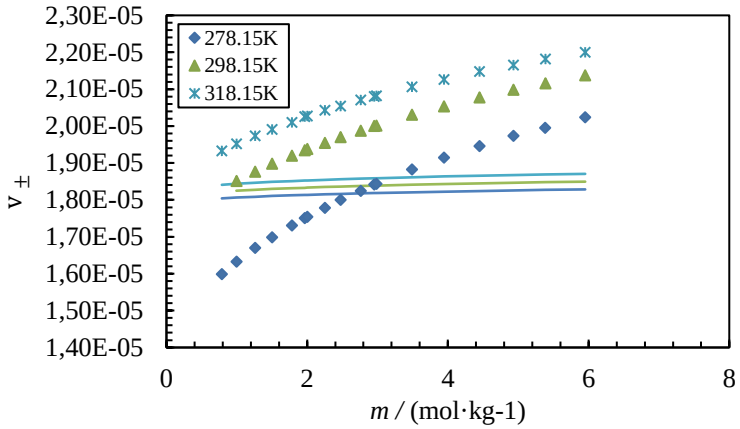

Figure 62 : Apparent molar volume in function of the salt concentration obtained from the optimisation of model 1.0 using optimisation strategy a. The symbols represent the experimental data and the lines represent the results obtained with the model. All isotherms follow the same line. The calculations were made at 1 bar.

2. Results from model 1.1 using strategy a.

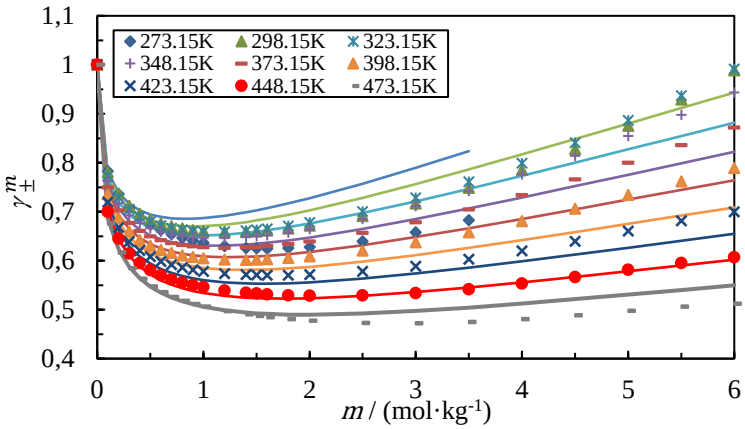

Figure 63 : Mean ionic activity coefficient in function of the salt concentration obtained from the optimisation of model 1.1 using optimisation strategy a. The symbols represent the experimental data and

the lines represent the results obtained with the model. The calculations were made at 1 bar for temperatures up to 373.15 K, then the saturation pressure of the solvent was used for temperatures above 373.15 K.

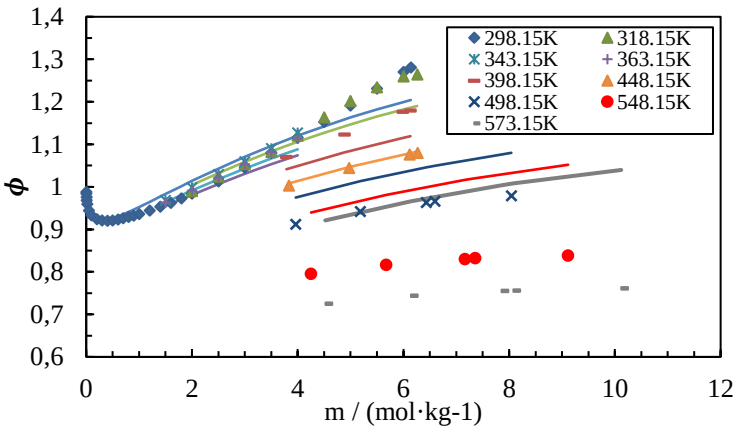

Figure 64 : Osmotic coefficient in function of the salt concentration obtained from the optimisation of model 1.1 using optimisation strategy a. The symbols represent the experimental data and the lines represent the results obtained with the model. The calculations were made at 1 bar for temperatures up to 373.15 K, then the saturation pressure of the solvent was used for temperatures above 373.15 K.

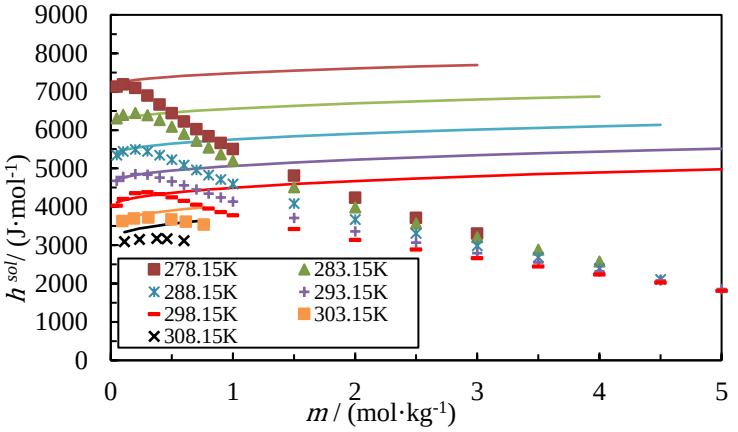

Figure 65 : Enthalpy of solution in function of the salt concentration obtained from the optimisation of model 1.1 using optimisation strategy a. The symbols represent the experimental data and the lines represent the results obtained with the model. The calculations were made at 1 bar.

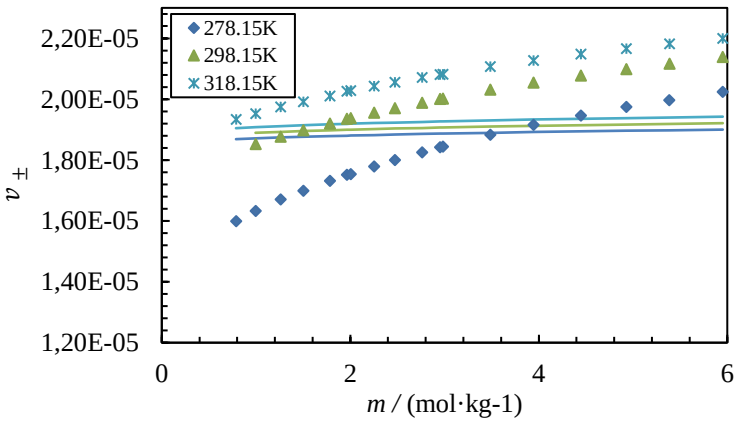

Figure 66 : Apparent molar volume in function of the salt concentration obtained from the optimisation of model 1.1 using optimisation strategy a. The symbols represent the experimental data and the lines

represent the results obtained with the model. All isotherms follow the same line. The calculations were made at 1 bar.

3. Results from model 1.2 using strategy a.

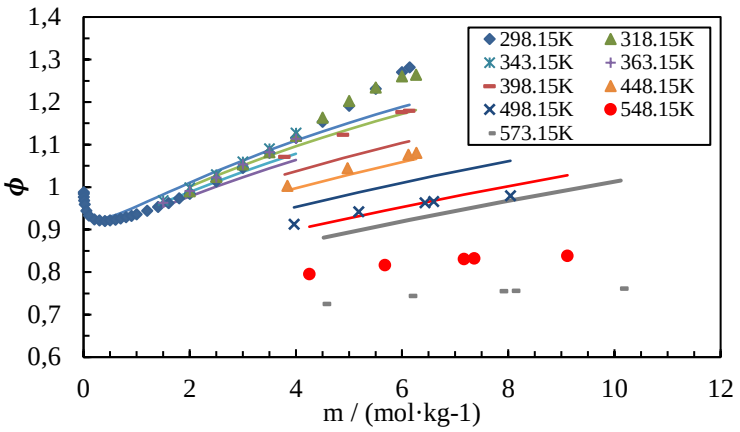

Figure 67 : Osmotic coefficient in function of the salt concentration obtained from the optimisation of model 1.2 using optimisation strategy a. The symbols represent the experimental data and the lines represent the results obtained with the model. The calculations were made at 1 bar for temperatures up to 373.15 K, then the saturation pressure of the solvent was used for temperatures above 373.15 K.

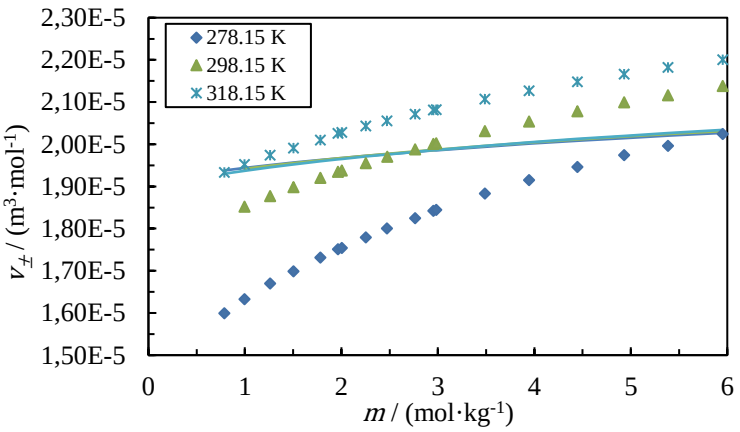

Figure 68 : Apparent molar volume in function of the salt concentration obtained from the optimisation of model 1.2 using optimisation strategy a. The symbols represent the experimental data and the lines represent the results obtained with the model. All isotherms follow the same line. The calculations were made at 1.

4. Results from model 1.0 using strategy b.

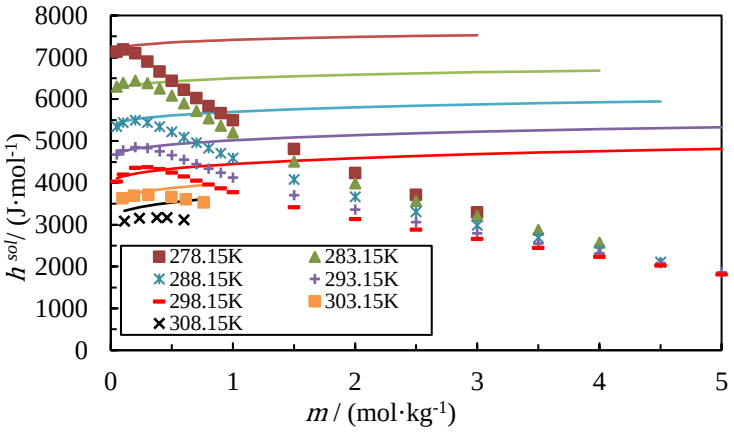

Figure 69 : Enthalpy of solution in function of the salt concentration obtained from the optimisation of model 1.0 using optimisation strategy b. The symbols represent the experimental data and the lines represent the results obtained with the model. The calculations were made at 1 bar.

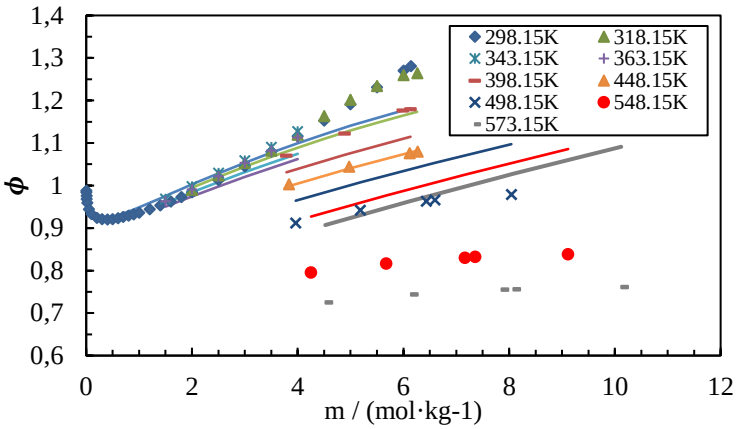

Figure 70 : Osmotic coefficient in function of the salt concentration obtained from the optimisation of model 1.0 using optimisation strategy b. The symbols represent the experimental data and the lines represent the results obtained with the model. The calculations were made at 1 bar for temperatures up to 373.15 K, then the saturation pressure of the solvent was used for temperatures above 373.15 K.

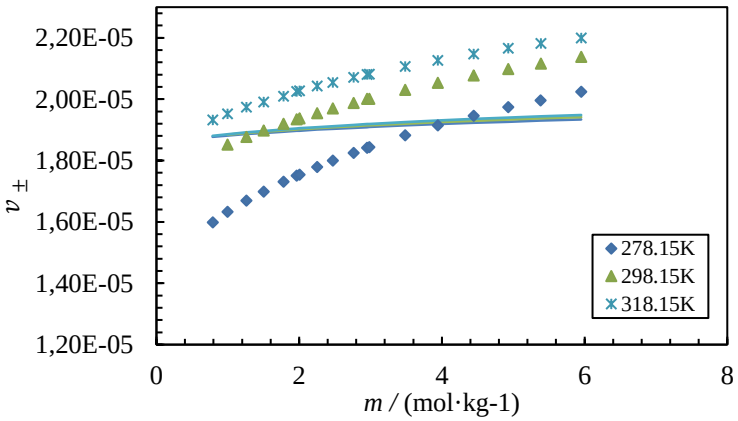

Figure 71 : Apparent molar volume in function of the salt concentration obtained from the optimisation of model 1.0 using optimisation strategy b. The symbols represent the experimental data and the lines represent the results obtained with the model. The calculations were made at 1 bar.

5. Results from model 2.0 using strategy a.

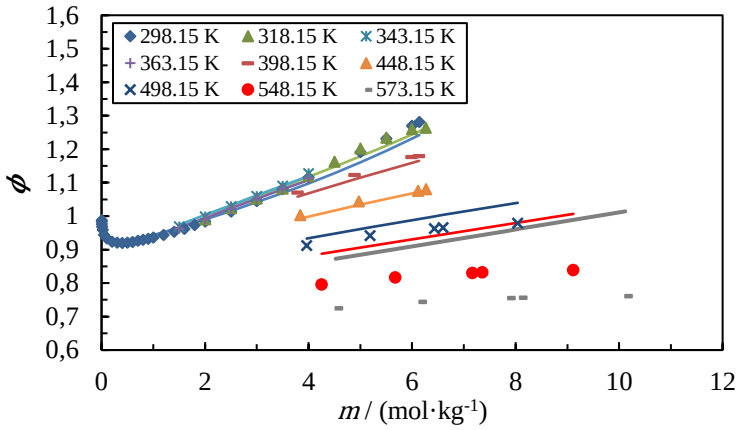

Figure 72 : Osmotic coefficient in function of the salt concentration obtained from the optimisation of model 2.0 using optimisation strategy a. The symbols represent the experimental data and the lines represent the results obtained with the model. The calculations were made at 1 bar for temperatures up to 373.15 K, then the saturation pressure of the solvent was used for temperatures above 373.15 K.

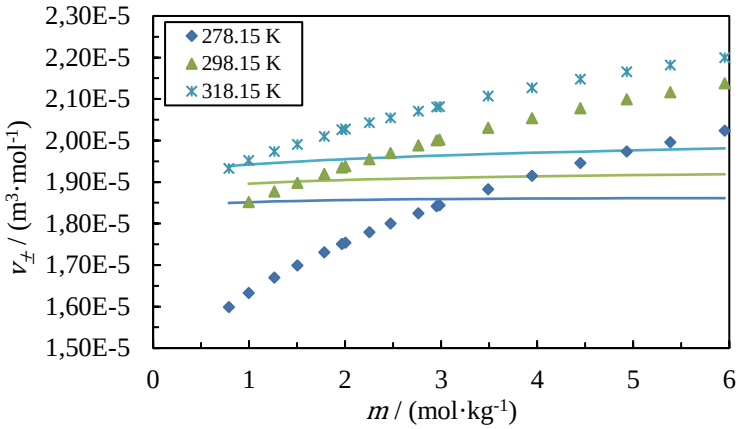

Figure 73 : Apparent molar volume in function of the salt concentration obtained from the optimisation of model 2.0 using optimisation strategy a. The symbols represent the experimental data and the lines represent the results obtained with the model. The calculations were made at 1 bar.

6. Results from model 2.1 using strategy a.

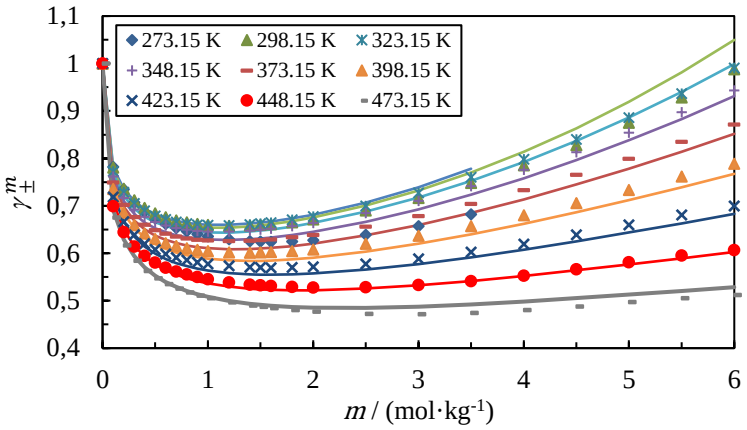

Figure 74 : Mean ionic activity coefficient in function of the salt concentration obtained from the optimisation of model 2.1 using optimisation strategy a. The symbols represent the experimental data and the lines represent the results obtained with the model. The calculations were made at 1 bar for temperatures up to 373.15 K, then the saturation pressure of the solvent was used for temperatures above 373.15 K.

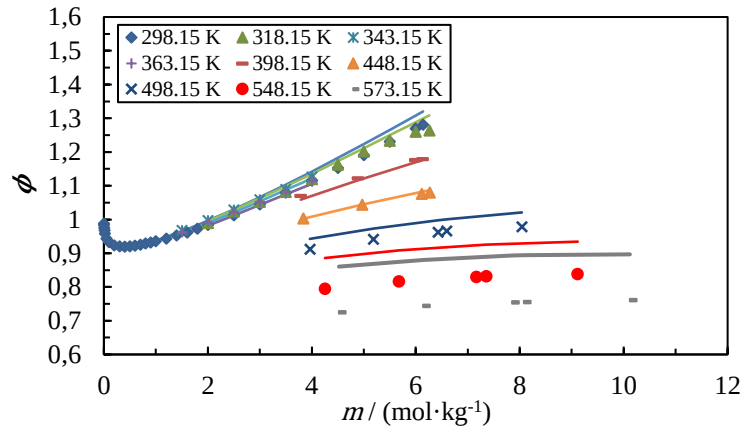

Figure 75 : Osmotic coefficient in function of the salt concentration obtained from the optimisation of model 2.1 using optimisation strategy a. The symbols represent the experimental data and the lines represent the results obtained with the model. The calculations were made at 1 bar for temperatures up to 373.15 K, then the saturation pressure of the solvent was used for temperatures above 373.15 K.

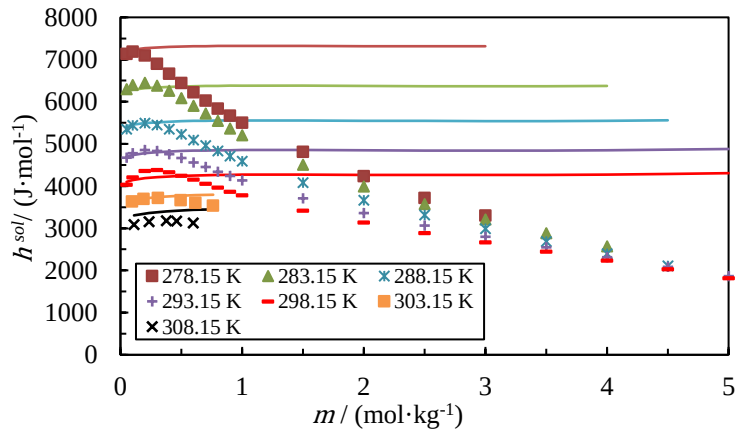

Figure 76 : Enthalpy of solution in function of the salt concentration obtained from the optimisation of model 2.1 using optimisation strategy a. The symbols represent the experimental data and the lines represent the results obtained with the model. The calculations were made at 1 bar.

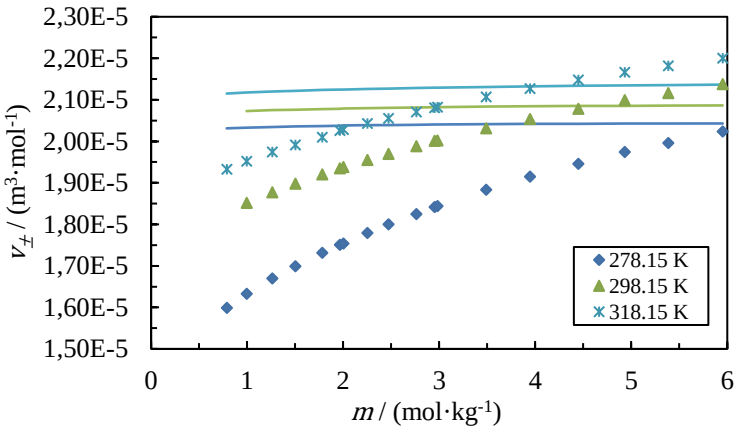

Figure 77 : Apparent molar volume in function of the salt concentration obtained from the optimisation of model 2.1 using optimisation strategy a. The symbols represent the experimental data and the lines represent the results obtained with the model. All isotherms follow the same line. The calculations were made at 1 bar.

7. Results from model 2.2 using strategy a.

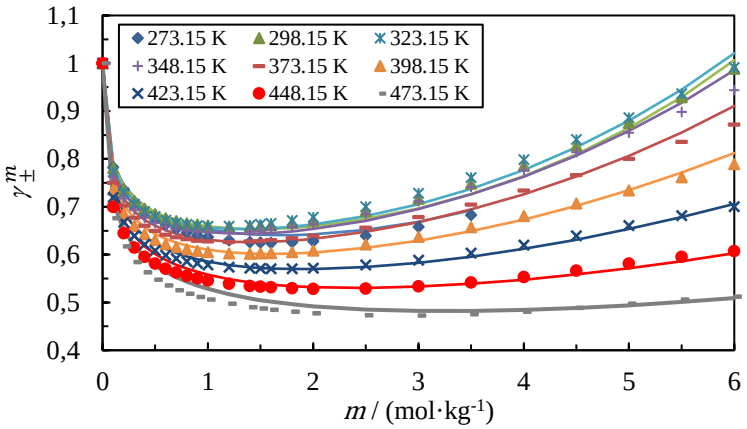

Figure 78 : Mean ionic activity coefficient in function of the salt concentration obtained from the optimisation of model 2.1 using optimisation strategy a. The symbols represent the experimental data and the lines represent the results obtained with the model. The calculations were made at 1 bar for temperatures up to 373.15 K, then the saturation pressure of the solvent was used for temperatures above 373.15 K.

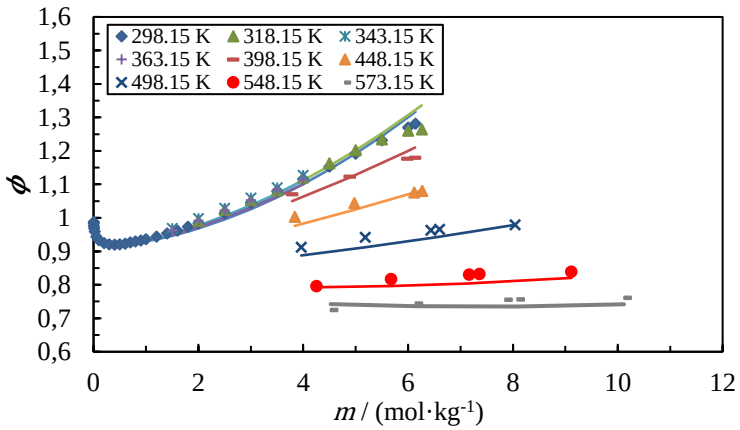

Figure 79 : Osmotic coefficient in function of the salt concentration obtained from the optimisation of model 2.1 using optimisation strategy a. The symbols represent the experimental data and the lines represent the results obtained with the model. The calculations were made at 1 bar for temperatures up to 373.15 K, then the saturation pressure of the solvent was used for temperatures above 373.15 K.

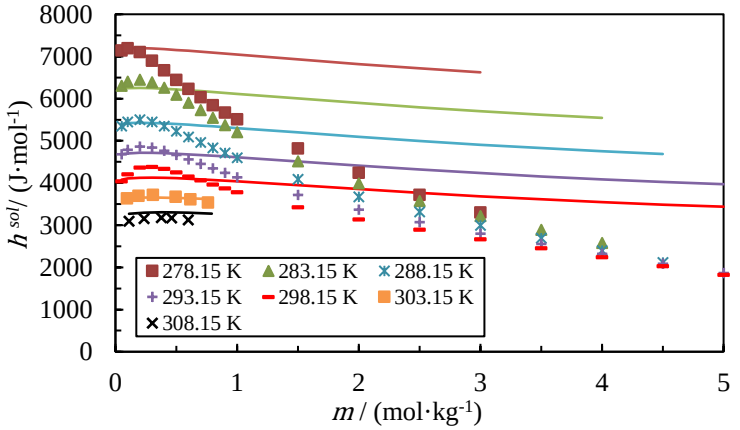

Figure 80 : Enthalpy of solution in function of the salt concentration obtained from the optimisation of model 2.1 using optimisation strategy a. The symbols represent the experimental data and the lines represent the results obtained with the model. The calculations were made at 1 bar.

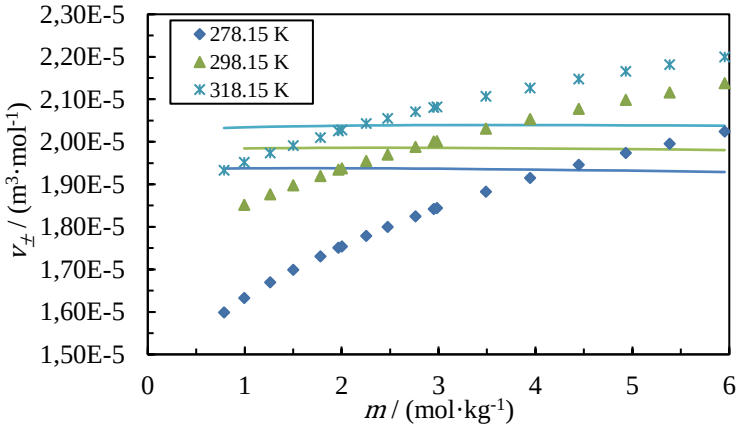

Figure 81 : Apparent molar volume in function of the salt concentration obtained from the optimisation of model 2.1 using optimisation strategy a. The symbols represent the experimental data and the lines represent the results obtained with the model. All isotherms follow the same line. The calculations were made at 1 bar.

Annex B - Terms contribution to $ln(\gamma_{\pm}^{m})$

1. Dispersive models

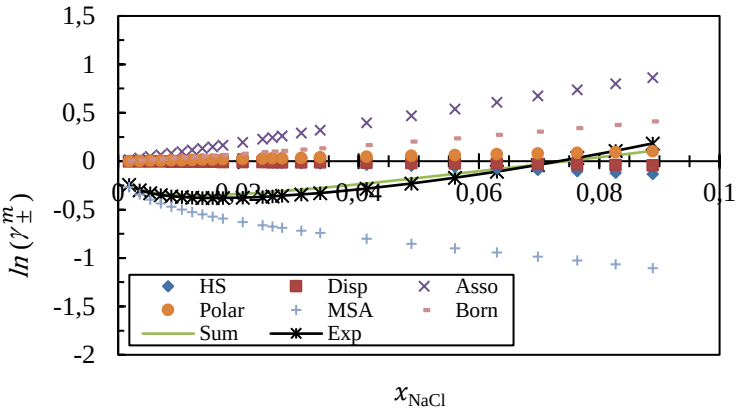

Figure 82 : Effect of the various terms on the logarithm of mean ionic activity coefficient for aqueous NaCl in function of the salt concentration at 298 K using model 1.0. Where hs=Hard sphere, disp=dispersion, asso=association, polar=polar, msa= MSA and born=Born terms, sum = sum of all terms and Exp= experimental data. The calculations were made at 1 bar.

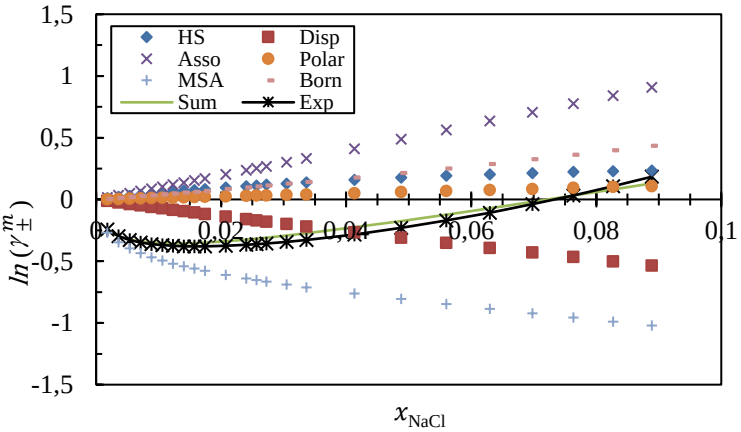

Figure 83 : Effect of the various terms on the logarithm of mean ionic activity coefficient for aqueous NaCl in function of the salt concentration at 298 K using model 1.1. Where hs=Hard sphere, disp=dispersion, asso=association, polar=polar, msa= MSA and born=Born terms, sum = sum of all terms and Exp= experimental data. The calculations were made at 1 bar

2. Associative models

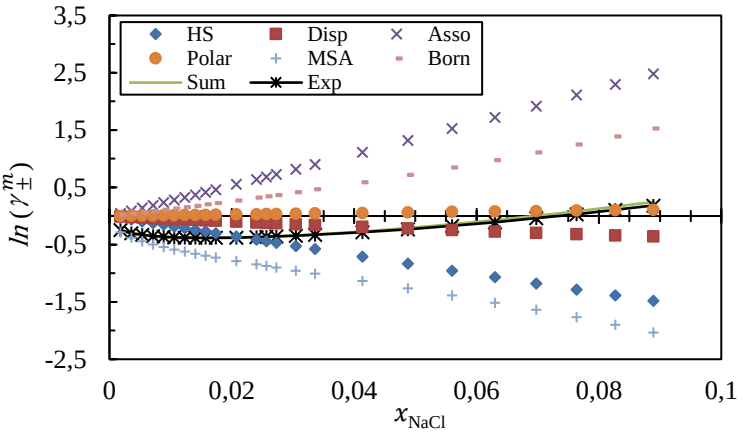

Figure 84 : Effect of the various terms on the logarithm of mean ionic activity coefficient for aqueous NaCl in function of the salt concentration at 298 K using model 2.1. Where hs=Hard sphere, disp=dispersion, asso=association, polar=polar, msa= MSA and born=Born terms, sum = sum of all terms and Exp= experimental data. The calculations were made at 1 bar.

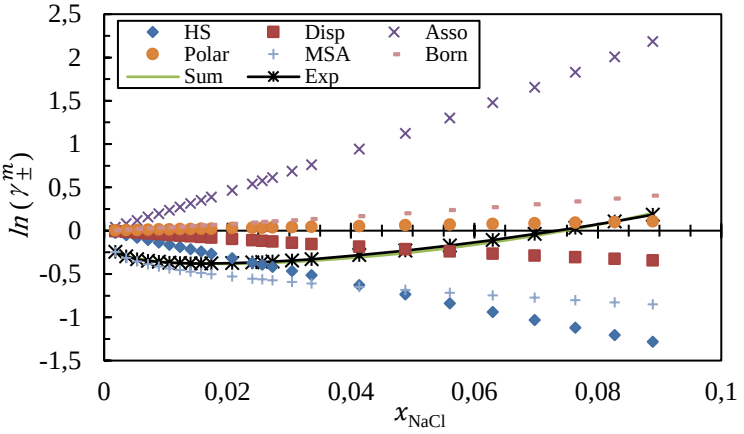

Figure 85 : Effect of the various terms on the logarithm of mean ionic activity coefficient for aqueous NaCl in function of the salt concentration at 298 K using model 2.2. Where hs=Hard sphere, disp=dispersion, asso=association, polar=polar, msa= MSA and born=Born terms, sum = sum of all terms and Exp= experimental data. The calculations were made at 1 bar.

Annex C - Dielectric constant as a function of salt concentration.

1. Schreckenberg model

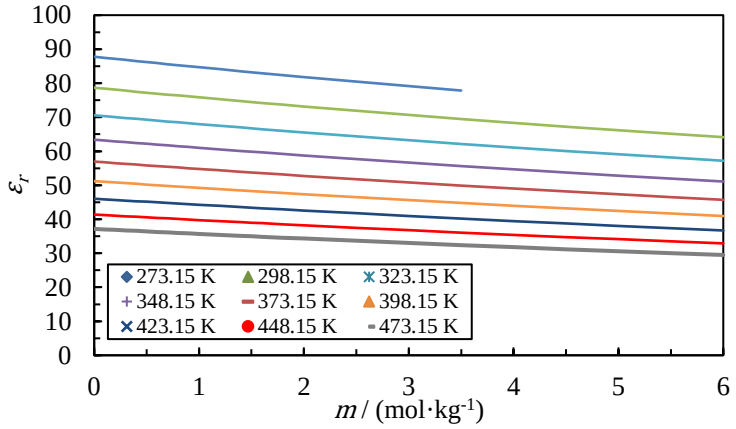

Figure 86 : Dielectric constant in function of the salt concentration at various temperatures, using Schreckenberg model. The calculations were made at 1 bar for temperatures up to 373.15 K, then the saturation pressure of the solvent was used for temperatures above 373.15 K.

2. Pottel model

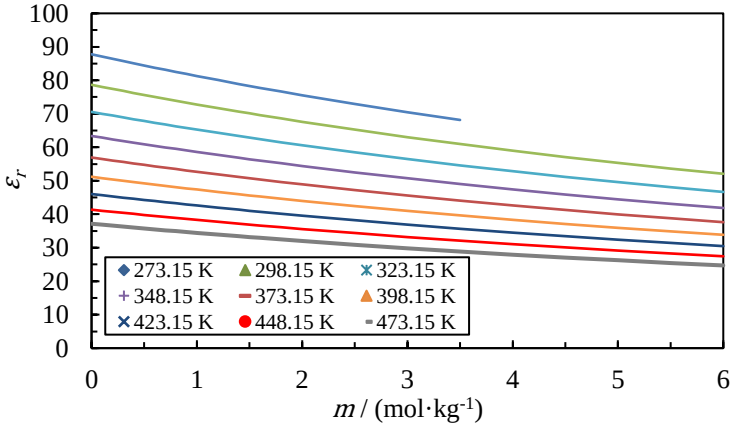

Figure 87 : Dielectric constant in function of the salt concentration at various temperatures, using Pottel model. The calculations were made at 1 bar for temperatures up to 373.15 K, then the saturation pressure of the solvent was used for temperatures above 373.15 K.

3. Simonin model

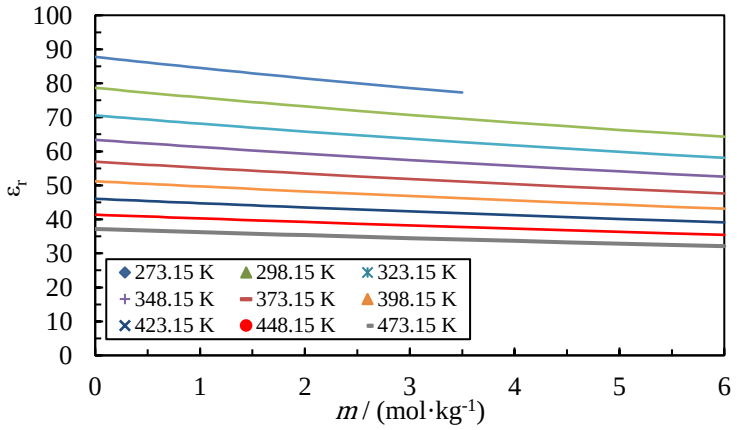

Figure 88 : Dielectric constant in function of the salt concentration at various temperatures, using Simonin model with parameters from model 2.0. The calculations were made at 1 bar for temperatures up to 373.15 K, then the saturation pressure of the solvent was used for temperatures above 373.15 K.

Annex D - Optimisations results from extension to 4 salts (NaCl, KCl, NaBr and KBr)

1. Dispersive model (Model 1.0)

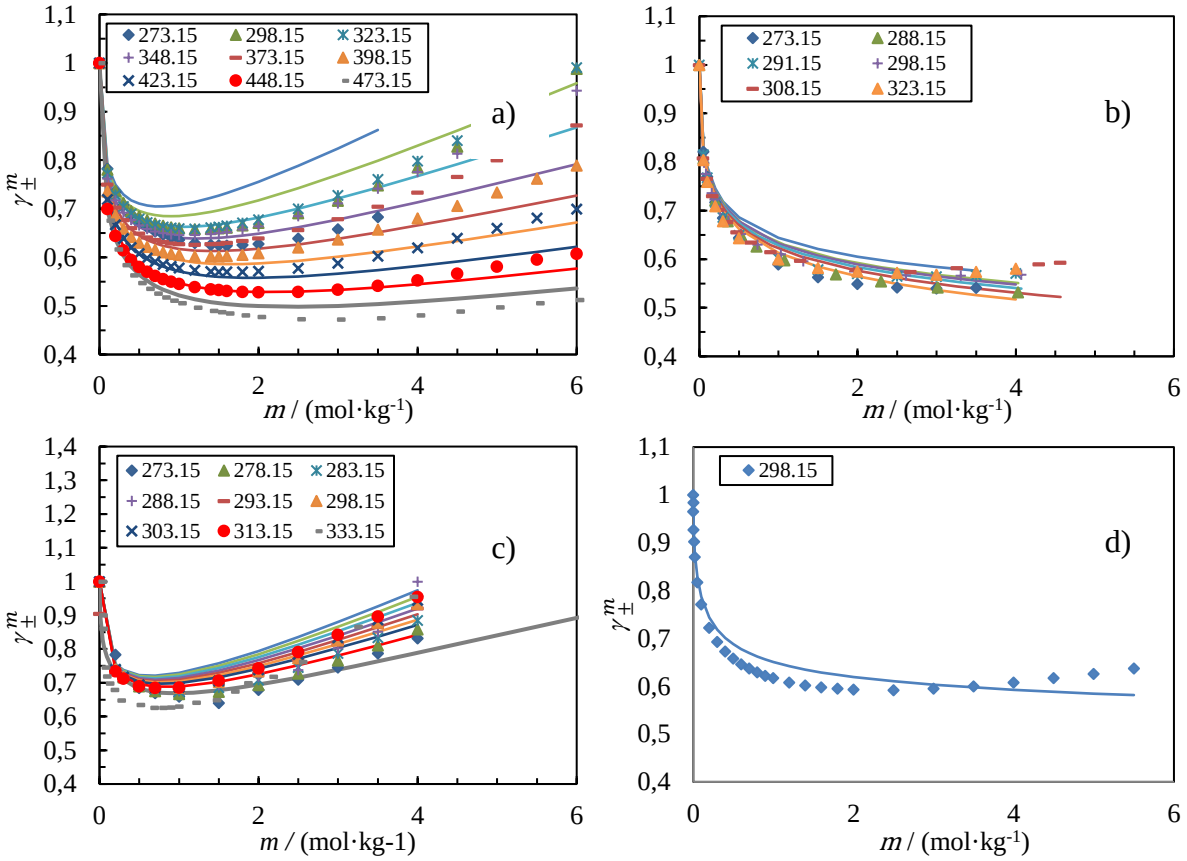

Figure 89 : Mean ionic activity coefficient in function of the salt concentration obtained from the optimisation of model 1.0. The symbols represent the experimental data and the lines represent the results obtained with the model. (a) NaCl ; (b) KCl ; (c) NaBr ; (d) KBr. The calculations were made at 1 bar for temperatures up to 373.15 K, then the saturation pressure of the solvent was used for temperatures above 373.15 K.

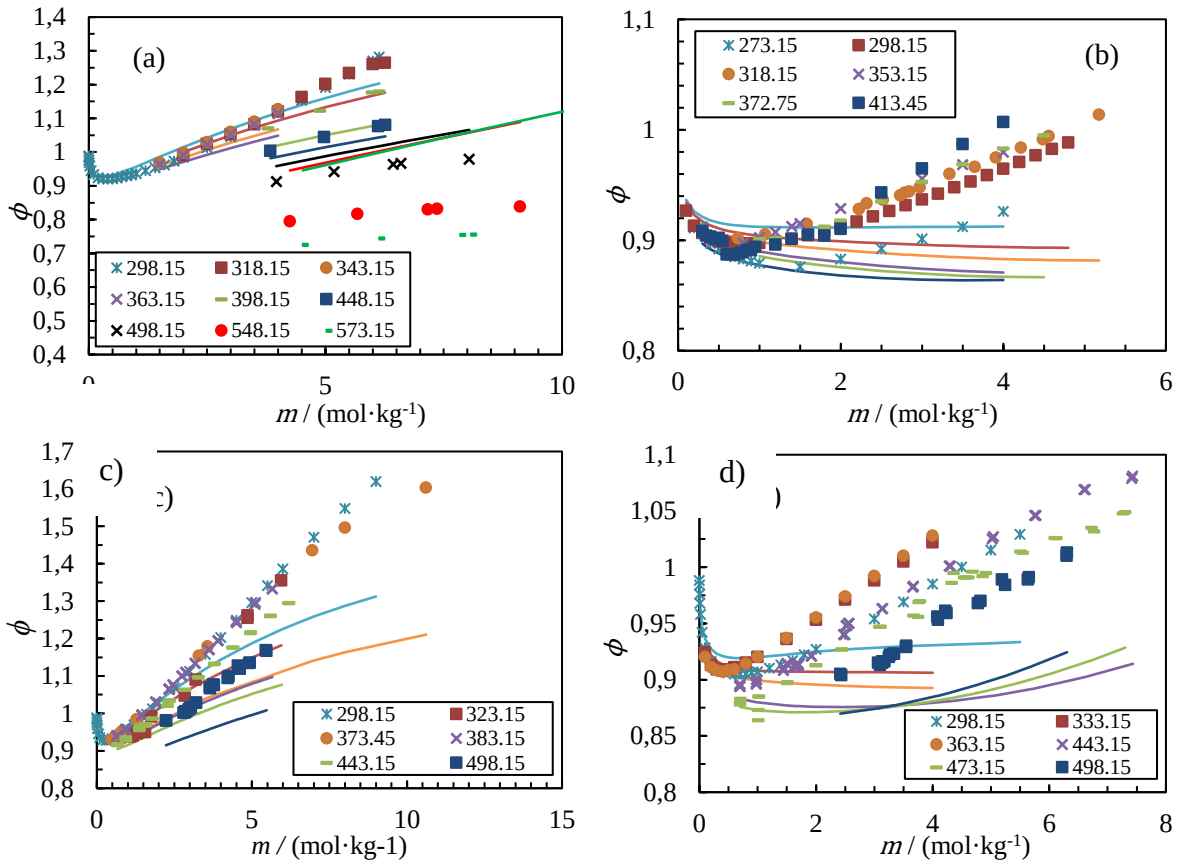

Figure 90 : Osmotic coefficient in function of the salt concentration obtained from the optimisation of model 1.0. The symbols represent the experimental data and the lines represent the results obtained with the model. (a) NaCl ; (b) KCl ; (c) NaBr ; (d) KBr. The calculations were made at 1 bar for temperatures up to 373.15 K, then the saturation pressure of the solvent was used for temperatures above 373.15 K.

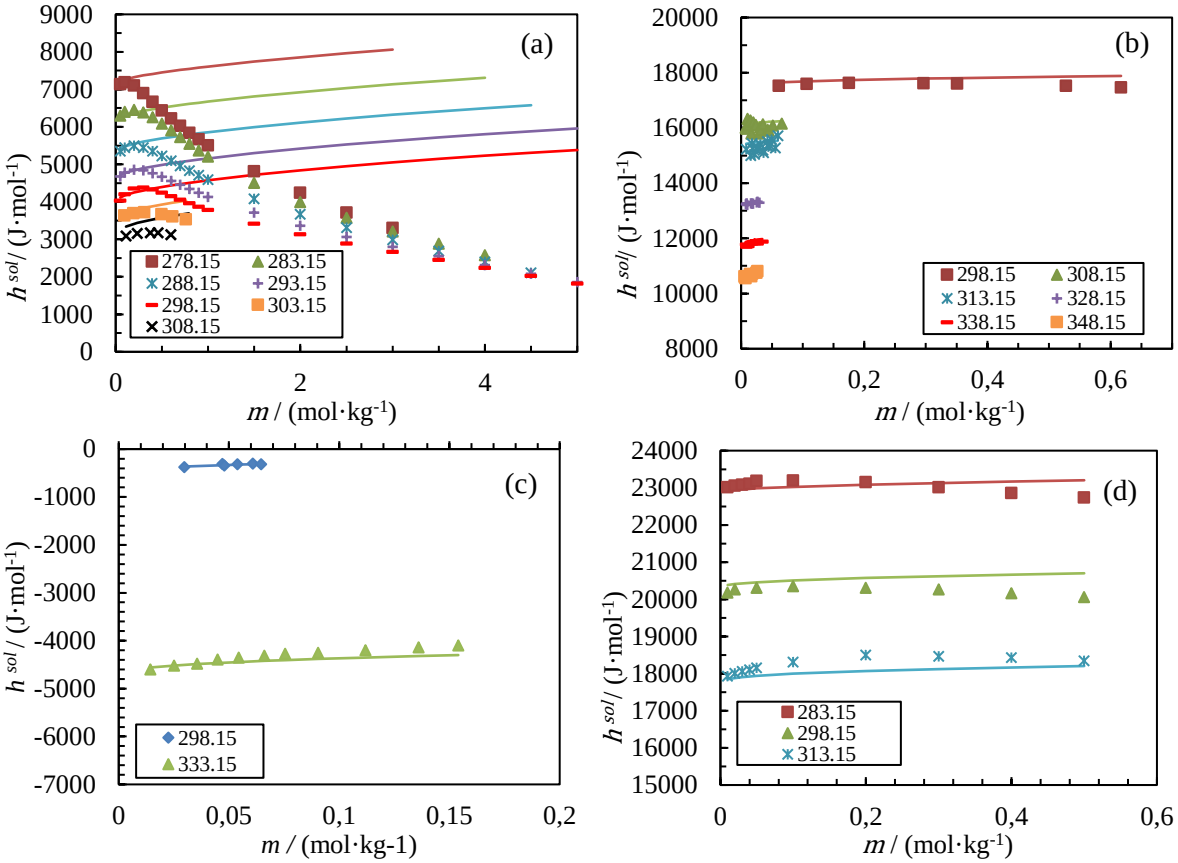

Figure 91 : Enthalpy of solution in function of the salt concentration obtained from the optimisation of model 1.0. The symbols represent the experimental data and the lines represent the results obtained with the model. (a) NaCl; (b) KCl ; (c) NaBr ; (d) KBr. The calculations were made at 1.

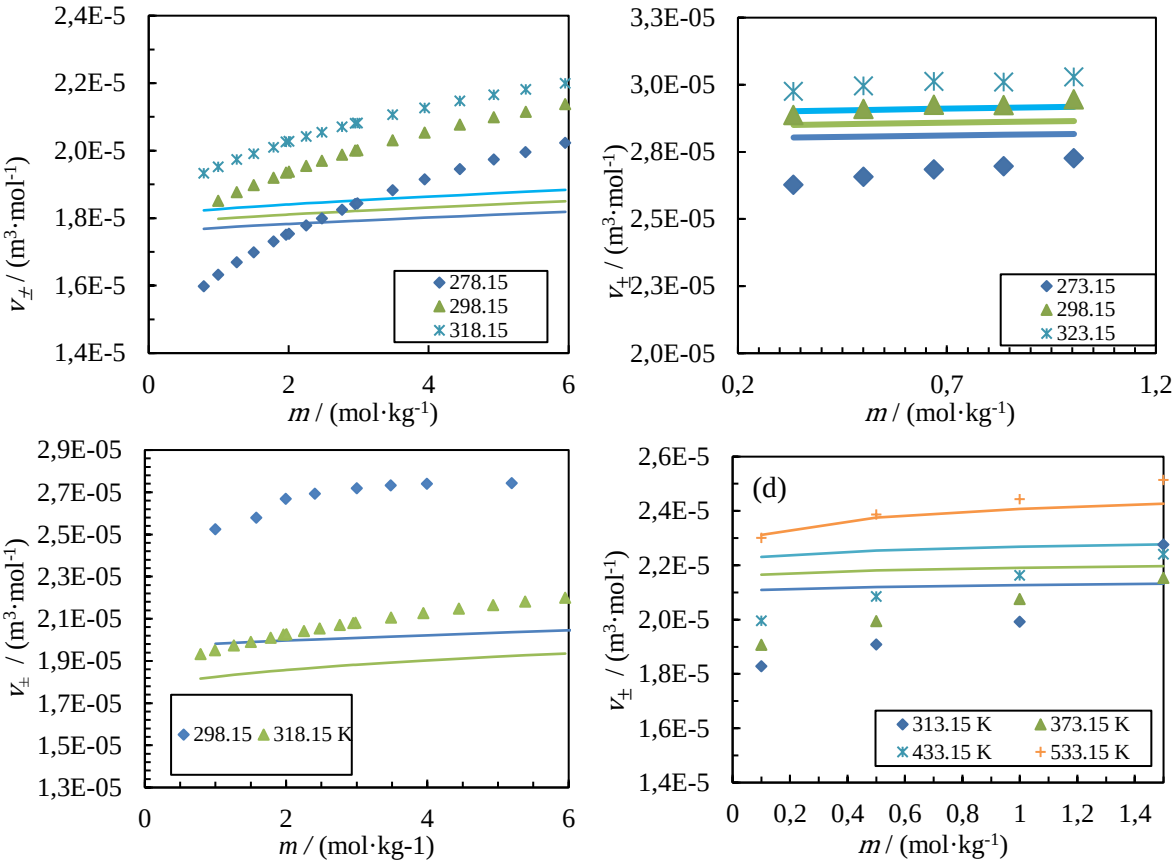

Figure 92 : Apparent molar volume in function of the salt concentration obtained from the optimisation of model 1.0. The symbols represent the experimental data and the lines represent the results obtained with the model. (a) NaCl ; (b) KCl ; (c) NaBr ; (d) KBr. The calculations were made at 1 bar for temperatures up to 373.15 K, then the saturation pressure of the solvent was used for temperatures above 373.15 K.

2. Associative model (Model 2.0)

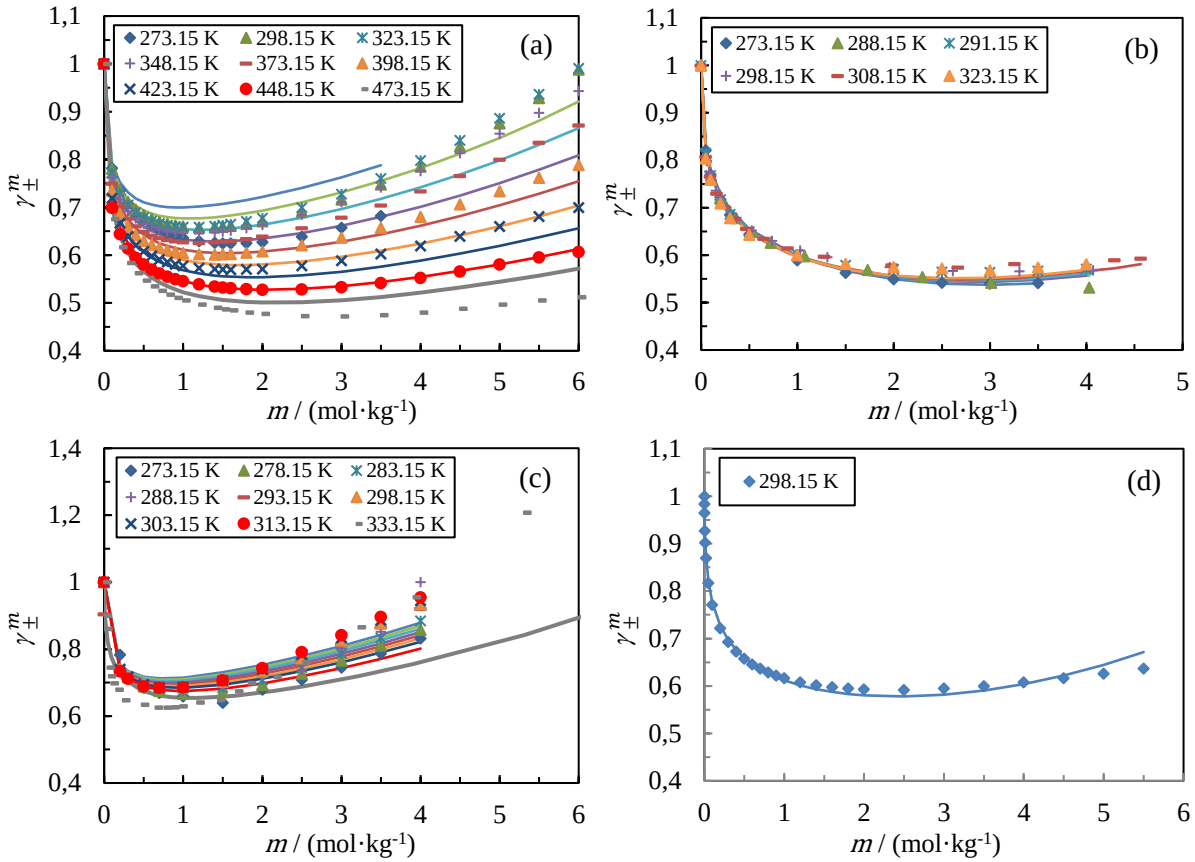

Figure 93 : Mean ionic activity coefficient in function of the salt concentration obtained from the optimisation of model 2.0. The symbols represent the experimental data and the lines represent the results obtained with the model. (a) NaCl ; (b) KCl ; (c) NaBr ; (d) KBr. The calculations were made at 1 bar for temperatures up to 373.15 K, then the saturation pressure of the solvent was used for temperatures above 373.15 K.

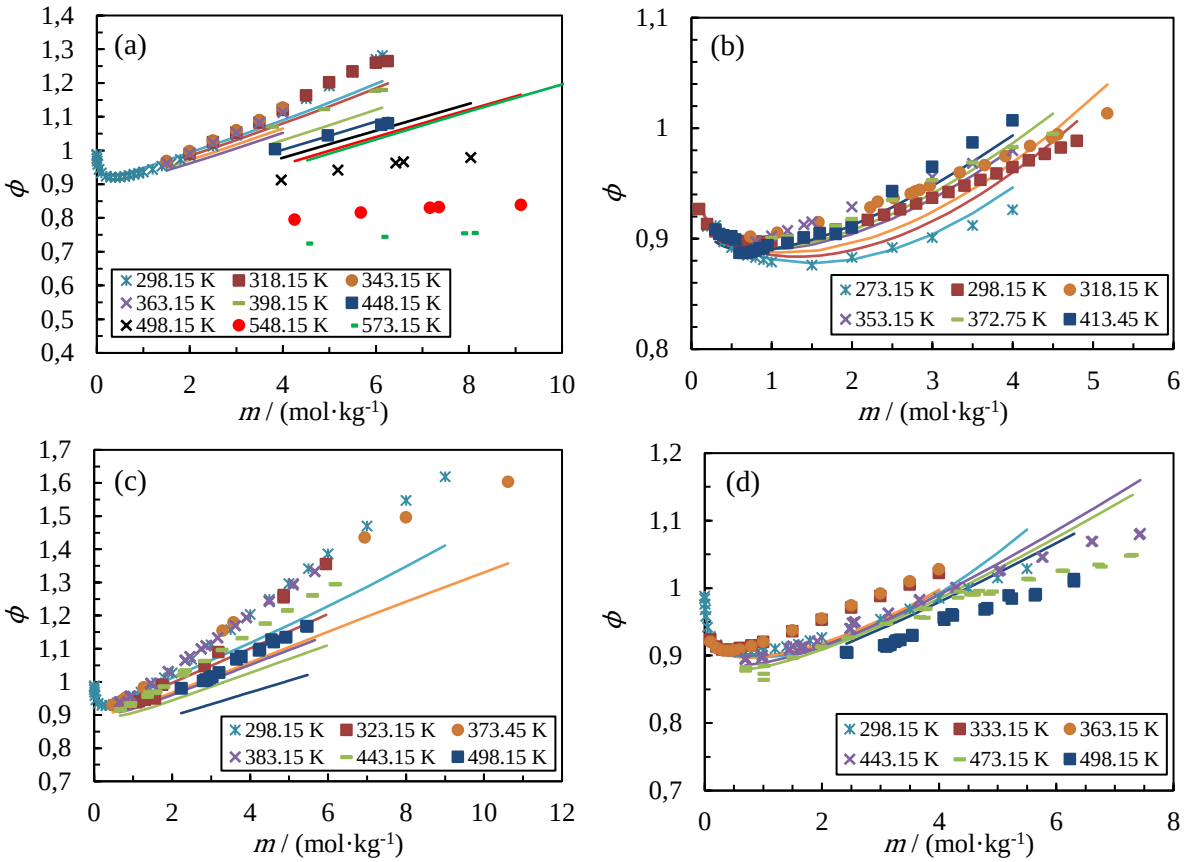

Figure 94 : Osmotic coefficient in function of the salt concentration obtained from the optimisation of model 2.0. The symbols represent the experimental data and the lines represent the results obtained with the model. (a) NaCl ; (b) KCl ; (c) NaBr ; (d) KBr. The calculations were made at 1 bar for temperatures up to 373.15 K, then the saturation pressure of the solvent was used for temperatures above 373.15 K.

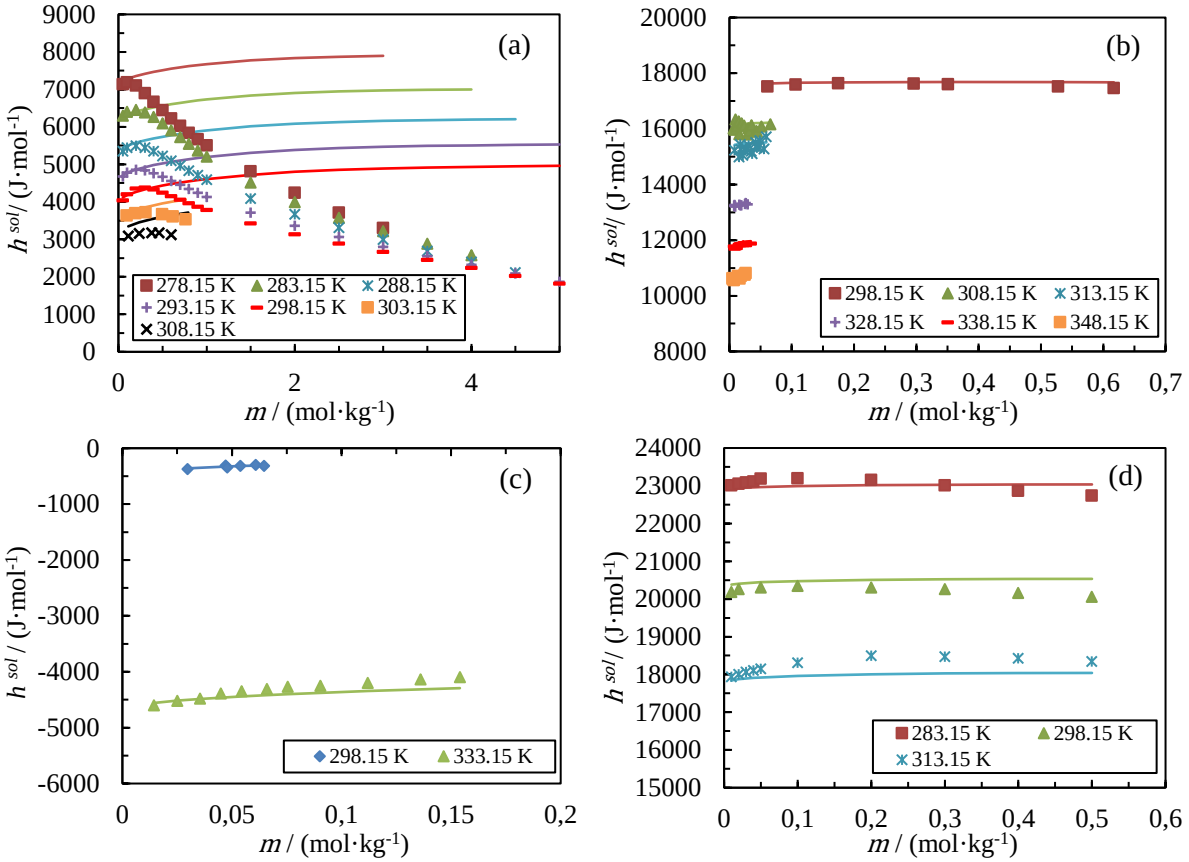

Figure 95 : Enthalpy of solution in function of the salt concentration obtained from the optimisation of model 2.0. The symbols represent the experimental data and the lines represent the results obtained with the model. (a) NaCl ; (b) KCl ; (c) NaBr ; (d) KBr. The calculations were made at 1 bar.

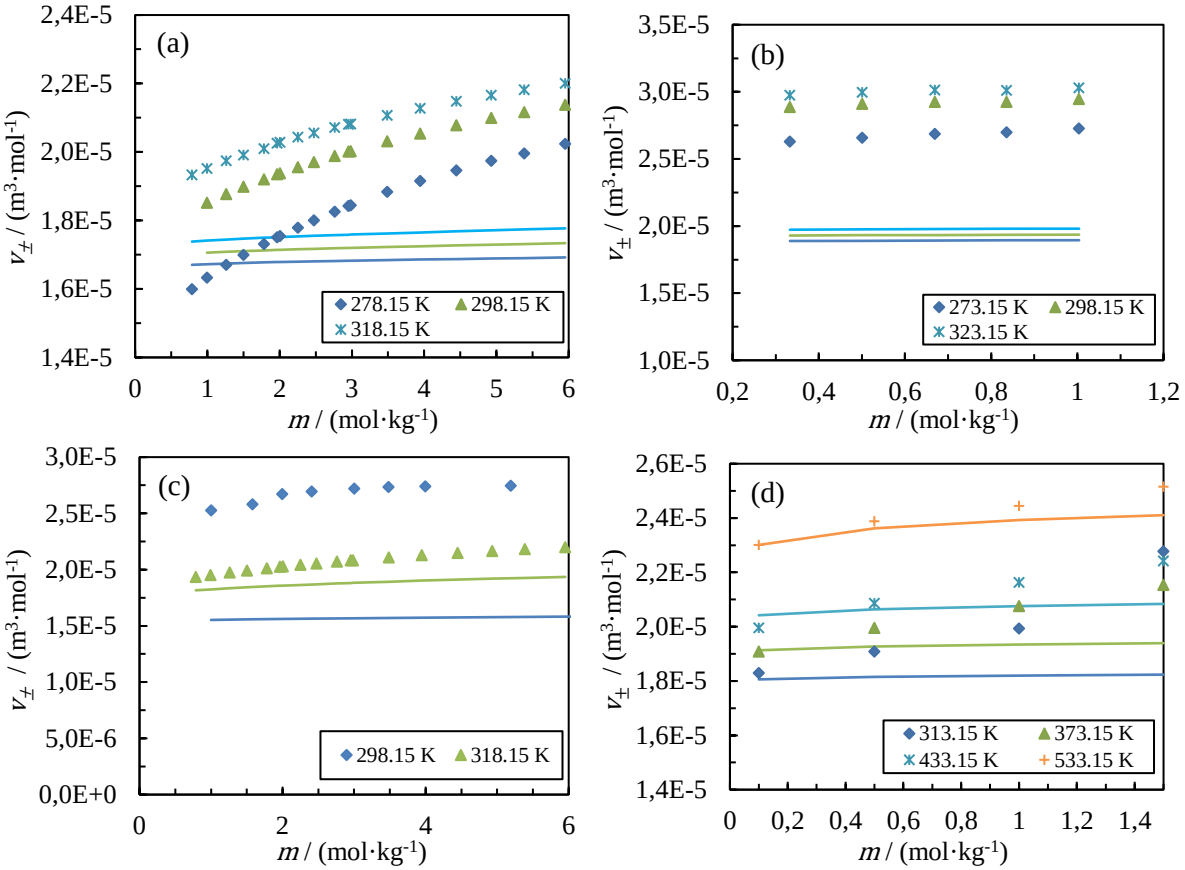

Figure 96 : Apparent molar volume in function of the salt concentration obtained from the optimisation of model 2.0. The symbols represent the experimental data and the lines represent the results obtained with the model. (a) NaCl ; (b) KCl ; (c) NaBr ; (d) KBr. The calculations were made at 1 bar for temperatures up to 373.15 K, then the saturation pressure of the solvent was used for temperatures above 373.15 K.

Annex E - Number of bonds for LiCl, LiBr and LiI using modified associative model 2.0Bj

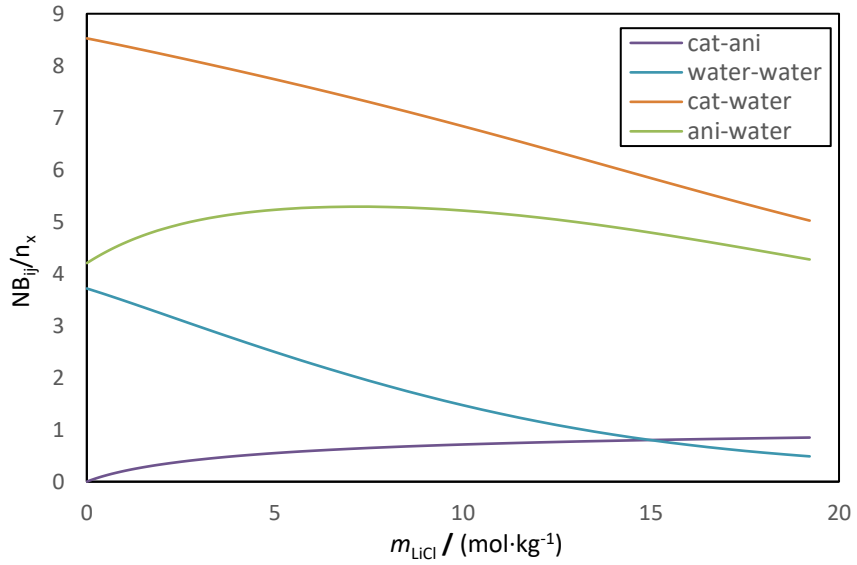

Figure 97 : Number of bonds per molecule as a function of salt concentration for aqueous LiCl at 298 K using modified associative model 2.0BJ with $M_{Li} = 9$ and $M_{Cl} = 8$. Cat-ani are the number of bonds between cation and anion, per ion ($n_X = n_{ion}$), water-water are the number of water-water bonds per water molecule ($n_X = n_{water}$), cat-water and ani-water are the number of bonds between cation and anion with water respectively, per ion molecule ($n_X = n_{ion}$)

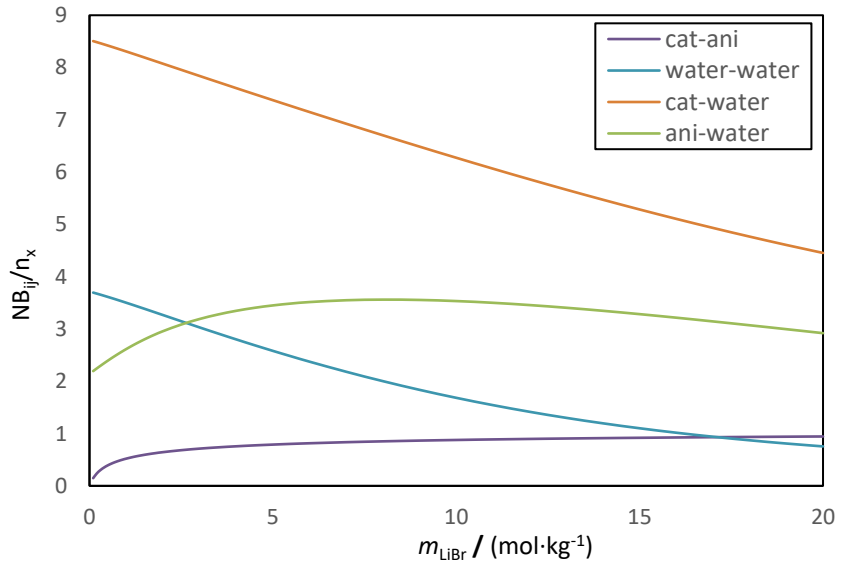

Figure 98 : Number of bonds per molecule as a function of salt concentration for aqueous LiBr at 298 K using modified associative model 2.0BJ with $M_{Li} = 9$ and $M_{Cl} = 7$. Cat-ani are the number of bonds between cation and anion, per ion ($n_X = n_{ion}$), water-water are the number of water-water bonds per water molecule ($n_X = n_{water}$), cat-water and ani-water are the number of bonds between cation and anion with water respectively, per ion molecule ($n_X = n_{ion}$).

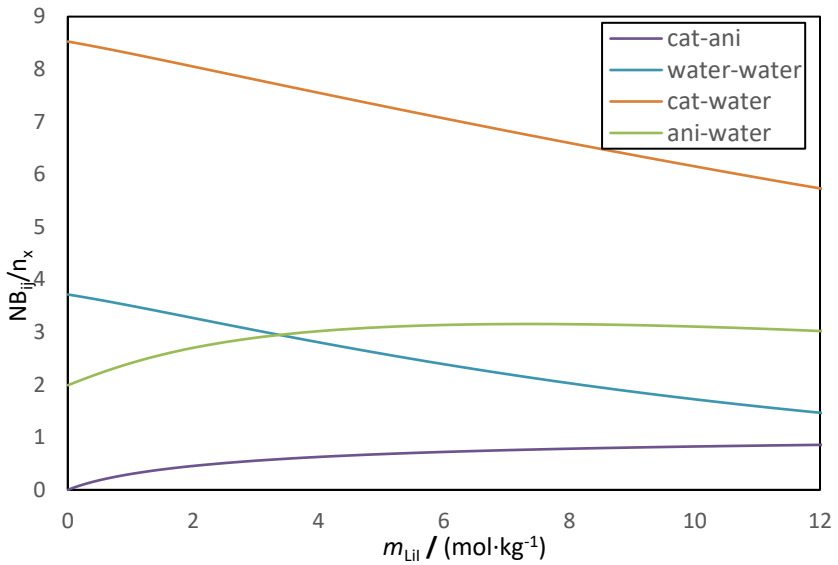

Figure 99 : Number of bonds per molecule as a function of salt concentration for aqueous LiI at 298 K using modified associative model 2.0BJ with $M_{Li} = 9$ and $M_{Cl} = 8$. Cat-ani are the number of bonds between cation and anion, per ion ($n_X = n_{ion}$), water-water are the number of water-water bonds per water molecule ($n_X = n_{water}$), cat-water and ani-water are the number of bonds between cation and anion with water respectively, per ion molecule ($n_X = n_{ion}$).